UNIVERSITEIT VAN PRETORIA
UNIVERSITY OF PRETORIA
YUNIBESITHI YA PRETORIA

DESIGN ADJUSTMENT FACTORS AND THE ECONOMICAL APPLICATION OF CONCRETE FLAT-SLABS WITH INTERNAL SPHERICAL VOIDS IN SOUTH AFRICA

by

CORNEILLE CHARLES MARAIS

A dissertation submitted in the partial fulfilment of the requirements for the degree of

MASTER OF ENGINEERING (STRUCTURAL ENGINEERING)

in the

FACULTY OF ENGINEERING, BUILT ENVIRONMENT AND INFORMATION TECHNOLOGY

UNIVERSITY OF PRETORIA

AUGUST 2009

UNIVERSITEIT VAN PRETORIA
UNIVERSITY OF PRETORIA
YUNIBESITHI YA PRETORIA

SUMMARY OF DISSERTATION

Design adjustment factors and the economical application of concrete flat-slabs with internal spherical voids in South Africa

by
Corneille Charles Marais

Supervisor: Dr John M Robberts
Co-Supervisor: Professor Ben van Rensburg
Department: Civil Engineering
University: University of Pretoria
Degree: Master of Engineering (Structural Engineering)

Keywords: spherical void formers, concrete flat slabs, shear strength, modelling, economy

Long span flat slab systems with internal spherical void formers have been used in Europe for a decade now. Cobiax® is the brand name of a successful system, recently introduced in South Africa. It is a bi-axial reinforced concrete flat slab system, with a grid of internal spherical void formers. The main advantage is the possibility of long spans due to the significant reduction in own weight, as well as the fast construction sequence with the use of flat slab formwork systems.

Design requirements of SANS 10100:2000 are affected. Vertical shear capacity is a concern due to loss of aggregate interlock. Research in Germany proved a factor of 0.55 to be a conservative shear resistance reduction factor for Cobiax slabs. Theoretical and preliminary laboratory South African research suggests that a greater factor of 0.85 might be used when considering the shear capacity of the steel cages. These cages' vertical legs also cross the cold joint caused by the two concrete pours required for Cobiax slabs, and proved to provide sufficient horisontal shear resistance if the correct cage diameters are used.

Laboratory tests in Germany supported by theoretical calculations further showed reduced deflections for Cobiax slabs. Although stiffness and own weight are reduced due to the voids, Cobiax slabs had smaller absolute deflections than solid slabs with the same thickness.

Cobiax research factors are safe to apply to SANS 10100-01:2000. The economy of Cobiax slabs was tested against that of coffer and post-tensioned slabs. Different span lengths and loads were considered. Based on 2007 material costs in South Africa, Cobiax slabs subject to the same loads and span lengths will be slightly more expensive than that of coffer slabs and post-tensioned slabs when considering only direct slab construction costs. Cobiax will be most appropriate where a flat soffit is required for high multi-storey buildings, requiring large spans with a light load application.

ACKNOWLEDGEMENT

This project report is based on a research project of Cobiax®. Permission to use the material is gratefully acknowledged. The opinions expressed are those of the old fitment and not necessarily represent the policy of Cobiax®.

I wish to express my appreciation to the following organisations and persons who made this project report possible:

a) The Cobiax organization for financial support and the University of Pretoria for the use of the laboratory facilities during the course of the study.

b) The following persons are gratefully acknowledged for their assistance during the course of the study.

I. Dr John Robberts
II. Prof Ben van Rensburg
III. Michael Stücklin
IV. Christian Roggenbuck
V. Chris Heesen
VI. Dévan Venter
VII. Jan Kotze
VIII. Johan Smit
IX. Kobus Nel
X. Ronélle Nel
XI. Oubaas & team
XII. Cobiax staff
XIII. Derrek Mostert
XIV. Herman Booysen
XV. Philip Pansengrow
XVI. Gerhard van den Berg
XVII. Pravesh Naidoo

c) Sandra my love.

TABLE OF CONTENTS

TABLE OF CONTENTS – Continued

APPENDICES

LIST OF TABLES

LIST OF TABLES - Continued

LIST OF FIGURES

LIST OF FIGURES - Continued

LIST OF FIGURES - Continued

LIST OF PHOTOS

1. INTRODUCTION

1.1. BACKGROUND

Various attempts have been made in the past to do reduce the weight of concrete slabs, without reducing the flexural strength of the slab. Reducing the own weight in this way would reduce deflections and make larger span lengths achievable. The economy of such a product will depend on the cost of the material that replaces the concrete with itself and air. Not all the internal concrete can be replaced though, since aggregate interlock of the concrete is important for shear resistance, concrete in the top region of the slab is necessary to form the compression block for flexural resistance, and concrete in the tension zone of the slab needs to bond with reinforcement to make the reinforcement effective for flexural resistance. Also the top and bottom faces of the slab need to be connected to work as a unit and to insure the transfer of stresses.

The idea of removing ineffective concrete in slabs is old, and coffers, troughs and core barrels were and are still used to reduce the self weight of structures with long spans. Disadvantages of these methods are:

- Coffers and troughs need to be placed accurately and this is time-consuming.
- Coffer and trough formwork are expensive.
- Extensive and specialised propping is required for coffers and troughs.
- Stripping of coffer and trough formwork is time-consuming.
- The slab soffits of coffers and troughs are not flat which could be a disadvantage when fixing services and installing the electrical lights.
- The coffer and trough systems are effective in regions of sagging bending but require the slab to be solid in regions of hogging bending.
- Coffer and trough slabs are very thick slabs, increasing the total building height, resulting in more vertical construction material like brickwork, services and finishes. This will increase cost.

Cobiax® was recently introduced to the South African market, after being used for a decade in the European market. This system consists of hollow plastic spheres cast into the concrete to create a grid of void formers inside the slab. The result is a flat slab soffit with the benefit of using flat slab formwork. With the reduction in concrete self weight, large spans can be achieved without the use of prestressed cables, providing the imposed loads are low.

The high density Polyethylene or Polypropylene spheres are fixed into 6mm diameter steel reinforcement cages, developed by German researchers. The rows of cages are placed adjacent to each other to form a grid of evenly spaced void formers. The cages with spheres are light-weight, allowing for quick placement and rapid construction. It completely replaces the need for concrete chairs normally required for construction purposes, and, as will be shown in this report, adds additional shear strength to the slab.

The cross-section of a Cobiax slab has top and bottom flanges which accommodates compressive stresses for either sagging or hogging bending. Although the cross-section is more complex when compared to a solid slab or coffer slab, flexural design poses no significant problem. However, when considering design for shear, the spherical void formers used in the Cobiax system result in concrete web widths that not only change through the depth of the section, but also in a horizontal direction. No design code of practice has specific design recommendations for such a system. Empirical methods were so far the most effective method to establish the shear resistance of Cobiax slabs, and this study may be furthered with the analysis of complex three-dimensional finite element software models in the future.

The Cobiax system has been used in numerous structures in Europe and the UK, confirming the acceptance of the system in Europe. Although design practice in Switzerland is similar to that followed in South Africa, German practice is significantly stricter. Every design requires an independent external review, placing much more stringent requirements on the promoters of new building systems to convince design engineers of the safety of such a system.

Extensive research on Cobiax shear resistance was carried out in Germany with the aim to calibrate codes such as the German DIN code, BS 8110 and Eurocode 2. As shown with experimental and numerical studies, the main conclusion was that a Cobiax slab will have a conservative shear resistance of $v_c' = Kv_c$ where K is a value less than unity and v_c is the shear capacity determined in the conventional manner for a solid slab with equal thickness, as prescribed by the relevant design code. This research recommends a very conservative value of $K = 0.55$ for any Cobiax slab.

When attempting to adopt this research in the South African environment, two problems were encountered:

- Since the original shear tests were conducted, the configuration of the Cobiax system has been subject to some adjustments with the aim of improving the system. A question arose regarding the applicability of the older test results with regards to the existing system.
- The design code of practice used in South Africa is SANS 10100:2000, which is primarily based on BS 8110. However, SANS 10100 recommendations regarding shear are stricter than in the original BS 8110 code. Theoretically, it would therefore be possible to adopt a larger K-value.

Another issue was that Cobiax slabs need to be casted in two pours. The first pour is approximately 70 mm to 80 mm high, followed with a second pour a few hours later after the first pour's concrete has hardened to a certain extent. This procedure is necessary to overcome the buoyancy problem of the spheres, in that the first pour extends above the bottom horizontal bars of the steel cages that hold the spheres in position. A concern exists with regards to the effect of the cold joint that forms, which will be investigated in this thesis.

The last important question regarding the use of Cobiax slabs is that of deflection – although the own weight of the slab is reduced, so is the stiffness.

For fire rating, natural frequency, creep and shrinkage of concrete, and other structural properties, the reader of this report is welcome to consult Cobiax research done in German Universities.

1.2. OBJECTIVES OF STUDY

The primary objective of this study is to establish the economical range of spans in which Cobiax flat slabs can be used for a certain load criteria, as well as addressing the safety of critical design criteria of Cobiax slabs in terms of SANS 10100:2000.

Vertical shear, horizontal shear and deflection will be investigated in order to motivate the safe use of German research factors in combination with SANS 10100:2000.

The economy of Cobiax slabs will also be investigated to establish graphs comparing Cobiax slabs, coffer slabs and post-tensioned slabs for different spans and load intensities. The aim of these graphs are to simplify the consulting engineer's choice when having to decide on the most economical slab system for a specific span length and load application.

1.3. SCOPE OF STUDY

This study partly focuses on establishing the shear capacity of Cobiax slabs without shear reinforcement by comparing experimental results to theoretical predictions for shear capacity. Current design practice in South Africa indicates that the most important parameters for shear resistance to be investigated are the slab depth and the quantity of flexural reinforcement. Increasing both these parameters leads to a higher shear capacity, but the relationship is not linear. Other factors influencing the shear capacity are concrete strength and shear span. However, these parameters are considered of lesser importance and are therefore kept constant to limit the number of specimens.

In addition to German research, this thesis will also investigate the effect of the steel cages holding the spheres. These cages will have both a contributing effect towards vertical shear capacity, as well as that of horizontal shear transfer at the cold joint region at the bottom of the slab. These criteria will be investigated with theoretical calculations, based on South African standards, as well as laboratory test results.

A closer look at deflection of Cobiax slabs will be of interest. A part of this thesis will analyse three by three span Cobiax slabs of different span lengths and load intensities. This will indicate the short-term deflections that can be expected for Cobiax slabs. The adjustment research factors provided by Cobiax for short-term deflections will be checked with simplified stiffness calculations.

A Cobiax slab is cast in two layers – an approximately 80mm thick bottom layer, followed by a second layer to the top of the slab. A few hours is required in-between the two pours to allow setting of the first layer, which hold the Cobiax cages in place and prevent the spheres from drifting during the second pour. To establish whether the top and bottom parts of the slab due to the two concrete pours work as a unit, the necessary calculations in accordance to the South African requirements will be performed. The horizontal shear resistance of the cages will be investigated for this purpose.

Together with the analysis of the Cobiax slabs mentioned above, similar slab patterns will be analysed to establish the economical range for Cobiax slabs. These other slabs will take the form of post-tensioned and coffer (or waffle) slabs. For different span ranges and load intensities, the slabs will be compared in the format of graphs. Finite element slab analysis will be used to obtain these comparative graphs, which will make the designer's decision easier when deciding on an economical design.

This range of slabs that will be investigated focus on commercial buildings only. Massive spans, as well as extreme live loads, will not be analysed for in this report. For these extreme cases a combination of post-tensioning and Cobiax might be an attractive solution.

It is assumed that the building in the particular application has only a few floors, in which case, the variation in foundation and column sizes should not have a significant influence on the relative costs associated with different types of slab systems.

1.4. METHODOLOGY

First this report investigated the shear strength of Cobiax slabs. By using local materials with the Cobiax system, experimental results were compared to theoretical calculations using SANS 10100. Twelve concrete slabs were tested experimentally to determine the shear strength at failure. Three slab depths (280 mm, 295 mm and 310 mm) and three reinforcement quantities were selected. For each reinforcement quantity, a solid sample with 280 mm thickness and no Cobiax or shear reinforcement was tested to serve as benchmark.

The ratio between the Cobiax and solid slab's shear strengths provided an experimental value for K. The shear capacity of the solid 280 mm slabs with varying quantities of reinforcement was predicted using SANS 10100:2000. These results were compared to the experimental results as well as results obtained from other codes of practice. By setting all partial material safety factors equal to one, the predicted capacities indicated the degree of accuracy in predicting the characteristic strength. Using the experimental value for K, capacities were predicted for the other Cobiax slab depths and compared to the experimental results. By including the partial material safety factors, the predicted capacities were compared to the experimental results to determine the margin of safety when using SANS 10100:2000.

The stiffness and elastic deflection of uncracked Cobiax slab sections were investigated with theoretical calculations. Average second moments of area (I-value) were developed for different thicknesses of Cobiax slabs, representing any section perpendicular to the direction of tension reinforcement. These results for different Cobiax slab thicknesses could be compared to the well established results provided by German research.

Finite element (FE) models were generated with Strand7 FE software for different span lengths and load intensities. These FE models consisted of three span by three span layouts, and were generated for Cobiax, coffer and post-tensioned slabs. For a specific layout, all spans were equal in length,

and all columns rigid, and pinned to the soffit of the slab. The FE models consisted of eight noded plate elements, with 10 or more plate elements for every span length.

Obtaining a fair comparison between the three systems, loading of the slabs needed to be approached in a similar manner. Live loads and additional or super-imposed dead loads were applied to all slabs in the normal manner. No lateral, wind or earthquake loads were considered.

The self weight of the different systems was the main concern. Cobiax and coffer slabs were taken as solid slabs with the total thickness, combined with an upward force compensating for the presence of the voids over 75% of the total slab area.

The unbonded post-tensioned slabs were loaded with uniform distributed loads (UDL) as generally would be calculated for post-tensioned cables due to the cables' change in inclination. These UDL`s were derived for parabolic cable curves. The direction of the UDL`s changed close to supports.

With a linear static analysis, a display of elastic deflection, shear, and Wood-Armer moment generated reinforcement areas could be obtained in the form of contour layouts. The maximum vertical shear contours for the two in-plane directions (x and y directions) were obtained using a MathCAD program. The stiffness reduction factors as a reduction in E-value were included for every Cobiax and Coffer slab before the analysis were done, resulting in realistic short-term deflections. A factor of 3.5 was applied to all slab systems' short-term deflections to estimate long-term deflections, assuming 60% of the live load to be permanent. For the purposes of this report, these long-term deflections for the cracked state of concrete were taken to at least satisfy a span/250 criterion.

With the vertical shear plots available, the horizontal shear resistance due to the vertical legs of the Cobiax cages at the horizontal cold joint could be calculated for the thickest Cobiax slab analysed. The thickest slab have the largest Cobiax cages, and therefore the least vertical steel legs crossing the horizontal cold joint of the slab, resulting in the most conservative occurrence.

The amount of concrete in each slab was calculated considering the voids and solid zones where applicable. The reinforcement quantities were calculated from the Strand7 contour plots. A specific slab's reinforcement contour plots were compared to that of a MathCAD program generated by Doctor John Robberts. Punching reinforcement quantities were obtained from Prokon analysis software.

The layouts consisted of the following span lengths, based on the highest minimum span and lowest maximum span generally used in practice for the three types of slab systems considered:

- 7.5 m
- 9.0 m
- 10.0 m
- 11.0 m
- 12.0 m

The above span lengths were then all combined with three sets of load combinations, derived from suggestions made by SABS 0160-1989:

1. Live Load (LL) = 2.0 kPa and Additional Dead Load (ADL) = 0.5 kPa
2. LL = 2.5 kPa and ADL = 2.5 kPa
3. LL = 5.0 kPa and ADL = 5.0 kPa

The cost comparisons took into account all material costs and labour, as well as delivery on site. The only way in which construction time is accounted for is via the cost of formwork. For large slab areas, repetition of formwork usage usually results in 5 day cycle periods for both flat-slab and coffer formwork. The assumption is based on the presence of an experienced contractor on site and no delays on the supply of the formwork.

Although the above cycle lengths may differ from project to project, as well as delivery costs of materials, site labour, construction equipment like cranes, and the location of the site, average cost rates for construction materials were assumed, based on contractors' and quantity surveyors' experience.

The outcome for all the different slab types and loading scenarios where then combined in easy to read graphs, which contractors, engineers and quantity surveyors can use to determine the most economical slab option for a specific application.

The economy of each slab analysis remained subject to all strength requirements of the South African design codes in terms of bending, torsion and shear. From a serviceability point of view they would all at least satisfy a span/250 long-term deflection criterion.

1.5 ORGANISATION OF THE REPORT

This report consists of the following chapters:

- Chapter 1 serves as an introduction to the report.
- Chapter 2 is a literature study on shear and deflection in Cobiax slabs, and general design and cost studies done previously on slab systems.
- Chapter 3 discusses the experimental work done on the shear capacity of Cobiax slabs.
- Chapter 4 discusses further technical issues of Cobiax slabs, and the cost comparison results obtained for long span slab systems.
- Chapter 5 contains the conclusions and recommendations of the study.
- The list of references follows the last chapter.
- The Appendices supporting the cost analysis follow.

2. LITERATURE REVIEW

2.1. INTRODUCTION

In this chapter the general design criteria of concrete slabs and beams are discussed, with the focus on the design of normal reinforced flat slabs, Cobiax flat slabs and post-tensioned flat slabs. The aim is to introduce the Cobiax slab system in terms of strength and serviceability requirements, as applicable to all types of flat slabs.

Shear resistance of reinforced concrete flat slabs with no shear reinforcement, bending behaviour, and different methods of analysis of these slabs have been scrutinised to introduce the Cobiax system. The SANS 10100, BS 8110 and Eurocode 2 design codes have been consulted to introduce the general structural behaviour of concrete beams and slabs, with the main focus on shear behaviour.

The analysis methodology of finite element slabs, with the inclusion of torsional effects in flat slabs via design formulae in accordance with Cope and Clark [1984], will also be discussed briefly.

Post-tensioned flat slab behaviour will be discussed for reference purposes, as required in *Chapter 4* where the economy of Cobiax flat slabs is compared to post-tensioned and coffer slabs.

Lastly, reference is made to existing economical models for Cobiax, coffer and post-tensioned slabs.

2.2. MECHANISM OF SHEAR RESISTANCE IN REINFORCED CONCRETE BEAMS WITHOUT SHEAR REINFORCEMENT

The behaviour of a reinforced concrete structural member failing in shear is complex and difficult to predict using analytical first principles. This is the reason why most design codes of practice follow an empirical approach to calculate shear resistance of concrete members. The following design codes of practice commonly used in South Africa will be discussed:

- BS 8110
- SANS 10100
- Eurocode 2

This report will focus on general concrete design codes used by most design engineers to predict shear in concrete slabs. More complex, yet more accurate methods to predict shear, like the modified compression field theory (MCFT), will therefore not be used in this report. Vecchio and Collins (1986) developed the MCFT. This theory presents a very accurate method to predict the shear behaviour of reinforced concrete elements. Relationships between average stresses and strains are guessed based on experimental observations, treating cracks in a distributed sense. The model for MCFT is non-linear elastic, and is able to predict full load deformation relationships.

Diagonal crack formation, according to Park & Paulay (1975), is as follows:

In reinforced concrete members, combinations of shear and flexure create a biaxial stress state. *Figure 2.2.1* illustrates the principal stresses that are generated in a typical beam.

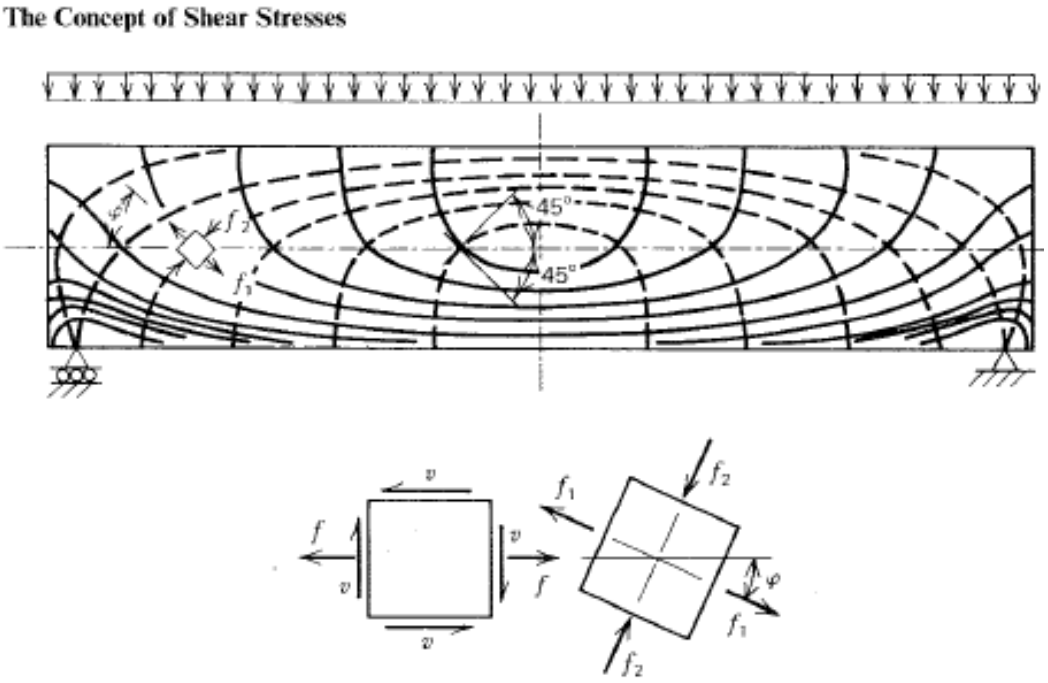

Figure 2.2.1 Trajectories of principal stresses in a homogeneous isotropic beam (Park & Paulay, 1975)

Once the tensile strength of the concrete member is exceeded by the principal tensile stresses, cracks develop. The extreme tensile fibres in the region with the largest bending moment are subjected to the most severe stresses and are therefore the position where the cracks start. These flexural cracks develop perpendicular to the member's axis. In the regions where high shear forces occur, large principal tensile stresses are generated. These principal tensile stresses form at more or less 45° to the axis of the member and are also called diagonal tension. These stresses cause inclined (diagonal tension) cracks.

The inclined cracks usually start from flexural cracks and develop further. Considering webs of flanged beams and situations where a narrowed cross section is dealt with, diagonal tension cracks will more often start in the location of the neutral axis. These are rather special cases though and not common, but may be considered applicable to this thesis, since the internal spheres in Cobiax slabs create a type of biaxial web system.

A reinforced concrete member under heavy loading reacts in two possible ways. One possibility is an immediately collapse after diagonal cracks form. The other is that a completely new shear carrying mechanism develops that is able to sustain additional load in a cracked beam.

When taking into account the tensile stresses of concrete when a principal stress analysis is performed, there are certain expectations in terms of the diagonal cracking load produced by flexure and shear. The actual loads are in fact much smaller than what would be expected. Three factors justify this:

- The redistribution of shear stresses between flexural cracks.
- The presence of shrinkage stresses.
- The local weakening of the cross section by transverse reinforcement causing a regular pattern of discontinuities along a beam.

Equilibrium in the shear span of a beam, according to Park & Paulay (1975), is as follows:

Figure 2.2.2 shows one side of a simply supported beam, with a constant shear force over the length of the beam. The equilibrium is maintained by internal and external forces, bounded on one side by a diagonal crack. In a reinforced concrete beam without web reinforcement, the external transverse force V is resisted mainly by combining three components:

- Shear force across the uncracked compression zone V_c (20 to 40%)
- A dowel force transmitted across the crack by flexural (tension) reinforcement V_d (15 to 20%).
- Vertical components of inclined shear stresses v_a transmitted across the inclined crack by means of interlocking of the aggregate particles. v_a is referred to as aggregate interlocking (35 to 50%).

Given in parenthesis is the approximate contribution of each component (Kong & Evans, 1987). The largest contribution results from aggregate interlock.

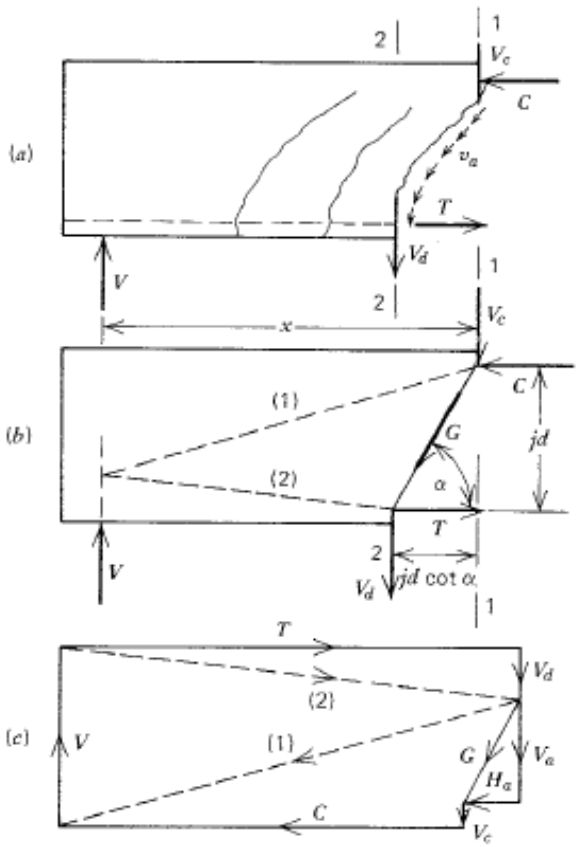

Figure 2.2.2 Equilibrium requirements in the shear span of a beam (Park & Paulay, 1975)

The equilibrium statement can be simplified assuming that the shear stresses transmitted by aggregate interlock can be converged into a single force G. The line of action of this force G will pass through two distinct points of the section as can be seen in *Figure 2.2.2.b*. This simplification allows the force polygon representing the equilibrium of the free body to be drawn as seen in *Figure 2.2.2.c*. The equilibrium condition can also be stated by the formula:

$V = V_c + V_a + V_d$ = the total shear capacity resulting from the three main shear carrying components, where V_c, V_a and V_d is as described above.

Shear failure mechanisms (Park & Paulay, 1975)

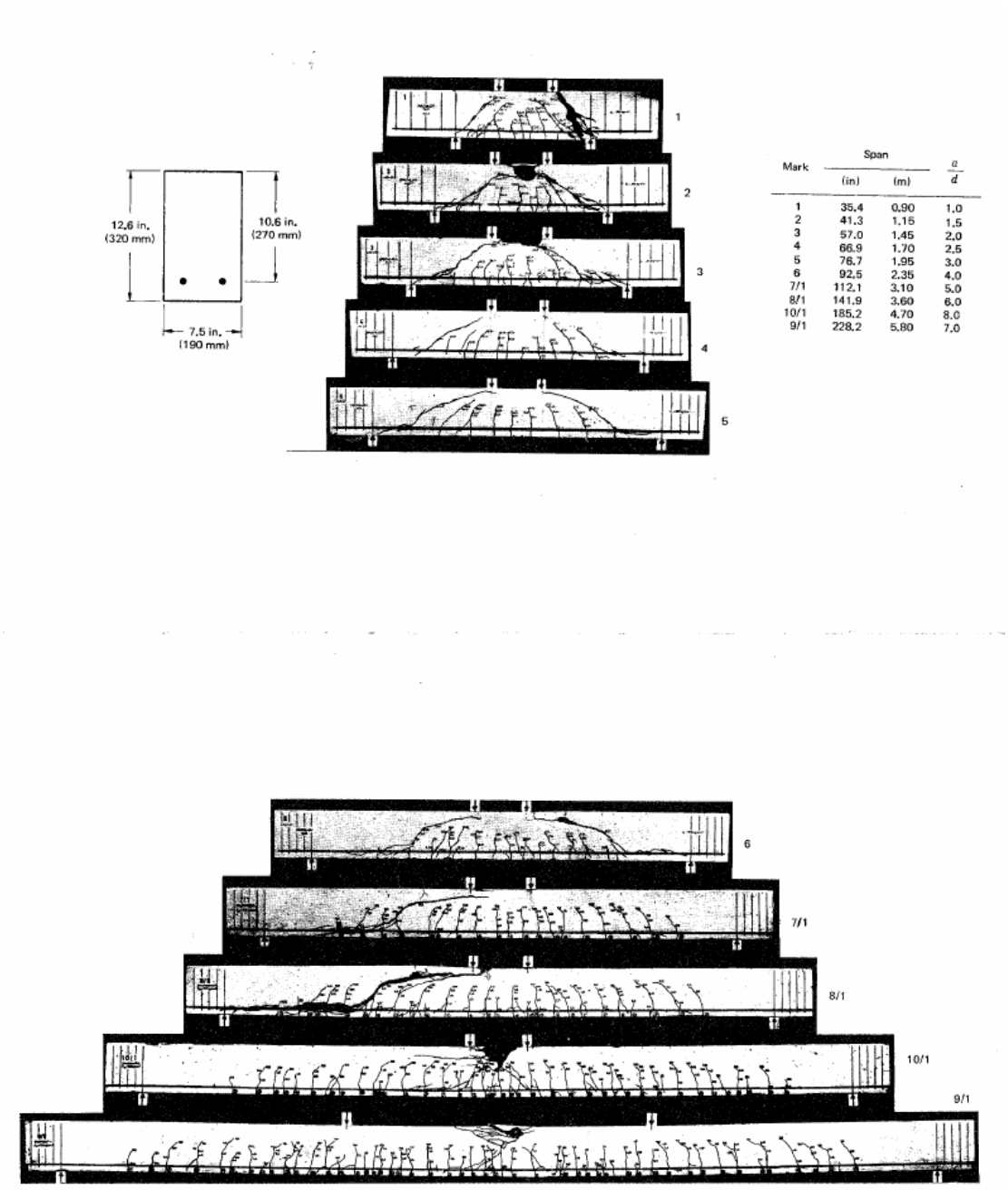

Mark	Span (in)	Span (m)	$\frac{a}{d}$
1	35.4	0.90	1.0
2	41.3	1.15	1.5
3	57.0	1.45	2.0
4	66.9	1.70	2.5
5	76.7	1.95	3.0
6	92.5	2.35	4.0
7/1	112.1	3.10	5.0
8/1	141.9	3.60	6.0
10/1	185.2	4.70	8.0
9/1	228.2	5.80	7.0

Figure 2.2.3 Crack patterns in beams tested by Leonhardt and Walther (Park & Paulay, 1975)

Three different $\frac{a}{d}$ ratio-sectors of mechanisms, according to which shear failure of simply supported beams loaded with point loads occur, can be established, where:

a = distance of a single point load to the face of the support

d = effective depth of the tension reinforcement

This was discovered by the testing of ten beams by Leonhardt and Walther (1965) (*Figure 2.2.3*). The beams had no shear reinforcement (stirrups), with material properties for all the specimens almost exactly the same.

Figure 2.2.4 shows the failure moments and the ultimate shear forces for these ten beams, plotted in terms of shear span versus depth ratio.

The three types can be described as follows:

Type1: For $3 < \frac{a}{d} < 7$ the failure of the beam mechanisms is precisely at, or shortly after the application of the load resulting in diagonal cracking. This means that the arch mechanism is incapable of sustaining the cracking load.

Type2: For $2 < \frac{a}{d} < 3$ a shear compression or flexural tension failure of the compression zone occur above the diagonal cracking load. This is in most cases an arch action failure.

Type3: For $\frac{a}{d} < 2.5$ failure occur by crushing or splitting of the concrete (i.e. arch action failure).

In *Figure 2.2.4* it can clearly be seen that for $1.5 < \frac{a}{d} < 7$ the flexural capacity of the beams is not attained and thus the design is governed by shear capacity.

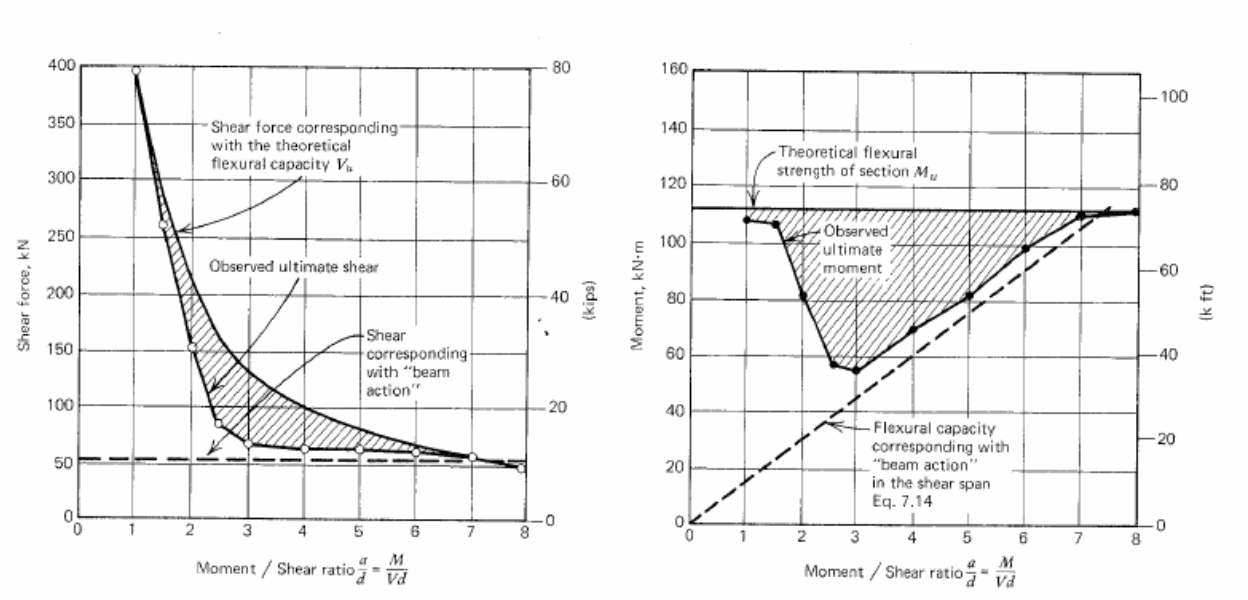

Figure 2.2.4 Moments and shears at failure plotted against shear span to depth ratio (Park & Paulay, 1975).

The shaded area of the right-hand figure displays the difference between the predicted flexural capacity and actual strength, with the largest difference in the $2.5 < \frac{a}{d} < 3$ range. This is the critical range where failure is least likely to be in bending, but without the benefits of the arch action.

From the left-hand-side of *Figure 2.2.4* it is clear that an a/d ratio of approximately 3 will result in both the lowest observed shear resistance (ranging from a/d = 3 to 7), as well as the greatest difference between the observed ultimate shear and the shear force corresponding with the theoretical flexural capacity. A beam with an a/d ratio of 3 will for this reason be the critical case to investigate for shear failure.

The experimental study by Leonhardt & Walther (1965) considered a constant area of tensile reinforcement. Kani (1966) tested a large number of beams with varying reinforcement and the results can be seen in *Figure 2.2.5*. Here the largest difference between the predicted flexural strength and the actual strength occurs at $\frac{a}{d} \approx 2.5$, with the magnitude of the difference increasing as the reinforcement ratio increases. M_u and M_{fl} refer to the predicted moment of resistance and the actual moment of resistance of the tested beams respectively.

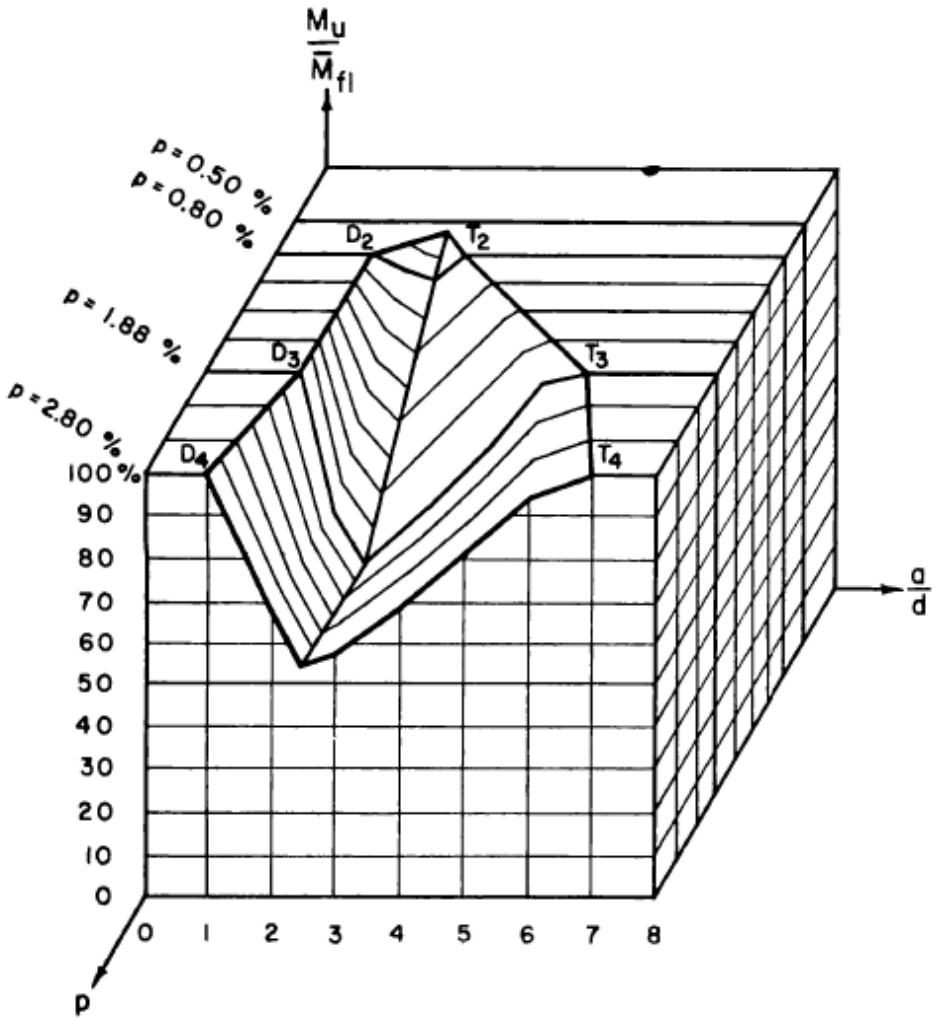

Figure 2.2.5: Shear capacity of beams with varying reinforcement ratios (Kani, 1969)

Apart from the *a*/*d* ratio, the following factors also influence the shear capacity of beams without shear reinforcement (Park & Paulay, 1975):

- *The area of tension reinforcement*. When providing more tension reinforcement, the depth of the neutral axis increases, providing a larger area of uncracked concrete in the compression zone. A greater area of concrete is available to develop dowel action. The reinforcement also tends to keep the shear crack closed, improving aggregate interlock.

- *The concrete strength*. Increasing the compressive strength of the concrete, increases the tensile strength, but not proportional. A greater tensile strength increases the capacity of the section to resist shear crack forming. A stronger concrete will also improve the aggregate interlock and dowel action.

- *The beam depth*. From experimental results showed that the shear capacity reduces as the beam depth increases.

The following sections of the report discuss design recommendations made by design codes of practice. The above parameters influencing the shear capacity has been incorporated.

2.3. SHEAR RESISTANCE ACCORDING TO BRITISH STANDARDS 8110

According to BS8110 Part 1 (1985) the shear resistance of a beam without shear reinforcement is:

$$V_c = v_c b d \qquad \text{(Equation 2.3.1.a)}$$

Where:

$$v_c = \frac{0.79\,\text{MPa}}{\gamma_{mv}} \left(\frac{100 A_s}{b\,d} \right)^{\frac{1}{3}} \left(\frac{f_{cu}}{25\,\text{MPa}} \right)^{\frac{1}{3}} \left(\frac{400}{d} \right)^{\frac{1}{4}} \qquad \text{(Equation 2.3.1.b)}$$

A_s = area of effectively anchored tension reinforcement, mm^2

f_{cu} = characteristic concrete cube strength, MPa

b = minimum width of section over area considered, mm

d = effective depth of the tension reinforcement, mm

γ_{mv} = partial material safety factor = 1.25

Equation 2.3.1.b is restricted to the following values:

- $f_{cu} \leq 40\,\text{MPa}$
- $\frac{100 A_s}{b\,d} \leq 3$
- $\frac{400}{d} \geq 1$

Experimental results and capacities predicted by BS8110 are shown in *Figure 2.3.1*. The important parameters such as reinforcement ratio and concrete strength were accommodated in the predicted capacity. In this figure a_v refers to the distance of a single point load to the face of the closest support, measured in mm. The scatter in experimental results should be noted. It is typical of shear failure that the tensile strength of concrete plays an important role.

The empirical approach used by most design codes of practice is to develop an equation that provides the best fit to the observed experimental strengths. The characteristic strength is then reduced by a partial factor of safety for material, or a capacity reduction factor to establish the design strength (see *Figure 2.3.1*). Where experimental data is lacking, the approach is either to be more conservative or to place limits on the applicability. It can be noted from *Figure 2.3.1* that the approach becomes more conservative with the increasing amount of tension reinforcement.

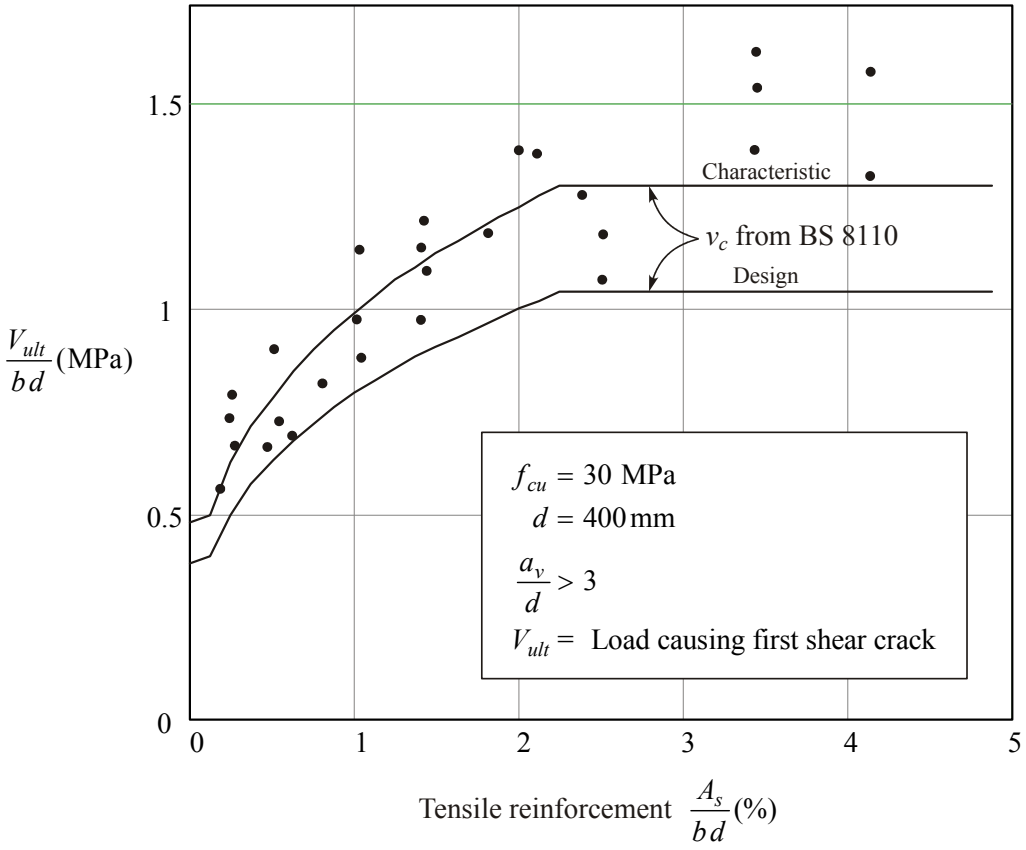

(a) Shear study Group (1969)

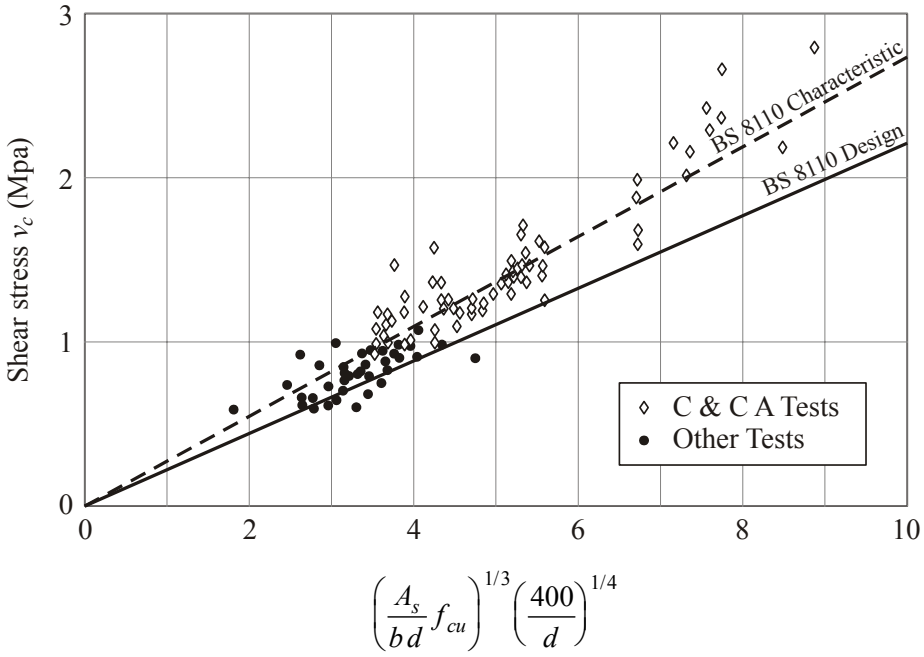

(b) Rowe et al. (1987)

Figure 2.3.1 Experimental results and capacities predicted by BS8110

2.4. SHEAR RESISTANCE ACCORDING TO SANS 10100-1:2000

The SANS 10100 recommendations for shear are based on BS 8110, but more conservative. The shear resistance of a beam without shear reinforcement is given by:

$$V_c = v_c bd$$

where:

$$v_c = \frac{0.75\,\text{MPa}}{\gamma_{mv}} \left(\frac{100 A_s}{b\,d} \right)^{\frac{1}{3}} \left(\frac{f_{cu}}{25\,\text{MPa}} \right)^{\frac{1}{3}} \left(\frac{400}{d} \right)^{\frac{1}{4}} \qquad \text{(Equation 2.4.1)}$$

The above equation is identical to the BS 8110 equation with the exception of the following modifications:

- γ_{mv} is taken to be 1.4 rather than 1.25
- The 0.79 factor is replaced by 0.75
- The limit $\frac{400}{d} \geq 1$ has been removed

All three modifications lead to a more conservative shear capacity.

The change in γ_{mv} accounts for the change in partial safety factors for loads. In previous editions of SANS 10100 the BS 8110 equation and corresponding load factors were used. A change in dead load factor from 1.4 to 1.2 in South Africa caused the code committee to believe it necessary to adjust the value of γ_{mv}. For a typical live load of approximately a third of the dead load, the adjusted γ_{mv} is:

$$\left(\frac{1.4 \times 3 + 1.6 \times 1}{1.2 \times 3 + 1.6 \times 1} \right) \times 1.25 = 1.394 \approx 1.4$$

One can reason that the change in γ_{mv} was necessary to account for the change in load factors. The strictness for bending failure had therefore been reduced in South Africa, but that of shear remained

unchanged. The reason for this was that a ductile failure mode applies for flexure, and a brittle failure mode applies for shear. Also no reason was given by the code committee for changing the 0.79 factor to 0.75. Keeping in mind that the general approach is to provide a characteristic prediction that best fits the experimental data with $\gamma_{mv} = 1$, the difference in shear capacity will be:

$$\frac{0.75}{0.79} = 0.9494$$

SANS 10100 predicts a shear capacity of 95% that of BS 8110 and will therefore be more conservative. The 400/*d* limit was not taken into account here and it can be shown that SANS 10100 becomes even more conservative for sections deeper than 400 mm. There is no published evidence to support this omission of the limit from SANS 10100 though, and an editor error might have occurred.

The flexural capacity of a section is determined in accordance with the SANS 10100 code as follows from the equilibrium of horizontal forces:

$$F_{st} = F_c \qquad \text{(Equation 2.4.2)}$$

where:

$F_c = \frac{0.67}{\gamma_{mc}} f_{cu} sb$ = force due to the concrete compression block (Equation 2.4.2.a)

$F_{st} = f_y A_s$ = force in tension reinforcement (Equation 2.4.2.b)

with:

$s = 0.9x$ = the compression block height (Equation 2.4.2.c)

where:

x = the distance from the top of the beam to the neutral axis (neutral axis depth)

The moment capacity of the beam is then given by:

$$M_r = F_{st} z \qquad \text{(Equation 2.4.3)}$$

where:

$$z = d - \frac{s}{2} = \text{lever arm of the force } F_{st} \qquad \text{(Equation 2.4.3.a)}$$

It was assumed that the tension reinforcement yields at ultimate. This assumption can be checked by calculating strains in the reinforcement and comparing them to the yield strain of the reinforcement. For the section dimensions and reinforcement quantities in this study, the reinforcement yields at ultimate for all concrete element designs.

The shear resistance of vertical links is:

$$V_s = A_{sv} f_{yv} \cot\beta \left(\frac{d}{s_v} \right) \qquad \text{(Equation 2.4.4)}$$

where:

V_s = shear resistance of all links that intersect the crack, N

β = the crack angle in degrees, shown to be 45º according to most research, with $\cot(\beta) = 1$

A_{sv} = cross-sectional area of vertical links, mm^2

f_{yv} = yield strength of vertical links, MPa

s_v = spacing of vertical link legs measured along the span of the beam, mm

The total resistance is then given by:

$$V = V_c + V_s$$

where:

V = total shear resistance, N

V_c = resistance of concrete and dowel action, N

2.5. SHEAR RESISTANCE ACCORDING TO EUROCODE 2

Eurocode 2 (EC 2) provides two methods of shear design - a Standard Method and a Variable Strut Inclination Method. The Variable Strut Inclination Method assumes that all the shear is resisted by the shear reinforcement alone, and no contribution from the concrete (Mosley et al., 1996). This research primarily considers the shear resistance of beams without shear reinforcement, and therefore the Variable Strut Inclination Method will not be used.

To calculate the concrete resistance without shear reinforcing, the Standard Method considers the following empirical equation:

$$V_{Rd1} = \tau_{Rd} * k * (1.2 + 40 * \rho_1) * b_w * d \qquad \text{(Equation 2.5.1)}$$

where:

τ_{Rd} = basic design shear strength = $0.035 f_{ck}^{1/3}$ (MPa), with f_{ck} limited to 40 MPa

f_{ck} = characteristic cylinder strength of concrete, (MPa)[3]

d = effective depth of section, mm

k = $1.6 - d$ {>1} or 1 where more than 50% of tension reinforcement is curtailed, unitless

A_{s1} = area of longitudinal tension reinforcement extending more than a full anchorage length plus one effective depth beyond the section considered, mm^2

b_w = minimum width of section over area considered, mm

ρ_1 = $\dfrac{A_{s1}}{b_w d}$

EC 2 has a design capacity in the form of a partial material safety factor for shear of γ_m = 1.5 that is applied to f_{ck}. To obtain a characteristic capacity ($\gamma_m = 1$), the equation showed to be true if written in the form:

$$\tau_{Rd} = 0.035\left(\frac{1}{1.5}\right)^{-\frac{2}{3}}\left(\frac{f_{ck}}{\gamma_m}\right)^{\frac{2}{3}} \qquad \text{(Equation 2.5.2)}$$

Shear capacity provided by shear reinforcement

Design codes like the British, South African, and European concrete codes follow a similar approach when considering the additional capacity provided by shear reinforcement. A simplified truss can be considered where equilibrium determines the resistance provided by the shear reinforcement V_s. The total resistance is the combined effect of V_s and V_c.

$$V = V_c + V_s$$

where:

V = total shear resistance
V_c = resistance of concrete and tension reinforcement

To find the shear resistance that the links provide, the following equation for vertical links was used:

$$V_s = A_{sv} f_{yv} \cot\beta\left(\frac{d}{s_v}\right) \qquad \text{(Equation 2.5.3)}$$

where

V_s = shear resistance of all links that intersect the crack
f_{yv} = yield strength of steel
A_{sv} = area of each stirrup leg that crosses the shear crack
s_v = centre to centre spacing of the links
d = depth of tension reinforcement

β = the crack angle being 45º according to research, with $\cot(\beta) = 1$

Experimental results showed that V_c and V_s can be added together (SANS 10100-1, 2000). The shear reinforcement has the beneficial affect that:

- The shear crack is smaller due to the shear reinforcement passing through the crack. This improves the aggregate interlock.
- Shear reinforcement that encloses the tension reinforcement will improve the dowel action, preventing the tension bars from breaking off the concrete cover under high loads.

2.6. COBIAX FLAT SLAB SHEAR RESISTANCE

The Cobiax system works on the principle of forming internal voids in biaxial slab systems (CBD-MS&CRO, 2006). The spherical, hollow balls are prefabricated from plastic (polypropylene or polyethylene) and fixed into 5 to 6 mm thick high yield steel bar cages. The number of balls that is fixed depends on the area that must be covered in the slab. It can range anything from a 1 x 4 (one row of four balls) to an 8 x 8 (eight rows of eight balls) or more, depending on ball sizes and handling capabilities of the user, e.g. crane capacity on site. The whole grid is thereafter placed onto the tension reinforcement and the cages fixed to it with wire. Concrete is poured in two stages, first 80 mm thick extending above the horizontal bars of the cages, and after a few hours, to the top of the required slab height. When the first pour hardens, it will keep the spheres in place, avoiding uplift due to buoyancy during the second pour (See *Figure 2.6.1* for an illustration of the above description). The result is a flat soffit, allowing the use of conventional flat slab formwork as for a regular solid slab (See *Photo 2.6.1*).

Photo 2.6.1 Flat soffit of a 16m span Cobiax flat-slab, Freistadt, Germany

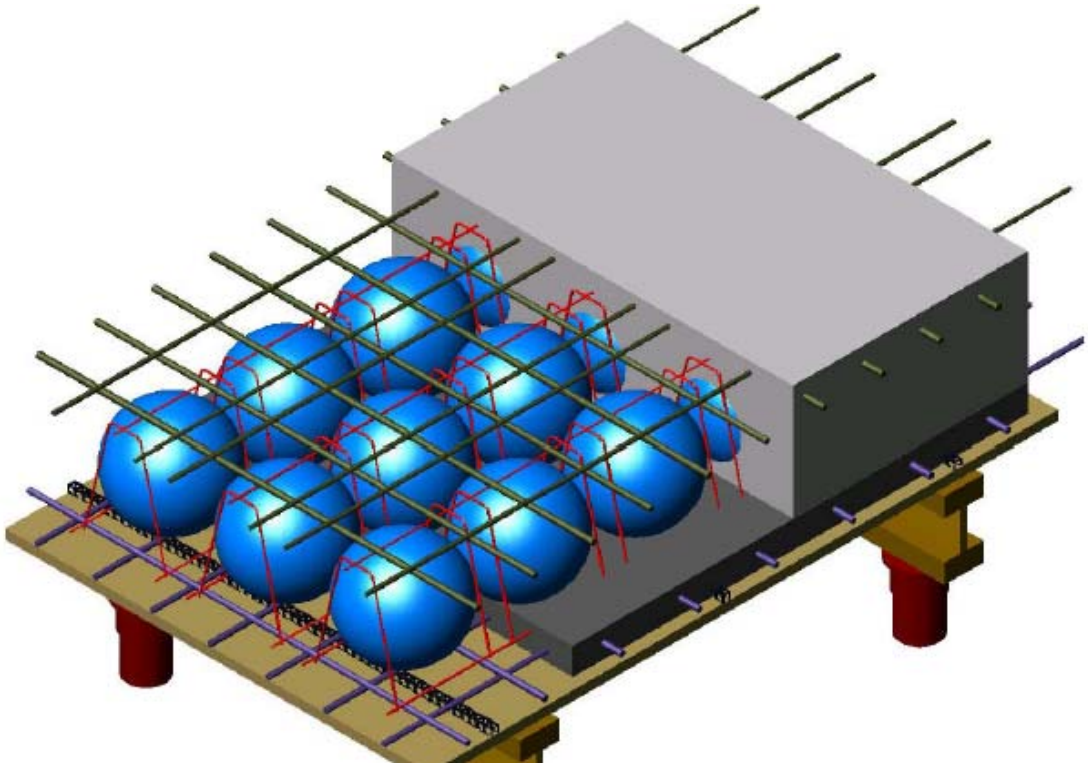

Figure 2.6.1 Typical illustration of a Cobiax slab and its components

Extensive researched have been done at the Technical University Darmstadt (TUD) in Germany on the shear capacity of Cobiax® slabs (Schellenbach-Held & Pfeffer, 1999). The method used to fix the spheres has been improved after 1999. These tests were carried out at the TUD, comparing the results to the Eurocode and DIN design code of practice. The methodology was as follows:

- Theoretical research was carried out on a system named "BubbleDeck", where the spheres were fixed by restraining it between the top end bottom reinforcing bars, and not by cages as used today in practice and in the research of this project report.
- The assumption was made that no shear reinforcement (stirrups) was present.
- The lost area of aggregate interlock was calculated by considering a diagonal plane along a shear crack, subtracting the voided area on the plane.
- No dowel action and compression block resistance were taken into account, implying that only *one* shear component was used, namely *aggregate interlock*.
- The estimated angle of the shear crack was taken as 30º or 45°.

The TUD followed up on these theoretical calculations with laboratory tests. Their test set-up contained four spheres in a cross-section so that the 3-dimensional truss could be created and to allow the bi-axial load bearing mechanism to form. The steel content of the TUD samples was approximately 1.3%. The $\frac{a}{d}$ ratio was taken as 3.7 that were considered to be the most unfavorable condition for shear resistance according to their interpretation of Kani's (1966) research.

The procedure followed to obtain the Cobiax shear factor was as follows (See *Figure 2.6.2*):

- A mean width was derived to estimate the least favorable cross section where:

$$A_{solid} = b^2 = \text{area of solid cross section}$$

$$A_{Bubble} = b^2 - \left(\frac{0.9}{2}\right) b^2 \pi = \text{area of BubbleDeck cross section}$$

$$b_m = \frac{0.36b^2}{b} = 0.36b = \text{mean width}$$

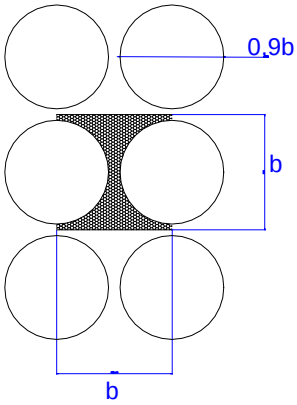

Figure 2.6.2 Mean width for cross section of BubbleDeck

Using the mean width in the DIN design code recommendations, a shear capacity of 36% is obtained for the BubbleDeck system when compared to a solid slab with the same thickness. Probe trials showed that even with the mean width taken into account the calculated shear capacity for the BubbleDeck is noticeably lower than the actual shear capacity. These findings resulted in more tests. The experimental tests that were then performed showed that the shear resistance of the BubbleDeck, when compared to a solid slab, ranged from 55 to 85%. The smallest value was adopted as the Cobiax shear factor, namely 0.55.

Further theoretical calculations were carried out assuming an angle for a shear crack of 30° and 45°. A plane along this angle was assumed to extend diagonally throughout the depth of the beam. The location of the plane was varied and the area of concrete surrounding the spheres was calculated as a ratio of the plane area without spheres. The smallest ratio obtained was 0.55 that corresponded well to the value derived from the test results. It was then argued that if aggregate interlock is the primary shear capacity mechanism, the shear capacity of a Cobiax® slab will be 0.55 of the capacity of a solid slab, based on the area of concrete that contribute to aggregate interlock.

However, it was shown in *Section 2.2* that the aggregate interlock only provides 30 – 50% of the shear capacity. Although TUD's theoretical calculations on the aggregate interlock supported their shear test results, it seems unlikely that the dowel action and compression zone in a Cobiax slab will not contribute to the shear capacity in the slab. Their theoretical approach to calculate the contribution of aggregate interlock in a Cobiax slab might therefore have overestimated the aggregate interlock's contribution to shear, and maybe not worth comparing to their test results. The general conclusion on their theoretical approach should have been that dowel action and the compression zone will indeed contribute to shear as previously discussed in this chapter, and that they should find a different approach to predict the aggregate interlock theoretically. The 0.55 shear reduction factor can therefore only be justified by their laboratory test results.

2.7. COBIAX FLAT SLAB DEFLECTION

The following discussion follows the research summary in the *Cobiax Technology Handbook of 2006*:

The presence of void former spheres in the Cobiax flat slab impacts and reduces its stiffness compared to a solid flat slab. In the *Cobiax Technology Handbook of 2006*, a table in the *Stiffness and Deflection* section indicates the stiffness factors of Cobiax flat slabs compared to solid flat slabs of the same thickness. The values are based on calculations done in deflection state I (uncracked), assuming a vertically centered position of the spheres, as well as a fixed position of the spheres at a distance of 50 mm from the bottom of the slab.

The presence of the spheres in deflection state II (cracked) has been researched with laboratory bending tests at the TUD. The results have revealed that the reduction factor in state I is the determining factor. The stiffness factors were derived from calculations done on the second moment of area I_{CB} (for the Cobiax flat slabs) and I_{SS} (for the solid flat slabs).

With these factors in hand and taking into account the reduced own weight of the Cobiax flat slab, the deflection calculation for Cobiax flat slabs can be carried out. The following are to be observed:

- Despite its reduced stiffness, the Cobiax flat slab’s absolute deflection is smaller than the one of a solid slab of same thickness for identical loads, except where the imposed load exceeds 1.5 times the amount of dead load.

- In common buildings the ratio of imposed load to dead load is generally significantly less than 1.5. In practice this means that the total defection of Cobiax flat slabs is usually smaller compared to solid slabs. Hence in most cases a smaller depth can be prescribed.

Long-term deflections for the cracked state can be calculated in accordance with SANS 10100:2000 or estimated by multiplying the short-term deflection for the un-cracked state with an applicable factor. Many engineers in South Africa recommend a factor between 2.5 and 4, as later discussed in *Chapter 4.2*. Otherwise creep and shrinkage deflections can be calculated in accordance with Appendix A of SANS 10100. Here the concrete type and properties, area of uncracked concrete, area of reinforcement, loads and age of concrete at loading will play a major roll.

The factor between 2.5 and 4 however, as well as how great a percentage of the live load to be taken as permanent (see SABS 0160:1989), remains the engineer's decision. It is suggested that the designer approaches the long-term deflection calculation exactly the same as he would have for a solid flat slab with the same thickness, but taking into account the reduced own weight due to the Cobiax voids, and reduced stiffness calculated as discussed later in *Chapter 4.4*.

2.8. FLAT PLATES

Flat slabs without column heads and drop head panels are normally referred to as flat plates. The strength of a flat plate type of slab is often limited by punching shear conditions close to the columns. As a result, they are used with light loads, for example in residential and office buildings, and with relatively short spans. The column head and drop panel provide the shear strength necessary for larger loads and spans as in the case of heavily loaded industrial structures, shopping malls and airport terminals. Park & Gamble [2000] suggest that column heads and drop panels are required for service live loads greater than 4.8 kN/m^2 and spans greater than 7 to 8 m. Shear reinforcement in the column regions can be used though to improve the shear strength of flat plates.

2.9. ELASTIC THEORY ANALYSIS OF SLABS

Elastic theory analysis applies to isotropic slabs that are sufficiently thick for in-plane forces to be unimportant and also thin enough for shear deformations to be insignificant. The thicknesses of most slabs usually lie in this range. Three basic principles of the Kirchhoff theory (Reddy, 1999) are as follows:

1. The equilibrium conditions must be satisfied at every point in the slab.
2. Stress is proportional to strain, resulting in bending moments proportional to curvature.
3. All boundary conditions must be complied with.

The procedure for the Kirchhoff plate theory can in turn be followed to derive the finite element equations for Reissner-Mindlin plates, introducing three boundary conditions at a given point, for moderately thick plates. This can be compared to the two boundary conditions introduced in thin plate theory. Here transverse shear stresses across the thickness of a plate element become important, although the stresses normal to the plate element are still assumed to be zero. The formulation of bending for Reissner-Mindlin elements remains the same as that of plane elastic elements (Fung, 2001).

Finite element software is commonly used for flat slab design in first world countries these days. The software programs have to be understood correctly though, both in terms of how the axis and orientation of applied loads and moments work, as well as how and how not to approach the finite element mesh construction. Very accurate results can be obtained for Wood-Armer moments, shear, and even area of reinforcement required for the different directions, using thin shell elements. This can be read from design output contour plots. Interpretation of these contours needs to be understood correctly though. Due to the accuracy of this method, and the fact that one can apply it to all types of slab systems, this analysis method will be used for the purposes of this report.

The assumption that plane sections will remain plane in a concrete slab with internal spherical void formers is a valid assumption, and shear deformations will be very small. The dome effect of the spheres inside the slab results in flanges that are thin for only a small area above and below each sphere, gaining thickness and stiffness rapidly further away from the sphere's vertical centerline. This geometry will tend to make a slab with spherical voids behave more like a solid slab than a flanged beam (Schellenbach-Held & Pfeffer, 1999).

2.10. LIMIT STATES AND OTHER METHODS OF ANALYSIS FOR SLABS

Limit States:

The basis of limit states analysis is that, because of plasticity, moments and shear are able to redistribute away from that predicted by the elastic analysis, before the ultimate load is reached. This occurs because there is only a small change in moment with additional curvature once the tension steel has yielded.

As soon as the highly stressed areas of a slab reach the yield moment, they tend to maintain a moment capacity that is close to the flexural strength with further increase in curvature. Yielding of slab reinforcement will then spread to other sections of the slab with further load increase (Marshall & Robberts, 2000).

Flat slabs can be analysed with four other methods, namely yield line, grillage analogy, equivalent frame, or finite elements as discussed above.

Yield Line:

Yield line is an upper bound method of analysis that determines the ultimate load by means of a collapse mechanism. A collapse mechanism consists of slab portions that are separated by lines of plastic hinges. The ultimate resisting moments between the plastic hinges are exceeded when an incorrect collapse mechanism is chosen. The upper bound method results in an ultimate load that is either too high or correct. It is therefore crucial to choose the correct collapse mechanism to avoid overestimation of the ultimate load. Yield line methods are not appropriate for prestressed flat slab design (Marshall & Robberts, 2000).

Equivalent Frame:

The Equivalent Frame analysis method closely models the true behaviour of a slab by a system of columns and beams analysed separately in both span directions. The method takes both vertical and horizontal loads on flat slabs into account (Marshall & Robberts, 2000).

Grillage Analysis

A grillage analysis is very suitable for the case of an irregular slab where an equivalent frame analysis is not suitable (Marshall & Robberts, 2000).

2.11. DESIGN SPECIFICS FOR FLAT SLABS

Division of panels

Flat slabs are divided into column strips and middle strips as displayed in *Figure 2.11.1*. The width of the column strip should be taken as half of the width of the panel. If drop-heads are present, the width is taken as the width of the drop-head. The width of the middle strip is taken as the difference between the width of the panel and that of the column strips, measured from a line running over the column centres into a direction towards the middle of the slab.

In accordance to SANS 10100, a drop-head, or thickening of the slab, should only be considered to affect the distribution of moments within the slab when the smaller dimension of the drop-head is at least one third of the smaller dimension of the surrounding panels.

Should adjacent panels have different widths, the width of the column strip between the two panels should be based on the wider panel.

Lateral distribution of reinforcement

SANS 10100 states that two thirds of the amount of reinforcement over the column, required to resist the negative moment in the column strip, should be placed in the central half width of column strip above the column.

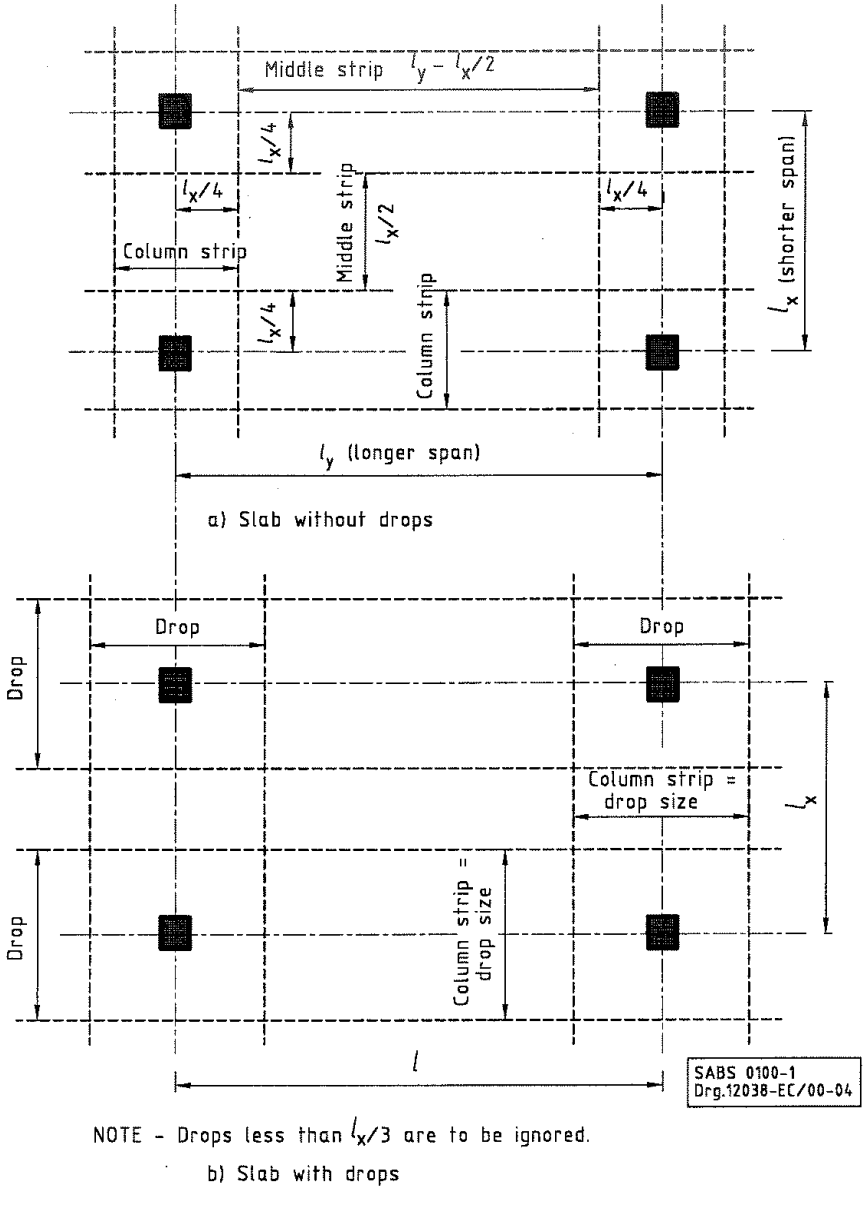

Figure 2.11.1: Division of flat slab panels into column and middle strips –- SANS 10100

Design formulae for moments of resistance of slabs to SANS 10100

$$K = \frac{M}{bd^2 f_{cu}} \qquad \text{(Equation 2.11.1)}$$

$$z = d\left\{0.5 + \sqrt{0.25 - \frac{K}{0.9}}\right\} \leq 0.95 \qquad \text{(Equation 2.11.2)}$$

$$A_s = \frac{M}{0.87 f_y z} \qquad \text{(Equation 2.11.3)}$$

Shear in flat slabs

In accordance with SANS 10100, the minimum required slab thickness for shear reinforcement to work effectively is 150 mm. The effectiveness of shear reinforcement will also reduce with a reduction in slab thickness from 200 mm. For slabs less that 200 mm thick, the allowable stress in the reinforcement should be reduced linearly from the full value at 200 mm to zero at 150 mm. SANS 10100 considers the magnification of shear at internal columns by moment transfer.

Two types of structural arrangements are recognised in the calculation of the effective shear force at an internal column. For the case where a structural bracing system exists, the ratio between adjacent spans does not exceed 1.25, and the maximum load is applied on all spans adjacent to the column, the effective shear force is defined by SANS 10100 as:

$V_{eff} = 1.15\ V_t$

where:

V_{eff}	is the design effective shear that includes moment transfer
V_t	is the design shear generated by the slab area surrounding the column

For a braced frame where the ratio between adjacent spans exceeds 1.25, or for unbraced frames, the effective shear force is the greater of the following:

$V_{eff} = 1.15\ V_t$ or

$$V_{eff} = (1 + \frac{1.5M_t}{V_t x})V_t$$

where:

V_t	is the design shear for a specific load arrangement transferred to the column
M_t	is the sum of design moments in a column
x	is the length of perimeter's side considered parallel to the axis of bending (see

Figure 2.11.2)

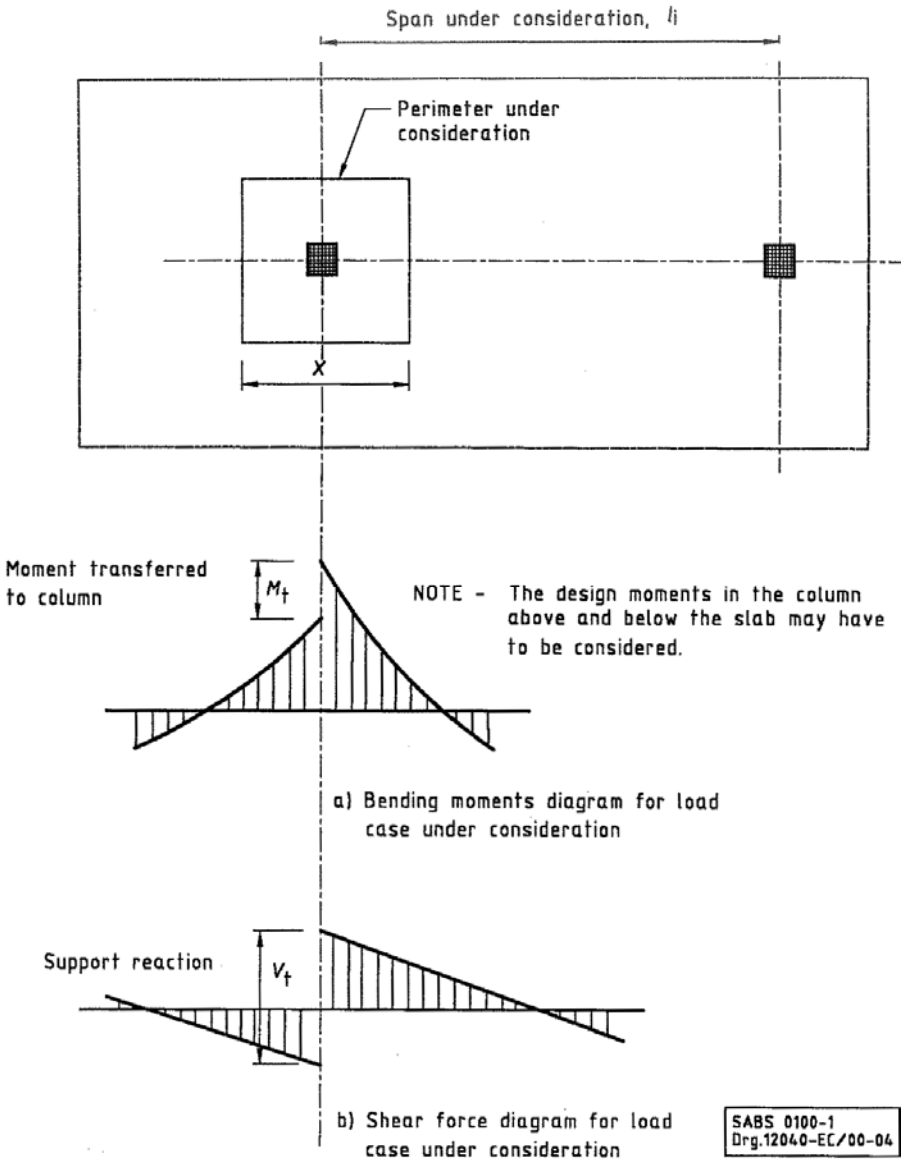

Figure 2.11.2: Shear at slab internal column connection – SANS 10100

SANS 10100 specifies the following equation for corner columns:

$V_{eff} = 1.25V_t$

For edge columns that are bent in a direction parallel to the edge and where the same assumptions mentioned above for internal columns are true:

$V_{eff} = 1.40V_t$

When any of the assumptions are not true:

$$V_{eff} = (1.25 + \frac{1.5M_t}{V_t x})$$

Punching shear design in accordance with SANS 10100 is approached considering the following:

Perimeter: a boundary of the smallest rectangle (or square) that can be drawn around a loaded area and that nowhere comes closer to the edges of the loaded area than some specified distance l_p (a multiple of 0.75*d*).

Failure zone: an area of slab bounded by perimeters 1.5*d* apart.

Effective length of a perimeter: the length of the reduced perimeter, where appropriate for the openings or external edges.

Effective depth d: the average effective depth for all effective tension reinforcement passing through a perimeter.

Effective steel area: the total area of all tension reinforcement that passes through a zone and that extends at least one effective depth or 12 times the bar size beyond the shear zone on either side.

SANS 10100 specifies a *maximum allowable design shear stress*, v_{max}, at the column face as the larger of the following:

$0.8\sqrt{f_{cu}}$ or 5.0 MPa

$$v_{max} = \frac{V}{u_0 d}$$

where:

V	is the design maximum value of punching shear force on the column
u_0	is the effective length of the perimeter that touches a loaded area
d	is the average effective depth of slab

A punching zone is an area of slab bounded by two perimeters 1.5*d* apart as shown in *Figure 2.11.3*, where d is the effective depth of the slab.

Punching failure around columns occurs when shear forces transferred to the columns exceeding the shear capacity at a specific failure perimeter.

The first check is at a distance 1.5*d* from the face of the column. If shear reinforcement is required, then at least two perimeters of shear reinforcement must be provided within the zone indicated in *Figure 2.11.3*. The first perimeter of reinforcement should be placed at approximately 0.5*d* from the face of the column.

The maximum permitted spacing of perimeters of reinforcement should not exceed 0.75*d*. The shear stress should then be checked on successive perimeters at 0.75*d* intervals until a perimeter is reached which does not require shear reinforcement, i.e. if the calculated shear stress does not exceed v_c, the permissible shear strength of the concrete, then no further checks are required after this zone.

For any particular perimeter, all reinforcement provided for the shear on previous perimeters should be taken into account.

The nominal design shear stress *v*, with $v = \frac{V}{ud}$

where:

V	is the design maximum value of punching shear force on column
u	is the effective length of the perimeter of the zone
d	is the effective depth of slab

SANS 10100 states that shear reinforcement is not required when the stress v is less than v_c, where v_c is:

$$v_c = \frac{0.75}{\gamma_m}\left(\frac{f_{cu}}{25}\right)^{1/3}\left(\frac{100A_s}{b_v d}\right)^{1/3}\left(\frac{400}{d}\right)^{1/4} \qquad \text{(Equation 2.11.4)}$$

where:

γ_m is the partial safety factor for materials (taken as 1.4)

f_{cu} is the characteristic strength of concrete (but not exceeding 40 MPa for the simple reason that no samples were tested with a higher strength to calibrate the formula)

$\left(\frac{100A_s}{b_v d}\right)^{1/3}$ shall not exceed 3,

where:

A_s is the area of anchored tension reinforcement (in the case of prestressed concrete the stressed and normal reinforcement should be considered)

b_v is the width of the section

d is the effective depth

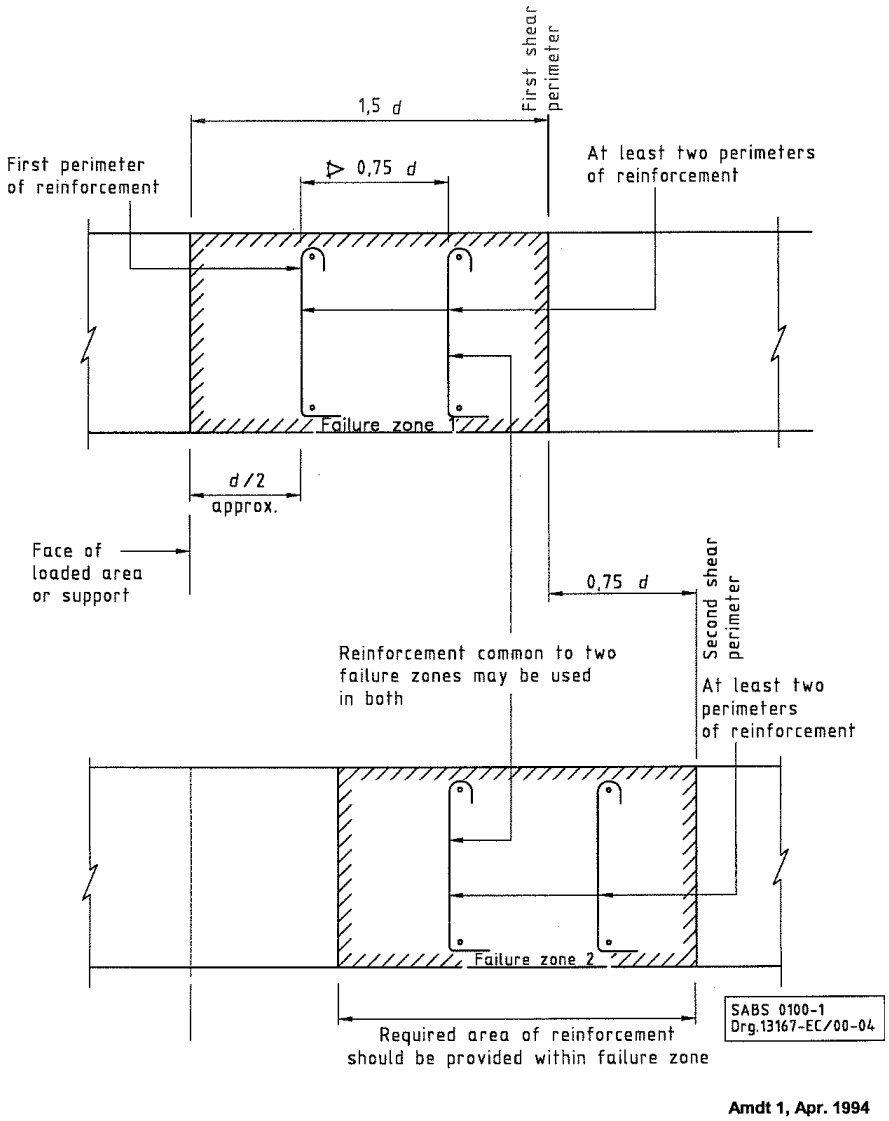

NOTE – *d* is the average effective depth for all effective reinforcement passing through a perimeter.

Figure 2.11.3: Punching shear zones – SANS 10100

SANS 10100 specifies two design formulae for the required area of shear reinforcement:

For $v_c < v < 1.6v_c$:

$$A_{sv} = \frac{(v - v_c)ud}{0.87 f_{yv}} \qquad \text{(Equation 2.11.5)}$$

For $1.6v_c < v < 2v_c$:

$$A_{sv} = \frac{5(0.7v - v_c)ud}{0.87 f_{yv}} \qquad \text{(Equation 2.11.6)}$$

where:

A_{sv} is the area of shear reinforcement

u is the effective length of the outer perimeter of the zone

v_c is the permissible shear strength of the concrete

v is the effective shear stress, $v = \frac{V_{eff}}{Ud}$

f_{yv} is the characteristic strength of the shear reinforcement

d is the effective depth of slab

v-$v_c \geq 0.4$ MPa

$v > 2v_c$ falls outside the scope of the design equations and the tension reinforcement used in the calculation of v_c must extend more than a distance d or 12 bar diameters beyond the shear perimeter.

Deflection in flat slabs in accordance with SANS 10100

Deflection is a serviceability limit state of great importance. In general, the long-term deflection (that includes effects of temperature, creep and shrinkage) of a floor or roof slab may not exceed span/250. This deflection can be measured from a datum point (zero deflection) at the slab soffit where columns are situated. The span length will then be measured along a diagonal line of a slab panel from column to column, as explained in *Chapter 4* of this report.

To prevent damage to flexible partitions, additional long-term deflections in the years to come after all partitions and finishes have been installed, should be limited to the lesser of span/350 or 20 mm. For brittle partitions, this limitation is span/500 or 10 mm.

SANS 10100 provides a method to ensure that deflections stay within the acceptable criteria of span/250. This method limits the span/effective depth ratio of the slab to specific values, depending on the structural arrangement. *Table 2.11.1* provides the basic span/250 ratios for rectangular beams for various support conditions. This table in SANS 10100 will be completely different for voided slabs, but may be used for solid flat-slabs. Where spans are larger than 10m, the span/depth ratio should be multiplied by a further 10/span factor to prevent damages to finishes and partitions. L/d ratios for flat slabs should also be multiplied by 0.9, and the normal length for span L must be taken as the longer span as opposed to the shorter span for slabs supported on all four sides.

Table 2.11.1 – Basic span/effective depth ratios for rectangular beams – SANS 10100 (Span/250)

Support conditions	**Ratio**
Truly simply supported beams	16
Simply supported beams with nominally restrained ends	20
Beams with one end continuous	24
Beams with both ends continuous	28
Cantilevers	7

Modification of span/effective depth ratios for tension reinforcement:

Deflection is influenced by the quantity of tension reinforcement and the stress in the reinforcement. The span/depth ratios must be modified according to the ultimate design moment and the service stress at the centre of the span, or at the support for a cantilever. The basic ratios from *Table 2.11.1* should be multiplied by the following factor.

$$Modification\ \ factor = 0.55 + \frac{(477 - f_s)}{120(0.9 + \frac{M}{bd^2})} \leq 2.0 \qquad \text{(Equation 2.11.7)}$$

where:

M	is the design ultimate moment at the centre of the span or, for cantilevers at the support
b	is the width of the section
d	is the effective depth of section
f_s	is the design estimate service stress in tension reinforcement

$$f_s = 0.87 f_y \times \frac{\gamma_1 + \gamma_2}{\gamma_3 + \gamma_4} \times \frac{A_{s,req}}{A_{s,prov}} \times \frac{1}{\beta_b} \qquad \text{(Equation 2.11.8)}$$

where:

f_y	is the characteristic strength of reinforcement
γ_1	is the self-weight load factor for serviceability limit states = 1.1
γ_2	is the imposed load factor for serviceability limit states = 1.0
γ_3	is the self-weight load factor for ultimate limit states = 1.2

γ_4 is the imposed load factor for ultimate limit states = 1.6

$A_{s,req}$ is the area of tension reinforcement required at mid-span to resist moment due to ultimate loads (at the support in the case of a cantilever)

A_{sprov} is the area of tension reinforcement provided at mid-span (at the support in the case of a cantilever)

β_b is the ratio of resistance moment at mid-span obtained from redistributed maximum moments diagram to that obtained from maximum moments diagram before redistribution. β_b may be taken as 1.0 if the percentage of redistribution is unknown.

Modification of span/effective depth ratios for compression reinforcement:

The presence of compression reinforcement (A'_s) will reduce deflection. Compression reinforcement is unlikely to be present in flat plates, but may be found in waffle slabs. The basic span/effective depth ratio may then be multiplied by a factor (see *Table 211.2*), depending on the compression reinforcement quantity.

Table 2.11.2: Modification factors for compression reinforcement – SANS 10100

1	2
$\frac{100A'_s}{bd}$	Factor*)
0.15	1.05
0.25	1.08
0.35	1.10
0.50	1.14
0.75	1.20
1.00	1.25
1.25	1.29
1.50	1.33
1.75	1.37
2.00	1.40
2.50	1.45
≥3.00	1.50
*) Obtain intermediate values by interpolation	

2.12. ANALYSIS AND DESIGN OF FLAT SLAB STRUCTURES

2.12.1 Analysis of structure: equivalent frame method

The equivalent frame method relates to a structure that is divided longitudinally and transversely into frames consisting of columns and slab strips.

For vertical loads, the width of slab defining the effective stiffness of the slab, is taken as the distance between the centres of the panels. For horizontal loads, the width is only half this value. The equivalent moment of area (I) of the slab can be taken as uncracked. Drops are taken into account if they exceed a third of the slab width. Column stiffness, including the effects of capitals, must be taken into account, except where columns are pinned to the slab soffit.

A flat slab supported on columns can sometimes fail in one direction, same as a one-way spanning slab. The slab should therefore be designed to resist the moment for the full load in each orthogonal direction. The load on each span is calculated for a strip of slab of width equal to the distance between centre lines of the panels.

SANS 10100:2000 specifies the following load arrangements:

1. all spans loaded with ultimate load ($1.2G_n + 1.6Q_n$)
2. all spans loaded with ultimate own-weight load ($1.2G_n$) and even spans loaded with ultimate impose load ($1.6Q_n$)
3. all spans loaded with ultimate own-weight load ($1.2G_n$) and odd spans loaded with ultimate impose load ($1.6Q_n$)

where:

G_n dead load
Q_n live load

SANS 10100 allows for the design negative moment to be taken at a distance $h_c/2$ from the centre-line of the column, provided that the sum of the maximum positive design moment and the average of the negative design moments in any one span of the slab for the whole panel width is at least:

$$\frac{nl_2}{8}\left(l_1 - \frac{2h_c}{3}\right)^2 \qquad \text{(Equation 2.12.1)}$$

where:

h_c diameter of column or of column head (which shall be taken as the diameter of a circle of the same area as the cross-section of the head)

l_1 panel length, measured from centres of columns, in the direction of the span under consideration

l_2 panel width, measured from centres of columns at right angles to the direction of the span under consideration

n total ultimate load per unit area of panel ($1.2g_n + 1.6q_n$)

2.12.2 Analysis of structure: simplified method

SANS 10100 also provides the designer with an option to use a simplified method of analysis if certain conditions are met. These conditions specified by SANS 10100 are:

1. All spans must be loaded with the same maximum design ultimate load.
2. Three or more rows of panels exist, with approximately equal span in the direction under consideration.
3. The column stiffness *EI/l* is not less than the *EI/l* value of the slab.
4. Hogging moments must be reduced by 20 percent and the sagging moments increased to maintain equilibrium.

The simplified method of determining moments may be used for flat slab structures where lateral stability does not depend on slab-column connections. If all of the above conditions are met, *Table 2.12.1* can be used to determine the slab moments and shear forces.

Table 2.12.1: Bending moments and shear force coefficients for flat slabs of three or more equal spans – SANS 10100

1	2	3	4
Position	**Moment**	**Shear**	**Total Column Moment**
Outer Support:			
Column	-0.04Fl*	0.45F	0.04Fl
Wall	-0.02Fl	0.4F	-
Near middle of end span	0.083Fl*	-	-
First interior support	-0.063Fl	0.6F	0.022Fl
Middle of interior span	0.071Fl	-	-
Internal support	-0.055Fl	0.5F	0.022Fl

* The design moments in the edge panel may have to be adjusted to comply with Clause 4.6.5.3.2

NOTES

1. *F* is the total design ultimate load on the strip of slab between adjacent columns (i.e. $1.2G_n + 1.6Q_n$)
2. l is the effective span = $l_1 - 2h_c/3$.
3. The limitations of 4.6.5.1.3 need not be checked.
4. These moments should not be redistributed and $\beta_b = 0.8$

2.12.3 Lateral distribution of moments and reinforcement

In elastic analysis, hogging moments concentrate towards the column centre-lines. SANS 10100 specifies that moments should be divided between the column strip and the middle strip in the proportions given in *Table 2.12.2.*

Table 2.12.2: Distribution of moments in panels of flat slabs designed as equivalent frames –SANS 10100

1	2	3
Moments	Apportionment between column and middle strips expressed as a percentage of the total negative or positive moment*	
	Column strip	Middle Strip
Negative Positive	75 55	25 45
* Where the column strip is taken as equal to the width of the drop-head, and the middle strip is thereby increased in width to a value exceeding half the width of the panel, moments must be increased to be resisted by the middle strip in proportion to its increased width. The moments resisted by the column strip may then be decreased by an amount that results in no reduction in either the total positive or the total negative moments resisted by the column strip and middle strip together.		

2.12.4 Wood and Armer Method for Concrete Slab Design (Wood and Armer, 1968)

Wood and Armer proposed a concrete slab design method, incorporating twisting moments. The method had been developed taking into account the normal moment yield criterion, to prevent yielding in all directions. Taking any point in a reinforced concrete slab, the moment normal to a direction resulting due to design moments M_x, M_y and M_{xy}, may not exceed the ultimate normal resisting moment in that direction.

This ultimate normal resisting moment is provided by ultimate resisting moments related to the reinforcement in the x-direction and reinforcement orientated at an angle θ to the x-axis, measured clockwise. M_x, M_y and M_{xy} can be obtained from a finite element or grillage analysis, where M_x is the moment about the y-axis, M_y the moment about the x-axis, and M_{xy} the twisting moment (see Figure 2.12.1 for sign convention).

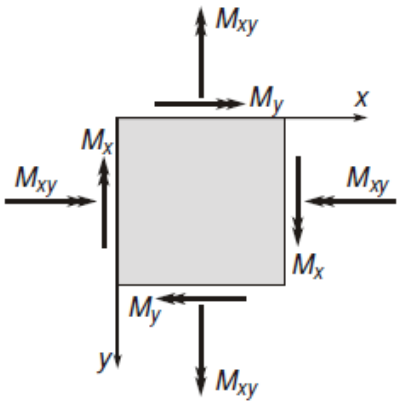

Figure 2.12.1: Equilibrium of a reinforced concrete membrane

The following equations can be used to calculate the moments to be resisted by the bottom steel reinforcement, where:

M^*_x is the moment to be resisted by reinforcement in the x-direction, and

M^*_θ is the moment to be resisted by reinforcement oriented at an angle θ to the x-axis.

$$M^*_x = M_x + 2M_{xy}\cot\theta + M_y\cot^2\theta + \left| (M_{xy} + M_y\cot\theta) / \sin\theta) \right| \quad \text{(Equation 2.12.2)}$$

$$M^*_\theta = (M_y / \sin^2\theta) + \left| (M_{xy} + M_y\cot\theta) / \sin\theta) \right| \quad \text{(Equation 2.12.3)}$$

if $M^*_x < 0$ then set $M^*_x = 0$

$$\text{and } M^*_\theta = (M_y + \left| (M_{xy} + M_y\cot\theta)^2 / (M_x + 2M_{xy}\cot\theta + M_y\cot^2\theta) \right|) / \sin^2\theta \quad \text{(Equation 2.12.4)}$$

or if $M^*_\theta < 0$ then set $M^*_\theta = 0$

$$\text{and } M^*_x = M_x + 2M_{xy}\cot\theta + M_y\cot^2\theta + \left| (M_{xy} + M_y\cot\theta)^2 / M_y) \right| \quad \text{(Equation 2.12.5)}$$

The top steel reinforcement is similar with sign changes as follows:

$$M^*_x = M_x + 2M_{xy}\cot\theta + M_y\cot^2\theta - \left| (M_{xy} + M_y\cot\theta) / \sin\theta) \right| \quad \text{(Equation 2.12.6)}$$

$$M^*_\theta = (M_y / \sin^2\theta) - \left| (M_{xy} + M_y\cot\theta) / \sin\theta) \right| \quad \text{(Equation 2.12.7)}$$

if $M^*_x > 0$ then set $M^*_x = 0$

$$\text{and } M^*_\theta = (M_y - \left| (M_{xy} + M_y\cot\theta)^2 / (M_x + 2M_{xy}\cot\theta + M_y\cot^2\theta) \right|) / \sin^2\theta \quad \text{(Equation 2.12.8)}$$

or if $M^*_\theta > 0$ then set $M^*_\theta = 0$

$$\text{and } M^*_x = M_x + 2M_{xy}\cot\theta + M_y\cot^2\theta - \left| (M_{xy} + M_y\cot\theta)^2 / M_y) \right| \quad \text{(Equation 2.12.9)}$$

These Wood-Armer moments obtained are typical of those utilised for the post-processing of finite element results. For the purposes of the study conducted in this dissertation, the main steel reinforcement directions are perpendicular to each other, and M^*_θ can be replaced by M^*_y, with $\theta = 90^o$, which simplifies the above equations.

2.13. DESIGN OF PRESTRESSED CONCRETE FLAT SLABS

2.13.1 Post-tensioning systems

In post-tensioned systems, the tendons are tensioned only after the concrete has been cast and developed sufficient strength. Post-tensioning can either be done using bonded or unbonded tendons. The following are points in favour of each technique:

Bonded:

- develops higher ultimate flexural strength
- localises the effects of damage
- does not depend on the anchorage after grouting

Unbonded:

- reduces friction losses
- grouting not required
- provides greater available level arm
- simplifies prefabrication of tendons
- generally cheaper
- can be constructed faster

Advantages of post-tensioned floors over conventional reinforced concrete in-situ floors are:

- Larger economical spans
- Thinner slabs
- Lighter structures
- Reduced storey height
- Reduced cracking and deflection
- Faster construction

2.13.2 Design codes of practice

British practise has generally formed the basis for prestressed concrete design in South Africa. The American code (ACI 318, 2005) is also used to a certain extent. Several technical reports have been compiled by the Concrete Society, each improving on the previous report. Report Number 2 of the South African Institution of Civil Engineers is an important reference and design manual for prestressed flat slabs. The recommendations following are based primarily on this technical report.

2.13.3 Load Balancing

The principle behind the load balancing design method is that the prestressing tendon applies a uniform upward load along the central length of a tendon span, and a downward load over the length of reverse curvature. This is illustrated in *Figure 2.13.1.*

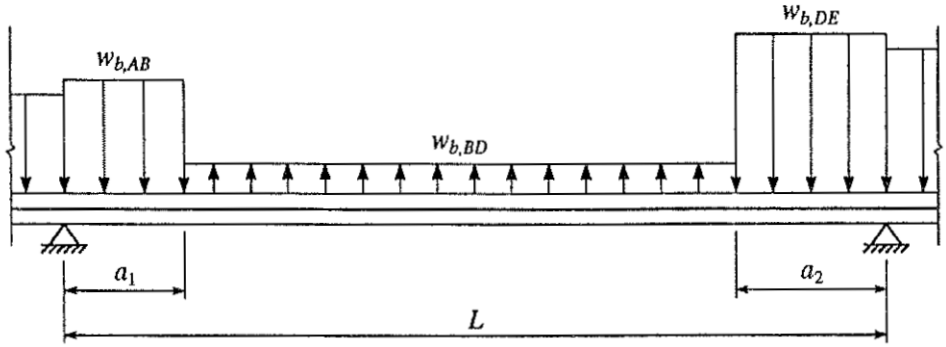

Figure 2.13.1: Tendon equivalent loads for a typical tendon profile
– Marshall & Robberts [2000]

Where the tendons are distributed uniformly in one direction and banded along the column lines in the direction perpendicular to the first, the concentrated band of tendons will provide an upward load to resist the downward load from the distributed tendons. The banded tendons act very much like beams, carrying the loads to the columns.

Tendons are placed in profile and in layout in such a manner to result in an upward normal force to counteract a specific portion of the slab's gravity. The effect of prestressing may then be included in the frame analysis or finite element model by applying these *equivalent* or *balanced* loads to the model, in combination with other general loadings.

2.13.4 Structural analysis of prestressed flat slabs

The equivalent frame method, grillage analysis and the finite element method of analysis may be used to analyse prestressed flat slabs. Marshall & Robberts [2000] suggest that yield line analysis is not suitable, since these slabs may not have sufficient plastic rotational capacity to allow the development of yield lines.

In the equivalent frame method, BS 8110 and SANS 10100 assume that the column is rigidly fixed to the slab over the whole width of the panel. If the ultimate hogging moment at the outer column exceeds the moment of resistance of the width of slab immediately adjacent to the column then this moment have to be reduced. The ACI 318 code allows for the loss of stiffness due to torsion, and

reduces the column's stiffness accordingly. Report No. 2 recommends that the ACI method of column stiffness calculation must be used for a frame method analysis.

2.13.5 Secondary effects

In the case of statically indeterminate structures, prestressing results in secondary forces and moments.

Primary prestressing forces and moments are due to the prestress force acting at an eccentricity from the centroid of the concrete section. The primary moment at any point is the product of the force in the tendon and the eccentricity.

Equivalent loads will generate the primary and secondary effects when applied to the frame for serviceability calculations. At ultimate limit state, primary and secondary effects are separated. The secondary effects are treated as applied loads. The primary effects contribute to the ultimate section capacity. The secondary effects can be obtained by subtracting the primary prestressing forces and moments from the equivalent load analysis. Allowance for secondary effects is not required for finite element modelling, since it is taken care of within the model during the analysis.

2.13.6 Design Parameters

Slab Depth

Slab depths depend on two main factors, strength and deflection. The slab must be deep enough to prevent shear and bending failure. Other methods used to prevent shear failure are:

1. Increasing the shear perimeter by using columns with capitals, or larger columns
2. Increasing the slab depth locally by means of drops
3. Application of punching shear reinforcement

Report No. 2 suggests the use of the following span/depth ratios to maintain acceptable deflection limits, although these may not be ideal for shear without the presence of column heads:

	Type of Construction Loading	**Span: Depth Ratio**
Flat Plates	Light	40 to 48
	Normal	34 to 42
	Heavy	28 to 36

The Modulus of Elasticity (E) of the slab affects deflection directly. According to SANS 10100, the Modulus of Elasticity is related to the cube strength of concrete (f_c) in the following manner:

$E = (20 + 0.2f_c)$ GPa

Report No. 2 suggests using a reduced value of 0.8E if the aggregates are not controlled (selected via inspection in accordance with SANS 10160).

Prestress Level

Report No. 2 does not recommend a minimum prestress level, but do suggest that when the prestressing is less than 0.7 MPa, greater care should be taken to ensure that deflections and cracking are not excessive.

The amount of load to be balanced is one of the most important design parameters. Report No. 2 mentions that a great deal of the advantage of prestressing is lost if less than half the dead load is balanced.

The tendon profile and amount of load to be balanced will govern the required prestress force. The amount of prestress influences the un-tensioned reinforcement requirements. The greater the level of prestress, the less un-tensioned reinforcement will be required. Various designs are possible for a particular layout and load application. The most economic design will depend on the relative costs of prestressing and un-tensioned reinforcement as well as the live to dead load ratio.

Tendon Profile and Layouts

The effect of prestressing must be maximised, by arranging the tendons in a profile to obtain the maximum drape. Tendons are usually fixed in parabolic profiles to provide a uniform upward load on the slab's internal region and downward load close to the supports. The tendons in external spans must be kept close to the mid-depth of the slab at the outside edge to avoid problems with bursting.

A popular system is where the tendons are concentrated over the columns in one direction, and spread uniformly in the other direction. This configuration facilitates placing of the tendons. If the column spacing is different in the two directions, the banded tendons should normally be placed in the direction of the shorter span.

2.13.7 Loading

At transfer of prestress, only own weight of the slab and prestress subject to all short-term losses, are included in the analysis.

At serviceability limit state, the analysis must include the full dead load, live load and prestress load, subject to all short-term and long-term losses.

At ultimate limit state, only the dead load and live load are included in the analysis with the prestressing secondary effects considered as a separate applied load case.

2.13.8 Lateral Loading

Wind loading is sometimes taken into account by approaching flat slab structures as frames. When analysing the frame, the slab portion of the frame is taken to have the stiffness of half the width of the panel. This allows for the effects of torsional flexibility.

2.13.9 Geometry of Tendons

A parabolic tendon profile is shown in *Figure 2.13.2*, in which points A, C and E are the tangents to the parabola, where B and D are the inflection points.

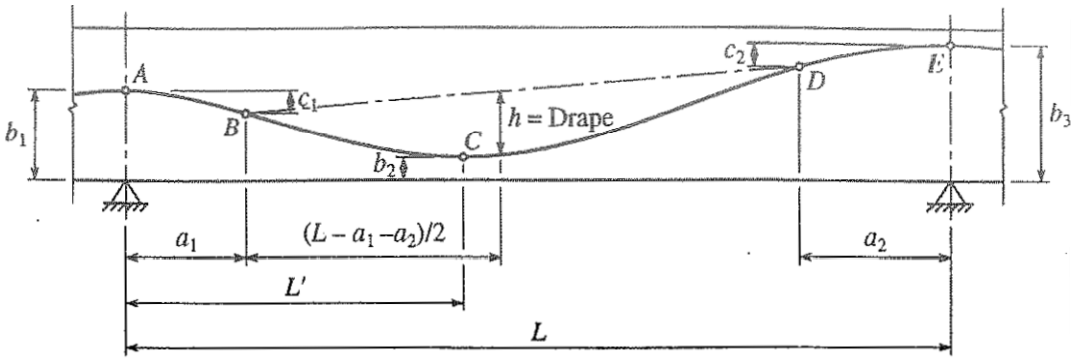

Figure 2.13.2: Tendon geometry for a typical tendon profile (Marshall & Robberts, 2000)

Report No. 2 indicates the geometrical parameters of the parabolic tendon to be as follows: (Notation modified by Marshall & Robberts [2000])

$$L' = \begin{cases} \dfrac{-m \pm \sqrt{m^2 - 4.l.n}}{2l} & for\ l \neq 0 \\ \dfrac{-n}{m} & for\ l = 0 \end{cases}$$

where:

$l = (b_3 - b_1)$

$m = (2L - a_2)\,(b_1 - b_2) - a_1\,(b_3 - b_2)$

$n = -\,(b_1 - b_2)\,(L - a_2)\,L$

$$c_1 = \frac{(b_1 - b_2)a_1}{L'} \qquad c_2 = \frac{(b_3 - b_2)a_2}{(L - L')}$$

$$h = drape = \frac{(b_1 - b_2)(L - a_1 - a_2)^2}{4L'(L' - a_1)}$$

The equivalent loads are:

$$w_{b,AB} = \frac{2Pc_1}{a_1^{\,2}}$$

$$w_{b,BD} = \frac{8Ph}{(l - a_1 - a_2)^2}$$

$$w_{b,DE} = \frac{2Pc_2}{a_2^{\,2}}$$

Values for a_1, a_2 and for the dimensions from the soffit of the slab b_1, b_2, b_3 should be assumed. The values of a_1 and a_2 are usually chosen to be 5% of the span. It is, however, preferable to utilise values providing an appropriate radius of the tendon over the column for the particular tendon diameter. Report No. 2 recommends a value of 100 tendon diameters.

2.13.10 Prestress losses

After the post-tensioning tendons are stressed, various losses occur which will reduce the initial tension in every tendon. The two types of losses that will occur are short-term and long-term losses.

Short term losses include:

1. Friction losses in the tendon
2. Anchorage seating
3. Elastic shortening of the structure

Long-term losses include:

1. Relaxation of the tendons
2. Concrete shrinkage
3. Creep of the concrete due to the prestress

Loss due to friction

Friction loss occurs due to two factors, namely wobble in the sheath and curvature of the tendon. In accordance with Report No. 2, the effective prestress at any distance *x*, immediately after stressing will be as follows:
(Notation modified by Marshall & Robberts [2000])

$$P_2 = P_1 e^{-(\mu\alpha + Kx)} \qquad \text{(Equation 2.13.1)}$$

where:

P_1, P_2 = tendon force at point 1 and 2 respectively
μ = friction factor, unitless
K = wobble factor, radians/m
α = total angle that the tendon has rotated between points 1 and 2, radians
x = horizontal projection along the length of the tendon between 1 and 2, m

In *Figure 2.13.2*, the angle through which the tendon has turned at mid span is as follows:

$$\alpha = Arctan\ (2\ c_1/a_1) + Arctan\ (2(b_1-b_2-c_1)/(x-a_1))$$

Report No. 2 recommends a value of K = 0.001 rad/m and μ = 0.06 for strands locally available. Marshall & Robberts [2000] recommend a value for K = 0.00025 rad/m.

Loss due to anchorage seating

Anchorage seating arises from the deformation of the anchorage components or, in the case of friction type wedges, from the slip that will take place to seat the grips when the tendon is anchored.

Marshall & Robberts [2000] presents the loss of prestress due to anchorage seating, for short tendons, as follows:

$$\Delta P_L = \frac{\delta A_{ps} E_p}{L} - pL \qquad \text{(Equation 2.13.2)}$$

where:

ΔP_L = loss of prestress due to anchorage seating
δ = anchorage seating
L = cable length
A_{ps} = Area of prestressed reinforcement
E_p = Modulus of elasticity of the prestressed reinforcement

The assumption in this equation is that the distance affected by anchorage seating extends over the entire length of the tendons. According to Technical Report No. 43, a typical value for anchorage seating is 6 mm.

Elastic shortening of the concrete

For post-tensioned slabs, the elastic shortening of a tendon that is being tensioned, will result in a loss of prestress in all tendons which have previously been tensioned and anchored.

According to Marshall & Robberts [2000], the loss due to elastic shortening can be determined as follows:

$$\Delta f_{pES} = \frac{1}{2}(f_{c,cgs})_{PJ'} n_{pt} \qquad \text{(Equation 2.13.3)}$$

where:

$(f_{c,cgs})_{PJ'}$ = stress in the concrete at the centroid of the prestressing steel due to the prestressing force acting on its own

$n_{pt} = E_p/E_{ct}$ = modular ratio

E_p = modulus of elasticity of the prestressing steel

E_{ct} = modulus of elasticity of the concrete at the time of tensioning

The loss of prestressing force as a result of elastic shortening, will be:

$$\Delta P_{ES} = -A_{ps}\Delta f_{pES}$$

According to Marshall & Robberts [2000], $(f_{c,cgs})_{PJ'}$ for unbonded tendons, is often taken as the average value of stress produced by the prestressing tendons at the centroid of the concrete section, rather than at the centroid of the prestressed steel.

Loss due to the relaxation of steel

The stress in the tendons always reduces with time because of the relaxation of the steel. The amount of relaxation will depend on the type of strand and the original stress.

SANS 10100-1 clause 5.8.2.2.2 states:

> "When there is no experimental evidence available, the relaxation loss for normal stress-relieved wire or strand may be assumed to decrease linearly from 10% for an initial prestress of 80%, to 3% for an initial prestress of 50%. This would apply when the estimated total creep and shrinkage strain of the concrete is less than 500×10^{-6}. When the creep plus shrinkage strain exceeds 500×10^{-6}, the loss for an initial stress of 80% should be reduced to 8,5%. Losses for low-relaxation tendons may be assumed to be half the above value."

Loss due to shrinkage of the concrete

Shrinkage strain is normally assumed to be uniform through the concrete. The loss of prestress due to shrinkage can be calculated as follows:

$\Delta f_{pS} = \varepsilon_S E_p$ (Equation 2.13.4)

where:

ε_S = shrinkage strain of the concrete from the time when curing of the concrete is stopped, to the time of transfer

E_p = modulus of elasticity of the prestressing steel

The corresponding loss of prestress force is:

$\Delta P_S = - \Delta f_{pS} n_{tnd} A_{ps,tnd}$

An estimate of the drying shrinkage of concrete may be obtained from *Figure 2.13.3*.

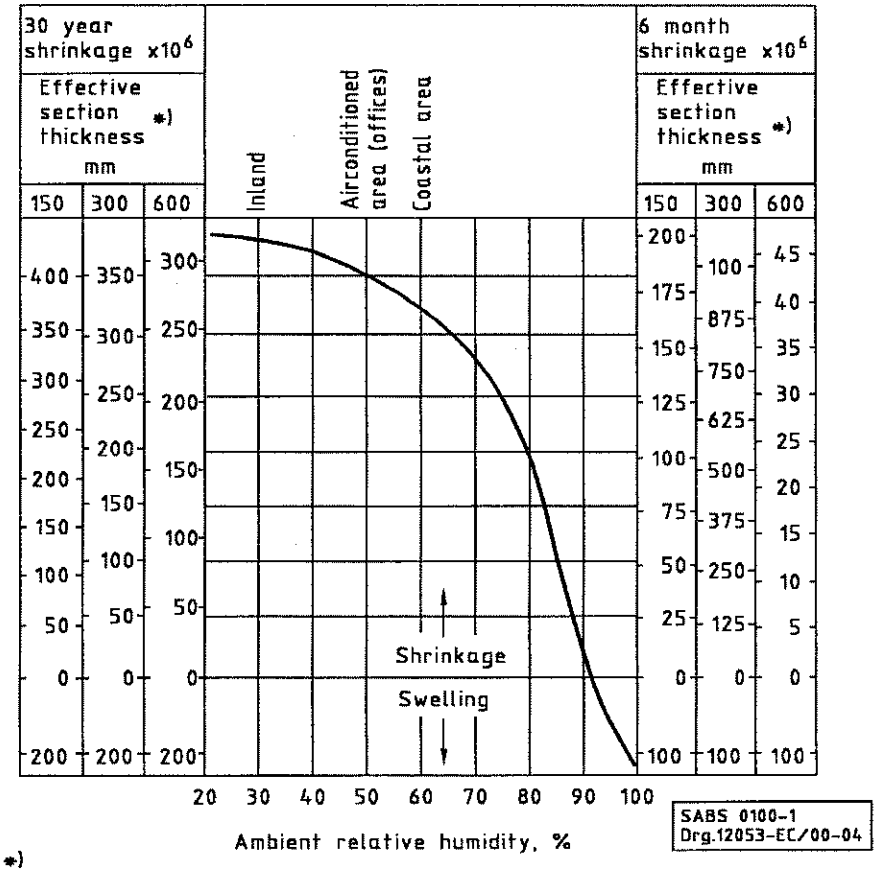

Figure 2.13.3: Drying shrinkage of normal-density concrete – SANS 10100

Creep loss

Creep loss is based on the strain in the concrete at the level of tendons.

$$\varepsilon_C = \phi_u \frac{f_{c,cgs}}{E_{ct}} \qquad \text{(Equation 2.13.5)}$$

where:

ϕ_u = creep coefficient as obtained from *Figure 2.13.4*

$f_{c,cgs}$ = stress in the concrete at the centroid of the prestressing steel due to prestress and the permanent loading

E_{ct} = modulus of elasticity of concrete

Loss of steel stress due to creep is:

$$\Delta f_{pC} = \varepsilon_C E_p \qquad \text{(Equation 2.13.6)}$$

The corresponding loss of prestress force is:

$$\Delta P_C = - \Delta f_{pC} n_{tnd} A_{ps,tnd}$$

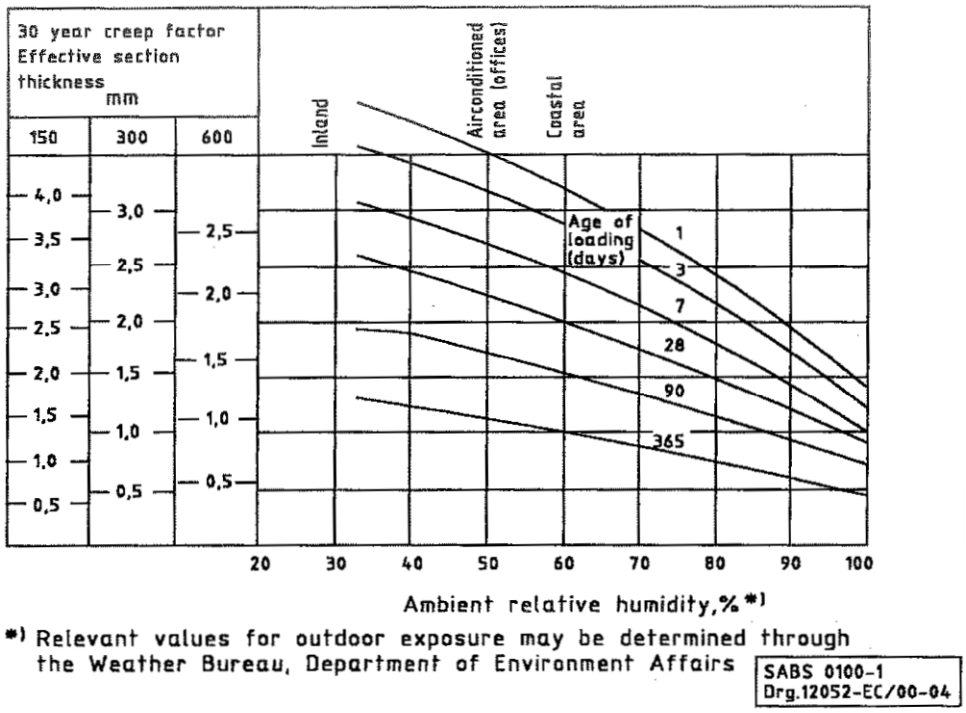

Figure 2.13.4: Effects of relative humidity, age of concrete at loading and section thickness upon creep factor – SANS 10100

2.13.11 Serviceability limit state

Permissible flexural stresses

The approach followed by Report No. 43 to control flexural cracking under service conditions, is to supply a limit to the tensile stress in the extreme tension fibre.

According to Report No. 43 these stresses can be calculated as follows:
(Notation modified by Marshall & Robberts [2000])

$$f_{top} = \frac{P}{A} + \frac{M}{Z_{top}} \qquad \text{(Equation 2.13.7)}$$

$$f_{bot} = \frac{P}{A} + \frac{M}{Z_{bot}} \qquad \text{(Equation 2.13.8)}$$

where:

f_{top}, f_{bot} = stress in the extreme top and bottom fibres respectively
A = area of the section
$Z_{top} = I/y_{top}$ = section modulus with respect to the extreme top fibre
$Z_{bot} = I/y_{bot}$ = section modulus with respect to the extreme bottom fibre
$M = M_a + P_e + M_s$ = total out-of-balance moment

M_a = applied moment due to dead and live load
P_e = primary moment due to prestress
M_s = secondary moment due to prestress

The prestressing force in this calculation includes all losses.

Report No. 43 limits these stresses for different conditions. A description is given in *Table 2.13.1*.

Table 2.13.1: Allowable average stresses in flat slabs, (two-way spanning), analysed using the equivalent frame method – Report No. 43

Location	**In compression**	**In tension**	
		With bonded reinforcement	**Without bonded reinforcement**
Support	$0.24f_{cu}$	$0.45\sqrt{f_{cu}}$	0
Span	$0.33f_{cu}$	$0.45\sqrt{f_{cu}}$	$0.15\sqrt{f_{cu}}$
Note: Bonded reinforcement may be either bonded tendons or un-tensioned reinforcement			

When examining the stresses at transfer of prestress, the prestressing force must include all short-term losses. The allowable stresses are obtained from *Table 2.13.1*, with the concrete compressive strength taken as that at transfer, namely f_{ci} *in MPa*.

Where these allowable tensile stresses are exceeded, un-tensioned reinforcement must be provided. In accordance with Report No. 43, this reinforcement should be designed to carry the full tensile force generated by the assumed tensile stresses in the concrete at a stress not exceeding *5/8* f_y, where f_y is the yield strength of the reinforcement.

2.13.12 Ultimate Limit State Design

Flexural strength

The stress in the tendon at ultimate may be expressed as follows:

$$f_{ps} = f_{se} + \Delta f_s \qquad \text{(Equation 2.13.9)}$$

where:

f_{se} is the effective prestress in the steel, including all losses

Δf_s is the additional stress induced in the steel by bending of the slab

SANS 10100 specifies the following semi-empirical formula for the calculation of the stress in the tendon at ultimate: (Notation modified by Marshall & Robberts [2000])

$$f_{ps} = f_{se} + \frac{7000}{l/d}\left[1 - 1.7\frac{f_{pu} n_{tnd} A_{ps}}{f_{cu} bd}\right] MPa \le 0.7 f_{pu} \qquad \text{(Equation 2.13.10)}$$

where:

l is defined in *Figure 2.13.5*

f_{pu} is the characteristic strength of tendons

f_{cu} is the characteristic cube strength of concrete

b is the width of the concrete section under consideration

d is the effective depth to the prestressing steel

This value of f_{ps} is based on an estimated length of the zone of inelasticity within the concrete of 10 times the neutral axis depth of the section. In the scenario where a member is continuous over supports, more than one zone of inelasticity may occur within the length of the tendon. This is provided for by adjusting the length l as indicated in *Figure 2.13.5*.

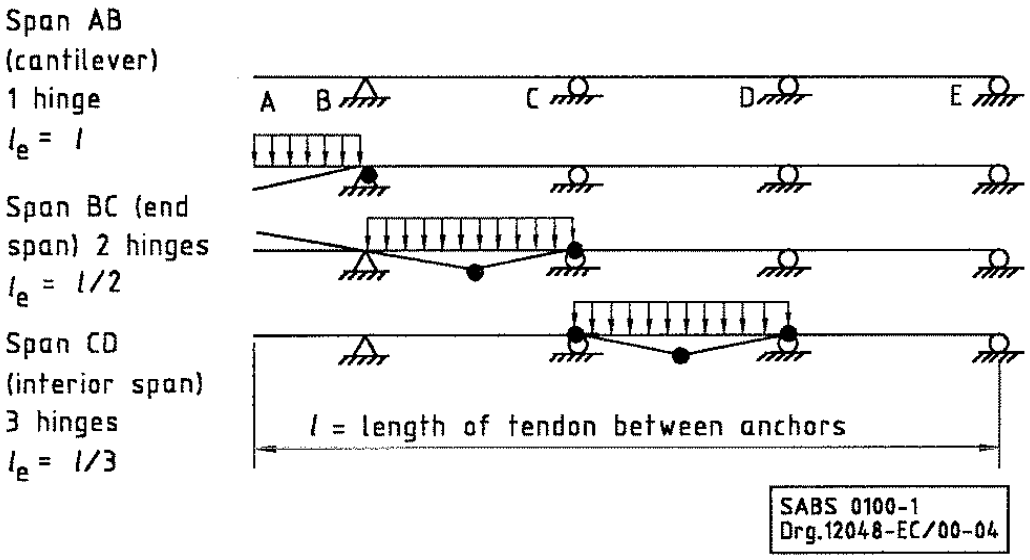

Figure 2.13.5 – Determination of *l* for use in Eq. 2.13.10 – SANS 10100

SANS 10100 states that non-prestressed bonded reinforcement (A_s) may be replaced by an equivalent area of prestressing tendons $A_s f_y / f_{pu}$.

Once the stress in the tendon at ultimate is known, the depth to the neutral axis, x, may be calculated by considering horizontal equilibrium of the section, and the ultimate moment, M_u, may be calculated by considering moment equilibrium.

According to SANS 10100 and BS 8110, the ultimate moments are redistributed to a maximum of 20%. Report No. 43 recommends that the maximum redistribution should rather be limited to 15%.

Shear

The design effective load for punching shear is calculated the same way as for a non-prestressed flat slab. Punching is considered at consecutive perimeters as well.

The punching shear resistance of a particular perimeter can be obtained by summing the shear capacities of each side of the perimeter. Report No. 43 recommends that the shear capacity of each side is calculated as follows:

$$V_{cr} = v_c b_v d + M_0 \frac{V}{M} \qquad \text{(Equation 2.13.11)}$$

where:

v_c is the shear strength of the concrete for the applicable side.

(The area of the prestressing tendons should only contribute to v_c if the tendons are bonded to the concrete).

b_v is the length of the side
d is the effective depth to the centroid of the tension steel

The value of V/M is calculated for the load case considered. V/M should be calculated at the position of the critical perimeter, however, Report No. 43 suggest that V/M may be conservatively calculated at the column centre-line.

M_0 is the decompression moment for the sides:

$$M_0 = -0.8P\frac{Z^*_t}{A} - 0.8P^*e^* \qquad \text{(Equation 2.13.12)}$$

where:

P = total prestressing force, over the full panel width, after all losses

A = the concrete section area over the full panel width

$Z^*_t = \frac{1}{6}bh^2 =$ section modulus for the top fibre over the width of the side of the critical perimeter

P^* = the total prestressing force for all tendons passing through the side of the critical perimeter

e^* = eccentricity of the prestress force , P^*, at the critical perimeter, measured positive below the centroid

Where the design effective load V_{eff} exceeds the punching shear capacity of a particular perimeter, the shear capacity of the slab should be increased. This can be achieved by either providing drops or column heads, or by providing shear reinforcement. The required amount of shear reinforcement is calculated in the same way as for a non-prestressed flat slab.

Shear reinforcement is considered to be ineffective in slabs less than 150 mm thick. The amount of shear reinforcement required is calculated with following equation:

$$\sum A_{sv} \leq \frac{(v - v_c)ud}{0.87 f_s} \qquad \text{(Equation 2.13.13)}$$

where:

A_{sv} = area of shear reinforcement

d = effective depth

u = shear perimeter

$(v\text{-}v_c) \geq 0.4\ MPa$

For slabs greater than 200 mm thick, $f_s = f_{yv}$

f_{yv} = characteristic strength of the shear reinforcement

To adjust for shear reinforcement being less effective in flat slab less than 200 mm thick, Report No. 2 recommends that for slabs between 150 mm and 200 mm thick (h), f_s can be taken as the lesser of :

$f_s = f_{yv}\,(h\text{-}150)/50$ and

$f_s = 425\,(h\text{-}150)/50$

2.13.13 Minimum un-tensioned reinforcement

Effective crack distribution must be achieved in accordance with Report No. 43 and Report No. 2, suggesting a minimum amount of un-tensioned reinforcement at column positions.

Report No. 43 recommends this minimum amount to be 0.075% of the gross concrete cross-section. This reinforcement should extend at least a fifth of the span into the span and may not be spaced at more than 300 mm centre to centre.

Report No. 2, however, recommends that this minimum amount should rather be $0.0015wh$, where w is the column width plus 4 times h, and h is the overall slab depth. The reinforcement should at least extend one sixth of the clear span on each side of the support. A further requirement is that no less reinforcement than 4 Y12 bars at a maximum spacing of 200 mm may be provided.

Both reports specify that the above-mentioned reinforcement should be concentrated over a distance of 1.5 times the slab depth either side of the column width.

Internal flat slabs panels have reserves of strength due to two way arching action and membrane stress. Exterior panels lack this reserve strength and are therefore more vulnerable. For this reason, Report No. 2 recommends that the exterior and corner spans be designed with additional non-prestressed reinforcement. Sufficient un-tensioned reinforcement should be provided in an external span to ensure that when 50% of the prestress is lost, the span will still be able to support the un-factored dead load and a quarter of the un-factored live load. It is also adequate, in the case of domestic and office buildings, that 0.25% reinforcement of the slab area is provided in the top at the first internal support and the bottom of the external span. This reinforcement should be concentrated mainly in the column band (75% in the column band and 25% in the slab band).

For internal spans, Report No. 2 recommends a minimum area of bottom reinforcement of 0.075% times the gross cross-sectional area of the band. Half of these bottom bars must have a minimum lap of 300 mm at support lines, and the rest should have a minimum length of half the span.

2.13.14 Crack control

In accordance with Report No. 2, crack widths are limited by an empirical formula, specifying a minimum amount of normal reinforcement to distribute cracks. This minimum reinforcement is as follows:

For end spans P_s = 0.5 P_{pr}, but not less than 0.05%

where: P_s = Percentage of normal reinforcement
P_{pr} = Percentage of prestressing steel

Internal spans do not require minimum steel. In the region of the columns, a minimum steel area of 0.3% must be provided over a width equal to the column width, plus three times the effective depth. Additional steel equal to 0.15% is required over the remaining column zone. Report No. 2 simplifies this by taking the minimum required quantity of steel over the column strip as 0.15 %.

2.14. ECONOMY OF DIFFERENT CONCRETE SLAB SYSTEMS

This paragraph's content is based on the *Cobiax Technology Handbook (2006)* and research done by *Goodchild, C.H. (1997)*. Goodchild's research scrutinises the economy of various slab systems, exposed to different load intensities and practical span ranges. The systems of importance to this report are Cobiax flat slabs and waffle slabs designed with flat slab methodology, as well as unbonded post-tensioned flat slabs.

Cobiax flat-slab system

Figure 2.14.1 is the preliminary design chart for Cobiax flat slabs. It is based on a simplified equal length three-span by three-span panel system, loaded with a 2 kPa superimposed dead load, and various sizes of live loads. These loads are indicated by different line colours on the chart, and for a certain span length a slab thickness can be established, using the correct design load on the chart. For that same span length a preliminary reinforcement content can be read from the chart, as well as a predicted long-term deflection where 60% of the live load was considered to be permanent.

Due to the simplicity of the model in this chart it is difficult to prepare estimates for structures with varying span lengths and load intensities. A suggestion is to base the slab thickness for a structure with relatively small variations in span lengths on the largest span, and the reinforcement content on an average span length. Interpolation can be performed for different load intensities.

Loadings displayed in *Figure 2.14.1* that will be applicable to the study of this research report will range from the indicated line for 2 kPa live load, to that of the 10 kPa live load. As mentioned earlier, these live loads will all be combined with a 2 kPa superimposed dead load. Due to the 280mm minimum thickness of a Cobiax slab governed by the smallest available Cobiax sphere size of 180 mm diameter, economical span ranges will range between 6.5 m and 13 m for the 10 kPa live load.

All assumptions in *Figure 2.14.1* are subject to the material properties written next to the chart. The required reinforcement contents allow for wastage, lapping of bars, and punching shear reinforcement quantities.

The 10 kPa live load on a 13 m span already requires a slab thickness of almost 600 mm and reinforcement content of approximately 70 kg/m^2. For such high reinforcement contents Cobiax can be combined with post-tensioned cables for more economical designs, a subject that will not be discussed in this report.

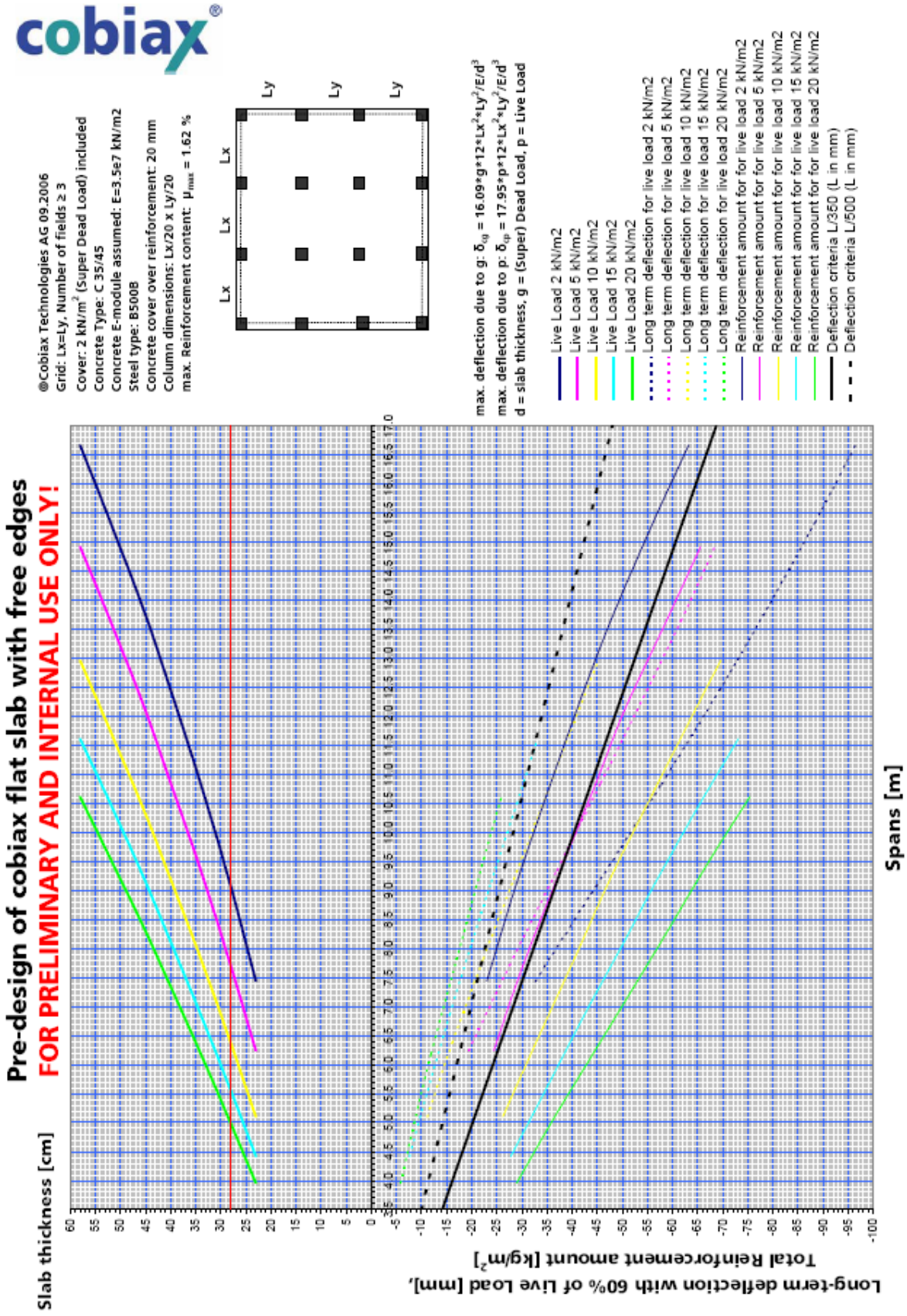

Figure 2.14.1: Preliminary Cobiax Design Chart (CBD-MS&CRO, 2006)

Waffle slabs and post-tensioned flat slabs

The assumptions made in the work of Goodchild are slightly different from that in *Figure 2.14.1* for a Cobiax slab. Nevertheless the studies of Goodchild and Cobiax demonstrate enough similarities to compare them with one another to establish economical span ranges for a certain range of load intensities.

Goodchild's studies also consider a continuous slab over supporting columns applied as pinned supports, with three equal spans that include the critical end-spans. Moment and shear factors from BS 8110 were restricted to spans not differing more than 15% to that of the largest span.

Goodchild states that different analysis methods can result in up to 15% difference in reinforcement weight. Reinforcement weight can further be influenced significantly by choosing various slab thicknesses for a specific slab under consideration. The calculation of reinforcement content in Goodchild's tables were based on BS 8110, and allowed 10% extra for wastage, curtailment and lapping of bars. It is based on the tension reinforcement required, and not on those provided, in order to display smooth curves. The reinforcement properties were taken to be f_y = 460 MPa for tension steel and f_{yv} = 250 MPa for shear steel.

The slab results in Goodchild's research allow for a mild exposure to weather and aggressive conditions, and a 1 hour fire rating in accordance with BS 8110. The concrete had a 35 MPa cube strength and 24 kN/m^3 density.

The imposed load, in this case live load, was chosen in accordance with BS 6399, where:

- 2.5 kPa General office loading and car parking
- 5.0 kPa High specification office loading, e.g. file rooms and areas of assembly
- 7.5 kPa Plant rooms and storage loading
- 10.0 kPa High specification storage loading

Goodchild assumed the superimposed dead load to be 1.5 kPa for finishes and services. Should this load be different for a specific slab design, both the design charts of Cobiax and Goodchild allow for the additional superimposed dead load to be adjusted to an equivalent live load. Goodchild further assumed a perimeter cladding load of 10 kN/m for his slab designs.

According to Goodchild, concrete, reinforcement and formwork costs result in up to 90% of the superstructure cost. Other factors that influence the structure's cost, and sometimes severely, are site constraints, incentives or penalties for early or late completion respectively, labour and crainage

on site, and foundations. Should a lighter slab type in e.g. a high-rise building justify a raft foundation instead of piling, it will be worth while to use this slab system, even if it is slightly more expensive per square meter than another slab system.

SANS 10100:2000 Clause 4.5.2 allows for coffer slabs to be designed with a flat slab methodology. This will insinuate three important adjustments to be made to the slab design, namely a reduction in the slab's shear capacity, stiffness, and own weight in the coffer zones. Goodchild also acknowledge this method of waffle slab design, and the economical ranges are discussed in *Figure 2.14.2* and *Table 2.14.1*.

Goodchild mentions that the slab thickness will be governed by deflection, punching shear and shear in ribs. His research assumption that no shear reinforcement is required in ribs where the shear capacity of the concrete rib without stirrups (v_c) is greater that the applied shear (v), is also apparent in SANS 10100 Clauses 4.3.4.1 and 4.4.5.2. Minimum tension reinforcement will nevertheless always be required for crack control in a coffer slab's flange zone. This steel area will amount to at least $0.0012*b*h_f$, where b is usually taken as a 1 m strip and h_f is the flange thickness.

As in the case of Cobiax flat slabs, these waffle slabs have also been allocated with 25% solid zone areas surrounding columns. According to Goodchild, only waffle slab spans of up to 12m will be economical and the major disadvantages of this system will be high formwork costs, greater floor thicknesses, and slow fixing of reinforcement.

Waffle slabs *designed as flat slabs (bespoke moulds)*

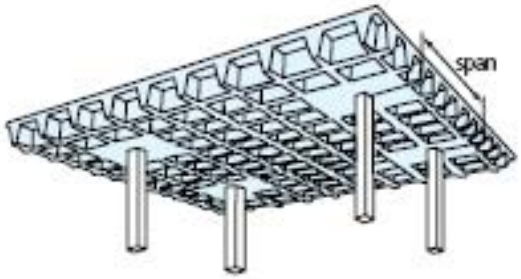

Introducing voids to the soffit of a flat slab reduces dead weight and these slabs are economical in spans up to 12 m in square panels. Thickness is governed by deflection, punching shear around columns and shear in ribs.

The charts assume a solid area adjacent to supporting columns up to span/2 wide and long. The chart and data include an allowance for an edge loading of 10 kN/m.

ADVANTAGES

- Profile may be expressed architecturally
- Flexibility of partition location and horizontal service distribution
- Lightweight

DISADVANTAGES

- Higher formwork costs than for other slab systems
- Slightly deeper members result in greater floor heights
- Difficult to prefabricate, therefore reinforcement may be slow to fix

SPAN: DEPTH CHART

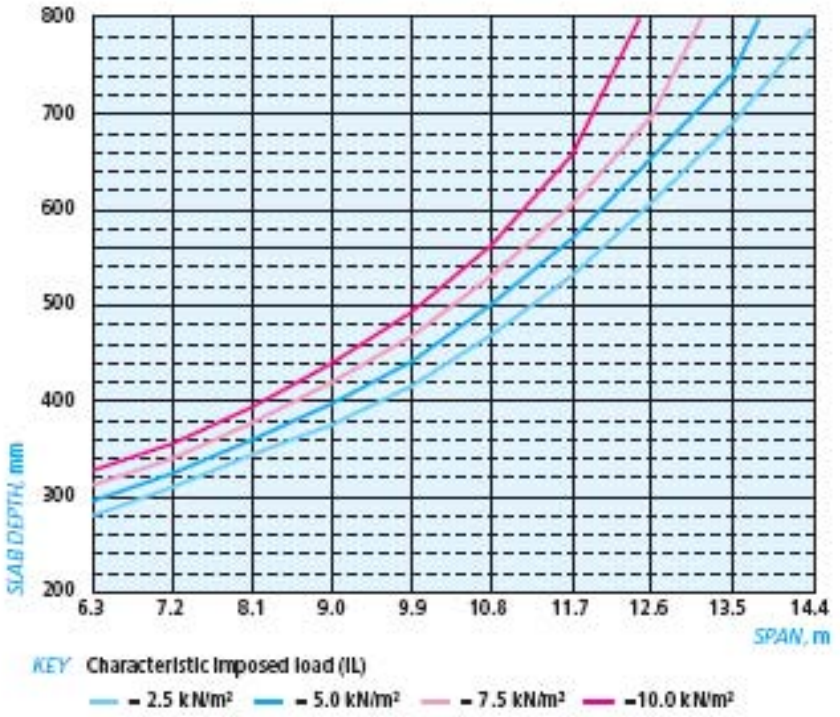

Figure 2.14.2: Waffle Slab Design Chart: Goodchild (1997)

Table 2.14.1: Waffle Slab Design: Goodchild (1997)

DESIGN ASSUMPTIONS

SUPPORTED BY	COLUMNS. Refer to column charts and data to estimate sizes, etc.
DIMENSIONS	Square panels, minimum of three spans x three bays. Ribs 150 mm wide @ 900 mm cc. Topping 100 mm. Moulds variable depth. Solid area = span/2 in each direction.
REINFORCEMENT	Max. bar sizes, ribs: 2T32B, T32T and R8 links. 25 mm allowed for A142 mesh T (@ 0.12%) in topping. 10% allowed for wastage, etc. f, may have been reduced.
LOADS	SDL of 1.50 kN/m² (finishes) and perimeter load of 10 kN/m (cladding) included. Ultimate loads to columns assume elastic reaction factors of 1.0 internally and 0.5 at ends. Self weight used accounts for 5:1 slope to ribs and solid areas as described above.
CONCRETE	C35, 24 kN/m³, 20 mm aggregate.
FIRE & DURABILITY	Fire resistance 1 hour; mild exposure.

MULTIPLE SPAN, m	6.3	7.2	8.1	9.0	9.9	10.8	11.7	12.6	13.5
THICKNESS, mm									
IL = 2.5 kN/m²	280	310	344	376	416	470	532	608	690
IL = 5.0 kN/m²	296	324	360	398	442	502	570	654	742
IL = 7.5 kN/m²	312	340	378	420	468	532	606	698	862
IL = 10.0 kN/m²	328	356	394	440	494	564	658	826	
ULTIMATE LOAD TO SUPPORTING COLUMNS, Internal (edge) per storey, MN									
IL = 2.5 kN/m²	0.5 (0.3)	0.7 (0.4)	0.9 (0.5)	1.2 (0.7)	1.5 (0.8)	1.9 (1.1)	2.4 (1.3)	3.1 (1.7)	3.9 (2.1)
IL = 5.0 kN/m²	0.7 (0.4)	0.9 (0.5)	1.2 (0.7)	1.5 (0.9)	1.9 (1.1)	2.5 (1.4)	3.1 (1.7)	4.0 (2.1)	4.9 (2.7)
IL = 7.5 kN/m²	0.8 (0.5)	1.1 (0.6)	1.5 (0.8)	1.9 (1.0)	2.4 (1.3)	3.0 (1.7)	3.8 (2.0)	4.8 (2.6)	6.2 (3.4)
IL = 10.0 kN/m²	1.0 (0.6)	1.4 (0.8)	1.7 (1.0)	2.3 (1.2)	2.8 (1.5)	3.6 (1.9)	4.5 (2.4)	5.9 (3.2)	
REINFORCEMENT, kg/m² (kg/m²)									
IL = 2.5 kN/m²	16 (56)	28 (99)	31 (98)	25 (67)	27 (66)	30 (64)	32 (60)	34 (56)	37 (53)
IL = 5.0 kN/m²	20 (66)	26 (79)	28 (78)	31 (78)	33 (76)	35 (70)	36 (63)	39 (60)	42 (56)
IL = 7.5 kN/m²	23 (72)	31 (92)	33 (88)	35 (84)	38 (83)	38 (72)	41 (68)	44 (63)	45 (52)
IL = 10.0 kN/m²	26 (78)	35 (100)	37 (94)	40 (90)	43 (88)	43 (77)	45 (68)	46 (56)	
COLUMN SIZES ASSUMED, mm square, Internal (perimeter)									
IL = 2.5 kN/m²	270 (260)	310 (300)	350 (340)	420 (390)	460 (440)	530 (510)	600 (570)	680 (650)	760 (730)
IL = 5.0 kN/m²	310 (290)	360 (340)	410 (390)	470 (440)	530 (500)	600 (570)	670 (640)	760 (720)	850 (810)
IL = 7.5 kN/m²	350 (320)	410 (370)	460 (420)	530 (490)	590 (550)	670 (620)	740 (700)	830 (790)	950 (900)
IL = 10.0 kN/m²	380 (340)	440 (400)	500 (460)	570 (530)	640 (590)	720 (670)	810 (750)	930 (870)	
DESIGN NOTES a = q_k > 1.25 g_k b = q_k > 5 kN/m² f = shear critical (initially v>2v$_c$) j = links in ribs close to solid areas									
IL = 2.5 kN/m²	fj	fj	fj	fj	fj	fj	fj	fj	fj
IL = 5.0 kN/m²	fj	fj	fj	fj	fj	fj	fj	fj	fj
IL = 7.5 kN/m²	bfj	bfj	bfj	bfj	bfj	bfj	bfj	bfj	bj
IL = 10.0 kN/m²	abfj	abfj	abfj	bfj	bfj	bfj	bfj	bfj	
LINKS, MAXIMUM NUMBER OF PERIMETERS IN SOLID AREAS (and percentage by weight of reinforcement, all links), no. (%)									
IL = 2.5 kN/m²	7 (6.7%)	6 (2.4%)	7 (2.3%)	7 (3.9%)	7 (4.2%)	6 (3.7%)	6 (4.4%)	5 (4.6%)	4 (5.2%)
IL = 5.0 kN/m²	7 (7.6%)	7 (4.1%)	7 (4.9%)	7 (4.3%)	7 (5.6%)	7 (5.1%)	5 (5.6%)	5 (6.6%)	5 (7.4%)
IL = 7.5 kN/m²	7 (7.5%)	6 (4.6%)	7 (6.0%)	7 (5.6%)	7 (6.9%)	6 (5.7%)	5 (7.1%)	5 (7.5%)	4 (9.8%)
IL = 10.0 kN/m²	6 (7.7%)	6 (5.5%)	7 (6.5%)	7 (6.5%)	6 (7.5%)	5 (6.7%)	5 (7.9%)	5 (9.8%)	

VARIATIONS TO DESIGN ASSUMPTIONS: difference in slab thickness for a characteristic imposed load (IL) of 5.0 kN/m²

Fire resistance	2 hours, 115 mm topping#	+20 mm	4 hours	not usually feasible
Exposure	Moderate #	+20 mm	Severe, C40 concrete#	+25 mm
Cladding load	No cladding load	- 20 mm	20 kN/m cladding	+ 40 mm if <12.6 m
	Edge beams	- 20 mm	Column head L/10 square	-0 mm
Holes	No holes, 225 holes	+0 mm	300 mm sq. holes	+ 0 mm if >8.1 m

175 rib width required

Thickness, mm	Span, m	8.1	9.0	9.9	10.8	11.7	12.6	13.5
	No shear links	486	550	608	644	700	794	882
	50 mm drop, L/2 wl	348	388	426	484	548	628	714
	2 spans	378	422	466	536	614	746	
Rectangular panels		For non-square panels use an equivalent square span to derive thickness						
	Long span, m		9.0	10.8	12.6	14.4	16.2	18.0
	Short span = 9.0 m		9.0	9.4	10.7	12.1	13.4	14.4
	Short span = 9.9 m			9.7	11.0	12.4	13.5	14.4
	Short span = 10.8 m			10.8	11.3	12.7	13.8	
	Short span = 11.7m				11.7	12.9	14.0	
	Short span = 12.6 m				12.6	13.2	14.3	
	Short span = 13.5 m					13.4	14.5	

Goodchild considers the benefits of post-tensioned flat-slabs to be the increase of span lengths, stiffness and water tightness, as well as reduced slab thickness, own weight, deflection, and construction time. The formwork will also be cheaper than that of coffers, since normal flat-slab formwork can be applied. Shear capacity is improved by the tensioned cables. The most beneficial tensioning method for normal building slabs is that of unbonded tendons (usually 12.9 or 15.7 mm diameter tendons covered in grease within a protective sheath). Bonded tendons will be more appropriate in bridges and uneconomical in building slabs. When concrete achieves sufficient strength, tendons are stressed utilising a simple hand-held jack and anchored off.

Figure 2.14.3 and *Table 2.14.2* display Goodchild's economical span range estimations for unbonded post-tensioned flat-slabs in buildings. His loading assumptions are the same as for the waffle slabs. His material property assumptions differ in that the cube strength of concrete is slightly higher, namely 40 MPa. The unbonded 15.7 mm diameter tendons each have an area (A_{ps}) of 150 mm^2 and strength (f_{pu}) of 1770 MPa. The other assumptions are that of the presence of edge beams, being at least 50% deeper than the slab.

The assumption of Goodchild that differs significantly from that made in this thesis, is that the post-tensioned slabs were designed to satisfy the requirements of a Class 2 tensioned member. He limits the allowable surface stresses and cracking of the slab by assuming a balanced load for the tendon design of 133% dead load added to 33% of the live load.

The assumption made in this thesis for economical design and South African conditions will be the use of 70% of the dead load only for calculation of the balanced load. This will result in a Class 3 tensioned member, allowing larger tension and cracking on the concrete surfaces. The rest of the load will be carried by normal reinforcement, where a Class 2 member will require much less normal reinforcement, usually limited to minimum reinforcement application. Since most building slabs are not directly exposed to weather conditions, and considering the fact that tendons are much more expensive than normal reinforcement, the Class 3 solution will be the most economical solution for South African requirements.

Goodchild also considers the maximum economical span range for post-tensioned slabs to be approximately 12m.

Flat slabs *with edge beams*

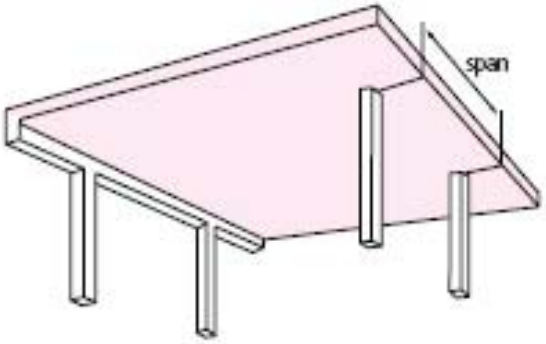

Popular overseas for apartment blocks, office buildings, hospitals, hotels etc, where spans are similar in both directions. Economical for spans of 7 to 12 m. Square panels are most economical.

ADVANTAGES

- Simple, fast construction and formwork
- Architectural finish can be applied directly to the underside of the slab
- Minimum thickness and storey heights
- Controlled deflection and cracking
- Flexibility of partition location and horizontal service distribution

DISADVANTAGES

- Holes, especially large holes near columns, require planning
- Punching shear provision around columns may be considered to be a problem but can be offset by using larger columns, column heads, drop panels or proprietary systems. Post-tensioning improves shear capacity

SPAN:DEPTH CHART

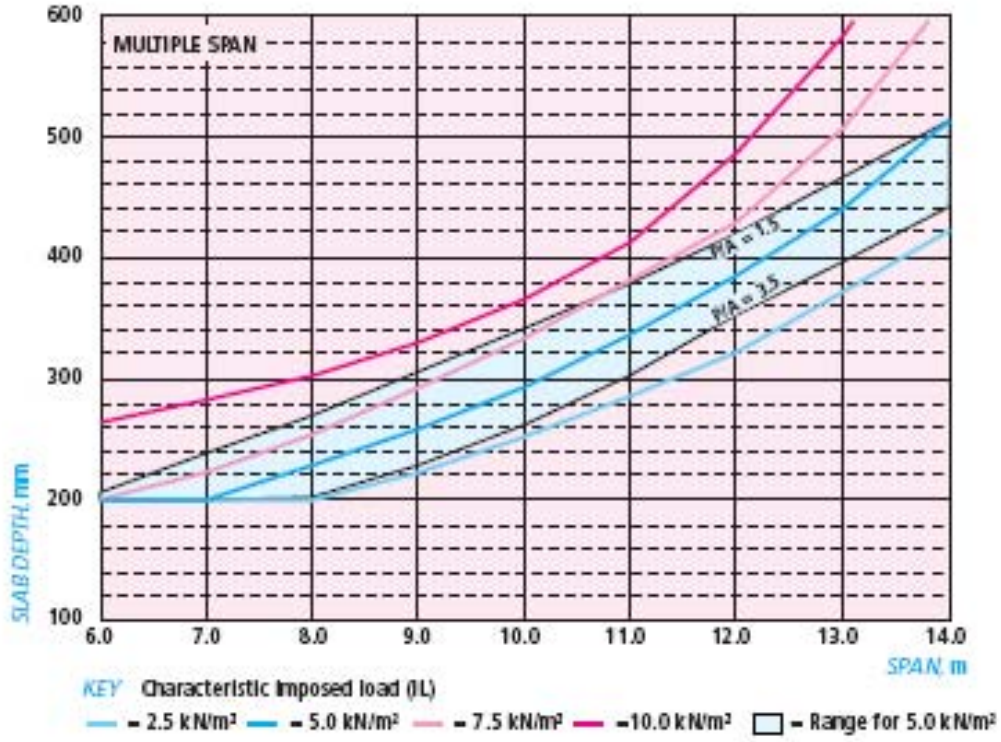

Figure 2.14.3: Unbonded Post-tensioned Flat Slab Design Chart: Goodchild (1997)

Table 2.14.2: Unbonded Post-tensioned Flat Slab Design: Goodchild (1997)

DESIGN ASSUMPTIONS

SUPPORTED BY	COLUMNS internally and BEAMS around perimeter. Refer to charts and data to estimate sizes, etc.
DESIGN BASIS	To CS TR43. Balanced load 133% DL + 33% IL . Maximum prestress (P/A) = 2.5 N/mm². See Section 7. Effectively Class 2 assumed. No restraint to movement assumed.
DIMENSIONS	Square panels, assuming three spans by three bays. Outside edge flush with columns. Minimum column size as data. Edge beams should be at least 50% deeper than slab.
LOADS	SDL of 1.50 kN/m² (finishes) assumed. Perimeter load of 10 kN/m (1.4 kN/m ult) included in loads on edge beams. Ultimate loads to columns and beams are the result of moment distribution analysis.
TENDONS	Unbonded 15.7 mm diam. Superstrand (A_{ps} 150 mm², f_{pu} 1770 N/mm²), B1, T2, B2 & T3. Max 5 per m.
CONCRETE	C40, 24 kN/m³, 20 mm aggregate. f_{ci} = 25 N/mm².
REINFORCEMENT	Assumed min. T10@250T both ways at supports, min T12@500B both ways and T8 links. 10% allowed for wastage and laps.
FIRE & DURABILITY	Fire resistance 1 hour; mild exposure (25 mm cover to all).

MULTIPLE SPAN, m	6.0	7.0	8.0	9.0	10.0	11.0	12.0	13.0	14.0
THICKNESS, mm									
IL = 2.5 kN/m²	200	200	200	222	252	286	322	372	424
IL = 5.0 kN/m²	200	200	228	258	294	338	386	442	516
IL = 7.5 kN/m²	200	222	254	292	334	382	430	508	620
IL = 10.0 kN/m²	264	282	302	330	366	414	488	584	710
ULTIMATE LOAD TO SUPPORTING COLUMNS, MN, INTERNAL, PER STOREY.									
IL = 2.5 kN/m²	0.61	0.83	1.09	1.45	1.93	2.49	3.22	4.16	5.27
IL = 5.0 kN/m²	0.80	1.09	1.50	2.01	2.62	3.43	4.39	5.58	7.11
IL = 7.5 kN/m²	0.99	1.40	1.92	2.55	3.35	4.31	5.44	6.97	9.05
IL = 10.0 kN/m²	1.28	1.79	2.39	3.11	4.02	5.12	6.57	8.43	10.88
ULTIMATE LOADS ON EDGE BEAMS, kN/m									
IL = 2.5 kN/m²	48	54	59	68	78	89	102	119	137
IL = 5.0 kN/m²	59	66	77	89	101	118	135	155	181
IL = 7.5 kN/m²	70	81	94	109	126	144	164	191	227
IL = 10.0 kN/m²	86	100	114	130	148	169	196	229	270
REINFORCEMENT (TENDONS), kg/m²									
IL = 2.5 kN/m²	14 (8)	13 (9)	13 (9)	12 (10)	12 (11)	11 (12)	11 (13)	12 (13)	14 (13)
IL = 5.0 kN/m²	14 (8)	14 (9)	13 (10)	13 (11)	13 (13)	13 (13)	14 (13)	16 (13)	18 (13)
IL = 7.5 kN/m²	15 (8)	14 (10)	14 (11)	13 (13)	13 (13)	14 (13)	17 (13)	19 (13)	21 (13)
IL = 10.0 kN/m²	15 (7)	15 (9)	15 (12)	15 (13)	16 (13)	18 (13)	19 (13)	22 (13)	24 (13)
COLUMN SIZES ASSUMED, INTERNAL, mm square									
IL = 2.5 kN/m²	280	330	380	440	500	570	650	740	830
IL = 5.0 kN/m²	320	370	440	510	580	660	750	840	950
IL = 7.5 kN/m²	350	410	480	560	640	730	820	920	1050
IL = 10.0 kN/m²	390	460	530	610	690	780	880	1000	1130
DESIGN NOTES	*o = limited by P/A of 2.5 N/mm²*		*p = B > response factor > 4*			*q = shrinkage per span > 10 mm*			
	r = tendons @ < 300 mm cc. (R @ 200 mm cc.)				*s = overall deflection, d_{dead} + d_{dyn} > 20 mm (S > 30 mm)*				
IL = 2.5 kN/m²	p	o	os	ors	orS	orS	oRS	RS	RS
IL = 5.0 kN/m²	p	o	or	ors	ors	Rs	Rs	Rs	RS
IL = 7.5 kN/m²	p	or	or	or	R	Rs	Rs	Rs	Rs
IL = 10.0 kN/m²			r	r	R	Rs	R	R	R
LINKS, maximum number of perimeters (and percentage by weight of bonded reinforcement), no. (%)									
IL = 2.5 kN/m²	2 (0.6%)	3 (0.8%)	5 (1.4%)	6 (1.6%)	7 (1.8%)	7 (1.6%)	8 (1.9%)	8 (1.7%)	7 (1.1%)
IL = 5.0 kN/m²	3 (1.0%)	5 (1.7%)	6 (1.9%)	7 (2.0%)	7 (1.8%)	8 (2.1%)	8 (1.8%)	7 (1.1%)	6 (0.7%)
IL = 7.5 kN/m²	4 (1.5%)	6 (2.2%)	7 (2.4%)	7 (2.1%)	8 (2.3%)	8 (1.9%)	7 (1.2%)	6 (0.8%)	5 (0.5%)
IL = 10.0 kN/m²	3 (1.1%)	5 (1.7%)	6 (2.0%)	7 (2.1%)	7 (1.7%)	7 (1.4%)	6 (0.9%)	5 (0.6%)	4 (0.4%)

VARIATIONS TO DESIGN ASSUMPTIONS: differences in slab thickness for a characteristic imposed load (IL) of 5.0 kN/m²

Fire resistance	2 hours	+0 mm	4 hours	+25 mm
Exposure	Moderate	+5 mm	Severe	+15 mm
Serviceability	Class 1	n/a	Column heads L/l 0 wide	-0 mm
Two spans	2 spans by 3 bays	see below	2 spans by 2 bays	see below
Rectangular bays	6.0 m wide bay -15 mm @ 8 m and beyond		9.0 m wide bay -15 mm @ 11.0 m and beyond	

Thickness, mm — Spans, m	8.0	9.0	10.0	11.0	12.0	13.0	14.0
P/A 1.5 N/mm² max	270	306	342	380	422	468	516
P/A 3.5 N/mm² max #	202	228	262	304	354	398	444
2 spans by 3 bays	230	260	294	346	400	496	608
2 spans by 2 bays	238	268	300	356	430	524	636
T16@350B both ways	220	246	274	306	360	424	516

max 7 tendons/m

3. EXPERIMENTAL WORK – SHEAR IN COBIAX SLABS

3.1. INTRODUCTION

In this chapter the task was to compare theoretical calculations for the shear strength of Cobiax slabs (discussed in Chapter 2) with force controlled shear tests performed on laboratory Cobiax slab specimens. This comparison had to be conducted to establish the shear strength reduction factor for a Cobiax slab, compared with a solid slab with the same thickness, tension reinforcement and concrete properties.

A Cobiax shear strength reduction factor of 0.55 times (Schellenbach-Held and Pfeffer, 1999) the shear strength of a concrete slab without shear reinforcement had been calculated at the Technical University of Darmstadt (TUD) in Germany. The Cobiax steel cages were omitted in the TUD tests. The objective of this chapter was to demonstrate that the presence of the steel cages holding the Cobiax spheres in position during construction, will act as shear reinforcement inside the slab, resulting in a less conservative shear strength reduction factor.

This method of multiplying the shear capacity of a solid slab with a shear strength reduction factor to obtain the shear strength of that slab with internal spherical voids, is a simplified method best supported by empirical test results. This method seems to be the easiest way to support the design engineer with answers for shear in Cobiax slabs, and also a faster way to predict shear strength when conducting a cost comparison between different slab types, as done in *Chapter 4* of this report.

Predicting the shear behaviour in concrete slabs with internal spherical voids is actually far more complex and could probably best be approached with powerful finite element software using three dimensional brick elements and non-homogenous material (concrete and steel reinforcement). One could with multiple analyses of different scenarios (slab content and dimensions) develop formulae that are typical for concrete slabs with internal spherical voids. This approach or a similar complex approach will not be conducted for the purposes of this report.

The experimental work comprised of the testing of twelve beam specimens of equal length and width, but having varying thicknesses and quantities of tension reinforcement, some with Cobiax spheres, and some solid. All beams, simulating strips of 600mm wide flat-slabs, were designed to fail in shear before failing in flexure, to allow for conclusions to be drawn regarding their shear capacities.

The samples were manufactured in Bloemfontein and transported to Pretoria on the day prior to testing. Three 150 x 150 cubes and three 150 x 150 x 700 beams were also manufactured and then tested on the same day as the sample beams so that the representative 13 day compression and flexural strengths could be established.

Due to casting and laboratory constrains the tests had to be carried out 13 days after casting. However, the age of testing has little significance seeing that all the tests were carried out on the same day. All predicted capacities are also based on the 13 day concrete strengths.

3.2. PREPARATION AND EXPERIMENTAL SETUP

Experimental Design

- A total of twelve sample beams were manufactured, each beam having a length of 1500 mm and a width of 600 mm.
- Three solid beams (without Cobiax spheres) were cast as well, having depths of 280 mm. In these beams the tension steel content was varied, each one having 3, 4 and 5 Y16 bars, respectively.
- For the 180 mm diameter Cobiax spheres used in the other 9 samples, the concrete webs or spheres were spaced at 200 mm centres in every sample. The beams were therefore dimensioned to contain two whole spheres in the centre, and two half spheres at the sides of every Cobiax sample. Every beam cross-section therefore contained 3 identical webs, central to the beam. (See Figure 3.2.1).

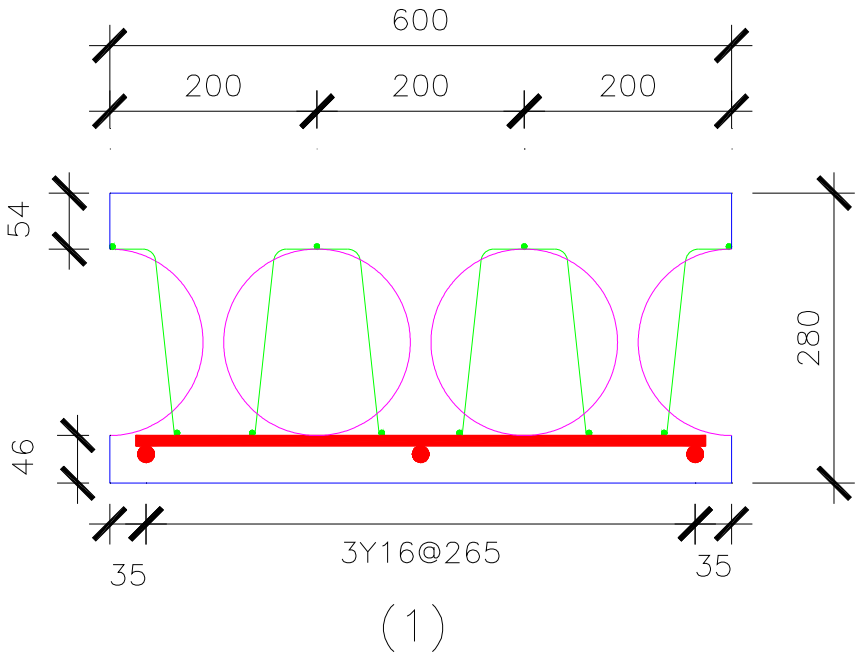

Figure 3.2.1 Cross section of a 280 mm thick Cobiax sample

- Three depths of 280, 295 and 310 mm were prepared for the Cobiax samples, with varying reinforcement quantities of 3, 4 and 5 Y16 bars for each depth. Details of the beams are presented in *Paragraph 3.5*.
- Cobiax cages (displayed in green in *Figure 3.2.1*) consist of 1 top and 2 bottom longitudinal bars, kept in place by transverse bars. Both the longitudinal and vertical bars of the cage will clearly contribute to the shear resistance. From a theoretical point of view these bars should be removed to obtain a true comparison between a solid slab and a voided slab containing spheres. However, this would result in some practical problems keeping the spheres in position during construction. On the other hand, the cages will always be present in a Cobiax slab, and it was therefore decided to use the Cobiax system exactly as it will be used in practice. It should be noted that vertical cage bars are not fully anchored around the main reinforcing bars when considering SABS 0144:1995 curtailment specifications. For this reason they will only partially contribute to the aggregate interlock capacity, and their contribution will reduce drastically after the welds between the vertical bars and bottom horizontal bars of the cages fail under large loads.

The following factors were considered in the parameter selection to investigate the design of the experimental setup:

- As stated in *Paragraph 2.2,* beams without shear reinforcement is likely to fail in shear before failing in flexure if the a_v / d ratio is less than approximately 6.

where:

a_v = distance of a single point load to the face of the support

d = effective depth of the tension reinforcement

It is therefore normal practice in beam design to provide shear reinforcement to increase the shear capacity so that flexural failure will happen before shear failure. The largest quantity of shear reinforcement will be required for an a_v / d ratio of approximately 2.5 to 4 (see discussion in Section 2). The a_v / d ratios for the beams were therefore kept within these limits to be able to produce conservative results. The actual ratios for the experimental beams are given in *Table 3.2.1*, with *H* the slab thickness.

Table 3.2.1 $\frac{a_v}{d}$ ratios

H (mm)	a_v (mm)	d (mm)	a_v/d
280	687.5	252	2.73
295	687.5	267	2.57
310	687.5	282	2.44

- For smaller $\frac{a_v}{d}$ ratios, arch action will increase the shear capacity of the beam, which is not desirable for the purpose of this research.
- The test apparatus was limited to a 600 mm wide slab.
- The beams had to be manufactured in Bloemfontein and then transported over a distance of 460km to Pretoria, having the effect of preparation of as small as possible samples to enable handling and transportation. The weight of every sample varied between 600 and 750 kg.
- The larger and heavier the samples were, the more difficult it would have been to position the beams correctly during the experimental setup.
- Budget constrains were also applicable.

The beams were simply supported with a span of 1350 mm (see *Photo 3.2.1* and *Figure 3.2.2*). Each sample's longitudinal centreline was aligned with the longitudinal centreline of the supports. The distance from the beam end to the centre of the support was 75mm. The knife edge load (P_u) was applied at the sample's midspan. The samples were tested in force control at a rate of 40 kN/min. Experience show that this rate is acceptable and will result in negligible dynamic effects. The failure

criterion is easily observed with a sudden drop in the applied force with a deflection that remains constant. Throughout the test the applied loads at midspan, as well as the displacements, were measured at 25 readings per second (25Hz).

Photo 3.2.1: Experimental setup

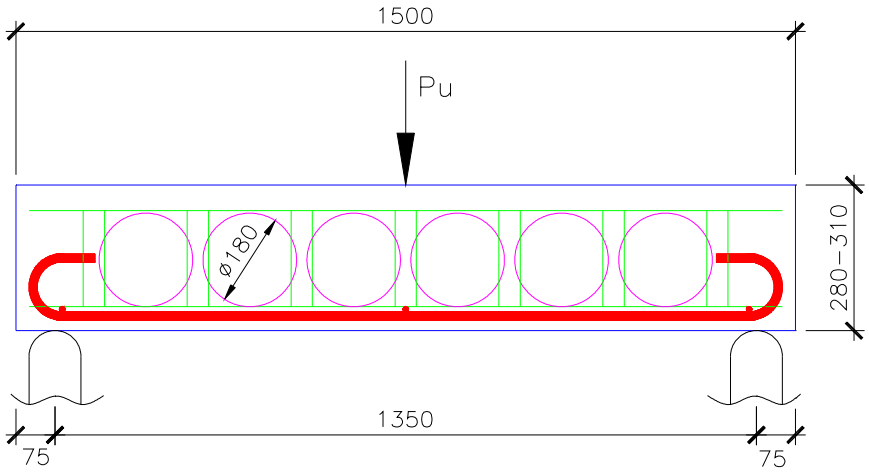

Figure 3.2.2 Experimental setup

The flexural capacity for each sample was calculated to ensure that shear failure would precede flexural failure. The results are presented in *Table 3.2.2*. *Figure 3.2.3* shows the results in graph format. These results are only an indication of the properties that will be required in the samples. The correct material properties are displayed later in this chapter. *Equations 2.4.1 to 2.4.3a* were used with all partial material safety factors set to unity.

- The slab thickness was varied by increasing the depth of the top flange, but keeping the thickness of the bottom flange constant for all beams. This was done to simulate construction practice.
- Reinforcement variation was decided on to assess the influence of tension reinforcement on the shear capacity.
- The reason for material factors being set to unity is to calculate the actual strength rather than the design strength.

Table 3.2.2 Comparison between moment failure loads and shear failure loads based purely on design values

SANS 10100					
fcu =	30	**MPa**	**Cover**	20	**mm**
fy =	450	**MPa**	**AY16 =**	201	**mm²**
b =	600	**mm**	**γm**	1.0	Material factor - Moment
L =	1350	**mm**	**γmc**	1.0	Material factor - Shear
Solid	**Height (mm)**	**d (mm)**	**Pm (kN)**	**Ps (kN)**	**Failure Mode**
280Y3	280	252	194	199	Moment
280Y4	280	252	254	219	Shear
280Y5	280	252	313	236	Shear
295Y3	295	267	206	204	Shear
295Y4	295	267	270	225	Shear
295Y5	295	267	333	242	Shear
310Y3	310	282	218	209	Shear
310Y4	310	282	286	230	Shear
310Y5	310	282	353	247	Shear
Pm =	Failure load for flexure (midspan point load)				
Ps =	Failure load for shear (midspan point load)				
Failure mode =	**"Moment" =**	Beam will fail in flexure			
	"Shear" =	Beam will fail in shear			

In *Table 3.2.2* the definitions of the symbols not explained in the table itself are:

fcu = characteristic concrete cube compression strength

fy = steel reinforcement yield strength

b = width of the specimen

L = span of the specimen

AY16 = area of a 16 mm diameter steel reinforcement bar

d = centroid depth of the tension reinforcement, measured from the top of the beam

The legends, for example *280Y3*, can be explained as follows:

280 = total thickness of the beam

Y3 = amount of steel reinforcement bars in the beam, spreaded over the 600 mm width

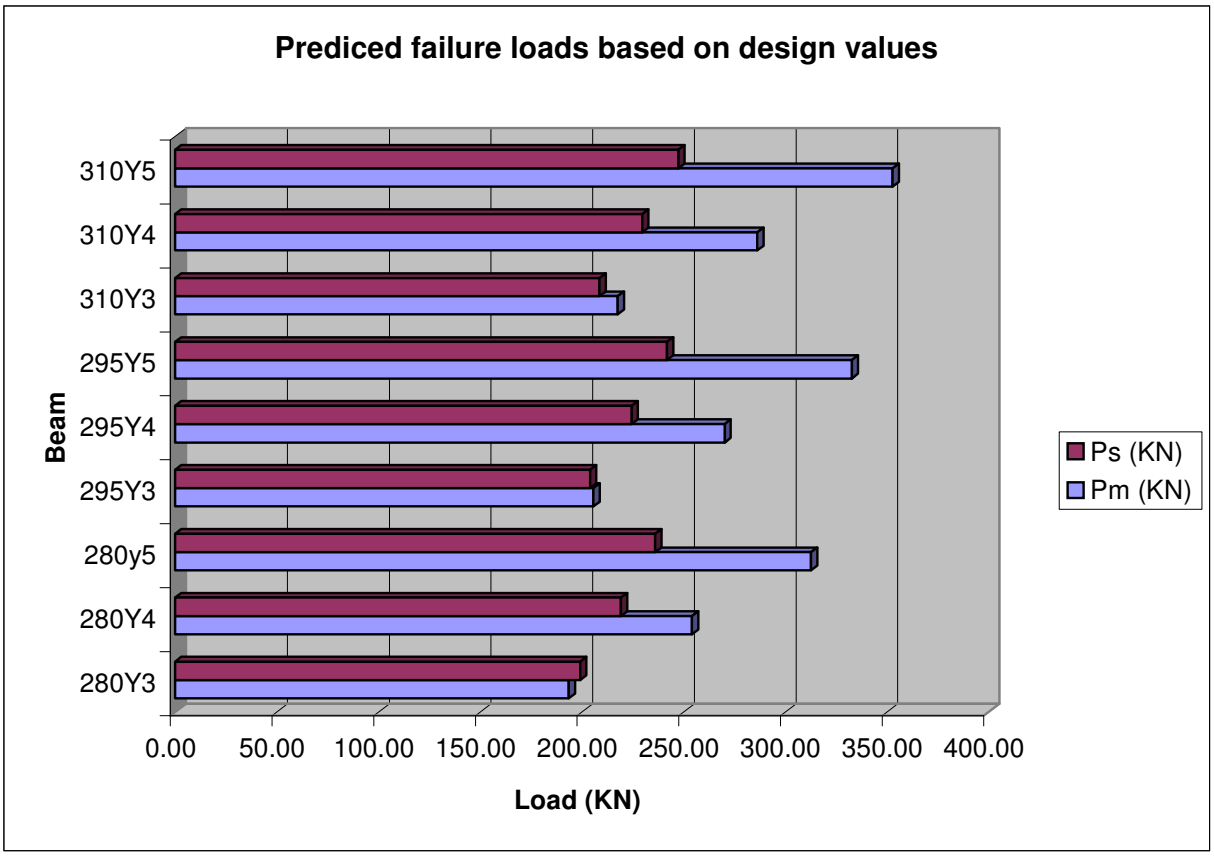

Figure 3.2.3 Predicted moment failure and shear failure loads based on design values

The Cobiax beams were expected to have a lower shear capacity than the solid beams. All calculations for the solid beams showed that shear failure would precede or happen simultaneously to flexural failure, and it was therefore concluded that the Cobiax beams would display a similar behaviour.

The depth of the stress block in flexure for the Cobiax beams never exceeded the minimum depth of the top flange during this research. For the 280 mm deep beam, the minimum depth of the top flange is 50 mm. The method used to design Cobiax slabs are for this reason the same as for solid slabs, where the presence of the voids only reduces the own-weight and slightly reduces the slab stiffness, as well as shear capacity.

The calculations indicated that the 280 mm solid slab with 3 Y16's (S280Y3) could fail in flexure before failing in shear. However, normally the flexural reinforcement will enter the work-hardening zone, and the flexural capacity will increase beyond that in shear. This configuration was accepted for this reason.

Sample Preparation

The samples were manufactured at Peri Wiehahn's premises in Bloemfontein. Following construction of the formwork, the tension reinforcement was positioned in the boxes, and the cages containing the Cobiax spheres were fixed to the tension reinforcement. The semi spheres were fixed to sides of the formwork boxes. Prior to casting, inspections were performed to ensure that all elements were correctly positioned in accordance with the design drawings.

The concrete was poured during the following day. A first concrete layer of approximately 70 mm was poured to ensure the tension reinforcement and bottom bars of the Cobiax cages were embedded by at least 20 mm. This prevented the spheres from floating to the top during casting, since they could not escape the cages that were then anchored in the bottom 70 mm of hardened concrete. This first concrete layer added sufficient dead weight to hold all components down during the second pour to the top of the slab. Lifting of cages would result in a smaller d value, that would extinguish the hope of any trustworthy results. The second and final pour was done approximately 4 hours later.

The second pour's concrete were utilised to construct the test cubes and beams, to ensure that a representative sample of the concrete forming the compression block (top concrete) was collected.

3.3. OBSERVATIONS

As can be seen from *Photos 3.3.1*, the shear cracks started from bending cracks in the case of the solid slabs. This is common for $2.5 < \frac{a_v}{d} < 6.0$.

In the case of the Cobiax slabs though, the crack sometimes started at the web, and then further developed down and back to the support along the tension reinforcement and also upwards to the top of the beam towards the line of load application. These observations are well justified by the predictions of Park & Paulay (1975). (See *Paragraph 2.2*)

Solid slab crack *Cobiax slab crack*

Photo 3.3.1: Observed crack patterns at failure

3.4. RESULTS

The following table is a summary of the failure loads obtained for each sample.

Table 3.4.1 Beams tested and results obtained
S = Solid slab
C = Cobiax Slab
Y3 = 3 x Y16 bars
Load = Load applied by hydraulic press for failure to occur

Beam	Load (kN)
S280Y3	242
S280Y4	326
S280Y5	354
C280Y3	268
C280Y4	279
C280Y5	330
C295Y3	259
C295Y4	301
C295Y5	343
C310Y3	276
C310Y4	271
C310Y5	353

Figure 3.4.1 shows the failure loads of all samples compared to SANS 10100 characteristic shear capacity (with $\lambda_{mv} = 1$) calculated for a solid section. The solid and Cobiax samples all exceeded the predicted capacity. From these results it would appear as if no reduction in capacity is required for the Cobiax slabs. However, further investigations were required in terms of material properties before any such conclusions could be made.

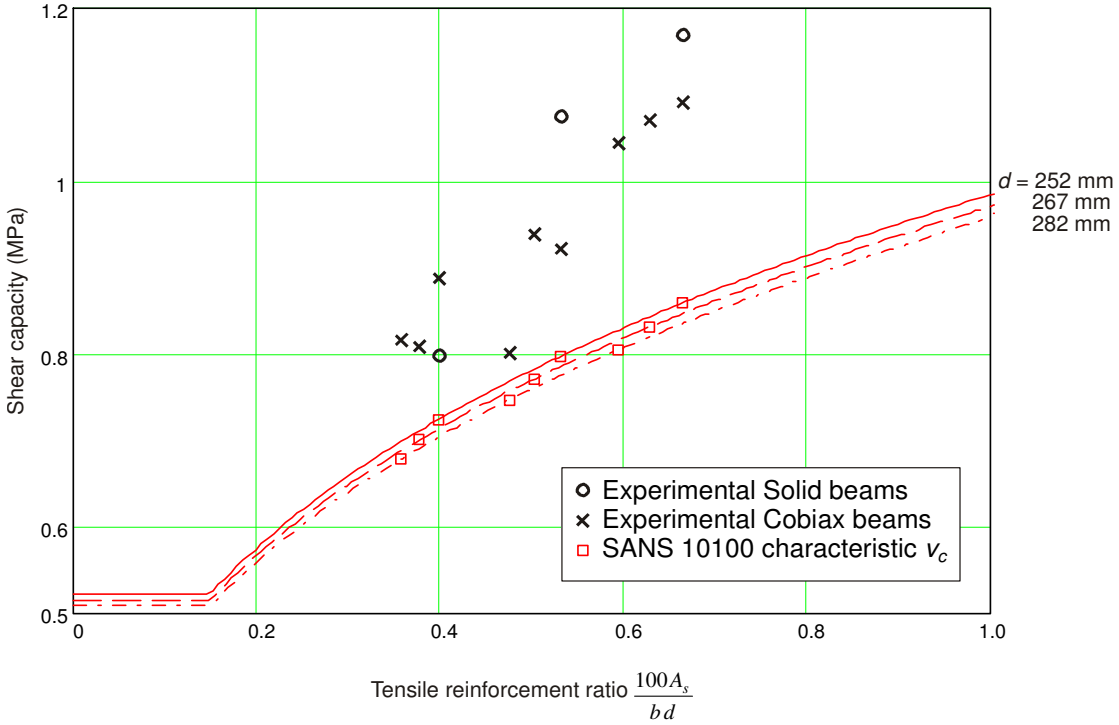

Figure 3.4.1: Failure stress of all beams compared to SANS 10100 characteristic shear capacity.

More detailed results are presented in the following sections, supported by a discussion on the observed behaviour.

Solid slabs

The load-deflection response of the solid slabs is illustrated in *Figure 3.4.2*. The behaviour is mostly brittle with an almost linear behaviour up to the peak load. After obtaining the peak load, there is a rapid reduction in resistance, characteristic of a shear failure. The exception is S280Y4 which exhibits a softening behaviour before reaching the peak load and a more gradual reduction in strength after reaching the maximum load.

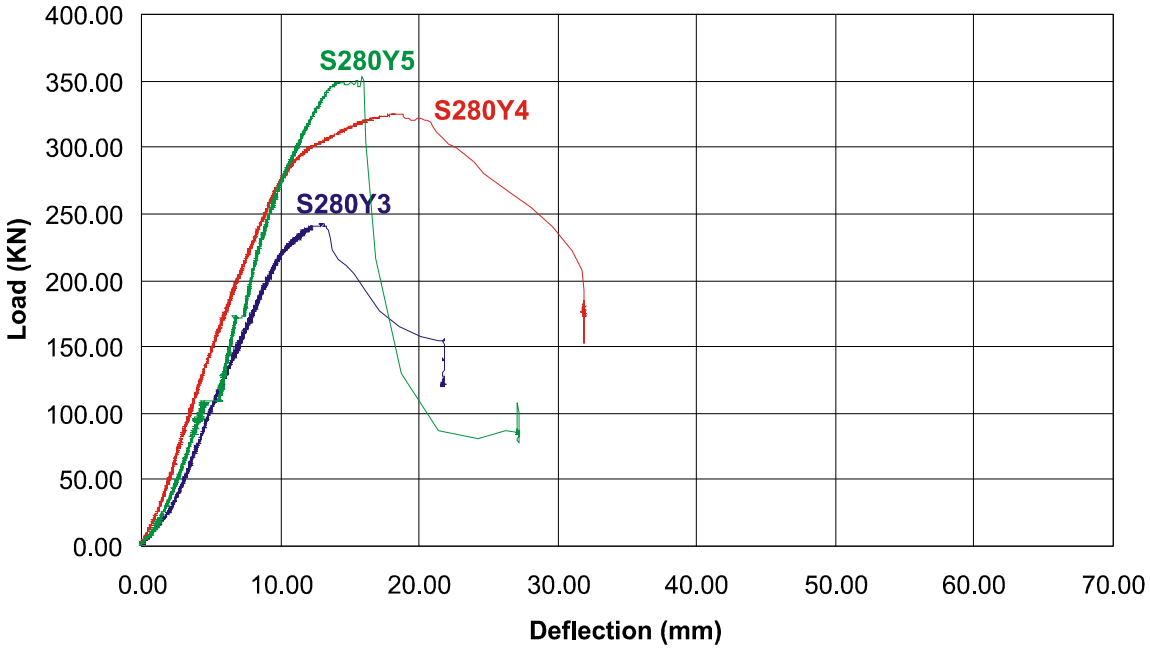

Figure 3.4.2: Load-deflection response of solid slabs

Figure 3.4.3 compares the experimental shear strength to characteristic values predicted by three design codes of practice discussed in *Chapter 2*, with material properties presented in *Table 3.2.2*. This figure clearly illustrates that the shear strength of beam S280Y3 is lower than expected and does not follow the anticipated trend. The reason for the difference could be a result of the typical scatter expected from experimental shear tests as discussed in *Paragraph 2.2*. Although the shear capacity for this beam is above that predicted by BS 8110 and SANS 10100, EC2 over predicts its strength. It is concluded that this beam had a lower than average shear strength.

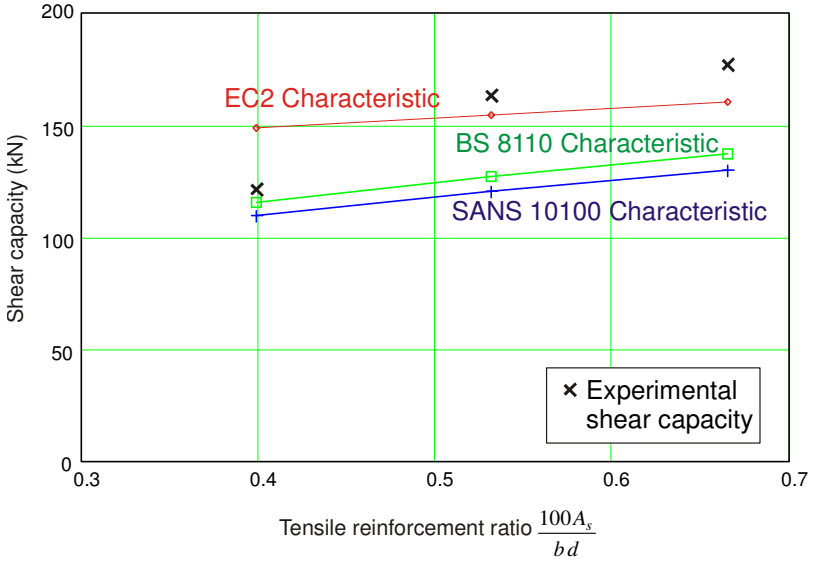

Figure 3.4.3: Shear capacity of 280 mm solid slabs compared to characteristic predicted values

Comparison of solid and Cobiax slabs

Figures 3.4.4 to 3.4.6 compare the load-deflection responses of 280 mm solid samples to that of the Cobiax samples. The peak loads achieved by the solids samples were higher than that of the Cobiax samples with the exception of one specimen, S280Y3.

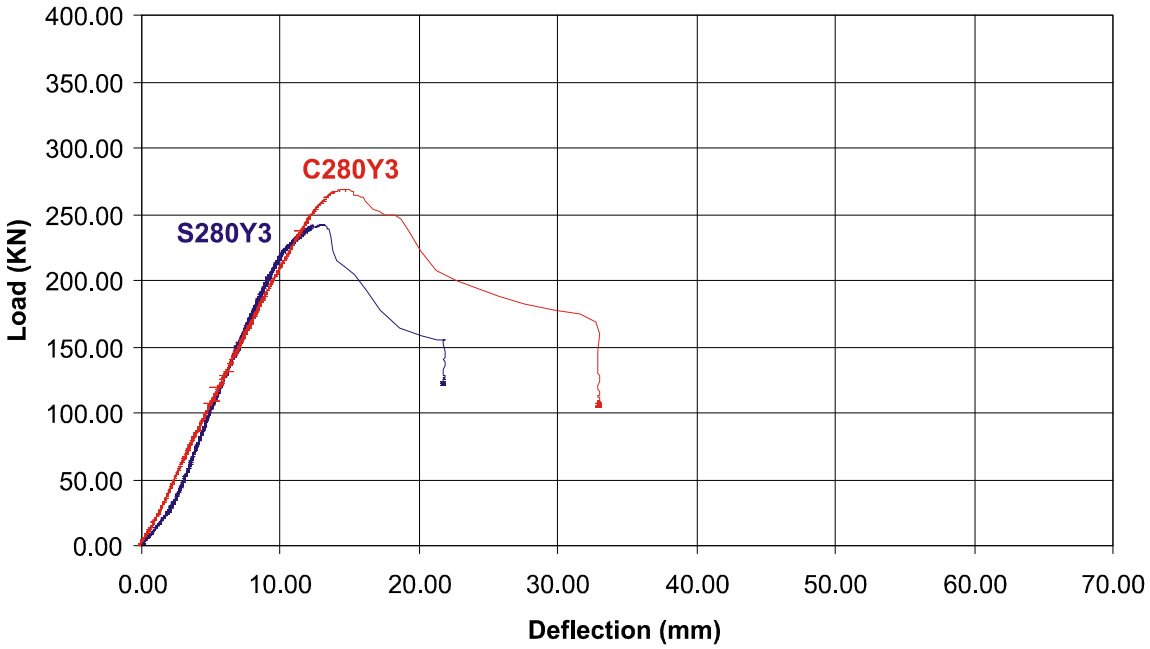

Figure 3.4.4: Load-deflection response of 280 mm slabs with 3 Y16's

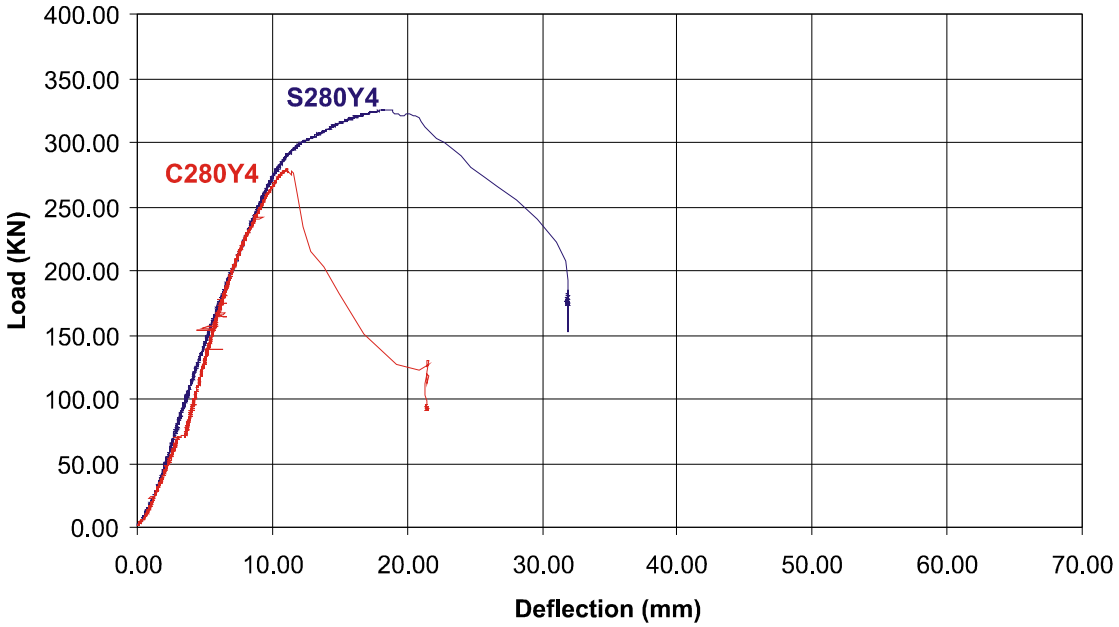

Figure 3.4.5: Load-deflection response of 280 mm slabs with 4 Y16's

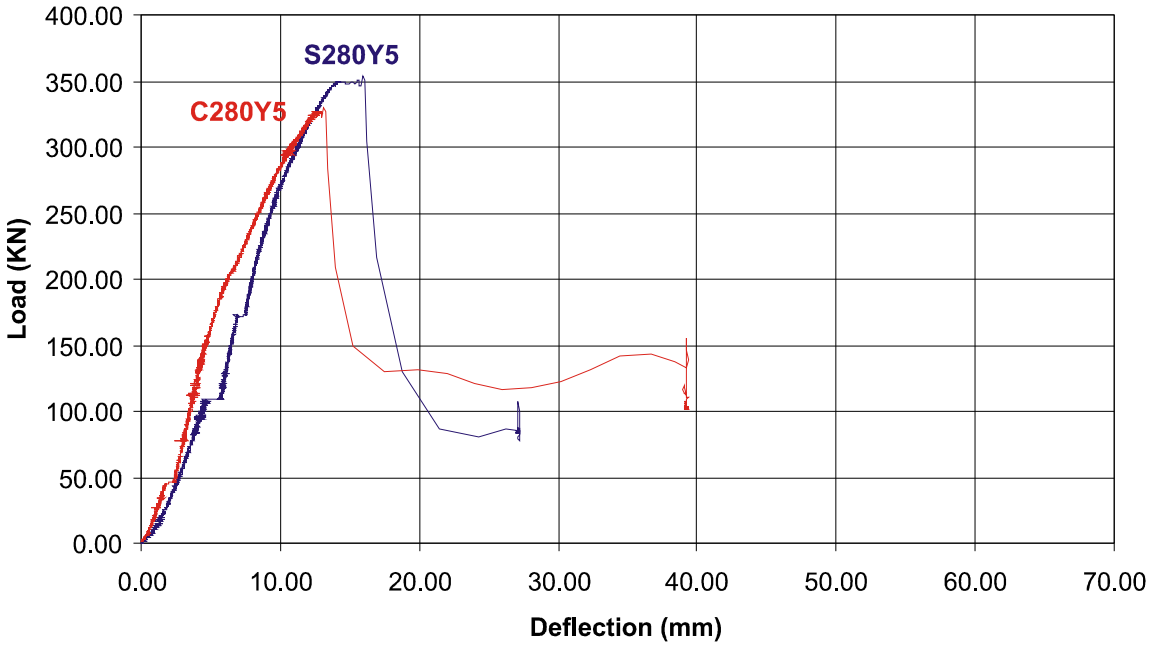

Figure 3.4.6: Load-deflection response of 280 mm slabs with 5 Y16's

The minimum Cobiax to solid slab capacity ratio obtained was 0.857 MPa.

Interesting to note is that the Cobiax slabs (see *Figures 3.4.4 to 3.4.8*) also resist the applied loads up to certain peak values, yet then tend to display more ductile behaviour than solid slabs without shear reinforcement, for two out of three cases, as the load decreases. This behaviour could also be

seen during a sample test, where the solid samples began to show shear cracks and then suddenly collapsed, compared to the Cobiax slabs that started to show shear cracks that opened much wider, allowing more deflection to occur. More Cobiax and solid samples are to be compared with regards to this ductile behaviour before any final conclusions can be made. It should be borne in mind that this higher ductility in the Cobiax slab specimens is of no real benefit, since the ductile behaviour occurs at a reduced load.

The observed ductility is not characteristic of a shear failure in beams without shear reinforcement and can only be attributed to the presence of the vertical legs of the Cobiax cages acting partially as shear reinforcement. Where the 45º angle crack crosses the path of these vertical bars, the vertical bars tend to hold the concrete on both sides of the crack together for much longer, until these bars are torn out of the concrete or sheared off.

Remainder of Cobiax slabs

The load deflection response of the remaining Cobiax slabs with thicknesses of 295mm and 310mm are illustrated in *Figures 3.4.7 and 3.4.8* respectively. The failure mode is similar to that observed for the 280 mm Cobiax slabs. Following the reduction in the peak load, a lower load value is reached, which remains constant for a significant deflection, indicating a greater ductility than observed for the 280 mm solid slabs.

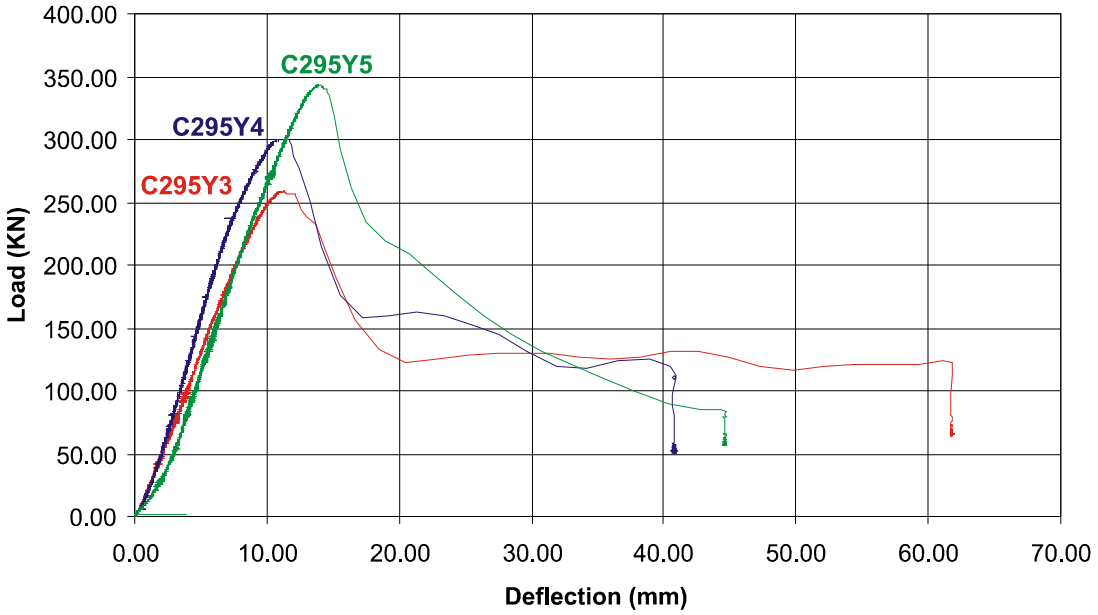

Figure 3.4.7: Load-deflection response of 295 mm Cobiax slabs

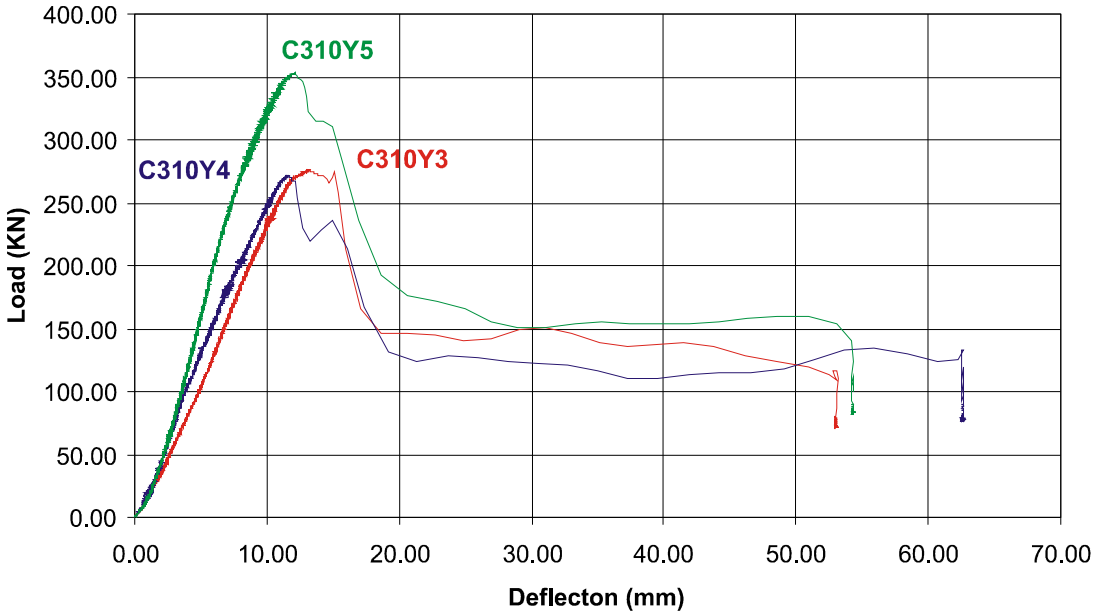

Figure 3.4.8: Load-deflection response of 310 mm Cobiax slabs

3.5. JUSTIFICATION OF RESULTS

The main observations from the results were:

1. The experimental results were significantly higher than predicted using characteristic material strengths.
2. The Cobiax results were higher than the values predicted using the actual material strengths and applying the 0.55 factor to the equivalent solid slab strength.
3. In one scenario the strength of the Cobiax beam even exceeded that of the equivalent solid slab.

Cases 1 and 2 will be discussed and the results justified:

1. The foremost reason for the significant difference between the values calculated before the experiment and the experimental results is that the concrete and reinforcement steel were much stronger than what was designed for. A ready-mix was used and the slump was adjusted due to a misunderstanding. The result was a much higher 13 day strength than was anticipated.

   The steel yield strength was also much higher than anticipated. The preliminary calculations have been done using $f_{cu} = 30\,MPa$ and $f_y = 450MPa$, but the actual values, as can be seen in *Table 3.5.1* and *Table 3.5.2*, were $f_{cu} = 45.1MPa$ and $f_y = 558.75MPa$. Beam specimens were also tested to establish the tension strength of the concrete.

Table 3.5.1 Concrete test cubes and beam results

Concrete			
Cube No	**MPa**	**Beam No**	**MPa**
A1	45.30	**B1**	2.23
A2	42.30	**B2**	3.70
A3	47.70	**B3**	3.35
Mean	**45.10**	**Mean**	**3.09**

Table 3.5.2 Steel test results

Steel						
	Size	**Yield Stress (MPa)**	**Tensile Stress (MPa)**	**Elongation (%)**	**Area (mm^2)**	**Length (m)**
C1	Y10	565	690	22	76.8	13
C2	Y10	530	645	20	76.2	13
C3	Y10	520	640	21	76.6	13
C4	Y10	620	720	21	77.6	13
Mean		**558.75**	**673.75**	**21**	**76.8**	**13**

The calculations had to be re-done using the actual material strengths and, as shown in *Table 3.5.3,* the failure loads were much closer to the experimental values (See *Figure 3.5.1*). K can be obtained from *Equation 2.11.1*.

Table 3.5.3 Comparison between predicted moment failure loads and shear failure loads based on actual values

SANS10100					
fcu =	45.1	**MPa**	**Cover**	20	**mm**
fy =	558.75	**MPa**	**AY16**	201	**mm^2**
b =	600	**mm**			
L =	1350	**mm**	**γm**	1.0	
K =	0.156		**γmc**	1.0	
Solid	**Height (mm)**	**d (mm)**	**Pm (kN)**	**Ps (kN)**	**Failure Mode**
280Y3	280	252	242	228	Shear
280Y4	280	252	319	251	Shear
280Y5	280	252	394	270	Shear
295Y3	295	267	257	234	Shear
295Y4	295	267	339	257	Shear
295Y5	295	267	419	277	Shear
310Y3	310	282	272	239	Shear
310Y4	310	282	359	263	Shear
310Y5	310	282	444	283	Shear

Pm =	Failure load for Flexure	
Ps =	Failure load for shear	
Failure mode	**"Moment"**	Beam will fail in flexure
	"Shear"	Beam will fail in shear

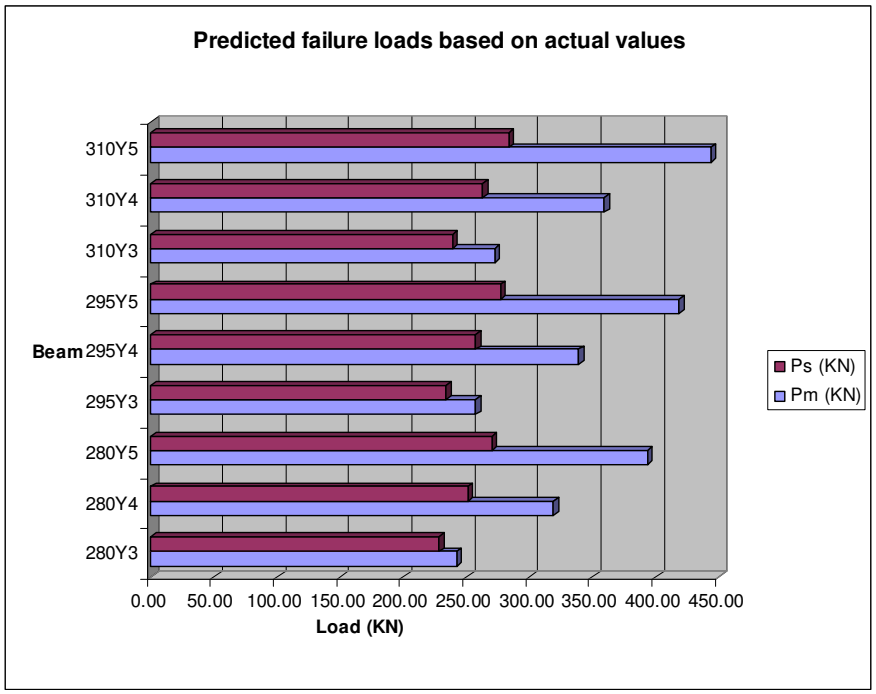

Figure 3.5.1 Predicted moment failure and shear failure loads based on design values

The P_{sc} values in *Tables 3.5.4 & 5* are the predicted failure loads for the Cobiax slabs based on previous research. Both the maximum TUD research factor (0.85) and minimum research factor (0.55) were used in the graphs (Schellenbach-Held and Pfeffer, 1999). Where the actual failure load values in column 2 of the tables exceeded the predicted German shear values, further investigation were required. So far Cobiax slab designers used the minimum shear value with 55% of the shear capacity of that of a solid slab with equal thickness and reinforcement strength and content.

In order to compare the SANS 10100, Eurocode 2 and test results, the results predicted by Eurocode2 was calculated as well, using *Equation 2.5.1*. *Table 3.5.4* and *3.5.5* display the SANS 10100 test results and EC 2 test results respectively.

Table 3.5.4 Comparison between test results and values predicted by SANS 10100

SANS10100					
fcu =	45.1	MPa	Cover	20	mm
fy =	558.75	MPa	AY16	201	mm²
b =	600	mm	γm	1.0	
L =	1350	mm	γmc	1.0	
	Actual Failure load	Predicted loads (kN)			
Beam	Pu (kN)	Ps (kN)		Psc (kN)	
			λcob =	0.85	0.55
S280Y3	242	228	-	-	-
S280Y4	326	251	-	-	-
S280Y5	354	270	-	-	-
C280Y3	268	228	C280Y3	186	121
C280Y4	279	251	C280Y4	205	133
C280Y5	330	270	C280y5	221	143
C295Y3	259	234	C295Y3	191	123
C295Y4	301	257	C295Y4	210	136
C295Y5	343	277	C295Y5	226	146
C310Y3	276	239	C310Y3	195	126
C310Y4	271	263	C310Y4	215	139
C310Y5	353	283	C310Y5	231	150

Pu =	Experimental failure load
Ps =	Failure load for an equivalent solid beam SANS 10100
Psc =	Failure load for a Cobiax slab = Factor x Ps
λcob =	Cobiax factor for shear capacity reduction

Table 3.5.5 Comparison between test results and values predicted by EUROCODE 2

EUROCODE 2					
fcu =	45.1	MPa	Cover	20	mm
fy =	558.75	MPa	AY16	201	mm²
b =	600	mm	τRd	0.581	
L =	1350	mm	γm	1.0	

	Actual failure load (KN)	Predicted loads (kN)			
Beam	Pu (kN)	Ps (kN)	Cobiax®	Psc (kN)	
			λcob =	0.85	0.55
S280Y3	242	322	-	-	-
S280Y4	326	335	-	-	-
S280Y5	354	347	-	-	-
C280Y3	268	322	C280Y3	274	177
C280Y4	279	335	C280Y4	284	184
C280Y5	330	347	C280y5	295	191
C295Y3	259	335	C295Y3	285	184
C295Y4	301	348	C295Y4	296	191
C295Y5	343	360	C295Y5	306	198
C310Y3	276	348	C310Y3	296	191
C310Y4	271	360	C310Y4	306	198
C310Y5	353	373	C310Y5	317	205

Pu =	Experimental failure load
Ps =	Failure load for an equivalent solid beam SANS 10100
Psc =	Failure load for a Cobiax slab = Factor x Ps
λcob =	Cobiax factor for shear capacity reduction

where:

$$\tau Rd = 0.035\left(\frac{1}{1.5}\right)^{-2/3} f_{cu}^{\,2/3}\text{, unitless}$$

From the above tables it is once again clear that SANS 10100 is more conservative in predicting shear failure. This should be noted where the actual shear failure loads of the solid samples are compared to the predicted values for solid samples. *Figure 3.5.2* and *3.5.3* show the comparisons made in *Table 3.5.4* and *3.5.5* respectively, taking λcob equal to 0.85. From *Figure 3.5.3* it can further be noted that EC 2 tends to be more conservative for a higher tension reinforcement content as well. One might argue that EC 2 is not conservative for low reinforcement content.

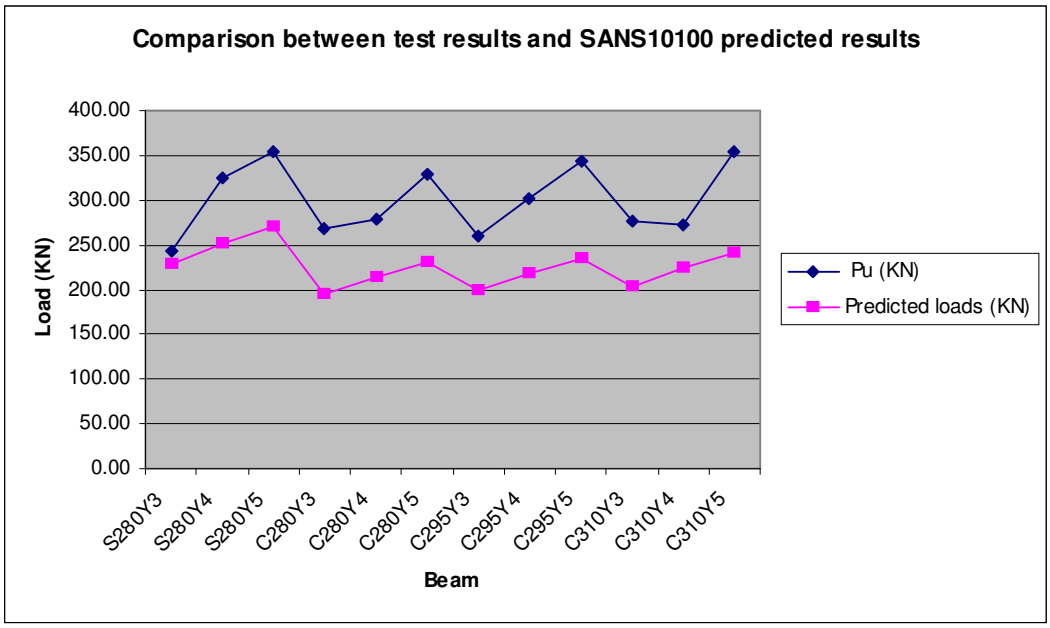

Figure 3.5.2 Comparison between predicted shear failure values and test results (SANS 10100)

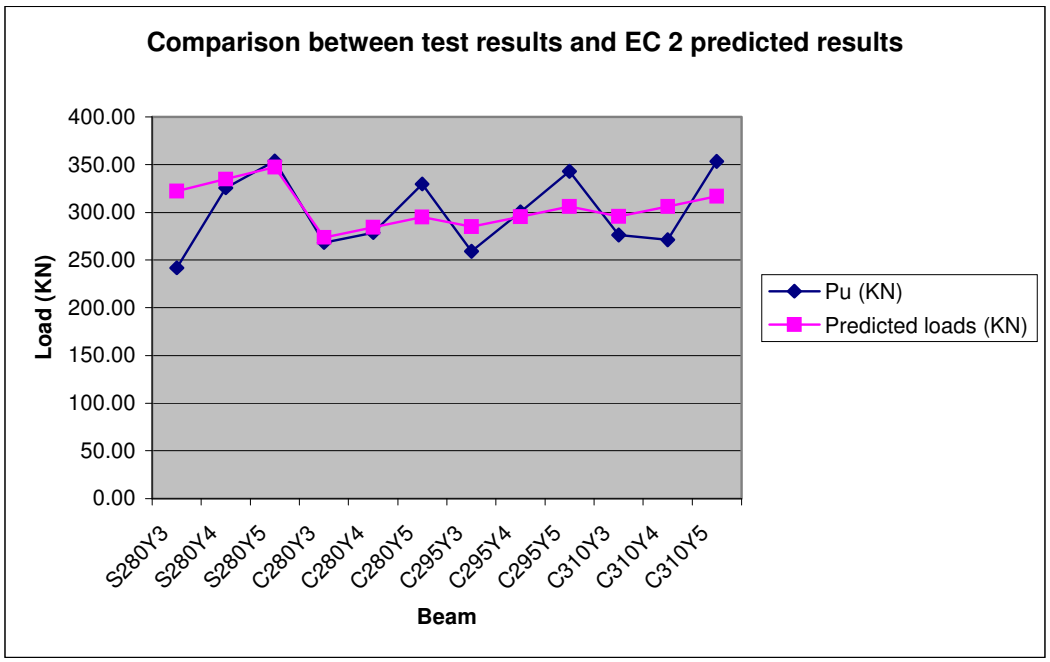

Figure 3.5.3 Comparison between predicted shear failure values and test results (EC 2)

2. Several years ago during the initial Cobiax research the steel cages currently used were not yet implemented. The fact that the Cobiax results are so high implies that the cages are contributing as shear reinforcement, in other words, increasing the shear capacity. It appears that the loss in shear capacity as a result of less aggregate interlock is compensated for by the increased capacity provided by the steel cages.

   Referring back to the experimental breaking loads (P_u) in *Table 3.5.4*, by dividing the failure load of the Cobiax sample by that of the solid sample with the same thickness and reinforcement content, 1.11, 0.86, and 0.93 are the ratios obtained. This amplifies the very essence of the shear research being done here. All three these ratios are much higher than the 0.55 ratio obtained from research in Germany where no steel cages were present in the testing samples. Therefore the steel cages must have some contribution to the shear capacity of a Cobiax slab, that has been discarded up to now.

   To verify the above statements, calculations were done according to SANS 10100 to obtain the shear resistance provided by the cages.

   The cages were fabricated using 5 mm diameter high tensile steel with a nominal yield stress of 450 MPa. The spacing of the cage bars in the vertical plane alternated between 41 mm and 159 mm. An average spacing of 100 mm was used for calculation purposes. The vertical cage bars were welded to the longitudinal bars in the cage (See *Figure 3.5.4*). Semi-spheres with cages cut in half were introduced to the sides of the samples. The longitudinal section shown below shows the true vertical cage dimensions for both the cut-in-half and full cages.

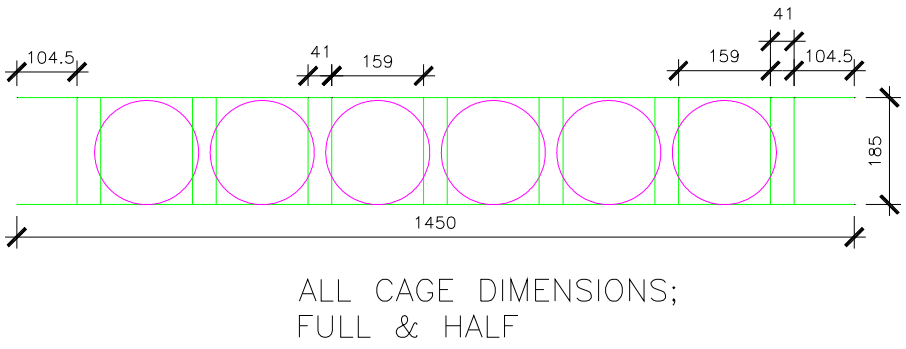

Figure 3.5.4 Cage spacing and dimensions

The maximum spacing permitted by SANS 10100 is 0.75 d = 0.75 x 252 = 189 mm. The maximum spacing of 159 mm spacing is less than this limit. SANS 10100 also requires a minimum amount of shear reinforcement calculated with $\frac{A_{sv}}{s_v} \geq 0.0012b$ where s_v = 100mm on average.

Then:

$A_{sv} = s_v*0.0012*600 = 72\ mm^2$

The shear reinforcement provided is 6 Y5 bars.

Then:

$A_{sv} = \frac{6*\pi*5^2}{4} = 117.8\ mm^2 > 72\ mm^2$

The shear reinforcement provided is more than what is required, therefore the only requirement not met is that the shear reinforcement must be anchored around the tension reinforcement. Yet, one can reason that some degree of anchorage is obtained via the welds of the vertical cage bars to the horizontal cage bars in the tension zone, and the horizontal bars will obtain a small degree of anchorage in this zone, which will drastically reduce when the weld fails under large loads.

Should one try to accommodate the shear resistance of these vertical cage bars, an approach could have been to subtract the shear resistance provided by the cages from the experimental results to obtain the capacity provided by the voided concrete. However, the resulting capacity will become unrealistically low when compared to earlier research. It is therefore concluded that the cages increase the shear capacity but not to the full possible value that could have been obtained by properly anchored shear links. This comment is confirmed when studying the load-deflection results that show a failure pattern tending more towards that of a brittle failure, than a ductile failure that would be expected in the presence of fully anchored shear reinforcement.

The following conclusions can be made in terms of the cages' influence:

- The cages provide additional longitudinal reinforcement which will increase the shear capacity v_c. This was conservatively ignored in preceding calculations, since it is

usually very poorly anchored, taken that the spot welds, connecting the vertical cage bars to the horizontal cage bars in the tension zone of the concrete, can easily fail.

- The presence of the vertical transverse bars in the cages add to the shear capacity v_s. They have met the requirement for maximum spacing and minimum reinforcement but were not anchored around the main reinforcing bars. Because of this, the vertical bars will add capacity to the aggregate interlock, but not as much to the dowel action. Therefore, the full value v_s predicted by the design code cannot be used.

It appears from this research that the 0.55 factor currently used may be too conservative. Comparing experimental results of the 280 mm slabs, this factor appears to be closer to 0.85. If this factor is applied to the design capacity obtained for an equivalent rectangular slab, the design should be sufficiently safe as illustrated in *Figure 3.5.5*. For these results, the smallest factor of safety will be 1.77.

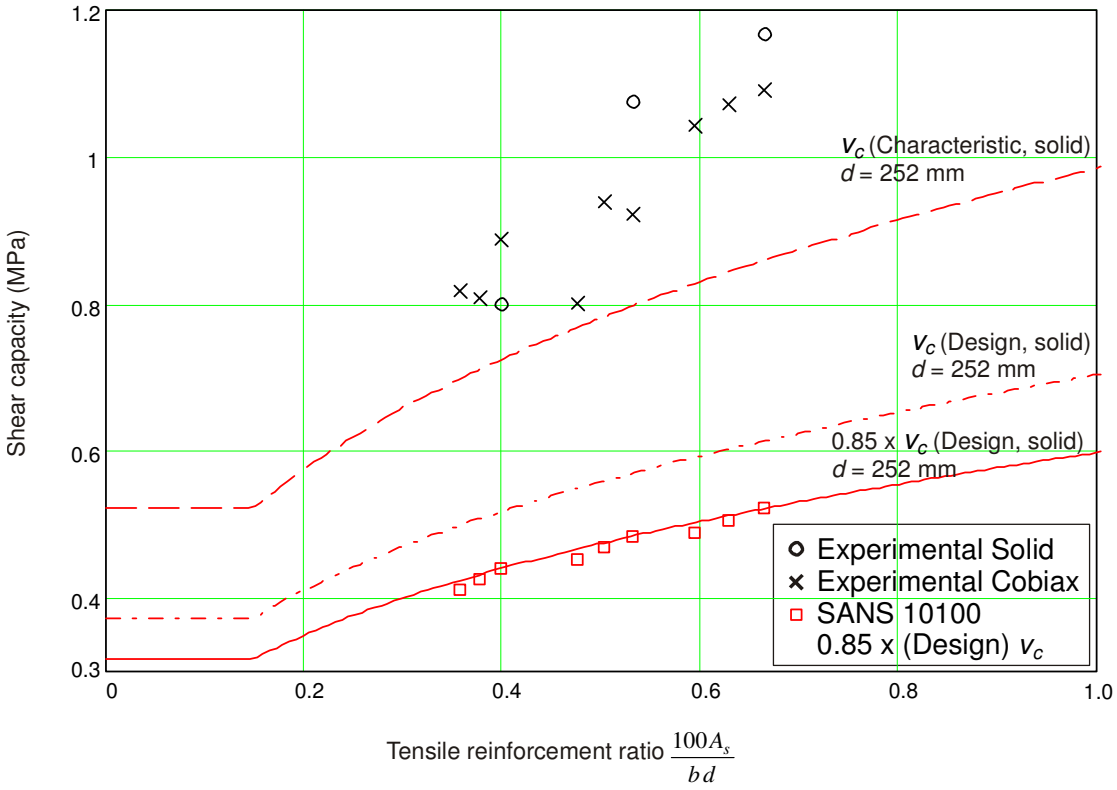

Figure 3.5.5 Design shear capacity of Cobiax slabs

Table 3.5.6 illustrates the shear resistance that fully anchored cages would have provided. *Equation 2.4.4* was used.

Table 3.5.6 Shear resistance of cages

SANS10100					
fcu =	45.1	MPa	Cover	20	mm
fy =	558.75	MPa	AY16 =	201	mm²
fyv =	450	MPa	AY5 =	19.63	mm²
b =	600	mm	γm	1.0	
L =	1350	mm	γmc	1.0	
sv =	100	mm	K =	0.156	

					Cage Resistance			
Solid	Height (mm)	d (mm)	Y16's	Asv (mm²)	Y5's	Asv (mm²)	Vs (KN)	Ps (KN)
280Y3	280	252	3	603	6	118	133.6	267
280Y4	280	252	4	804	6	118	133.6	267
280Y5	280	252	5	1005	6	118	133.6	267
295Y3	295	267	3	603	6	118	141.5	283
295Y4	295	267	4	804	6	118	141.5	283
295Y5	295	267	5	1005	6	118	141.5	283
310Y3	310	282	3	603	6	118	149.5	299
310Y4	310	282	4	804	6	118	149.5	299
310Y5	310	282	5	1005	6	118	149.5	299

Vs =	Shear resistance provided by cages
Ps =	Shear load resistance provided by cages = 2Vs

Comparing *Table 3.5.4* with *Table 3.5.6* it is clear that the shear resistance added to a solid slab with Cobiax cages inside should have more than doubled up the capacity of the sample strength. This can be visualised by adding the *Ps* value from *Table 3.5.4* to that of *Table 3.5.6*. The theoretical vertical point load at the centre of the beam (*Ps*) has been obtained by doubling the theoretical shear reinforcement capacity (*Vs*). This will approximately be true for a simply supported beam with a point load in the centre, where only vertical shear reinforcement has the ability to resist shear (off course this is not the case in reality, but *Ps* is nevertheless required for calculations to follow).

The question arises what the capacity would have been of Cobiax samples without cages, plus the *Ps* value in *Table 3.5.6*? Should the value be higher than the *Pu* value in *Table 3.5.4*, it would be a clear indication that some of the shear capacity of the vertical cage bars does not contribute to the shear strength, and the best reason being that these bars are not fully anchored around the tension reinforcement. At the TUD they only considered aggregate interlock, with the absence of some aggregate along a 45º angle through the Cobiax slab, to contribute to shear capacity (Schellenbach-Held and Pfeffer, 1999). This area of aggregate interlock was established as follows:

There are two full and two half spheres in a cross section as shown by *Figure 3.2.1*. This means a total area of three spheres. In the cross section, the sphere is a circle with a maximum diameter of 180mm.

$$A_{circle} = \pi r^2$$

where:

r = radius of circle

The effective area that provides aggregate interlock in a Cobiax slab is:

$$A_{eff} = bd - 3A_{circle}$$

This is for a cross section that is perpendicular to the plan view of the beam. To compensate for the extra area that will be available because of a 30 or 45° crack, a further factor has to be introduced. To be conservative, a 45° angle is assumed which will produce the smallest increase in area, therefore:

$$A_{eff} = \lambda_{area} bd - 3A_{circle}$$

with:

$$A_{circle} = \pi r^2$$

$$\lambda_{area} = \frac{1}{\sin 45^\circ} = 1.41 = \text{slope area increasing factor}$$

where:

$r = 90mm$

The effective shear resistance is then:

$$V_{ceff} = V_c Eff.Ratio$$

where:

$$Eff.Ratio = \frac{A_{eff}}{bd}$$

The force required to cause a V_{ceff} shear value will yield values similar to those found in *Table 3.5.4* under the $0.55P_{sc}$ column. This is simply because the effective ratio derived above will be in the vicinity of 0.55 for a worst case scenario. The TUD researchers therefore ignored the compression

block and dowel-action, and only concentrated on the loss of aggregate interlock along the 45º plane of a typical shear crack (Schellenbach-Held and Pfeffer, 1999).

In *Table 3.5.7* the contribution of fully anchored vertical cage bars (P_s), the theoretical force required to break a Cobiax slab where only aggregate interlock contributes to shear resistance ($0.55P_{sc}$), and the two forces added together (Pt) are displayed. These P_t forces should have been equal to that of the actual breaking loads (P_u) of the various samples, should the vertical cage bars at all have been fully anchored around the tension reinforcement. Since the P_t values are greater than the P_u values, it shows that the vertical bars are not fully anchored.

A rough estimate of how effective the vertical cage bars are, can be obtained by the following calculation:

$(P_u - 0.55P_{sc})/P_s$

According to this calculation the vertical bars are roughly between 44% to 70% effective in shear. This conclusion should be approached with great caution, since theoretical and test results were mixed, as well as the contribution of other shear resistance parameters has been ignored, like dowel-action.

The better way to test the effectiveness of these vertical bars will be to break several solid samples with and without the cages placed inside, with no spheres present whatsoever. The contribution to shear capacity of the cages will then be clearly demonstrated from the empirical test results.

Table 3.5.7 Rough indication of the cages` shear capacity

Cobiax	Ps (kN)	0.55Psc (kN)	Pt (kN)	Pu (kN)	(Pu – 0.55Psc)/Ps
280Y3	267	121	388	268	0.553
280Y4	267	133	400	279	0.548
280Y5	267	143	410	330	0.700
295Y3	283	123	406	259	0.479
295Y4	283	136	419	301	0.582
295Y5	283	146	429	343	0.695
310Y3	299	126	425	276	0.502
310Y4	299	139	438	271	0.442

3.6. CONCLUSION

The main conclusion of this chapter is that the shear reduction factor for Cobiax flat slabs can be increased from 0.55, to at least 0.86, in accordance with the test results discussed. This increase in the shear reduction factor is accepted to be the result of the presence of the Cobiax steel cages (previously omitted at the TUD) in the test samples. Although it has been shown that the steel cages' vertical bars do not contribute as much to the shear strength as fully anchored shear reinforcement, the cages indeed increased the shear capacity of the Cobiax slabs.

Firstly the conclusion is of importance to demonstrate that the 0.55 shear reduction factor can conservatively be applied when designing Cobiax slabs in accordance with SANS 10100. Secondly this opens up the opportunity to utilise higher shear reduction factors, that might benefit the feasibility of Cobiax slabs. This second statement will require further investigation before it can be accepted and implemented into the design of Cobiax slabs.

Interesting to note from this chapter is that the EC 2 calculation for the shear resistance of slabs without shear reinforcement is less conservative than that of SANS 10100. When comparing the theoretical design code results with the laboratory test results, EC 2 tends to provide the designer with slightly more accurate results though.

The feasibility study of Cobiax flat slabs, discussed in *Chapter 4*, could be conducted with ease of mind that the utilisation of the 0.55 shear reduction factor would not compromise the integrity of a Cobiax slab design in accordance with SANS 10100.

2.15. CONCLUSION

The content of this chapter indicated that numerous similarities and differences exist between design codes for concrete beams and slabs. The difference in answers for shear resistance of concrete beams is marginal though.

The strength and serviceability design procedures of SANS 10100, BS 8110 and EC 2 for concrete flat slabs can be applied to Cobiax flat slabs, with applicable adjustment factors to Cobiax slabs due to its unique cross-section.

Various analysis methods for concrete flat slabs have also been discussed. The remainder of this report will utilise finite element analysis methodology to establish the difference in cost between Cobiax, coffer and post-tensioned flat slabs in accordance with SANS 10100. This cost comparison will only be applicable to the South African environment.

3. EXPERIMENTAL WORK – SHEAR IN COBIAX SLABS

3.1. INTRODUCTION

In this chapter the task was to compare theoretical calculations for the shear strength of Cobiax slabs (discussed in Chapter 2) with force controlled shear tests performed on laboratory Cobiax slab specimens. This comparison had to be conducted to establish the shear strength reduction factor for a Cobiax slab, compared with a solid slab with the same thickness, tension reinforcement and concrete properties.

A Cobiax shear strength reduction factor of 0.55 times (Schellenbach-Held and Pfeffer, 1999) the shear strength of a concrete slab without shear reinforcement had been calculated at the Technical University of Darmstadt (TUD) in Germany. The Cobiax steel cages were omitted in the TUD tests. The objective of this chapter was to demonstrate that the presence of the steel cages holding the Cobiax spheres in position during construction, will act as shear reinforcement inside the slab, resulting in a less conservative shear strength reduction factor.

This method of multiplying the shear capacity of a solid slab with a shear strength reduction factor to obtain the shear strength of that slab with internal spherical voids, is a simplified method best supported by empirical test results. This method seems to be the easiest way to support the design engineer with answers for shear in Cobiax slabs, and also a faster way to predict shear strength when conducting a cost comparison between different slab types, as done in *Chapter 4* of this report.

Predicting the shear behaviour in concrete slabs with internal spherical voids is actually far more complex and could probably best be approached with powerful finite element software using three dimensional brick elements and non-homogenous material (concrete and steel reinforcement). One could with multiple analyses of different scenarios (slab content and dimensions) develop formulae that are typical for concrete slabs with internal spherical voids. This approach or a similar complex approach will not be conducted for the purposes of this report.

The experimental work comprised of the testing of twelve beam specimens of equal length and width, but having varying thicknesses and quantities of tension reinforcement, some with Cobiax spheres, and some solid. All beams, simulating strips of 600mm wide flat-slabs, were designed to fail in shear before failing in flexure, to allow for conclusions to be drawn regarding their shear capacities.

The samples were manufactured in Bloemfontein and transported to Pretoria on the day prior to testing. Three 150 x 150 cubes and three 150 x 150 x 700 beams were also manufactured and then tested on the same day as the sample beams so that the representative 13 day compression and flexural strengths could be established.

Due to casting and laboratory constrains the tests had to be carried out 13 days after casting. However, the age of testing has little significance seeing that all the tests were carried out on the same day. All predicted capacities are also based on the 13 day concrete strengths.

3.2. PREPARATION AND EXPERIMENTAL SETUP

Experimental Design

- A total of twelve sample beams were manufactured, each beam having a length of 1500 mm and a width of 600 mm.
- Three solid beams (without Cobiax spheres) were cast as well, having depths of 280 mm. In these beams the tension steel content was varied, each one having 3, 4 and 5 Y16 bars, respectively.
- For the 180 mm diameter Cobiax spheres used in the other 9 samples, the concrete webs or spheres were spaced at 200 mm centres in every sample. The beams were therefore dimensioned to contain two whole spheres in the centre, and two half spheres at the sides of every Cobiax sample. Every beam cross-section therefore contained 3 identical webs, central to the beam. (See Figure 3.2.1).

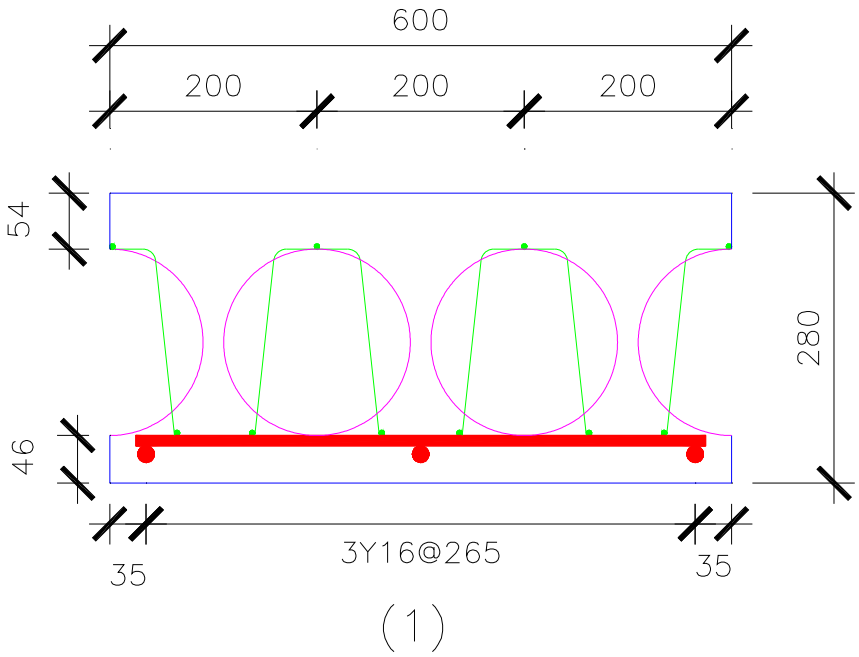

Figure 3.2.1 Cross section of a 280 mm thick Cobiax sample

- Three depths of 280, 295 and 310 mm were prepared for the Cobiax samples, with varying reinforcement quantities of 3, 4 and 5 Y16 bars for each depth. Details of the beams are presented in *Paragraph 3.5*.
- Cobiax cages (displayed in green in *Figure 3.2.1*) consist of 1 top and 2 bottom longitudinal bars, kept in place by transverse bars. Both the longitudinal and vertical bars of the cage will clearly contribute to the shear resistance. From a theoretical point of view these bars should be removed to obtain a true comparison between a solid slab and a voided slab containing spheres. However, this would result in some practical problems keeping the spheres in position during construction. On the other hand, the cages will always be present in a Cobiax slab, and it was therefore decided to use the Cobiax system exactly as it will be used in practice. It should be noted that vertical cage bars are not fully anchored around the main reinforcing bars when considering SABS 0144:1995 curtailment specifications. For this reason they will only partially contribute to the aggregate interlock capacity, and their contribution will reduce drastically after the welds between the vertical bars and bottom horizontal bars of the cages fail under large loads.

The following factors were considered in the parameter selection to investigate the design of the experimental setup:

- As stated in *Paragraph 2.2,* beams without shear reinforcement is likely to fail in shear before failing in flexure if the a_v / d ratio is less than approximately 6.

where:

a_v = distance of a single point load to the face of the support

d = effective depth of the tension reinforcement

It is therefore normal practice in beam design to provide shear reinforcement to increase the shear capacity so that flexural failure will happen before shear failure. The largest quantity of shear reinforcement will be required for an a_v / d ratio of approximately 2.5 to 4 (see discussion in Section 2). The a_v / d ratios for the beams were therefore kept within these limits to be able to produce conservative results. The actual ratios for the experimental beams are given in *Table 3.2.1*, with *H* the slab thickness.

Table 3.2.1 $\frac{a_v}{d}$ ratios

H (mm)	a_v (mm)	d (mm)	a_v/d
280	687.5	252	2.73
295	687.5	267	2.57
310	687.5	282	2.44

- For smaller $\frac{a_v}{d}$ ratios, arch action will increase the shear capacity of the beam, which is not desirable for the purpose of this research.
- The test apparatus was limited to a 600 mm wide slab.
- The beams had to be manufactured in Bloemfontein and then transported over a distance of 460km to Pretoria, having the effect of preparation of as small as possible samples to enable handling and transportation. The weight of every sample varied between 600 and 750 kg.
- The larger and heavier the samples were, the more difficult it would have been to position the beams correctly during the experimental setup.
- Budget constrains were also applicable.

The beams were simply supported with a span of 1350 mm (see *Photo 3.2.1* and *Figure 3.2.2*). Each sample's longitudinal centreline was aligned with the longitudinal centreline of the supports. The distance from the beam end to the centre of the support was 75mm. The knife edge load (P_u) was applied at the sample's midspan. The samples were tested in force control at a rate of 40 kN/min. Experience show that this rate is acceptable and will result in negligible dynamic effects. The failure

criterion is easily observed with a sudden drop in the applied force with a deflection that remains constant. Throughout the test the applied loads at midspan, as well as the displacements, were measured at 25 readings per second (25Hz).

Photo 3.2.1: Experimental setup

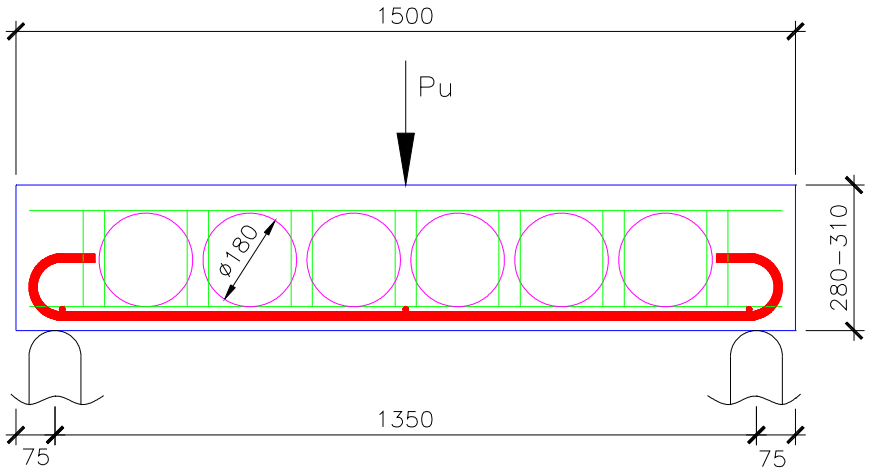

Figure 3.2.2 Experimental setup

The flexural capacity for each sample was calculated to ensure that shear failure would precede flexural failure. The results are presented in *Table 3.2.2*. *Figure 3.2.3* shows the results in graph format. These results are only an indication of the properties that will be required in the samples. The correct material properties are displayed later in this chapter. *Equations 2.4.1 to 2.4.3a* were used with all partial material safety factors set to unity.

- The slab thickness was varied by increasing the depth of the top flange, but keeping the thickness of the bottom flange constant for all beams. This was done to simulate construction practice.
- Reinforcement variation was decided on to assess the influence of tension reinforcement on the shear capacity.
- The reason for material factors being set to unity is to calculate the actual strength rather than the design strength.

Table 3.2.2 Comparison between moment failure loads and shear failure loads based purely on design values

SANS 10100					
fcu =	30	**MPa**	**Cover**	20	**mm**
fy =	450	**MPa**	**AY16 =**	201	**mm²**
b =	600	**mm**	**γm**	1.0	Material factor - Moment
L =	1350	**mm**	**γmc**	1.0	Material factor - Shear
Solid	**Height (mm)**	**d (mm)**	**Pm (kN)**	**Ps (kN)**	**Failure Mode**
280Y3	280	252	194	199	Moment
280Y4	280	252	254	219	Shear
280Y5	280	252	313	236	Shear
295Y3	295	267	206	204	Shear
295Y4	295	267	270	225	Shear
295Y5	295	267	333	242	Shear
310Y3	310	282	218	209	Shear
310Y4	310	282	286	230	Shear
310Y5	310	282	353	247	Shear
Pm =	Failure load for flexure (midspan point load)				
Ps =	Failure load for shear (midspan point load)				
Failure mode =	**"Moment" =**	Beam will fail in flexure			
	"Shear" =	Beam will fail in shear			

In *Table 3.2.2* the definitions of the symbols not explained in the table itself are:

fcu = characteristic concrete cube compression strength

fy = steel reinforcement yield strength

b = width of the specimen

L = span of the specimen

AY16 = area of a 16 mm diameter steel reinforcement bar

d = centroid depth of the tension reinforcement, measured from the top of the beam

The legends, for example *280Y3*, can be explained as follows:

280 = total thickness of the beam

Y3 = amount of steel reinforcement bars in the beam, spreaded over the 600 mm width

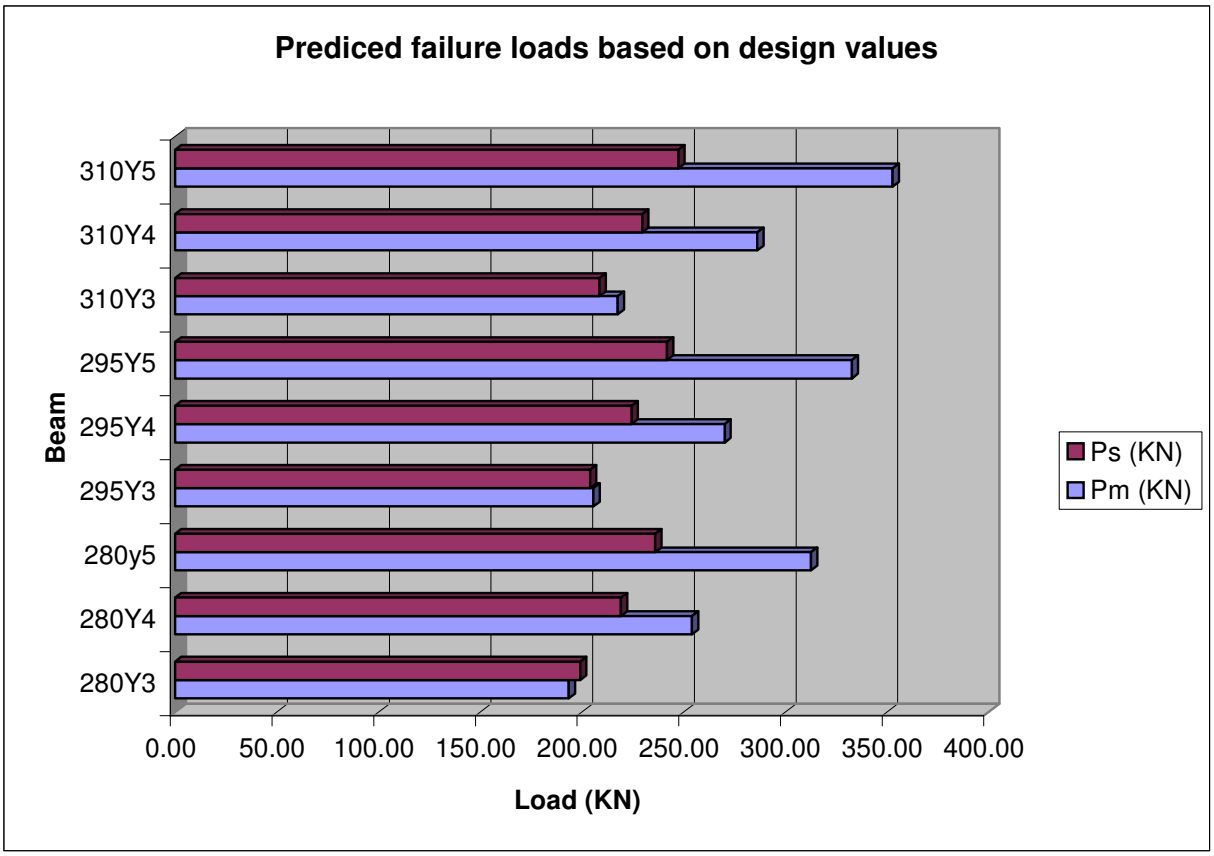

Figure 3.2.3 Predicted moment failure and shear failure loads based on design values

The Cobiax beams were expected to have a lower shear capacity than the solid beams. All calculations for the solid beams showed that shear failure would precede or happen simultaneously to flexural failure, and it was therefore concluded that the Cobiax beams would display a similar behaviour.

The depth of the stress block in flexure for the Cobiax beams never exceeded the minimum depth of the top flange during this research. For the 280 mm deep beam, the minimum depth of the top flange is 50 mm. The method used to design Cobiax slabs are for this reason the same as for solid slabs, where the presence of the voids only reduces the own-weight and slightly reduces the slab stiffness, as well as shear capacity.

The calculations indicated that the 280 mm solid slab with 3 Y16's (S280Y3) could fail in flexure before failing in shear. However, normally the flexural reinforcement will enter the work-hardening zone, and the flexural capacity will increase beyond that in shear. This configuration was accepted for this reason.

Sample Preparation

The samples were manufactured at Peri Wiehahn's premises in Bloemfontein. Following construction of the formwork, the tension reinforcement was positioned in the boxes, and the cages containing the Cobiax spheres were fixed to the tension reinforcement. The semi spheres were fixed to sides of the formwork boxes. Prior to casting, inspections were performed to ensure that all elements were correctly positioned in accordance with the design drawings.

The concrete was poured during the following day. A first concrete layer of approximately 70 mm was poured to ensure the tension reinforcement and bottom bars of the Cobiax cages were embedded by at least 20 mm. This prevented the spheres from floating to the top during casting, since they could not escape the cages that were then anchored in the bottom 70 mm of hardened concrete. This first concrete layer added sufficient dead weight to hold all components down during the second pour to the top of the slab. Lifting of cages would result in a smaller d value, that would extinguish the hope of any trustworthy results. The second and final pour was done approximately 4 hours later.

The second pour's concrete were utilised to construct the test cubes and beams, to ensure that a representative sample of the concrete forming the compression block (top concrete) was collected.

3.3. OBSERVATIONS

As can be seen from *Photos 3.3.1*, the shear cracks started from bending cracks in the case of the solid slabs. This is common for $2.5 < \frac{a_v}{d} < 6.0$.

In the case of the Cobiax slabs though, the crack sometimes started at the web, and then further developed down and back to the support along the tension reinforcement and also upwards to the top of the beam towards the line of load application. These observations are well justified by the predictions of Park & Paulay (1975). (See *Paragraph 2.2*)

Solid slab crack *Cobiax slab crack*

Photo 3.3.1: Observed crack patterns at failure

3.4. RESULTS

The following table is a summary of the failure loads obtained for each sample.

Table 3.4.1 Beams tested and results obtained
S = Solid slab
C = Cobiax Slab
Y3 = 3 x Y16 bars
Load = Load applied by hydraulic press for failure to occur

Beam	Load (kN)
S280Y3	242
S280Y4	326
S280Y5	354
C280Y3	268
C280Y4	279
C280Y5	330
C295Y3	259
C295Y4	301
C295Y5	343
C310Y3	276
C310Y4	271
C310Y5	353

Figure 3.4.1 shows the failure loads of all samples compared to SANS 10100 characteristic shear capacity (with $\lambda_{mv} = 1$) calculated for a solid section. The solid and Cobiax samples all exceeded the predicted capacity. From these results it would appear as if no reduction in capacity is required for the Cobiax slabs. However, further investigations were required in terms of material properties before any such conclusions could be made.

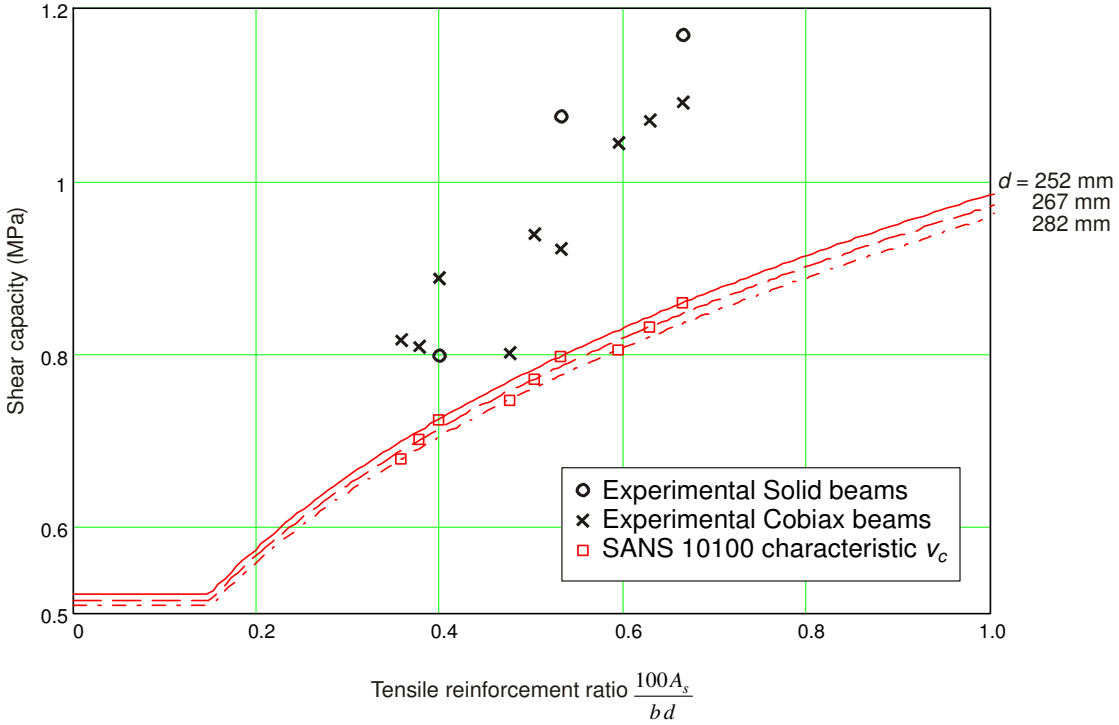

Figure 3.4.1: Failure stress of all beams compared to SANS 10100 characteristic shear capacity.

More detailed results are presented in the following sections, supported by a discussion on the observed behaviour.

Solid slabs

The load-deflection response of the solid slabs is illustrated in *Figure 3.4.2*. The behaviour is mostly brittle with an almost linear behaviour up to the peak load. After obtaining the peak load, there is a rapid reduction in resistance, characteristic of a shear failure. The exception is S280Y4 which exhibits a softening behaviour before reaching the peak load and a more gradual reduction in strength after reaching the maximum load.

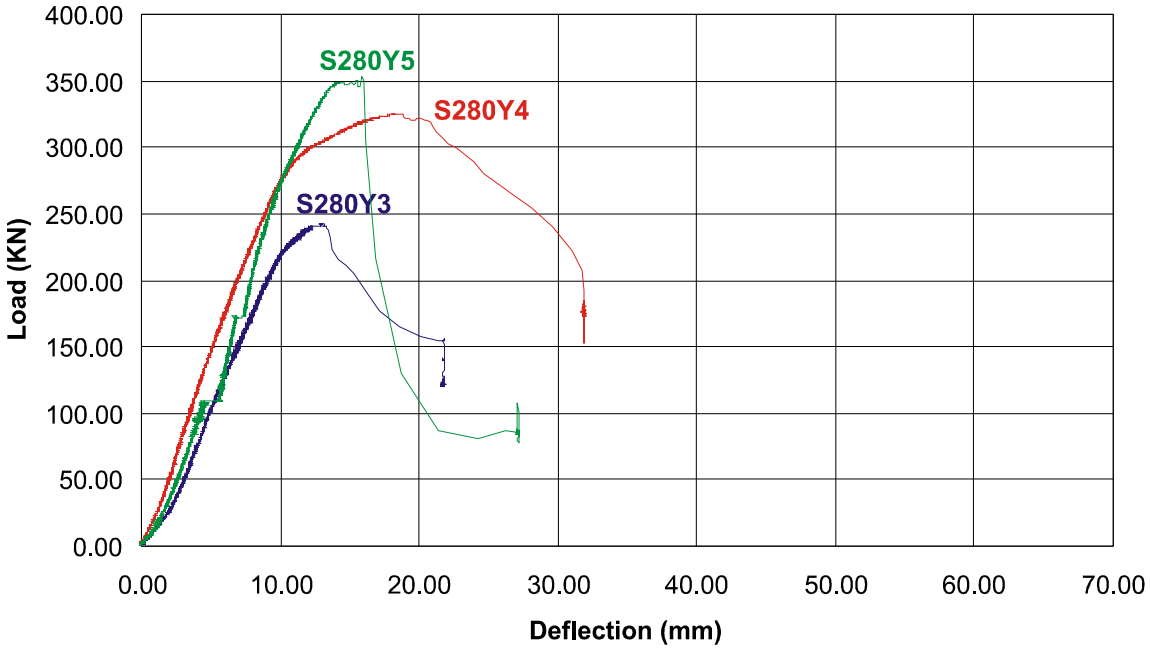

Figure 3.4.2: Load-deflection response of solid slabs

Figure 3.4.3 compares the experimental shear strength to characteristic values predicted by three design codes of practice discussed in *Chapter 2*, with material properties presented in *Table 3.2.2*. This figure clearly illustrates that the shear strength of beam S280Y3 is lower than expected and does not follow the anticipated trend. The reason for the difference could be a result of the typical scatter expected from experimental shear tests as discussed in *Paragraph 2.2*. Although the shear capacity for this beam is above that predicted by BS 8110 and SANS 10100, EC2 over predicts its strength. It is concluded that this beam had a lower than average shear strength.

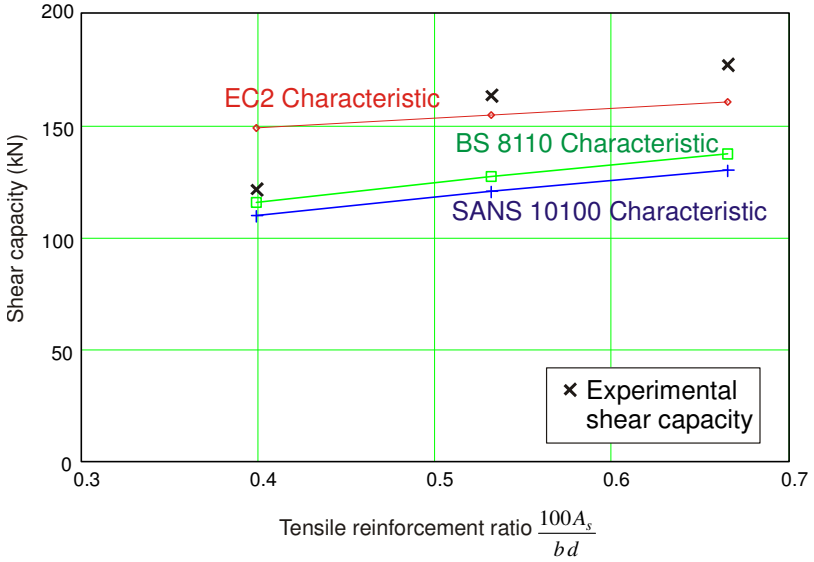

Figure 3.4.3: Shear capacity of 280 mm solid slabs compared to characteristic predicted values

Comparison of solid and Cobiax slabs

Figures 3.4.4 to 3.4.6 compare the load-deflection responses of 280 mm solid samples to that of the Cobiax samples. The peak loads achieved by the solids samples were higher than that of the Cobiax samples with the exception of one specimen, S280Y3.

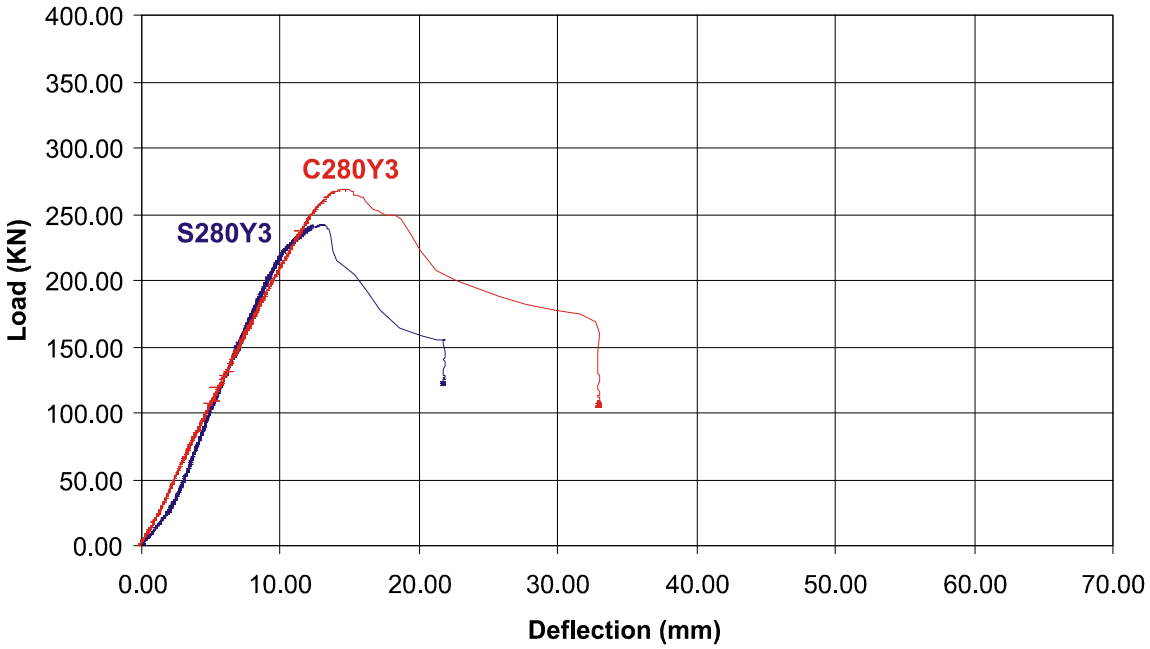

Figure 3.4.4: Load-deflection response of 280 mm slabs with 3 Y16's

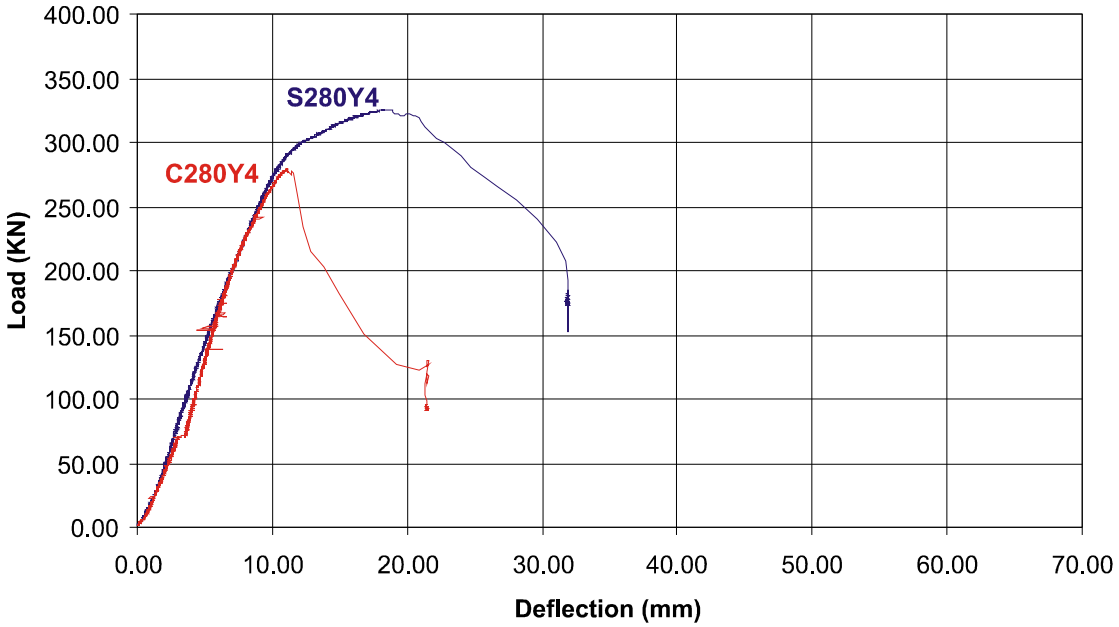

Figure 3.4.5: Load-deflection response of 280 mm slabs with 4 Y16's

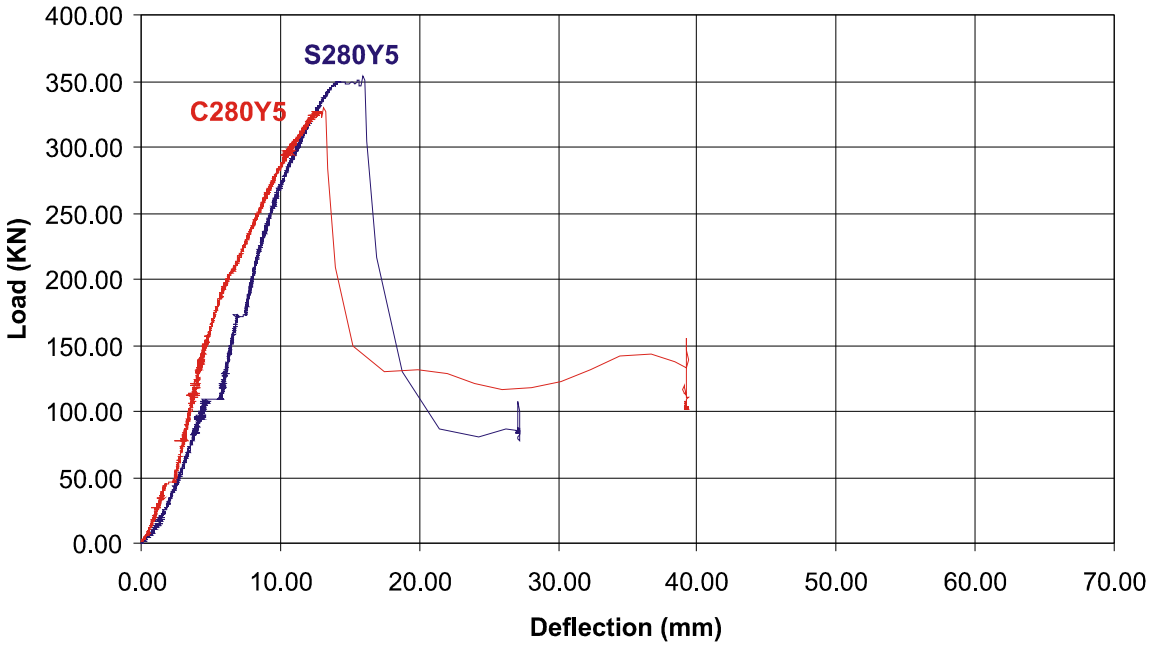

Figure 3.4.6: Load-deflection response of 280 mm slabs with 5 Y16's

The minimum Cobiax to solid slab capacity ratio obtained was 0.857 MPa.

Interesting to note is that the Cobiax slabs (see *Figures 3.4.4 to 3.4.8*) also resist the applied loads up to certain peak values, yet then tend to display more ductile behaviour than solid slabs without shear reinforcement, for two out of three cases, as the load decreases. This behaviour could also be

seen during a sample test, where the solid samples began to show shear cracks and then suddenly collapsed, compared to the Cobiax slabs that started to show shear cracks that opened much wider, allowing more deflection to occur. More Cobiax and solid samples are to be compared with regards to this ductile behaviour before any final conclusions can be made. It should be borne in mind that this higher ductility in the Cobiax slab specimens is of no real benefit, since the ductile behaviour occurs at a reduced load.

The observed ductility is not characteristic of a shear failure in beams without shear reinforcement and can only be attributed to the presence of the vertical legs of the Cobiax cages acting partially as shear reinforcement. Where the 45º angle crack crosses the path of these vertical bars, the vertical bars tend to hold the concrete on both sides of the crack together for much longer, until these bars are torn out of the concrete or sheared off.

Remainder of Cobiax slabs

The load deflection response of the remaining Cobiax slabs with thicknesses of 295mm and 310mm are illustrated in *Figures 3.4.7 and 3.4.8* respectively. The failure mode is similar to that observed for the 280 mm Cobiax slabs. Following the reduction in the peak load, a lower load value is reached, which remains constant for a significant deflection, indicating a greater ductility than observed for the 280 mm solid slabs.

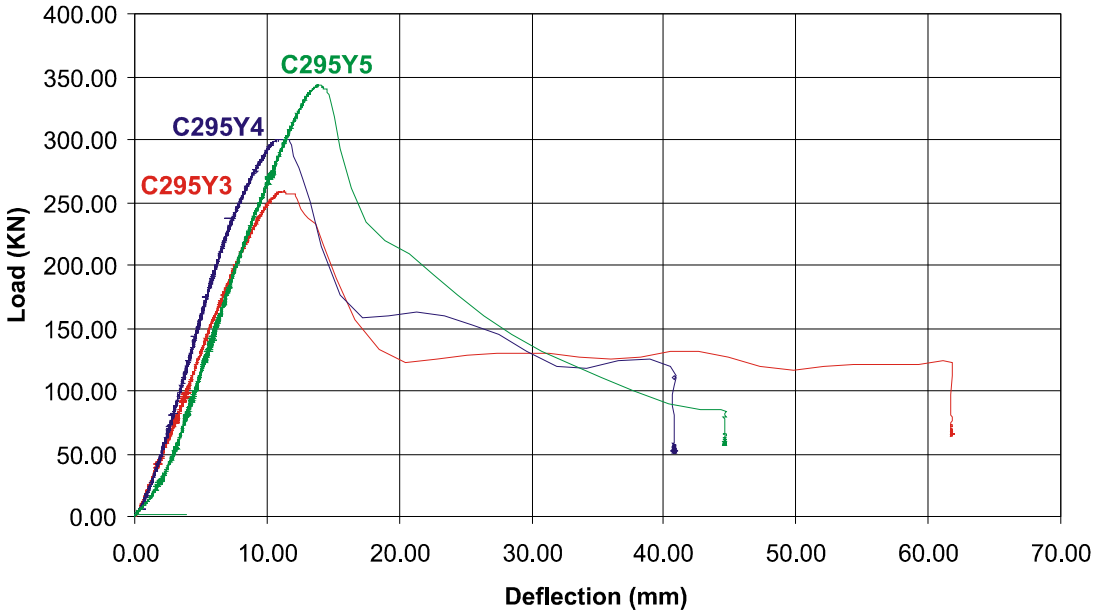

Figure 3.4.7: Load-deflection response of 295 mm Cobiax slabs

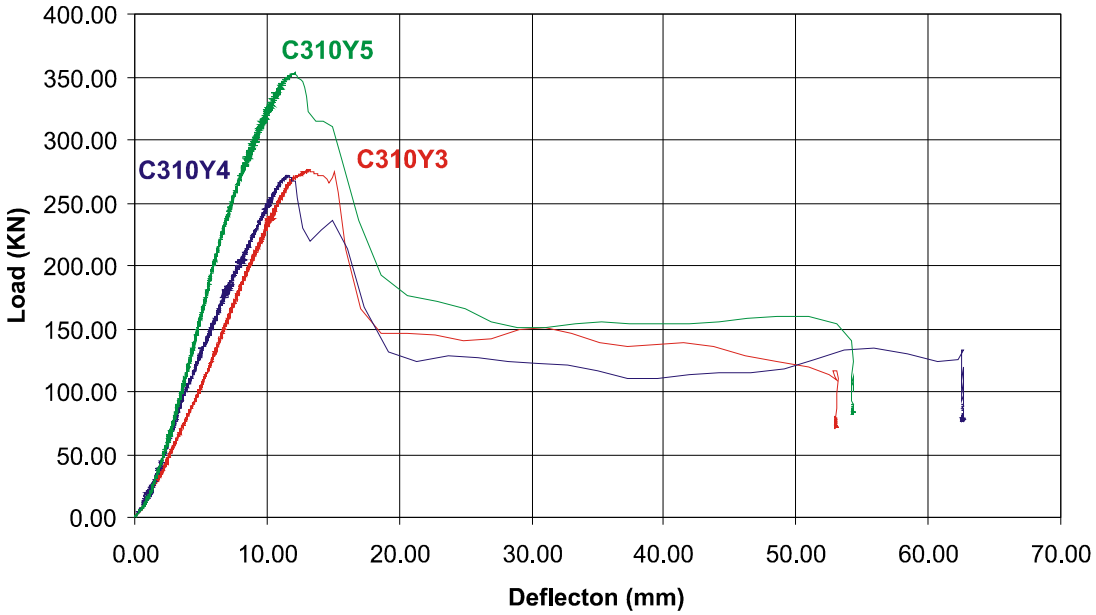

Figure 3.4.8: Load-deflection response of 310 mm Cobiax slabs

3.5. JUSTIFICATION OF RESULTS

The main observations from the results were:

1. The experimental results were significantly higher than predicted using characteristic material strengths.
2. The Cobiax results were higher than the values predicted using the actual material strengths and applying the 0.55 factor to the equivalent solid slab strength.
3. In one scenario the strength of the Cobiax beam even exceeded that of the equivalent solid slab.

Cases 1 and 2 will be discussed and the results justified:

1. The foremost reason for the significant difference between the values calculated before the experiment and the experimental results is that the concrete and reinforcement steel were much stronger than what was designed for. A ready-mix was used and the slump was adjusted due to a misunderstanding. The result was a much higher 13 day strength than was anticipated.

   The steel yield strength was also much higher than anticipated. The preliminary calculations have been done using $f_{cu} = 30\,MPa$ and $f_y = 450MPa$, but the actual values, as can be seen in *Table 3.5.1* and *Table 3.5.2*, were $f_{cu} = 45.1MPa$ and $f_y = 558.75MPa$. Beam specimens were also tested to establish the tension strength of the concrete.

Table 3.5.1 Concrete test cubes and beam results

Concrete			
Cube No	**MPa**	**Beam No**	**MPa**
A1	45.30	**B1**	2.23
A2	42.30	**B2**	3.70
A3	47.70	**B3**	3.35
Mean	**45.10**	**Mean**	**3.09**

Table 3.5.2 Steel test results

Steel						
	Size	**Yield Stress (MPa)**	**Tensile Stress (MPa)**	**Elongation (%)**	**Area (mm^2)**	**Length (m)**
C1	Y10	565	690	22	76.8	13
C2	Y10	530	645	20	76.2	13
C3	Y10	520	640	21	76.6	13
C4	Y10	620	720	21	77.6	13
Mean		**558.75**	**673.75**	**21**	**76.8**	**13**

The calculations had to be re-done using the actual material strengths and, as shown in *Table 3.5.3,* the failure loads were much closer to the experimental values (See *Figure 3.5.1*). K can be obtained from *Equation 2.11.1*.

Table 3.5.3 Comparison between predicted moment failure loads and shear failure loads based on actual values

SANS10100					
fcu =	45.1	**MPa**	**Cover**	20	**mm**
fy =	558.75	**MPa**	**AY16**	201	**mm^2**
b =	600	**mm**			
L =	1350	**mm**	**γm**	1.0	
K =	0.156		**γmc**	1.0	
Solid	**Height (mm)**	**d (mm)**	**Pm (kN)**	**Ps (kN)**	**Failure Mode**
280Y3	280	252	242	228	Shear
280Y4	280	252	319	251	Shear
280Y5	280	252	394	270	Shear
295Y3	295	267	257	234	Shear
295Y4	295	267	339	257	Shear
295Y5	295	267	419	277	Shear
310Y3	310	282	272	239	Shear
310Y4	310	282	359	263	Shear
310Y5	310	282	444	283	Shear

Pm =	Failure load for Flexure	
Ps =	Failure load for shear	
Failure mode	**"Moment"**	Beam will fail in flexure
	"Shear"	Beam will fail in shear

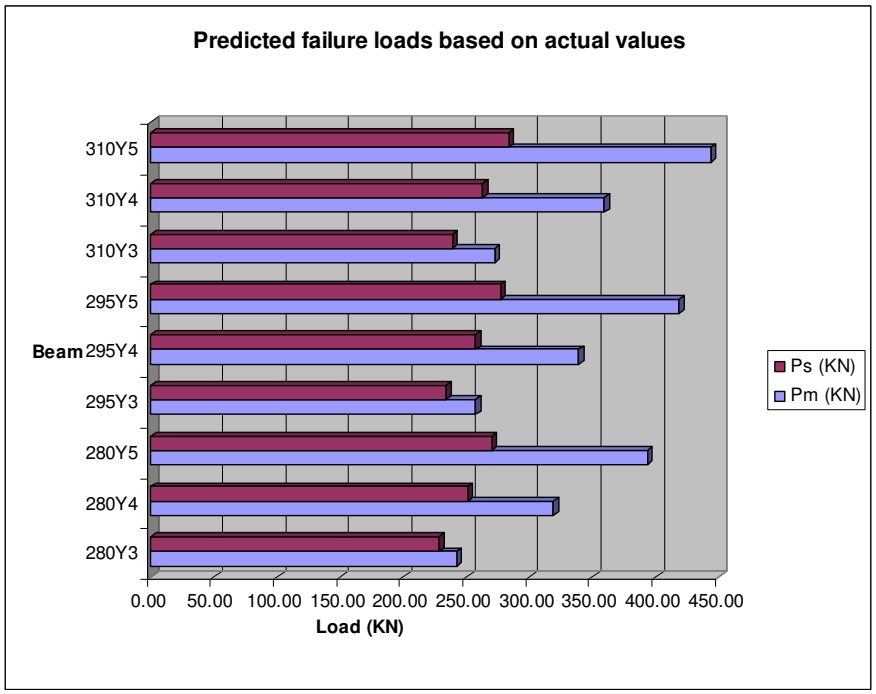

Figure 3.5.1 Predicted moment failure and shear failure loads based on design values

The P_{sc} values in *Tables 3.5.4 & 5* are the predicted failure loads for the Cobiax slabs based on previous research. Both the maximum TUD research factor (0.85) and minimum research factor (0.55) were used in the graphs (Schellenbach-Held and Pfeffer, 1999). Where the actual failure load values in column 2 of the tables exceeded the predicted German shear values, further investigation were required. So far Cobiax slab designers used the minimum shear value with 55% of the shear capacity of that of a solid slab with equal thickness and reinforcement strength and content.

In order to compare the SANS 10100, Eurocode 2 and test results, the results predicted by Eurocode2 was calculated as well, using *Equation 2.5.1*. *Table 3.5.4* and *3.5.5* display the SANS 10100 test results and EC 2 test results respectively.

Table 3.5.4 Comparison between test results and values predicted by SANS 10100

SANS10100					
fcu =	45.1	MPa	Cover	20	mm
fy =	558.75	MPa	AY16	201	mm²
b =	600	mm	γm	1.0	
L =	1350	mm	γmc	1.0	
	Actual Failure load	Predicted loads (kN)			
Beam	Pu (kN)	Ps (kN)		Psc (kN)	
			λcob =	0.85	0.55
S280Y3	242	228	-	-	-
S280Y4	326	251	-	-	-
S280Y5	354	270	-	-	-
C280Y3	268	228	C280Y3	186	121
C280Y4	279	251	C280Y4	205	133
C280Y5	330	270	C280y5	221	143
C295Y3	259	234	C295Y3	191	123
C295Y4	301	257	C295Y4	210	136
C295Y5	343	277	C295Y5	226	146
C310Y3	276	239	C310Y3	195	126
C310Y4	271	263	C310Y4	215	139
C310Y5	353	283	C310Y5	231	150

Pu =	Experimental failure load
Ps =	Failure load for an equivalent solid beam SANS 10100
Psc =	Failure load for a Cobiax slab = Factor x Ps
λcob =	Cobiax factor for shear capacity reduction

Table 3.5.5 Comparison between test results and values predicted by EUROCODE 2

EUROCODE 2					
fcu =	45.1	MPa	Cover	20	mm
fy =	558.75	MPa	AY16	201	mm²
b =	600	mm	τRd	0.581	
L =	1350	mm	γm	1.0	

	Actual failure load (KN)	Predicted loads (kN)			
Beam	Pu (kN)	Ps (kN)	Cobiax®	Psc (kN)	
			λcob =	0.85	0.55
S280Y3	242	322	-	-	-
S280Y4	326	335	-	-	-
S280Y5	354	347	-	-	-
C280Y3	268	322	C280Y3	274	177
C280Y4	279	335	C280Y4	284	184
C280Y5	330	347	C280y5	295	191
C295Y3	259	335	C295Y3	285	184
C295Y4	301	348	C295Y4	296	191
C295Y5	343	360	C295Y5	306	198
C310Y3	276	348	C310Y3	296	191
C310Y4	271	360	C310Y4	306	198
C310Y5	353	373	C310Y5	317	205

Pu =	Experimental failure load
Ps =	Failure load for an equivalent solid beam SANS 10100
Psc =	Failure load for a Cobiax slab = Factor x Ps
λcob =	Cobiax factor for shear capacity reduction

where:

$$\tau Rd = 0.035\left(\frac{1}{1.5}\right)^{-2/3} f_{cu}^{\,2/3}\text{, unitless}$$

From the above tables it is once again clear that SANS 10100 is more conservative in predicting shear failure. This should be noted where the actual shear failure loads of the solid samples are compared to the predicted values for solid samples. *Figure 3.5.2* and *3.5.3* show the comparisons made in *Table 3.5.4* and *3.5.5* respectively, taking λcob equal to 0.85. From *Figure 3.5.3* it can further be noted that EC 2 tends to be more conservative for a higher tension reinforcement content as well. One might argue that EC 2 is not conservative for low reinforcement content.

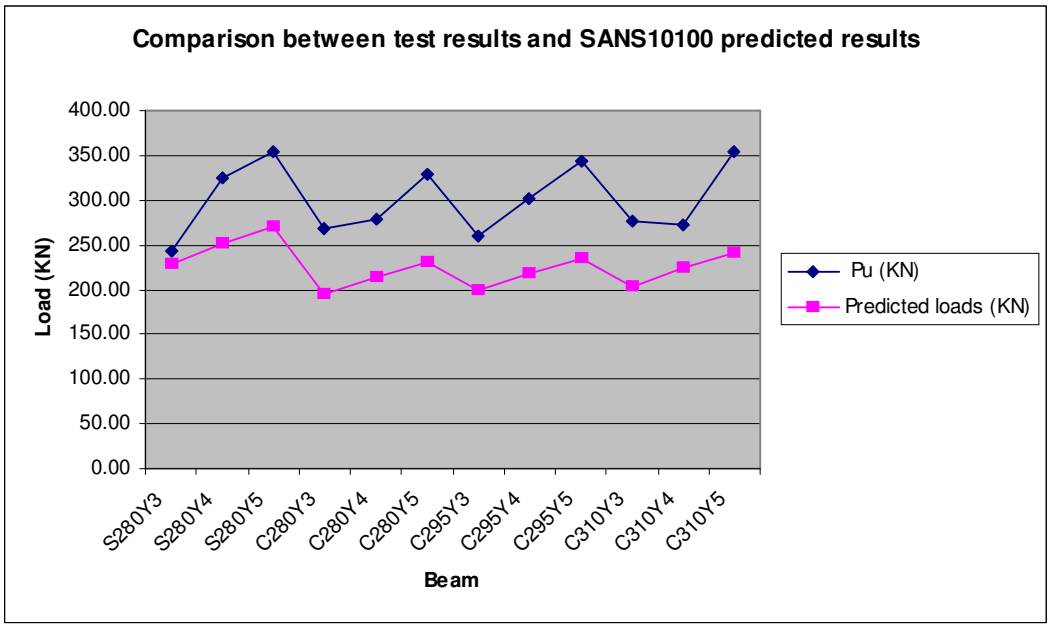

Figure 3.5.2 Comparison between predicted shear failure values and test results (SANS 10100)

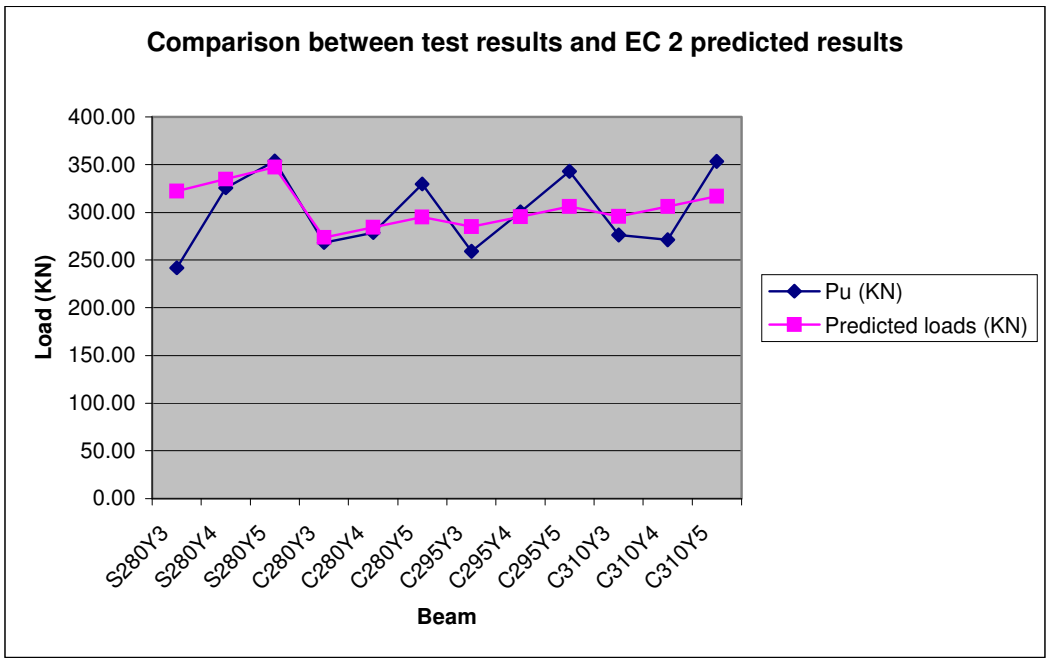

Figure 3.5.3 Comparison between predicted shear failure values and test results (EC 2)

2. Several years ago during the initial Cobiax research the steel cages currently used were not yet implemented. The fact that the Cobiax results are so high implies that the cages are contributing as shear reinforcement, in other words, increasing the shear capacity. It appears that the loss in shear capacity as a result of less aggregate interlock is compensated for by the increased capacity provided by the steel cages.

   Referring back to the experimental breaking loads (P_u) in *Table 3.5.4*, by dividing the failure load of the Cobiax sample by that of the solid sample with the same thickness and reinforcement content, 1.11, 0.86, and 0.93 are the ratios obtained. This amplifies the very essence of the shear research being done here. All three these ratios are much higher than the 0.55 ratio obtained from research in Germany where no steel cages were present in the testing samples. Therefore the steel cages must have some contribution to the shear capacity of a Cobiax slab, that has been discarded up to now.

   To verify the above statements, calculations were done according to SANS 10100 to obtain the shear resistance provided by the cages.

   The cages were fabricated using 5 mm diameter high tensile steel with a nominal yield stress of 450 MPa. The spacing of the cage bars in the vertical plane alternated between 41 mm and 159 mm. An average spacing of 100 mm was used for calculation purposes. The vertical cage bars were welded to the longitudinal bars in the cage (See *Figure 3.5.4*). Semi-spheres with cages cut in half were introduced to the sides of the samples. The longitudinal section shown below shows the true vertical cage dimensions for both the cut-in-half and full cages.

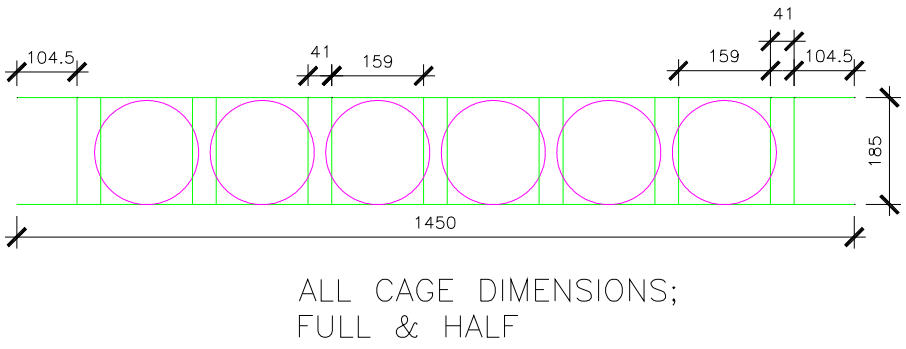

Figure 3.5.4 Cage spacing and dimensions

The maximum spacing permitted by SANS 10100 is 0.75 d = 0.75 x 252 = 189 mm. The maximum spacing of 159 mm spacing is less than this limit. SANS 10100 also requires a minimum amount of shear reinforcement calculated with $\frac{A_{sv}}{s_v} \geq 0.0012b$ where s_v = 100mm on average.

Then:

$A_{sv} = s_v*0.0012*600 = 72\ mm^2$

The shear reinforcement provided is 6 Y5 bars.

Then:

$A_{sv} = \frac{6*\pi*5^2}{4} = 117.8\ mm^2 > 72\ mm^2$

The shear reinforcement provided is more than what is required, therefore the only requirement not met is that the shear reinforcement must be anchored around the tension reinforcement. Yet, one can reason that some degree of anchorage is obtained via the welds of the vertical cage bars to the horizontal cage bars in the tension zone, and the horizontal bars will obtain a small degree of anchorage in this zone, which will drastically reduce when the weld fails under large loads.

Should one try to accommodate the shear resistance of these vertical cage bars, an approach could have been to subtract the shear resistance provided by the cages from the experimental results to obtain the capacity provided by the voided concrete. However, the resulting capacity will become unrealistically low when compared to earlier research. It is therefore concluded that the cages increase the shear capacity but not to the full possible value that could have been obtained by properly anchored shear links. This comment is confirmed when studying the load-deflection results that show a failure pattern tending more towards that of a brittle failure, than a ductile failure that would be expected in the presence of fully anchored shear reinforcement.

The following conclusions can be made in terms of the cages' influence:

- The cages provide additional longitudinal reinforcement which will increase the shear capacity v_c. This was conservatively ignored in preceding calculations, since it is

usually very poorly anchored, taken that the spot welds, connecting the vertical cage bars to the horizontal cage bars in the tension zone of the concrete, can easily fail.

- The presence of the vertical transverse bars in the cages add to the shear capacity v_s. They have met the requirement for maximum spacing and minimum reinforcement but were not anchored around the main reinforcing bars. Because of this, the vertical bars will add capacity to the aggregate interlock, but not as much to the dowel action. Therefore, the full value v_s predicted by the design code cannot be used.

It appears from this research that the 0.55 factor currently used may be too conservative. Comparing experimental results of the 280 mm slabs, this factor appears to be closer to 0.85. If this factor is applied to the design capacity obtained for an equivalent rectangular slab, the design should be sufficiently safe as illustrated in *Figure 3.5.5*. For these results, the smallest factor of safety will be 1.77.

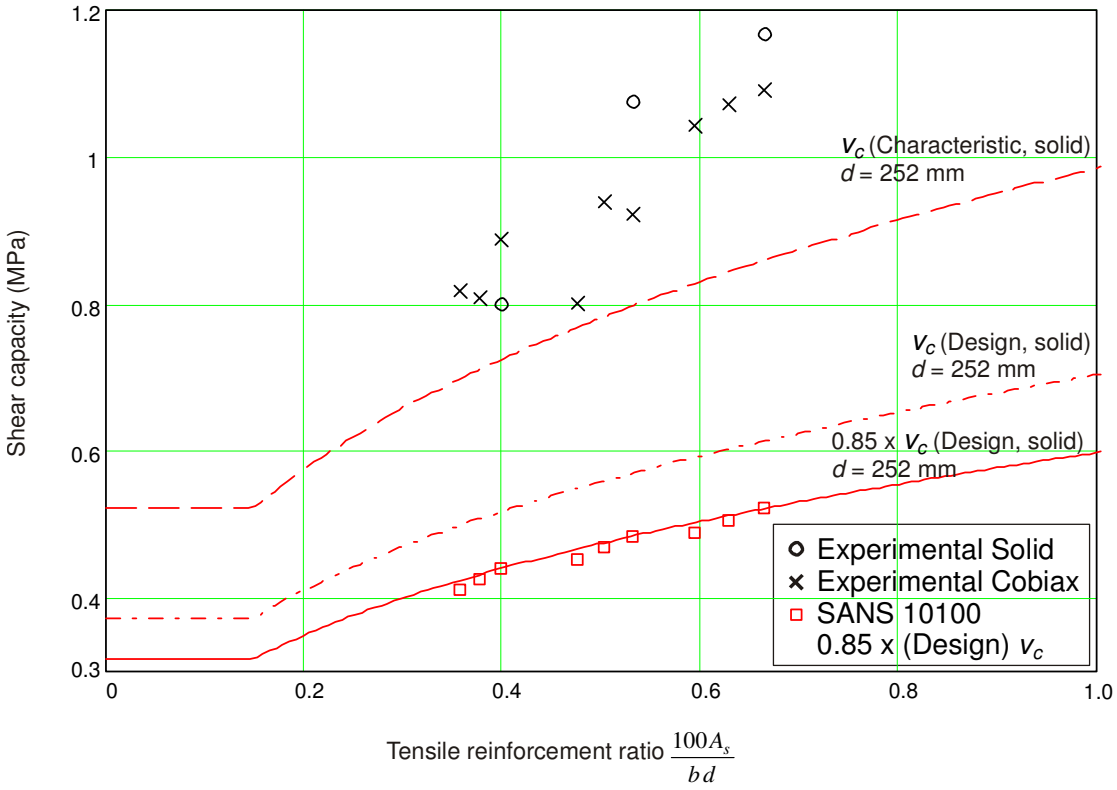

Figure 3.5.5 Design shear capacity of Cobiax slabs

Table 3.5.6 illustrates the shear resistance that fully anchored cages would have provided. *Equation 2.4.4* was used.

Table 3.5.6 Shear resistance of cages

SANS10100					
fcu =	45.1	MPa	Cover	20	mm
fy =	558.75	MPa	AY16 =	201	mm²
fyv =	450	MPa	AY5 =	19.63	mm²
b =	600	mm	γm	1.0	
L =	1350	mm	γmc	1.0	
sv =	100	mm	K =	0.156	

					Cage Resistance			
Solid	Height (mm)	d (mm)	Y16's	Asv (mm²)	Y5's	Asv (mm²)	Vs (KN)	Ps (KN)
280Y3	280	252	3	603	6	118	133.6	267
280Y4	280	252	4	804	6	118	133.6	267
280Y5	280	252	5	1005	6	118	133.6	267
295Y3	295	267	3	603	6	118	141.5	283
295Y4	295	267	4	804	6	118	141.5	283
295Y5	295	267	5	1005	6	118	141.5	283
310Y3	310	282	3	603	6	118	149.5	299
310Y4	310	282	4	804	6	118	149.5	299
310Y5	310	282	5	1005	6	118	149.5	299

Vs =	Shear resistance provided by cages
Ps =	Shear load resistance provided by cages = 2Vs

Comparing *Table 3.5.4* with *Table 3.5.6* it is clear that the shear resistance added to a solid slab with Cobiax cages inside should have more than doubled up the capacity of the sample strength. This can be visualised by adding the *Ps* value from *Table 3.5.4* to that of *Table 3.5.6*. The theoretical vertical point load at the centre of the beam (*Ps*) has been obtained by doubling the theoretical shear reinforcement capacity (*Vs*). This will approximately be true for a simply supported beam with a point load in the centre, where only vertical shear reinforcement has the ability to resist shear (off course this is not the case in reality, but *Ps* is nevertheless required for calculations to follow).

The question arises what the capacity would have been of Cobiax samples without cages, plus the *Ps* value in *Table 3.5.6*? Should the value be higher than the *Pu* value in *Table 3.5.4*, it would be a clear indication that some of the shear capacity of the vertical cage bars does not contribute to the shear strength, and the best reason being that these bars are not fully anchored around the tension reinforcement. At the TUD they only considered aggregate interlock, with the absence of some aggregate along a 45º angle through the Cobiax slab, to contribute to shear capacity (Schellenbach-Held and Pfeffer, 1999). This area of aggregate interlock was established as follows:

There are two full and two half spheres in a cross section as shown by *Figure 3.2.1*. This means a total area of three spheres. In the cross section, the sphere is a circle with a maximum diameter of 180mm.

$$A_{circle} = \pi r^2$$

where:

r = radius of circle

The effective area that provides aggregate interlock in a Cobiax slab is:

$$A_{eff} = bd - 3A_{circle}$$

This is for a cross section that is perpendicular to the plan view of the beam. To compensate for the extra area that will be available because of a 30 or 45° crack, a further factor has to be introduced. To be conservative, a 45° angle is assumed which will produce the smallest increase in area, therefore:

$$A_{eff} = \lambda_{area} bd - 3A_{circle}$$

with:

$$A_{circle} = \pi r^2$$

$$\lambda_{area} = \frac{1}{\sin 45^\circ} = 1.41 = \text{slope area increasing factor}$$

where:

$r = 90mm$

The effective shear resistance is then:

$$V_{ceff} = V_c Eff.Ratio$$

where:

$$Eff.Ratio = \frac{A_{eff}}{bd}$$

The force required to cause a V_{ceff} shear value will yield values similar to those found in *Table 3.5.4* under the $0.55P_{sc}$ column. This is simply because the effective ratio derived above will be in the vicinity of 0.55 for a worst case scenario. The TUD researchers therefore ignored the compression

block and dowel-action, and only concentrated on the loss of aggregate interlock along the 45º plane of a typical shear crack (Schellenbach-Held and Pfeffer, 1999).

In *Table 3.5.7* the contribution of fully anchored vertical cage bars (P_s), the theoretical force required to break a Cobiax slab where only aggregate interlock contributes to shear resistance ($0.55P_{sc}$), and the two forces added together (Pt) are displayed. These P_t forces should have been equal to that of the actual breaking loads (P_u) of the various samples, should the vertical cage bars at all have been fully anchored around the tension reinforcement. Since the P_t values are greater than the P_u values, it shows that the vertical bars are not fully anchored.

A rough estimate of how effective the vertical cage bars are, can be obtained by the following calculation:

$(P_u - 0.55P_{sc})/P_s$

According to this calculation the vertical bars are roughly between 44% to 70% effective in shear. This conclusion should be approached with great caution, since theoretical and test results were mixed, as well as the contribution of other shear resistance parameters has been ignored, like dowel-action.

The better way to test the effectiveness of these vertical bars will be to break several solid samples with and without the cages placed inside, with no spheres present whatsoever. The contribution to shear capacity of the cages will then be clearly demonstrated from the empirical test results.

Table 3.5.7 Rough indication of the cages` shear capacity

Cobiax	Ps (kN)	0.55Psc (kN)	Pt (kN)	Pu (kN)	(Pu – 0.55Psc)/Ps
280Y3	267	121	388	268	0.553
280Y4	267	133	400	279	0.548
280Y5	267	143	410	330	0.700
295Y3	283	123	406	259	0.479
295Y4	283	136	419	301	0.582
295Y5	283	146	429	343	0.695
310Y3	299	126	425	276	0.502
310Y4	299	139	438	271	0.442

3.6. CONCLUSION

The main conclusion of this chapter is that the shear reduction factor for Cobiax flat slabs can be increased from 0.55, to at least 0.86, in accordance with the test results discussed. This increase in the shear reduction factor is accepted to be the result of the presence of the Cobiax steel cages (previously omitted at the TUD) in the test samples. Although it has been shown that the steel cages' vertical bars do not contribute as much to the shear strength as fully anchored shear reinforcement, the cages indeed increased the shear capacity of the Cobiax slabs.

Firstly the conclusion is of importance to demonstrate that the 0.55 shear reduction factor can conservatively be applied when designing Cobiax slabs in accordance with SANS 10100. Secondly this opens up the opportunity to utilise higher shear reduction factors, that might benefit the feasibility of Cobiax slabs. This second statement will require further investigation before it can be accepted and implemented into the design of Cobiax slabs.

Interesting to note from this chapter is that the EC 2 calculation for the shear resistance of slabs without shear reinforcement is less conservative than that of SANS 10100. When comparing the theoretical design code results with the laboratory test results, EC 2 tends to provide the designer with slightly more accurate results though.

The feasibility study of Cobiax flat slabs, discussed in *Chapter 4*, could be conducted with ease of mind that the utilisation of the 0.55 shear reduction factor would not compromise the integrity of a Cobiax slab design in accordance with SANS 10100.

4. ECONOMY OF INTERNAL SPHERICAL VOID FORMING CONCRETE FLAT SLAB SYSTEMS

4.1. BACKGROUND

Finding a practical method to compare costs of different slab systems is complex in the sense that the layout and application of most structures vary significantly, leaving the designer with almost endless possibilities. Many different techniques have been tried in the past, most of them with valid application in practice (refer to the work done by Goodchild (1997) described in *Chapter 2.14*). This report will focus on the most practical "real-life" design approaches, complementing the methodology that most South Africa design engineers will follow to achieve an economical design. Many assumptions will nevertheless be made to generalise the process of comparing slabs.

Two slab systems identified to be compared with a spherical void forming concrete flat-slab system (SVFS) are coffer slabs and unbonded post-tensioned slabs. Cost results for the SVFS will be based on the only existing such system in South Africa. All three slab systems have already been discussed in *Chapter 2*. The reason for their comparison with the relatively new SVFS is because they serve the same function and are well known as cost effective systems for large span slabs in South Africa. The material for the construction of these three large span slab systems is readily available in the country as well.

Same as for many other cost comparative studies on slab systems, these slabs were all modeled as shown in *Figure 4.1*. These three by three equal continuous spans provide the researcher with a relatively conservative, yet practical system, displaying both the behaviour of an internal span and external spans. Other motivation for this layout is that expansion joints will occur at distances less than 40 m apart as a good design practice to minimise crack widths. Large span systems with three continuous spans will quickly approach this 40m bench-mark, as span lengths increase.

The finite element layouts consisted of the following span lengths, based on the highest minimum and lowest maximum value generally used in practice for the three types of slab systems:

- 7.5 m
- 9.0 m
- 10.0 m
- 11.0 m
- 12.0 m

The above span lengths were all combined with three sets of load combinations each, for all three types of slab systems, derived from suggestions made by SABS 0160-1989:

1. Live Load (LL) = 2.0 kPa and Additional Dead Load (ADL) = 0.5 kPa
2. LL = 2.5 kPa and ADL = 2.5 kPa
3. LL = 5.0 kPa and ADL = 5.0 kPa

Self weight (SW) was applicable to all designs. Combination 1 was referred to as "Light Loading", combination 2 as "Medium Loading" and combination 3 as "Heavy Loading" throughout this report. Combination 1 would generally resemble the loading found on normal parking slabs, combination 2 that of normal office loading, and combination 3 that of retail buildings or office areas with single skin brick walls as internal partitions, combined with the storing of heavy equipment. Live load mainly refers to people and loose equipment on floor areas that can be moved around. Additional or superimposed dead load mainly refers to finishes, services and partitions.

4.2. MAIN ASSUMPTIONS

The following summary of assumptions for this cost study was based on common building types, design methodology, and available materials:

Cost and structural features

All designs were done using SANS 10100-01:2000 design requirements and fulfilled the requirements of minimum reinforcement, deflection and punching shear resistance. The total cost described the direct cost only, which included material, formwork, labour, site delivery, and contractor's mark-ups, but excluding VAT.

The formwork cost has been simplified by assuming normal 3 m high storeys and the construction of large floor areas where repetition was possible. No column- or drop-heads were allowed for below any of the slab systems for all models analysed, making formwork application easier and cheaper.

Column dimensions of 450 mm x 450 mm were assumed for all columns of every model and slab system analysed. All columns were assumed to be pinned to the slab soffit. This resulted in a slightly more conservative slab design, since no moments (accept minimum moments due to eccentricity) were carried by the columns. Buildings with four storeys or less were assumed, since

this will result in very small differences in column and foundation costs for the different slab systems analysed.

The models such as displayed in *Figure 4.1* were all completely surrounded by expansion joints, allowing the slab to stop near the centre of the edge columns. All span lengths were measured from centre to the centre of columns.

Material properties

The concrete cube strength for all models was taken to be 30 MPa. The elasticity of concrete was taken equal to 26 GPa. Reinforcement yield strength was set equal to 450 MPa.

Loading

Dead Load (DL) consisted of SW and ADL. Only one load combination was considered for ultimate limit state (ULS), namely 1.2DL + 1.6LL. Serviceability limit state (SLS) had factors 1.1DL + 0.6LL. The 0.6 factor was used due to the fact that 60% of the live load was taken as permanent loading when estimating long-term deflections. This 60% is a good estimate, supported by SABS 0160 design code. All 45 models were loaded with these ULS and SLS load combinations, and to simplify the cost comparisons, no pattern loading was introduced to any of the models.

Deflection

In accordance with SANS 10100 the maximum long-term deflection allowed for concrete structures is span/250. In accordance with SABS 0160 the maximum deviation for any slab or beam may not exceed 30 mm or span/300, whichever is the lesser, where this deviation can be measured to the top or bottom of the slab's horizontal position of zero deviation. These requirements were fulfilled by insuring that no long-term deflection exceeded span/250 or 60 mm, whichever is the lesser, where the 60 mm had been obtained from a maximum deviation (precamber) to the top of 30 mm, plus the maximum allowed downward deviation of 30 mm.

It should be clear that the final downward deviation described in SABS 0160 refers to differential deflection. The "span" can therefore refer to the distance between any two points, with the resulting maximum difference in vertical displacement along a line between these two points. The points of zero deflection are the columns. The line between two points can therefore conveniently be taken on a diagonal line or orthogonal line between two columns. The deflection on an orthogonal line

runs along a column band, usually with a small differential deflection. The diagonal line will generally contain the maximum differential deflection, and when it is divided by its maximum deflection, it normally yields the smaller value, closer to the 250 limit, therefore being the critical case to consider. The Cobiax company interpreted the DIN 1045-1 code in such a manner that they decided to base their span/deflection criteria on the diagonal span between columns (CBD-MS&CRO, 2006).

The L/d ratios described in SANS 10100 should not be confused with the other criterion of span/250. The "L" in the L/d ratio criterion refers to the critical span, which is usually the longer of the two orthogonal spans of a flat slab panel. This is a different application than that found in SABS 0160. Neither codes discuss the deflection limits very clearly, and experience shows that various engineers have different interpretations of deflection limits.

Long-term deflections were not calculated according to the formulae of code requirements, but rather the general rule of thumb were applied by multiplying the short-term elastic deflections with a factor. Experience shows that this factor usually varies between 2.5 and 4.0 according to most design engineers, and will depend on the type of aggregate, the curing of the concrete, temperature exposure, loading of the slab, and on so forth. These elements will in turn result in the creep and shrinkage of the concrete, causing long-term deflections to occur. A factor of 3.5 was assumed for all slab types in this report.

It should be noted that the aim of this report is not to investigate long-term deflection behaviour of different slab types, and therefore the factor is used. Interesting enough, from analysis run by Prokon software for post-tensioned slab design, the output of this software indicated a long-term deflection factor between 3.0 and 3.5 to be quite applicable to all span and load ranges of post-tensioned slabs. Although no special verification of Prokon software was attained for long-term deflection results in prestressed beams, the software had been utilised by the majority of structural engineers throughout South-Africa for more than a decade. The fact that constructed prestressed beams and slabs that had been designed using Prokon did not yield any problems that the public was made aware of, justifies at least that the deflection predictions of Prokon were either correct or conservative.

Table 4.1 displays deflection results for the three slab types compared in this chapter. These deflection results were obtained from various Strand7 finite element analysis output contours. The finite element analysis methodology will be discussed later in this chapter.

As mentioned, the span from any column to column, divided by the maximum deflection along that line, may not result in a value lower than 250. The maximum deflection along a diagonal line between two columns in *Figure 4.1* will be larger than that of the shorter span length in an *x* or *y* direction (referred to as "Span" in *Table 4.1*). After investigating the span/deflection (span/x or diagonal/x) ratios, the worst case scenarios had been listed in *Table 4.1*. These ratios were always critical (smallest) along the diagonal span for coffer and Cobiax slabs, yet both scenarios had to be listed for post-tensioned slabs.

Table 4.1: Deflections

Load	Span (mm)	Cobiax Deflection (diagonal) (mm)			Coffer Deflection (diagonal) (mm)		
		Elastic	Long-term	Diagonal/x	Elastic	Long-term	Diagonal/x
7.5m light load	7500	7.6	27	399	5.3	19	572
7.5m medium load	7500	10.2	36	297	6.8	24	446
7.5m heavy load	7500	7.7	27	394	9.4	33	322
9m light load	9000	13.5	47	269	10.8	38	337
9m medium load	9000	13.3	47	273	14.0	49	260
9m heavy load	9000	9.3	33	391	11.4	40	319
10m light load	10000	15.6	55	259	16.4	57	246
10m medium load	10000	13.9	49	291	12.8	45	316
10m heavy load	10000	11.0	39	367	11.3	40	358
11m light load	11000	16.1	56	276	15.0	53	296
11m medium load	11000	14.8	52	300	12.6	44	353
11m heavy load	11000	11.8	41	377	16.4	57	271
12m light load	12000	16.9	59	287	14.6	51	332
12m medium load	12000	15.9	56	305	17.8	62	273
12m heavy load	12000	13.8	48	353	23.1	81	210

Load	Span (mm)	Post-tension Deflection (diagonal) (mm)			Post-tension Deflection (normal) (mm)		
		Elastic	Long-term	Diagonal/x	Elastic	Long-term	Span/x
7.5m light load	7500	7.7	27	394	6.0	21	357
7.5m medium load	7500	9.2	32	328	7.2	25	298
7.5m heavy load	7500	11.3	40	268	8.7	30	246
9m light load	9000	10.3	36	353	8.0	28	321
9m medium load	9000	11.9	42	306	9.4	33	274
9m heavy load	9000	13.5	47	269	10.5	37	245
10m light load	10000	11.4	40	354	8.9	31	321
10m medium load	10000	12.9	45	313	10.0	35	286
10m heavy load	10000	14.1	49	287	11.0	39	260
11m light load	11000	12.7	44	350	9.9	35	317
11m medium load	11000	13.9	49	320	11.1	39	283
11m heavy load	11000	15.9	56	280	12.4	43	253
12m light load	12000	14.9	52	325	11.9	42	288
12m medium load	12000	15.7	55	309	12.6	44	272
12m heavy load	12000	12.7	44	382	10.2	36	336

Reinforcement

Cover on reinforcement was taken to be 25 mm for all slabs, satisfying safe fire protection requirements of over 2 hours fire exposure. In contrast with the assumptions of Goodchild (1997) for his analysis discussed in *Chapter 2.14,* reinforcement content for all models was based on the reinforcement provided and not those required. The reinforcement provided was always kept to a minimum, but never allowed to be less than the SANS 10100 minimum reinforcement specifications. Curtailment and lap lengths (SABS 0144, 1995) were provided for by multiplying the total reinforcement per m^2 of slab area by 1.1, therefore allowing for 10% extra reinforcement. In practice this 10% would normally represent the correct amount of reinforcement very well.

A good designer will try to design the reinforcement as such that the reinforcement provided is always more than the reinforcement required, yet kept to a minimum. A better simulation of the reality can be obtained for the use of a cost analysis, by using this amount of reinforcement provided, rather than the exact amount required. The reinforcement content chosen for each slab was therefore approximately 5 percent more than the amount required. It should be borne in mind though that it is not practically possible to read off the exact amount of reinforcement required when interpreting a finite element contour plot.

Spacings of reinforcement provided were also kept to standard spacings such as 125 mm or 300 mm increments for example. In areas where top and bottom reinforcement occurs, the spacings were set to have the same increment to simplify construction.

The three tables in *Appendix A* show the reinforcement areas as provided for all the models. Using the 7.5m span scenario as an example, typical finite element output displays of the models' required reinforcement content are shown in *Appendix B, C and D.*. These were obtained ustilising Strand7 (2006) software, with the plate elements set up in accordance to SANS 10100 criteria for the direct calculation of reinforcement using Wood-Armer moments.

The 7.5 m span Cobiax slab with light loading was used to demonstrate the accuracy of the reinforcement contours in *Appendix B*. This was done by comparing the top and bottom reinforcement in the y-direction with a MathCad generated contour plot (by Dr John Robberts, 2007) based on the gauss point values obtained from Strand7. The plots from the Strand7 concrete module are very similar to those generated by Dr John Robberts's program, and therefore one can assume the reinforcement results to be quite accurate.

The Strand7 finite elements used for al three slab systems consisted of rectangular eight-noded plate elements. Each plate element represented a finite volume of the concrete slab. Applicable concrete properties and plate thicknesses were applied to all plate elements for the various scenarios.

The "B" and "T" in *Appendix B-D* mean "Bottom" and "Top" reinforcement respectively. Only the slightly more conservative *y*-direction of reinforcement is displayed, since the internal lever arms between the compression block and tension reinforcement were smaller in this direction for all the models. The same amount of steel provided for this y-direction was provided for the x-direction.

The steel provided as displayed in *Appendix A* was based on the following assumptions:

- Bottom reinforcement for column strips was taken to be a mm^2/m value read at a position measured in the *x*-direction, one sixteenth of the span away from the y-direction line connecting column centers. This was done for both edge and internal spans, and bottom reinforcement was provided according to these values. The maximum reinforcement contours at the above positions (usually closer to midspan) were used.
- The same has been done for the middle strips, but the steel content was read at a position five sixteenths away from the y-direction line connecting column centers.
- The bottom steel was taken to be continuous over the whole slab in both directions.
- At the same distances away from the y-direction column line as for bottom steel, but measured right on top of the x-direction column line connecting internal columns, the amount of top steel could be found for column and middle strips.
- Top steel were stopped at a distance of 0.3 times the span length past a line connecting the column face, accept for coffer slabs, where minimum reinforcement was required according to SANS 10100 throughout the 100 mm topping. Cobiax in Europe claims that no minimum reinforcement is required in the midspan (compression) region of a Cobiax slab (CBD-MS&CRO, 2006) due to the fact that the top flange thickness rapidly increases to the full slab depth between voids, being thin only for a small area above each sphere.
- The reinforcement spacings of column and middle strips were allowed to have different spacing increments, since there is no practical reason why these spacings should be the same, as long as the top and bottom steel had the same increments.
- No reinforcement spacing was taken smaller than 100 mm or larger than 300 mm centre to centre.

- Coffer slab tension reinforcement had to be grouped in the webs. The steel provided was based on two or four bars with a specific diameter in the bottom of each web, matching the required steel displayed in *Appendix C*.

4.3. FORMWORK

Appendix E shows the formwork cost analysis done by Jan Kotze (2007) at Wiehahn Formwork (Pty) Ltd for both Cobiax flat-slabs and coffer slabs. All formwork material, delivery on site and labour were included in this analysis, but VAT excluded. The analysis was based on large slab areas where repetition of formwork usage resulted in 5 day cycle periods for both flat-slab (Cobiax and post-tensioned slabs) and coffer formwork. The assumption is based on the presence of an experienced contractor on site and no delays in the supply of the formwork.

A 450 mm thick Cobiax flat-slab with 315 mm diameter spheres was compared with a 525 mm thick coffer slab with 425x425x900 coffers and a 100 mm topping. This comparison resembles the average formwork conditions for the three slab systems, assuming that since formwork designs are conservative, the formwork costs will vary only slightly for different slab and coffer depths. The 425 mm deep coffer mould is also known as the most commonly used and available coffer in South Africa.

In *Appendix E* the total nett rate for the post-tension and Cobiax flat-slab formwork will be R64/m^2. The total net rate for a coffer slab will be R114/m^2. These rates are displayed in *Table 4.6*. Therefore coffer formwork will be approximately R50/m^2 more expensive than flat-slab formwork for large slab areas. For small projects this difference will increase due to the fact that the first cycle or two for coffers takes longer, resulting in an extended hire period.

4.4. COBIAX SLABS

Punching Shear

Eight-noded rectangular plate finite element models were created for all three load combinations and five span lengths, resulting in 15 models for the Cobiax slabs alone. *Figure 4.1* displays square areas around the columns which result in approximately 25% of the total slab area. These areas will remain solid to accommodate shear greater than 55% of that of a solid slab's v_c-value, with the same thickness as the specific Cobiax slab under investigation (see *Chapter 3* for a discussion).

The Cobiax solid zones obtained from a Strand7 analysis are shown in *Appendix F*, where the white areas around the columns are to be left solid (i.e. spheres omitted), and the remaining area should be supplied with the applicable Cobiax spheres (where the applied shear is lower than $0.55v_c$). Only one such analysis is shown in *Appendix F*, since all Cobiax models for the different scenarios resulted in almost exactly similar shear contour patterns. Comparing *Figure 4.1* with the Cobiax plot in *Appendix F*, it is clear that the size of the square solid zones assumed in *Figure 4.1* simulate the real solid zone scenario quite accurately, and therefore the Cobiax models in this report can be used with confidence.

The slab thicknesses of Cobiax slabs were mainly determined by using the punching shear design software of Prokon, set up to fulfill SANS 10100 requirements. The vertical column reaction resulting from the ULS loading combination was obtained for an internal column, using Strand7 software. A simplified punching shear design was then performed by entering this vertical load and other material factors into the Prokon punching shear software.

Chapter 3 indicated that SANS 10100-01 is more conservative than EC 2 for punching shear requirements, and compared to the test results maybe a bit too conservative. The ultimate shear (v) may not exceed $2v_c$. Enough tension reinforcement had to be added over the column zone to cross the critical shear perimeters, to prevent the utilisation of uneconomically thick slabs. The more tension reinforcement, the higher the value of v_c. The Prokon punching shear calculation output for an internal column is displayed in *Appendix G*, using the 7.5m span scenario as an example for the Cobiax models.

The area of punching reinforcement could be found from *Appendix G* type output, and then multiplied by the length of half a shear clip for the specific slab thickness, to calculate the volume of punching reinforcement for one column. This volume could in turn be multiplied by the 7850 kg/m^3 to obtain the steel weight in kg. The weight could then be multiplied by the total number of columns, taking into account that the eight edge columns are “half” columns and four corner columns are “quarter” columns. This means that only half a shear zone exists for edge columns and only quarter a shear zone exists for corner columns.

Lastly this total steel weight for the punching reinforcement could be divided by the total slab area for the specific model (see *Figure 4.1*), resulting in a very low steel content per m^2, usually being far less than 1.0 kg/m^2 for most of the models. Therefore one can conclude that punching reinforcement will only contribute to a very small percentage of the total reinforcement content. Nevertheless this approximated punching reinforcement was added to the reinforcement content displayed later in this report in *Tables 4.7 to 4.9*.

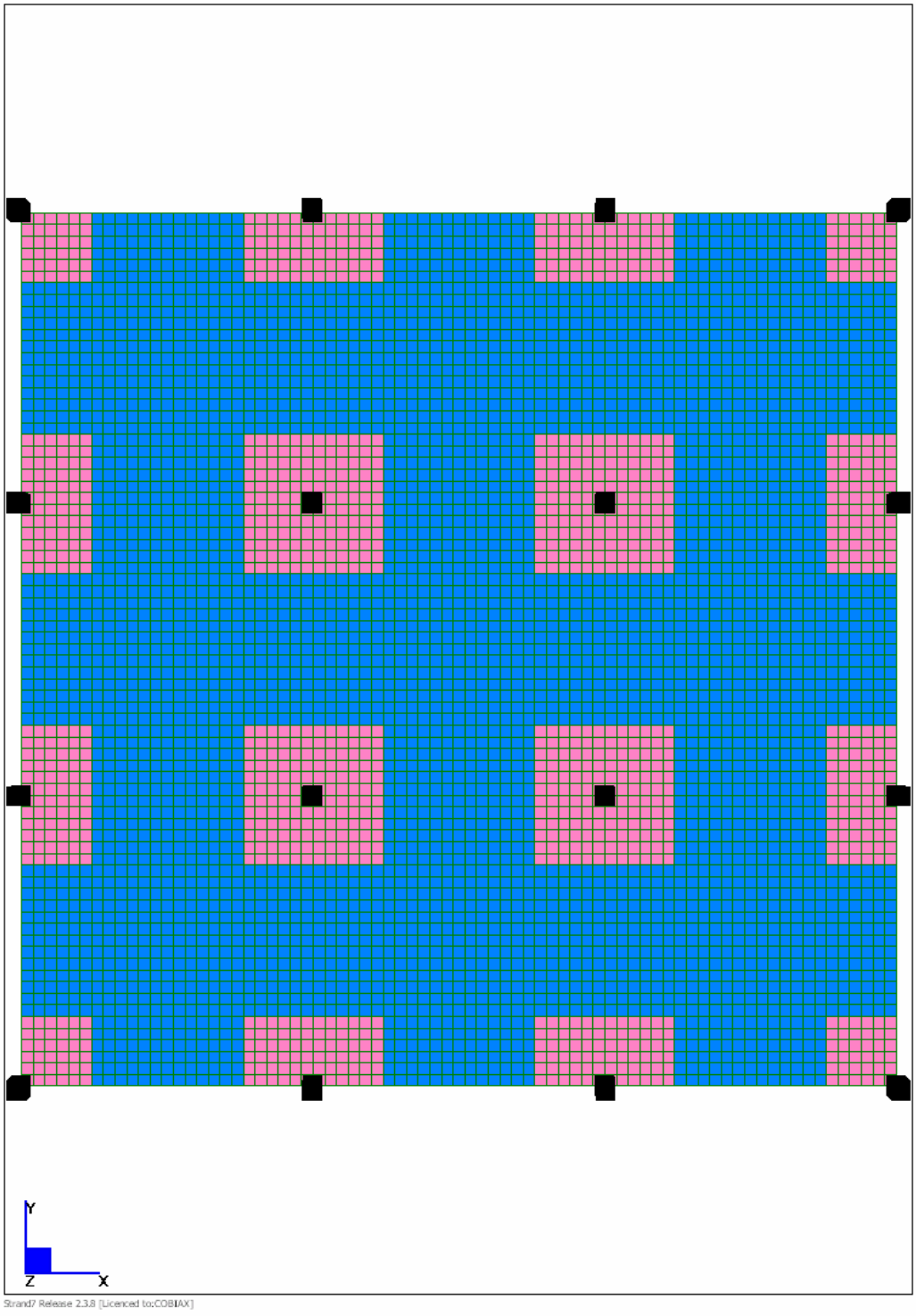

Figure 4.1: Cobiax and Coffer slab solid zone layouts

Deflection

A stiffness reduction factor had to be calculated for all types of Cobiax slabs. The formula for elastic deflection calculation is:

$$deflection = \frac{kwL^4}{EI}$$

Where:

k = a factor depending on the support conditions of the specific span
w = SLS load
L = span length
E = elasticity of concrete
I = second moment of area, in other words the stiffness of the slab

Whether a stiffness reduction factor is applied to either the E or the I value in the formula above will make no difference. The E-value of the pink areas (voided zones) of the Cobiax models (see *Figure 4.1*) were simply reduced by the stiffness reduction factors in *Table 4.2* for the applicable slab thickness. By also adding an upward load over these voided zones for reduction in dead load, obtained from *Table 4.2*, one could obtain the correct elastic deflection values for any Cobiax slab.

The reduction in dead load was simply the displaced concrete weight (25 kN/m^3) as a result of the hollow spheres in the voided areas, which differs for all different sizes of spheres. The calculation of the stiffness reduction factors are more complicated though.

Figure 4.2 shows a section through a Cobiax slab on the left hand side, displaying only two spheres, cut exactly where the diameter is greatest. This section will be exactly the same for the perpendicular direction. Should half a sphere be taken to perform calculations with, an x-distance can be calculated to the centroid of the hemisphere, where x = 3r/8, with al symbols explained in *Table 4.2*. With the formula for a circle (Pythagoras) $r^2 = x^2 + y^2$ one can easily obtain the y-value.

Section A-A in *Figure 4.2* was taken at the x-position, displaying a new cross section on the right hand side of the figure. This cross-section is representative of the voided part of the Cobiax slab when calculating the second moment of area. In *Table 4.2* I_s is calculated with the formula $I = bh^3/12$ and represents the second moment of area of a flat slab with no Cobiax void. $I_c = \pi r^4/4$ represents the second moment of area of a circle with radius y. I_c can then be subtracted from I_s and then divided by I_s to provide a ratio of the stiffness of a voided slab to that of a solid slab.

Along an imaginary line through the cetroids of the spheres in a Cobiax slab, 90% of that line will be inside the spheres (voids) and 10% of that line will run through solid zones (regions between spheres). Due to the gradual change in void size and thus cross-section of the slab along the line, one may assume that the stiffness of a Cobiax slab will be given by combining the voided zone's (90%) and the solid zone's (10%) stiffnesses to obtain an average stiffness. Stiffness reduction factors follow in *Table 4.2*, which complement those obtained at the Technical University of Darmstadt (TUD) very well, where both empirical tests, as well as theoretical calculations were performed.

It should be noted that one can simply adjust the slab thickness in *Table 4.2* to obtain a new stiffness ratio, but that one cannot use this excel program to calculate the stiffness for different vertical positions of the spheres within the slab thickness. For the purposes of this report it was assumed that the spheres were all placed mid-height in the slab.

Multiplying the E-value of 26 GPa with this stiffness reduction factor as explained earlier, will then provide the designer with a new E-value (see *Table 4.2*) for the purpose of deflection calculations with either hand calculation methods or finite element software.

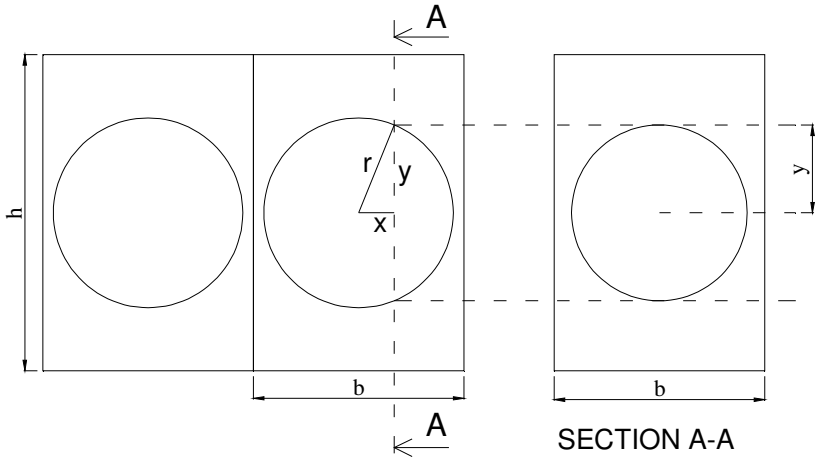

Figure 4.2: Cobiax stiffness calculation method

Table 4.2: Cobiax Stiffness Reduction Factors

Sphere Diameter – 2r (mm)	180	180	225	225	270	315
Slab Thickness – h (mm)	280	300	340	360	400	450
Sphere Spacing c/c – b (mm)	200	200	250	250	300	350
Radius - r (mm)	90	90	112.5	112.5	135	157.5
Centroid hemisphere - x (mm)	33.8	33.8	42.2	42.2	50.6	59.1
New radius - y (mm)	83.4	83.4	104.3	104.3	125.1	146.0
Is solid (mm^4)	3.66E+08	4.50E+08	8.19E+08	9.72E+08	1.60E+09	2.66E+09
Ic circle (mm^4)	3.81E+07	3.81E+07	9.29E+07	9.29E+07	1.93E+08	3.57E+08
Sphere factor (Is-Ic)/Is	0.896	0.915	0.887	0.904	0.880	0.866
Solid factor Is/Is	1.0	1.0	1.0	1.0	1.0	1.0
Sphere %	0.9	0.9	0.9	0.9	0.9	0.9
Solid %	0.1	0.1	0.1	0.1	0.1	0.1
Stiffness Reduction Factor	0.91	0.92	0.90	0.91	0.89	0.88
E-value of Concrete for Strand7 (GPa)	23.566	24.021	23.345	23.763	23.182	22.858
Reduction in dead load (kPa)	1.909	1.909	2.386	2.386	2.863	3.340
Sphere Diameter (mm)	315	360	360	405	450	
Slab Thickness (mm)	460	500	520	570	620	
Sphere Spacing c/c (mm)	350	400	400	450	500	
Radius - r (mm)	157.5	180	180	202.5	225	
Centroid hemisphere - x (mm)	59.1	67.5	67.5	75.9	84.4	
New radius - y (mm)	146.0	166.9	166.9	187.7	208.6	
Second moment of area for the solid region between voids - Is solid (mm^4)	2.84E+09	4.17E+09	4.69E+09	6.94E+09	9.93E+09	
Second moment of area for the voided region - Ic circle (mm^4)	3.57E+08	6.09E+08	6.09E+08	9.75E+08	1.49E+09	
Sphere factor (Is-Ic)/Is (stiffness ratio of the average voided cross-sectional area in terms of a fully solid cross-section)	0.874	0.854	0.870	0.860	0.850	
Solid factor Is/Is (stiffness ratio of a fully solid cross-sectional area in terms of a fully solid cross-section)	1.0	1.0	1.0	1.0	1.0	
Sphere % (percentage of all possible cross-sections through the slab that will obtain internal voids)	0.9	0.9	0.9	0.9	0.9	
Solid % (percentage of all possible cross-sections through the slab that will be fully solid)	0.1	0.1	0.1	0.1	0.1	
Stiffness Reduction Factor	0.89	0.87	0.88	0.87	0.87	
E-value of Concrete for Strand7 (GPa)	23.058	22.580	22.960	22.714	22.497	
Reduction in dead load (kPa)	3.340	3.817	3.817	4.294	4.771	

Referring back to *Table 4.1,* since the diagonal/x ratios are reasonably larger than 250 for the case of Cobiax slabs, it demonstrates that punching shear has governed the calculation of the slab thickness for all span lengths and load combinations, especially for the heavier load combinations. In the TUD deflection was found to be the governing factor, since their punching shear requirements are not as strict as in South Africa, combined with the use of Halfen® Shear Stirrups in Europe. These two factors allow for thinner Cobiax slabs to be used, resulting in more economical designs, still being within the maximum deflection specifications.

Horizontal Shear Resistance

The cold joint in a Cobiax slab due to the two pour system needs some investigation. Laboratory tests done in the TUD confirmed that a Cobiax slab constructed with two pours will behave the same as a slab with no cold joint. This is probably the best way to confirm the effective horizontal shear capacity, which is obtained by friction at the surface of the cold joint and the vertical cage bars passing through the cold joint. A concrete slump between 120 mm and 140 mm will generally result in easier workability of the first concrete layer of a Cobiax slab, and are therefore strongly recommended for this layer.

In South Africa a decision has been made to continue with the Cobiax cages into the solid zones, to act as reinforcement chairs separating top and bottom reinforcement. Both the solid and voided zones of a Cobiax slab will be performed in two pours. Since the vertical shear from an ultimate limit state (ULS) loading condition is used in the formula for horizontal shear calculation, the critical position for the testing of horizontal shear will be where the punching shear reinforcement is discontinued and only the cages continue. This position where the relevant vertical shear (in the y-direction) can be obtained is shown in *Appendix H*, on the line where the white zone changes to a coloured zone.

The contour plot in this appendix is for the 12 m span Cobiax slab exposed to heavy loading. The highest vertical shear will exist for this slab, as well will the vertical cage bars be the furthest apart, providing the least shear resistance of al slabs investigated for the purpose of this dissertation. The large spacing of vertical cage bars is due to the largest Cobiax sphere size (450 mm diameter) used for this 620 mm thick slab.

TMH7 Part 3 (1989) is a South African code that provides a method to test the longitudinal shear capacity at horizontal cold joints. *Section 5.4.2.3* provides formulae for this shear resistance. The V_l value for ultimate vertical shear force per meter width referred to in this section is obtained from the well-known formula:

$V_1 = VAy/I$

Where:

V = 375 kN/m, which is the vertical shear at the critical position for a meter width.

A = 1m x (0.62 – 0.1)m = 0.52m^2, or

A = 1m x 0.1m = 0.1m^2,

where a 100 mm first pour height and 1 m slab width are assumed, and A is the area either below or above the cold joint.

y = (0.62/2)m – (0.52/2)m = 0.05m, or

y = (0.62/2)m – (0.1/2)m = 0.26m,

where y is the distance from the centroid of slab area either above or below the cold joint, measured to the centroid of the area of the total slab thickness.

Therefore:

Ay = 0.52m x 0.05m = 0.026m^3, or

Ay = 0.1m x 0.26m = 0.026m^3,

which should be exactly the same.

I = $bh^3/12$ = [1m x (0.62m)^3]/12 = 19.861 x 10^{-3} m^4

Then:

V_1 = 1x(375 x 0.026)/19.861 x 10^{-3} = 491 kN/m,

for a 1 m length along the span of the slab.

This V_1 value should in accordance with TMH7 Part 3 not exceed the lesser of:

$k_1 f_{cu} L_s$ = 2700 kN/m (or N/mm)

$v_1 L_s + 0.0007 A_e f_y$ = 593 kN/m (or N/mm)

Where:

$k_1 = 0.09$ for surface type 2 described as a surface where laitance removal was performed with air or water, and no other surface treatment conducted.

f_{cu} = 30MPa which is the characteristic cube strength of concrete

L_s = 1000mm which is the width of the shear plane (or cold joint)

v_1 = 0.45MPa which is the ultimate longitudinal shear stress in the concrete taken from *Table 30* of *TMH7 Part 3*, for surface type 2.

$A_e = 16 \times \pi d^2/4 = 452$ mm^2,

which is the area of anchored reinforcement per unit length crossing the shear plane, and where *d* is the vertical cage bar diameter. This unit length was taken to be 1 m when calculating V_1. For 450 mm diameter Cobiax spheres, 16 cage bars of 6 mm diameter each will cross this shear plane for every square meter of slab area.

f_y = 450MPa which is the characteristic strength of the cage reinforcement.

TMH7 Part 3 as well as *SANS 10100* stipulates that the minimum reinforcement crossing the shear plane should be:

0.15% x Area of contact = 0.0015 x 1 m^2 = 1500 mm^2

This value is greater than that of A_e, and therefore the vertical cage reinforcement is insufficient. A simple investigation will show that only 6 mm diameter cage bars for the 180 mm and 225 mm diameter Cobiax spheres will exceed the 1500 mm^2/m^2 minimum horizontal shear reinforcement requirement. These sphere sizes include all Cobiax slabs up to 360 mm thickness. For thicker Cobiax slabs the minimum horizontal shear reinforcement requirements will not be satisfied.

The spacing of the vertical cage reinforcement bars may not exceed the lesser of four times the minimum thickness of the second concrete pour or 600mm. The maximum spacing of these bars is less than 500 mm for all sizes of Cobiax cages, and therefore this requirement of *TMH7 Part 3* is met.

Since the TUD laboratory tests showed the Cobiax slabs to be safe, one might question whether this was also true for slab thicknesses exceeding 360 mm, which will not meet the minimum horizontal shear reinforcement requirements. Also, whether or not the cage reinforcement is truly fully anchored, remains unclear and needs further investigation.

A counter argument may be that almost no vertical shear rebar will be required through the cold joint, since the code requirements are based on precast members that may be a couple of days old before receiving a topping, while the second pour of a Cobiax slab generally follows within four hours of the first pour. This will allow for less differential creep and shrinkage to take place at the cold joint, which will limit the reduction in shear strength on this plane.

A South African solution will be to increase the cage reinforcement thickness for Cobiax slabs thicker than 360 mm. Setting A_e = 1500 mm^2 for a 1 m^2 area of cold joint and then dividing A_e by the area of a single cage bar, choosing different bar diameters, will indicate the number of these bars required to cross the 1 m^2 area. The following number of bars will satisfy minimum horizontal shear reinforcement requirements for different reinforcement diameters through a 1 m^2 area:

- 53 bars for 6 mm diameter bars
- 30 bars for 8 mm diameter bars
- 19 bars for 10 mm diameter bars
- 14 bars for 12 mm diameter bars

The number of bars crossing a 1 m^2 area for different Cobiax cages are:

- 100 bars for 180 mm diameter Cobiax sphere cages
- 64 bars for 225 mm diameter Cobiax sphere cages
- 44 bars for 270 mm diameter Cobiax sphere cages
- 33 bars for 315 mm diameter Cobiax sphere cages
- 25 bars for 360 mm diameter Cobiax sphere cages
- 20 bars for 405 mm diameter Cobiax sphere cages
- 16 bars for 450 mm diameter Cobiax sphere cages

The above summary clearly shows that the following cage reinforcement diameters are required:

- 6 mm diameter bars for 180 mm and 225 mm diameter Cobiax sphere cages
- 8 mm diameter bars for 270 mm and 315 mm diameter Cobiax sphere cages
- 10 mm diameter bars for 360 mm and 405 mm diameter Cobiax sphere cages
- 12 mm diameter bars for 450 mm diameter Cobiax sphere cages

Although this would result in a very practical solution for satisfying the minimum horizontal shear reinforcement requirements for Cobiax slabs, unfortunately it will increase the cost of the Cobiax item.

4.5. COFFER SLABS

Punching Shear

Eight-noded finite element plate models were created for all three load combinations and five span lengths in Strand7, resulting in 15 models for the coffer slabs alone. *Figure 4.1* displays square areas around the columns which result in approximately 25% of the total slab area. These areas will remain solid to accommodate shear that cannot be resisted by the webs of the coffers alone.

The coffer solid zones obtained from a Strand7 analysis are shown in *Appendix F*, where the white areas around the columns are to be left solid, and the remaining area should be supplied with the applicable coffer moulds. One can limit the solid zones to approximately 25% of the slab area, and simply add some shear stirrups in the webs where additional shear is required. For the 10 m span slab model under light loading in *Appendix F* one would typically have to add shear stirrups in just over half a meter of web length away from the solid zone. This will only be required in some areas of the slab and the rest of all the webs can be left without stirrups. The example in *Appendix F* was the most critical case of all coffer models analysed, having the largest solid zones. Comparing *Figure 4.1* with the coffer plot in *Appendix F*, it is clear that the size of the square solid zones assumed in *Figure 4.1* simulate the real solid zone scenario quite accurately, and therefore the coffer models in this report can be used with confidence.

The same procedure used for Cobiax slabs was used for coffer slab punching shear design, utilising Prokon software. The Prokon punching shear calculation output for an internal column is displayed in *Appendix I*, using the 7.5m span scenario as an example for the coffer models. Here punching

reinforcement also made up a very small percentage of the total reinforcement content. Nevertheless this approximated punching reinforcement was added to the reinforcement content displayed later in this report in *Tables 4.7 to 4.9*. The same reasoning for obtaining valid results from a Prokon design discussed in Chapter 4.2, applies here.

Deflection

The slab thicknesses of coffer slabs were mainly governed by deflection. Coffer thicknesses could only be 425, 525 and 625 mm thick, where commonly available coffer sizes with 100 mm toppings had been used, which is the maximum allowable topping. This provides a strange non-constant long-term deflection variation between coffer slabs with different span lengths and loading conditions. The deflection became too severe for the 12 m span coffer slab under heavy loading (see *Table 4.1*). One can also show that from 13 m span lengths, even for the light load combination, no commonly available coffer slab will meet the deflection requirements. Therefore one can assume that the use of coffer slabs ends with approximately 12 m lengths, unless a special coffer mould with increased depth, or post-tensioning in combination with the coffers, is used.

A stiffness reduction factor had to be calculated for all types of coffer slabs. The same approach was followed as that used for Cobiax slabs. The E-value of the pink areas (voided zones) of the coffer models (see *Figure 4.1*) was simply reduced by the stiffness reduction factors in *Table 4.3* for the applicable slab thickness. By also adding an upward load over these voided zones for reduction in dead load, obtained from *Table 4.3*, one could obtain the correct elastic deflection values for any coffer slab.

The reduction in dead load was simply the displaced concrete weight (25 kN/m^3) as a result of the coffer voids outside the solid regions, which differs for the different sizes of coffer moulds.

In *Table 4.3* I_{solid} was calculated with the formula $I_{solid} = b_f(A+h_f)^3/12$ and represented the second moment of area of a flat slab with no coffer voids. I_{coffer} was equal to a T-section's second moment of area, with a tapering web (calculated with areas A_1, A_2 and A_3). The stiffness reduction factor here was directly obtained by calculating the I_{coffer}/I_{solid} ratio. Unlike with Cobiax slabs, the change along the span length to a totally solid section does not happen gradually, but very suddenly, and therefore it would be dangerous to assume that part of the span along the coffers will have the stiffness value of a completely solid slab.

Multiplying the E-value of 26 GPa with this stiffness reduction factor as explained earlier, will then provide the designer with a new E-value (see *Table 4.3*) for the purpose of deflection calculations

with either hand calculation methods or finite element software. *Figure 4.2B* explains the symbols used in *Table 4.3* for the coffer system.

Table 4.3: Coffer Stiffness Reduction Factors

Coffer Type (+100mm topping)	900x900x325	900x900x425	900x900x525
A - Coffer height (mm)	325	425	525
B – Web width at soffit of topping (mm)	258	298	338
B_{av} – Average web width (mm)	193	213	233
C – Minimum web width at bottom (mm)	128	128	128
h_f - Flange Thickness (mm)	100	100	100
b_f - Flange Width (mm)	900	900	900
A_1 – Flange area of section (mm²)	90000	90000	90000
A_2 – Web area of section (mm²)	41600	54400	67200
A_3 – Tapering web area of section (mm²)	10562.5	18062.5	27562.5
y - Centroid from bottom (mm)	295.2	357.5	417.7
I_{coffer} - Second moment of area (mm^4)	2.00E+09	3.84E+09	6.56E+09
I_{solid} (mm^4)	5.76E+09	1.09E+10	1.83E+10
Stiffness reduction factor = I_{coffer}/I_{solid}	0.35	0.35	0.36
E-value of Concrete for Strand7 (GPa)	9.037	9.203	9.316
Reduction in dead load (kPa)	4.875	6.025	7.125

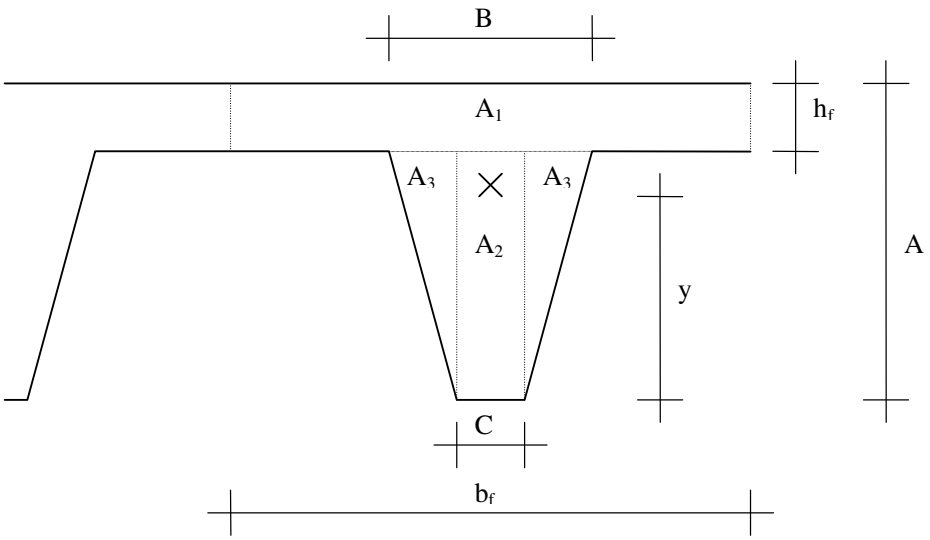

Figure 4.2B: Coffer system

4.6. POST-TENSIONED SLABS

Punching Shear

Eight-noded finite element plate models were created in Strand7 for all three load combinations and five span lengths, resulting in 15 models for the unbonded post-tensioned slabs alone. Punching shear reinforcement was designed with the help of the Prokon Captain software, and results are displayed only for the 7.5m span scenario in *Appendix J*. The presence of the cables in the slabs contributed significantly to shear resistance, making very thin slabs possible. Punching shear reinforcement made up a very small percentage of the total reinforcement content. Nevertheless this approximated punching shear reinforcement was added to the reinforcement content displayed later in this report in *Tables 4.7 to 4.9*.

Deflection

Appendix K discusses the cable design methodology of every post-tensioned slab model in detail, using a Mathcad software program mainly developed by Dr John Robberts. Only the calculations for the light load scenario on the 7.5m span slab system are displayed as an example. The cables were banded (100 mm c/c spacings) in the x-direction and uniformly distributed in the y-direction. The equivalent loads on the slabs after long-term losses occurred (*Appendix K*) were applied to the slabs for both directions of cables. The forces were applied in the form of uniform distributed loads (UDL), being downward over supports and upward away from supports over distances as calculated in *Appendix K*. The application of this UDL significantly reduces deflections.

By taking the cables to balance only 70% of the dead load, which is an average value that designers may use, one can assume a class 3 structure in accordance with TMH7 Part 3 (1989) as a result, where additional normal reinforcement will be critical to carry the remainder of the loads.

The results in *Appendix K* were tested against those obtained in Prokon, and very similar deflections and equivalent loadings were obtained. The slab thicknesses were determined with a formula that would normally suggest a thickness satisfying punching, deflection and vibration requirements. Punching shear requirements dictated slab thicknesses for the lighter loadings, and deflection that of heavy loading (see *Table 4.1*). The deflections seen in this table were both for the maximum obtained on a diagonal line between columns, and that for a normal span length, between two columns.

As from 12 m span lengths, heavy loading on post-tensioned slabs causes the slab thickness to be dictated by punching shear requirements. Post-tensioned slabs rapidly increase in thickness beyond 12 m spans and become uneconomical due to unacceptable volumes of concrete, also resulting in heavier columns and foundations. The number of cables also becomes excessive for spans greater than 12 m, causing congestion of cables to occur.

Post-tension content

The cost of post-tensioning was calculated as displayed in the *Appendix K* example, and from there a cost per kg could be established as displayed in *Table 4.4*, resulting in an average cost for the post-tensioning content displayed in *Table 4.6*.

Table 4.5 was used to create *Figure 4.3*. This figure displays the difference in post-tensioning content for different span lengths and load intensities. The increase of post-tensioning weight versus increase in span length ratio was almost linear.

Table 4.4: Calculation of Post-tension cost per kg of tendons and anchors

Load	Cost (R/m²)	Weight (kg)	Weight (kg/m²)	Cost (R/kg)
7.5m light load	49	659	1.3	38
7.5m medium load	65	878	1.7	38
7.5m heavy load	81	1098	2.2	38
9m light load	63	1252	1.7	37
9m medium load	80	1581	2.2	37
9m heavy load	96	1911	2.6	37
10m light load	74	1830	2.0	36
10m medium load	95	2343	2.6	36
10m heavy load	110	2709	3.0	36
11m light load	85	2577	2.4	36
11m medium load	104	3141	2.9	36
11m heavy load	120	3625	3.3	36
12m light load	97	3514	2.7	36
12m medium load	114	4130	3.2	36
12m heavy load	124	4484	3.5	36
				37

Table 4.5: Post-tension Content

Load	Span (m)	Weight (kg/m²)
Light	7.5	1.3
	9	1.7
	10	2.0
	11	2.4
	12	2.7
Medium	7.5	1.7
	9	2.2
	10	2.6
	11	2.9
	12	3.2
Heavy	7.5	2.2
	9	2.6
	10	3.0
	11	3.3
	12	3.5

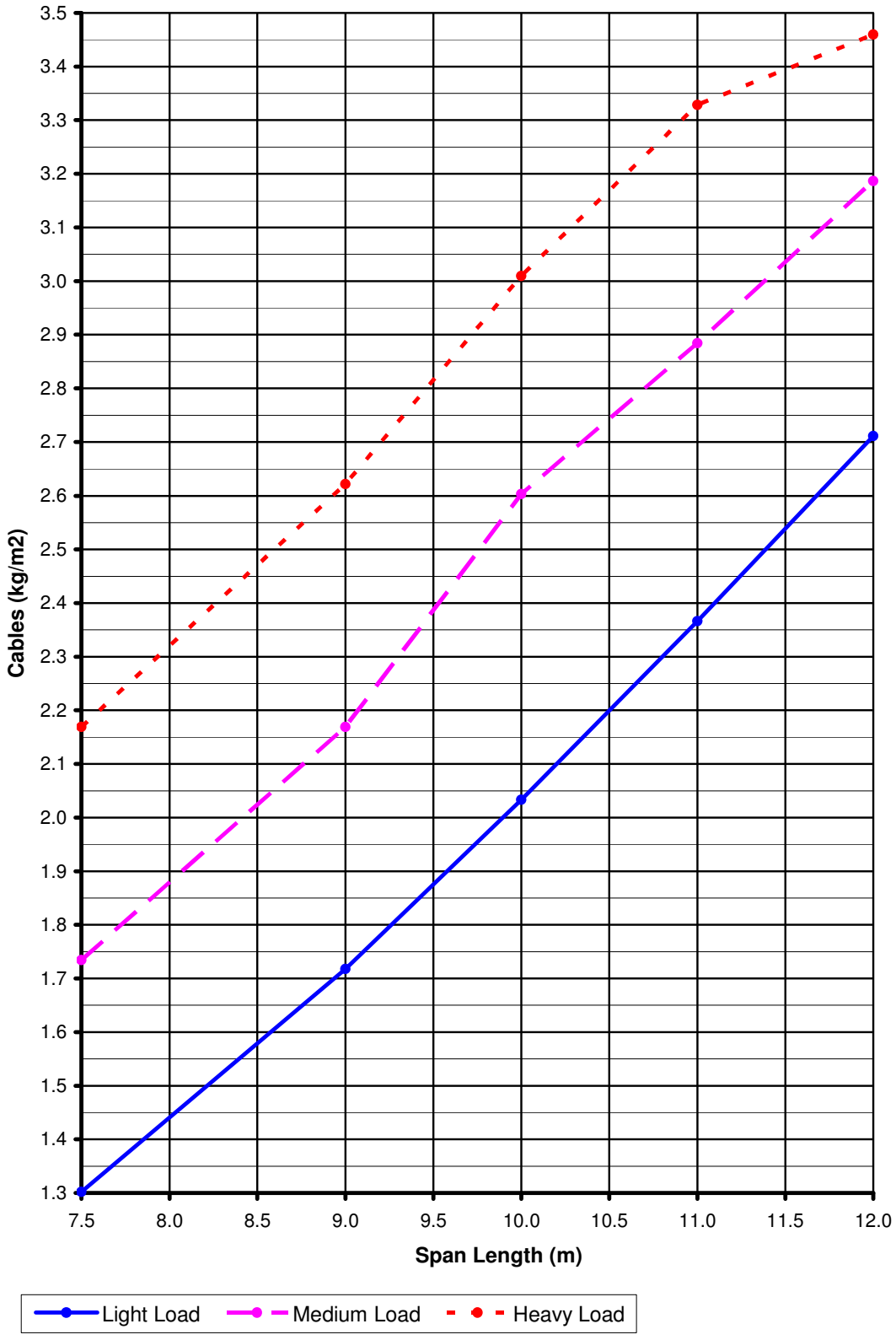

Figure 4.3: Post-tension Content

4.7. RESULTS

The values used in *Table 4.6* can vary from location to location in South Africa, and therefore only resemble the average rates for materials during December 2007. These values were based on various engineers', contractors' and quantity surveyors' opinions.

The values in *Table 4.6* were used to create *Tables 4.7 to 4.9*, where the concrete content of coffer and Cobiax slabs were calculated, assuming 25% of the slab to be solid. *Table 4.7* contains the results for light loading, *Table 4.8* for medium loading, and *Table 4.9* for heavy loading. These tables were used to generate the graphs in *Figures 4.4 to 4.15*, which were scrutinised to explain the economy of the different slab systems for different loadings and span lengths.

Table 4.6: Material Cost 2007

Concrete (R/m³)	1100
Reinforcement (R/kg)	9.50
Cost Post-tension (R/kg)	36.50
Flat-slab Formwork (R/m²)	64
Coffer Formwork (R/m²)	114
Cobiax Component	
Cobiax sphere diameter (mm)	(R/m²)
180	139
225	140
270	150
315	186
360	215
405	233
450	240
*NOTES Costs exclude VAT Costs include: - Delivery on site - Labour - Reinforcement cages and spheres (Cobiax) - 10% contractor's mark-up (Cobiax) - Cables, sleeves & anchors (Post-tension)	

Table 4.7: Cobiax, Coffer & Post-tensioned Slab Cost Comparison - Light Load

Additional Dead Load = 0.5 kPa

Live Load = 2.0 kPa

Span (m)	Concrete (m^3/m^2)			Reinforcement (kg/m^2)		
	Cobiax	Coffer	Post-tension	Cobiax	Coffer	Post-tension
7.5	0.223	0.279	0.220	16.8	13.3	15.9
9.0	0.243	0.279	0.270	23.8	19.5	21.3
10.0	0.268	0.279	0.310	28.4	24.5	24.9
11.0	0.314	0.344	0.350	30.6	28.5	30.2
12.0	0.360	0.411	0.380	35.3	31.1	33.6
Span (m)	Slab Thickness (mm)			Cost (R/m^2)		
	Cobiax	Coffer	Post-tension	Cobiax	Coffer	Post-tension
7.5	280	425	220	608	547	504
9.0	300	425	270	696	606	626
10.0	340	425	310	769	653	715
11.0	400	525	350	851	763	822
12.0	460	625	380	981	861	900

Table 4.8: Cobiax, Coffer & Post-tensioned Slabs Cost Comparison - Medium Load

Additional Dead Load = 2.5 kPa

Live Load = 2.5 kPa

Span (m)	Concrete (m^3/m^2)			Reinforcement (kg/m^2)		
	Cobiax	Coffer	Post-tension	Cobiax	Coffer	Post-tension
7.5	0.223	0.279	0.230	22.0	16.5	20.9
9.0	0.268	0.279	0.280	29.8	24.6	28.2
10.0	0.314	0.344	0.325	31.6	28.6	29.8
11.0	0.360	0.411	0.370	35.1	31.2	35.7
12.0	0.405	0.411	0.410	42.8	37.1	36.8
Span (m)	Slab Thickness (mm)			Cost (R/m^2)		
	Cobiax	Coffer	Post-tension	Cobiax	Coffer	Post-tension
7.5	280	425	230	657	578	578
9.0	340	425	280	783	655	719
10.0	400	525	325	860	765	800
11.0	460	625	370	979	863	915
12.0	520	625	410	1132	919	981

Table 4.9: Cobiax, Coffer & Post-tensioned Slabs Cost Comparison - Heavy Load

Additional Dead Load = 5.0 kPa

Live Load = 5.0 kPa

Span (m)	Concrete (m^3/m^2)			Reinforcement (kg/m^2)		
	Cobiax	Coffer	Post-tension	Cobiax	Coffer	Post-tension
7.5	0.288	0.279	0.250	29.1	26.6	34.1
9.0	0.350	0.344	0.310	33.0	31.3	43.4
10.0	0.385	0.411	0.360	39.3	34.6	47.4
11.0	0.441	0.411	0.400	45.0	43.1	47.6
12.0	0.477	-	0.510	51.3	-	47.6

Span (m)	Slab Thickness (mm)			Cost (R/m^2)		
	Cobiax	Coffer	Post-tension	Cobiax	Coffer	Post-tension
7.5	360	425	250	798	674	742
9.0	450	525	310	948	790	913
10.0	500	625	360	1076	895	1020
11.0	570	625	400	1210	976	1078
12.0	620	-	510	1316	-	1204

Concrete content

Figure 4.4 and *Figure 4.8* indicated the Cobiax slab system to provide the greatest concrete savings for the light and medium load conditions respectively. Due to the rigidness of coffer slab thicknesses, it can be seen in *Figure 4.4* that coffer slabs had the highest concrete content for light loading, from where post-tensioned slabs required slightly more concrete between 9 m and 11 m spans, but then again coffers the most for 12 m span slabs. The dots, instead of lines, used in the graphs for concrete content and slab thickness of coffer slabs were due to the fact that a line could never represent coffer slabs, having only three possible slab depths.

For medium loading (*Figure 4.8*) the concrete content of post-tensioned slabs almost matched those of the Cobiax slabs, and coffer slabs showed to be the heaviest. For heavy loading (*Figure 4.12*) the concrete content of Cobiax and coffer slabs will be approximately the same, with coffer slabs delivering no results for the 12 m span design as explained in earlier discussions. Interesting is to note that for the case of heavy loading, the post-tensioned slabs will be the lightest slab system.

Only direct material cost benefits were taken into account when looking at the concrete content. It should be borne in mind though that, especially for high buildings, lighter slab systems can result in

enormous cost savings on support and foundation structures. The Cobiax system clearly displays this benefit for light loading, and therefore might be an attractive slab option for multi-level car park structures.

Reinforcement content

For light and medium loading conditions (*Figure 4.5 and 4.9*), coffer slabs will require the least reinforcement due to its larger slab depth, and therefore greater internal lever arms between the compression block and tension steel of the section. Post-tensioned slabs have the benefit of the cables balancing a great percentage of the total load, and therefore Cobiax slabs end up requiring the most reinforcement for light and medium loading conditions.

Figure 4.13 showed that for heavy loading conditions coffer slabs still require the least reinforcement, but in this case, post-tensioned slabs the most. This scenario occurred due to the fact that because of the high live load, a much smaller percentage of the total load has been balanced by the cable forces. The thin post-tension slabs therefore resulted in sections with small internal lever arms, requiring a lot of tension reinforcement. Due to the rapid increase in thickness of post-tensioned slabs close to 12 m spans for heavy loading, in order to resist punching effects, the thicker post-tension slab for a 12 m span had a greater lever arm. This explained why the reinforcement content was less than that of Cobiax slabs for these conditions.

Slab thickness

For all loading conditions (see *Figures 4.6, 4.10 and 4.14*) post-tension slabs had the smallest slab thicknesses and coffer slabs the largest. Although this was not taken into account for this cost study, again for high buildings with multi-level floors, Cobiax and post-tension slabs may have cost benefits in terms of vertical services and construction material required such as brickwork. Finishes to buildings with excessive heights can also result in high costs.

Direct material cost

The graphs comparing costs of the different slab systems, as displayed in *Figures 4.7, 4.11 and 4.15*, showed that the Cobiax system will be the most expensive and coffer slabs the cheapest for all loading conditions over large span lengths. *Table 4.6* clearly states what this cost study took into account, mainly being direct material costs. As earlier mentioned many other costs should also be taken into account to obtain a true display of the cost effectiveness of a slab system. Sadly in South

Africa very few quantity surveyors, contractors and engineers go the distance to calculate the indirect cost effects of different slab systems.

Preliminary cost estimates

The graphs in *Figures 4.3 to 4.15* can be used by designers to do preliminary cost estimates. For concrete content and slab thickness, should the spans differ, e.g. 9 m by 11 m spans, the designer should always take the reading on the graph for the largest span length to accommodate deflection requirements, thus 11 m in this example. Reinforcement and post-tensioning content may be obtained from a reading at the average span length, for this example at a 10 m span.

Take for instance the medium loading condition for a slab with a 9 m by 11 m column grid. From *Figure 4.8* at an 11 m span length, the concrete content for a Cobiax slab system will be 0.36 m^3/m^2. The slab thickness (*Figure 4.10*) for this same scenario will be 460 mm, also for an 11 m span length, and the reinforcement content (*Figure 4.9*) approximately 31.6 kg/m^2, taken at the average span length of 10 m. A 460 mm thick Cobiax slab will require 315 mm Cobiax spheres, resulting in a Cobiax component cost (see *Table 4.6*) of $R186/m^2$ in the year of 2007. Flat-slab formwork will be required, costing $R64/m^2$. Using the cost rates in *Table 4.6*, the total cost per square meter for this scenario will be:

$0.36 \times R1100 + 31.6 \times R9.5 + R186 + R64 = R946.20/m^2$

More conservatively the designer can read the cost directly from *Figure 4.11*, at the highest span length of 11 m, which will indicate a cost of R978.93 for this system. This will overestimate the more likely cost of the slab by 3.5%.

The preliminary cost and quantity estimates for Cobiax slabs can not be established at this time in South Africa with the Cobiax preliminary design graph in *Figure 2.14.1*, since this graph was based on European design standards that are much less strenuous on shear requirements, as well as assuming the use of Halfen shear reinforcement and 35 MPa concrete cylinder strength (43.75 MPa cube strength). These factors will cause Cobiax slabs not to be dominated by punching requirements, but rather deflection requirements, making much thinner Cobiax slabs possible. The designer should refer to the figures in this chapter only for South African Cobiax slab cost estimates.

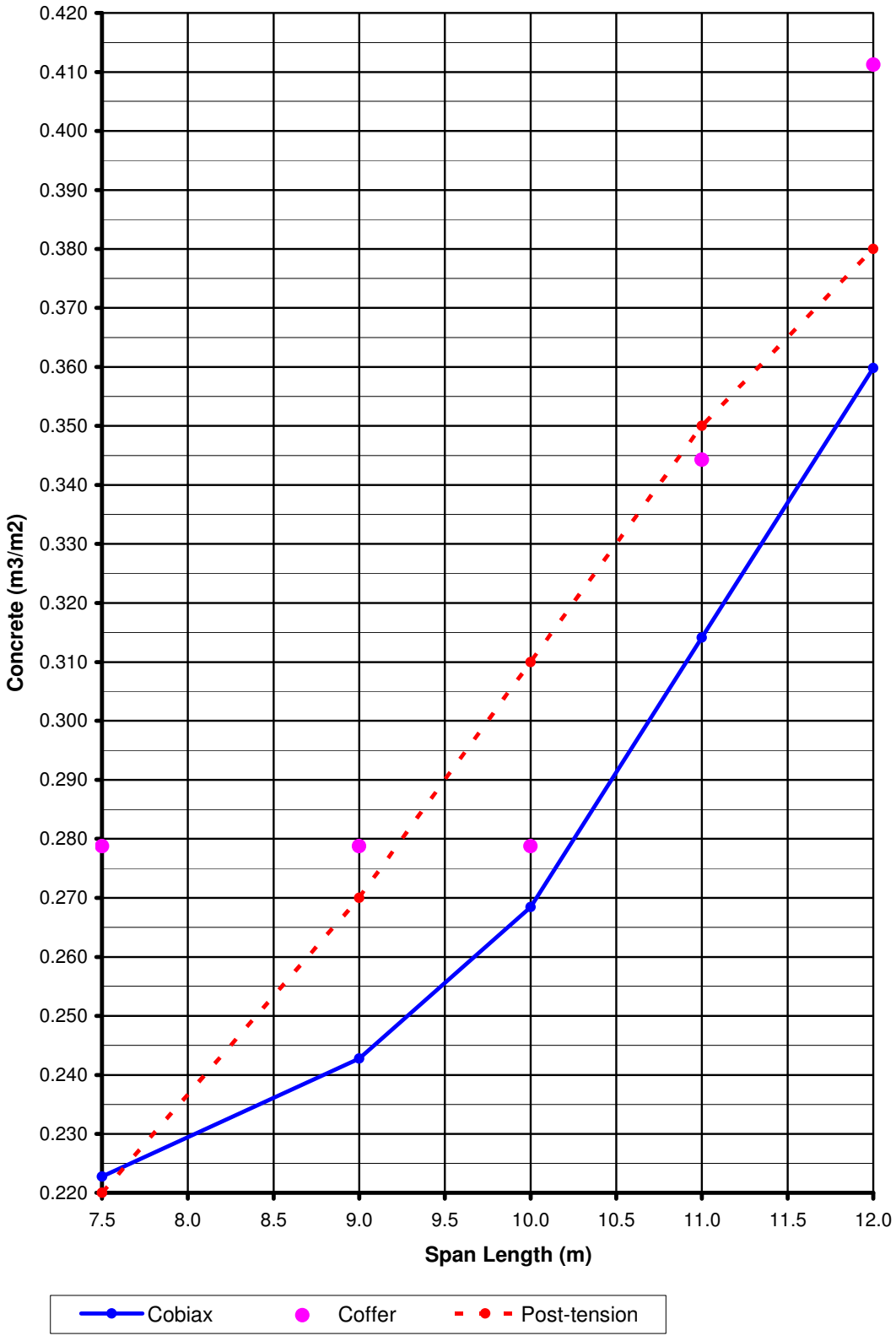

Figure 4.4: Concrete Content of Slab Systems [SDL=0.5kPa & LL=2.0kPa]

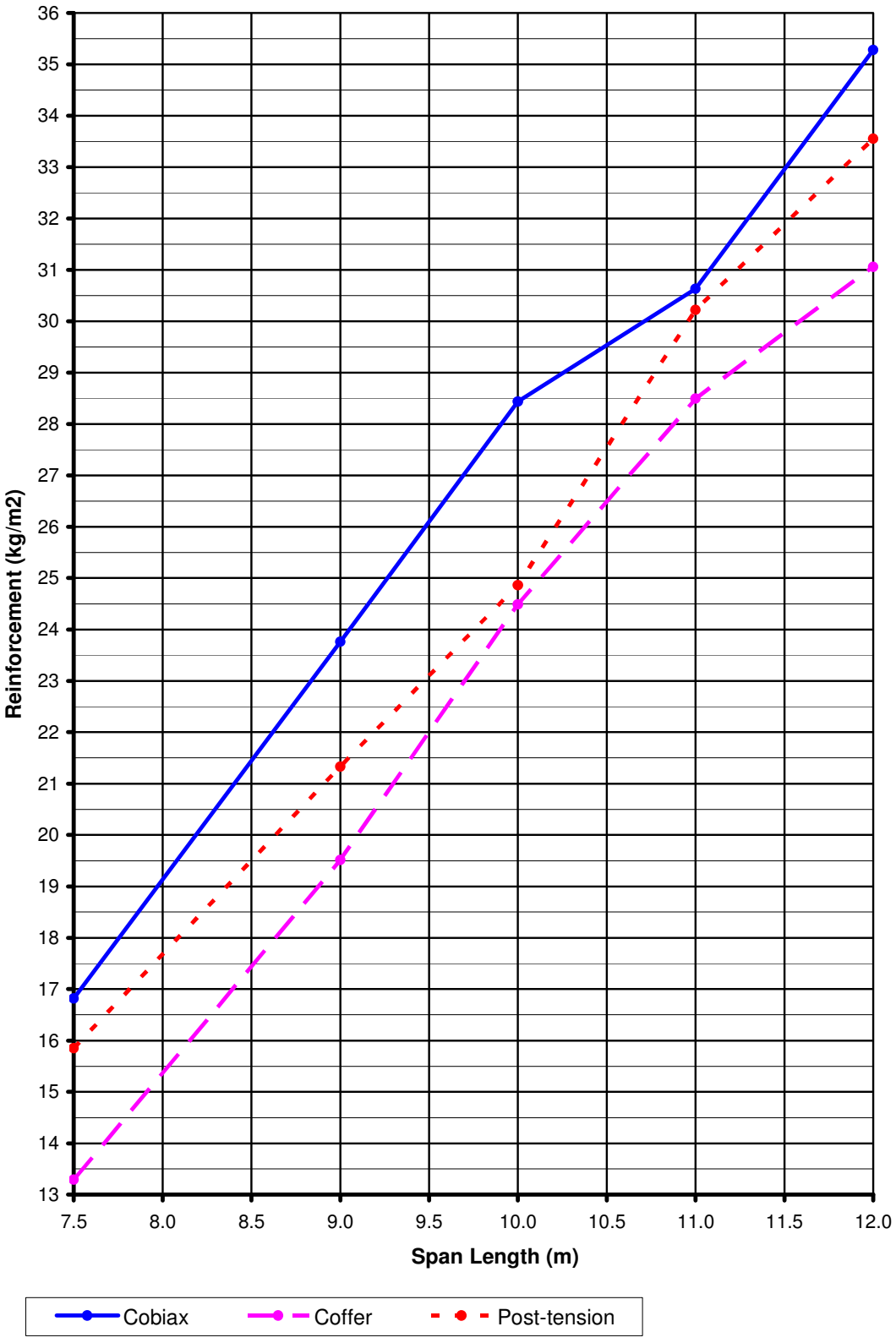

Figure 4.5: Reinforcement Content of Slab Systems [SDL=0.5kPa & LL=2.0kPa]

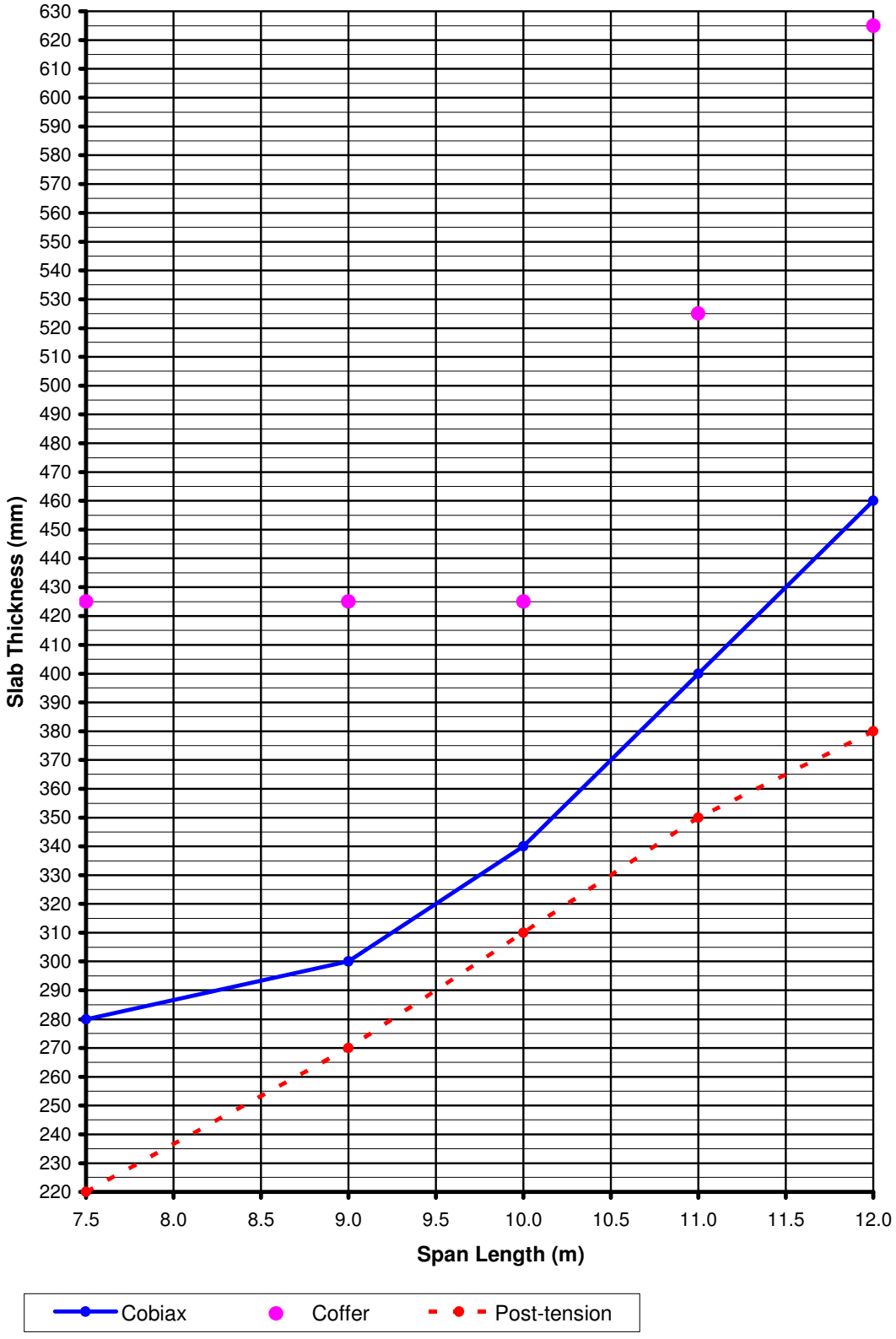

Figure 4.6: Slab Thickness of Slab Systems [SDL=0.5kPa & LL=2.0kPa]

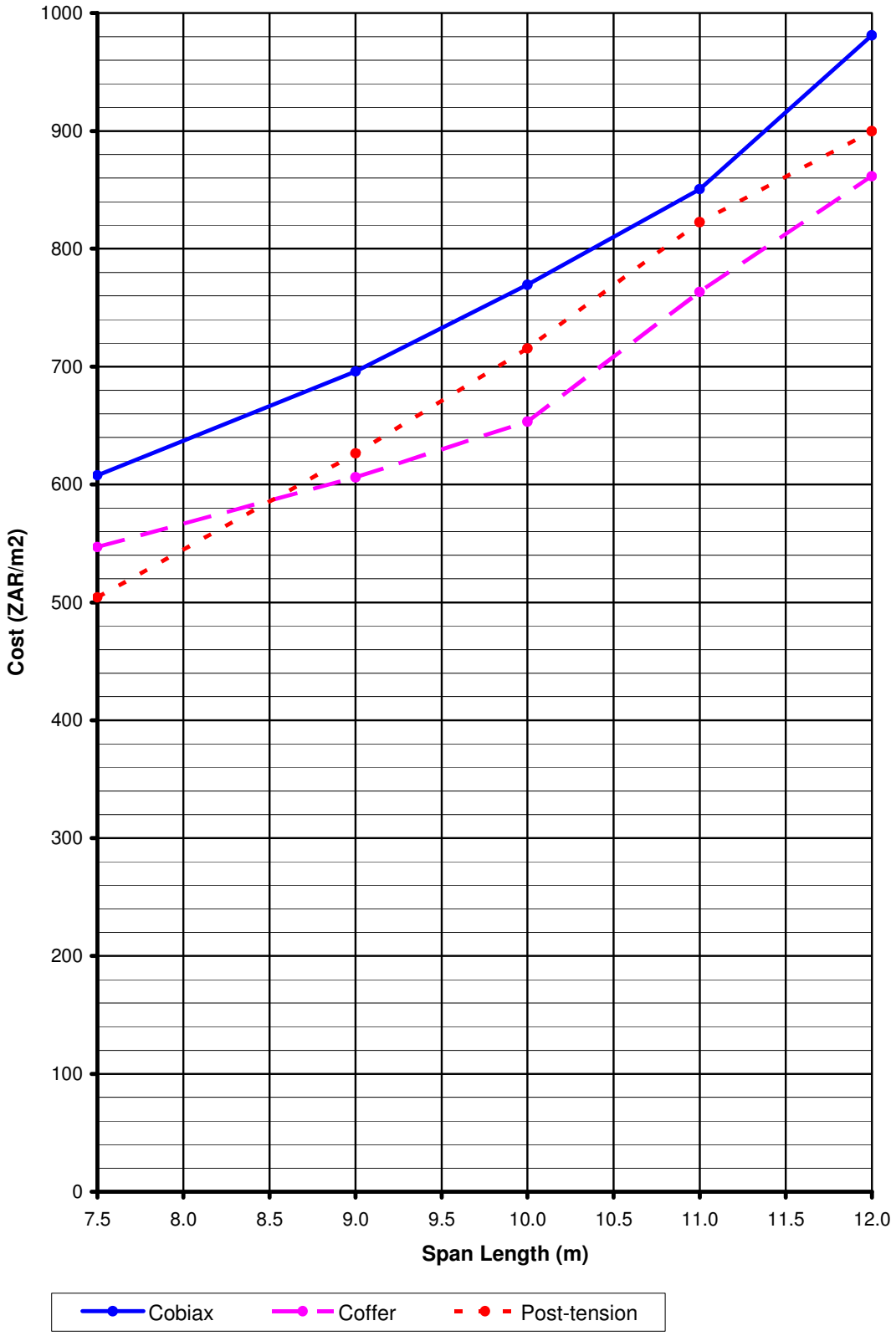

Figure 4.7: Cost of Slab Systems [SDL=0.5kPa & LL=2.0kPa]

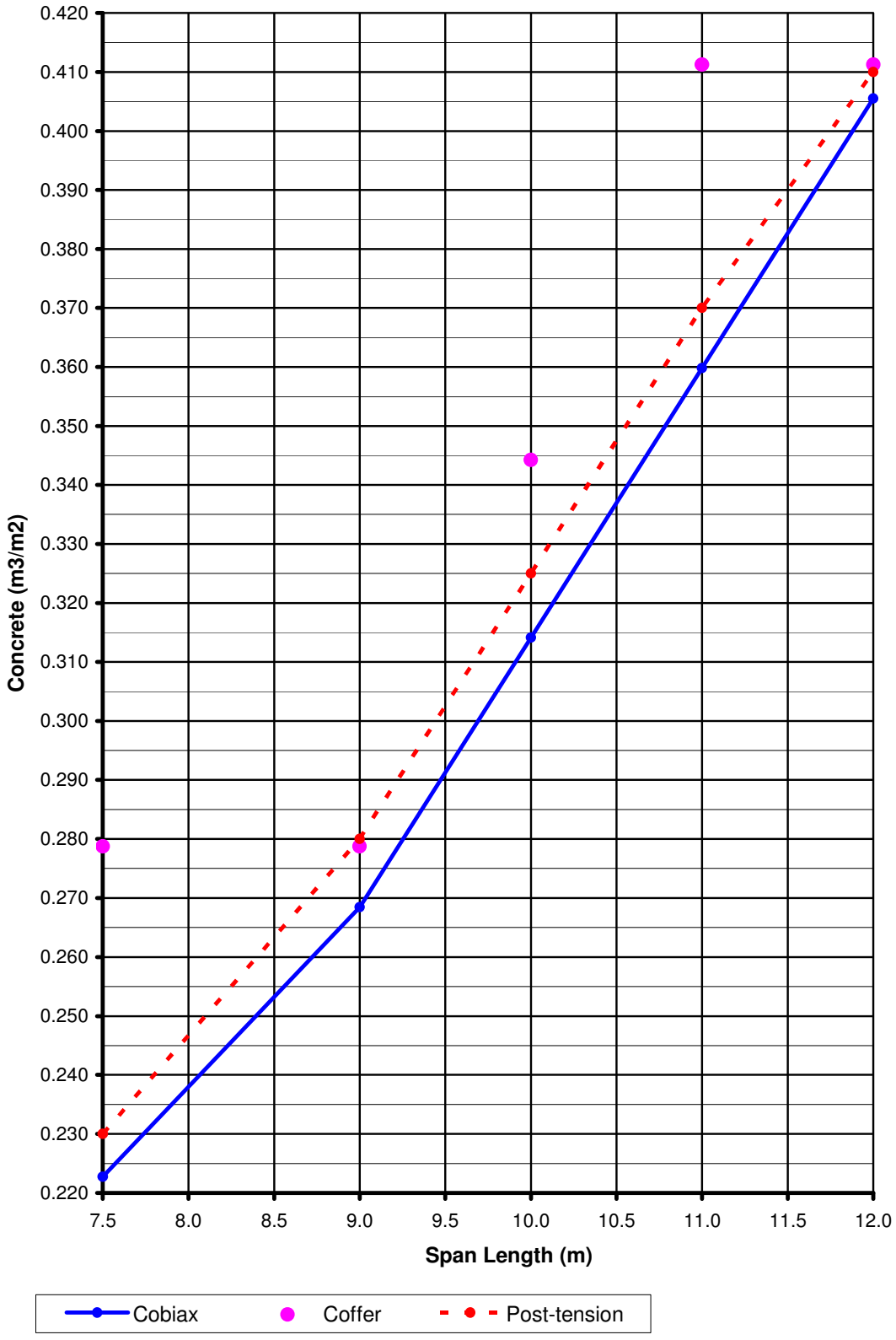

Figure 4.8: Concrete Content of Slab Systems [SDL=2.5kPa & LL=2.5kPa]

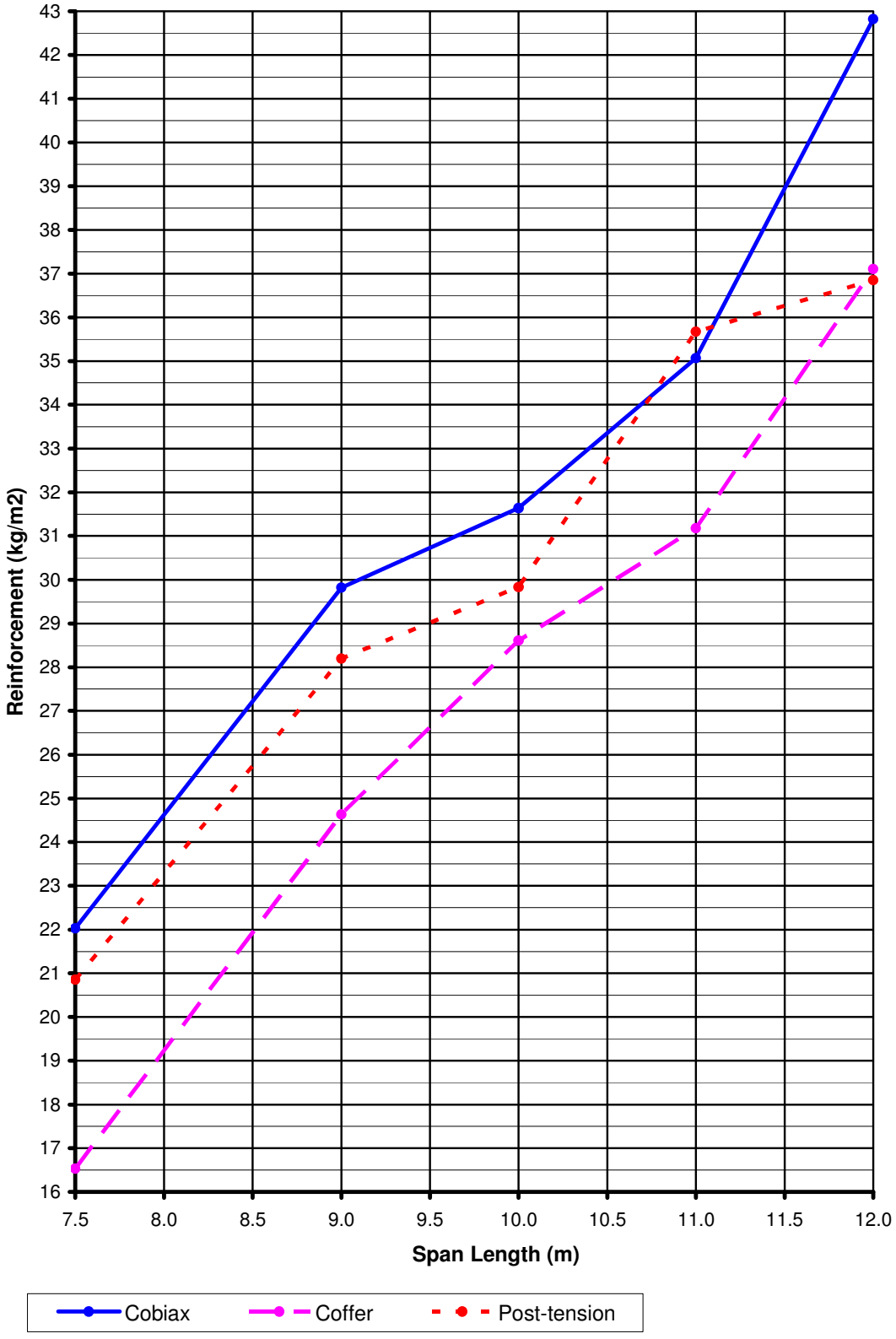

Figure 4.9: Reinforcement Content of Slab Systems [SDL=2.5kPa & LL=2.5kPa]

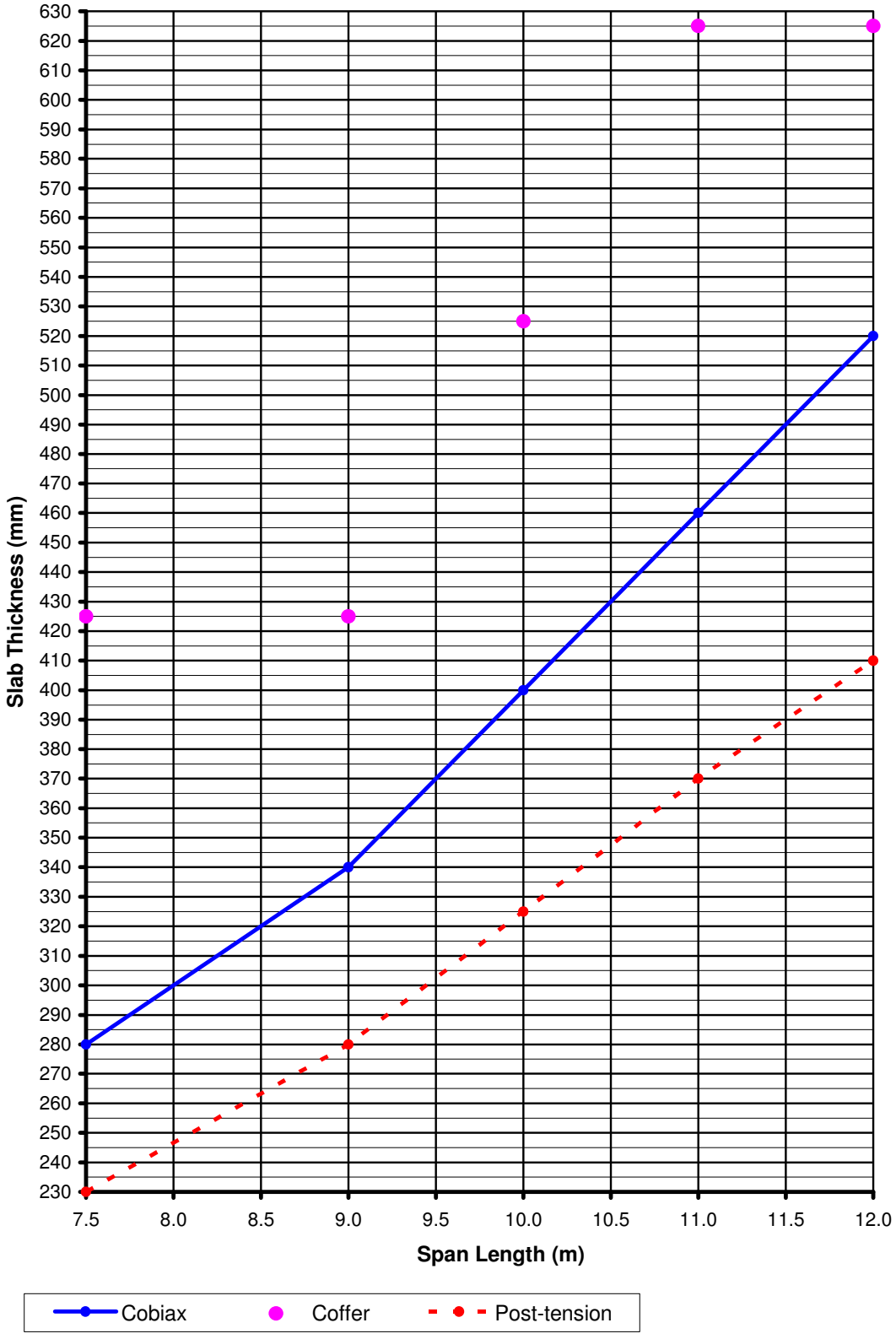

Figure 4.10: Slab Thickness of Slab Systems [SDL=2.5kPa & LL=2.5kPa]

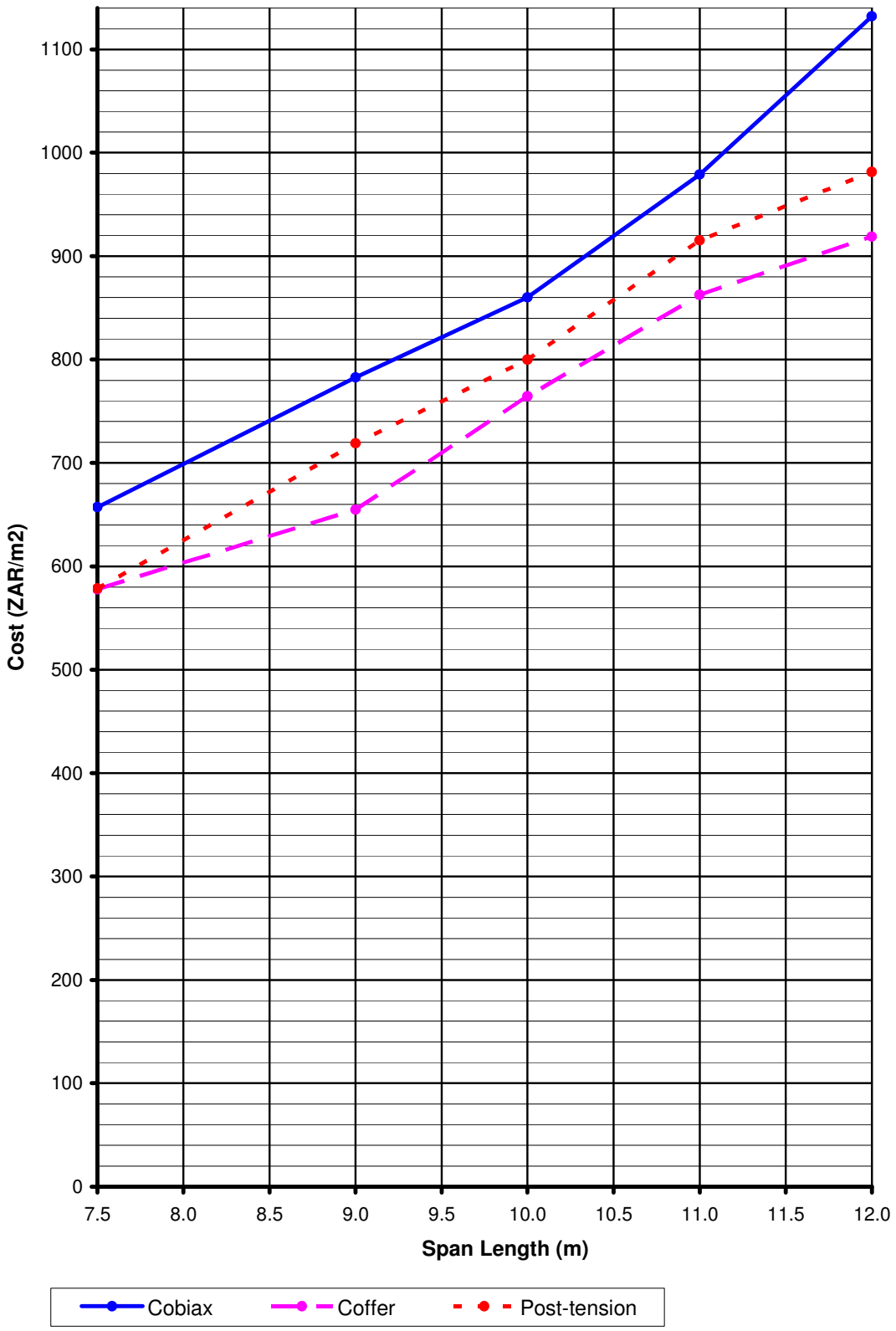

Figure 4.11: Cost of Slab Systems [SDL=2.5kPa & LL=2.5kPa]

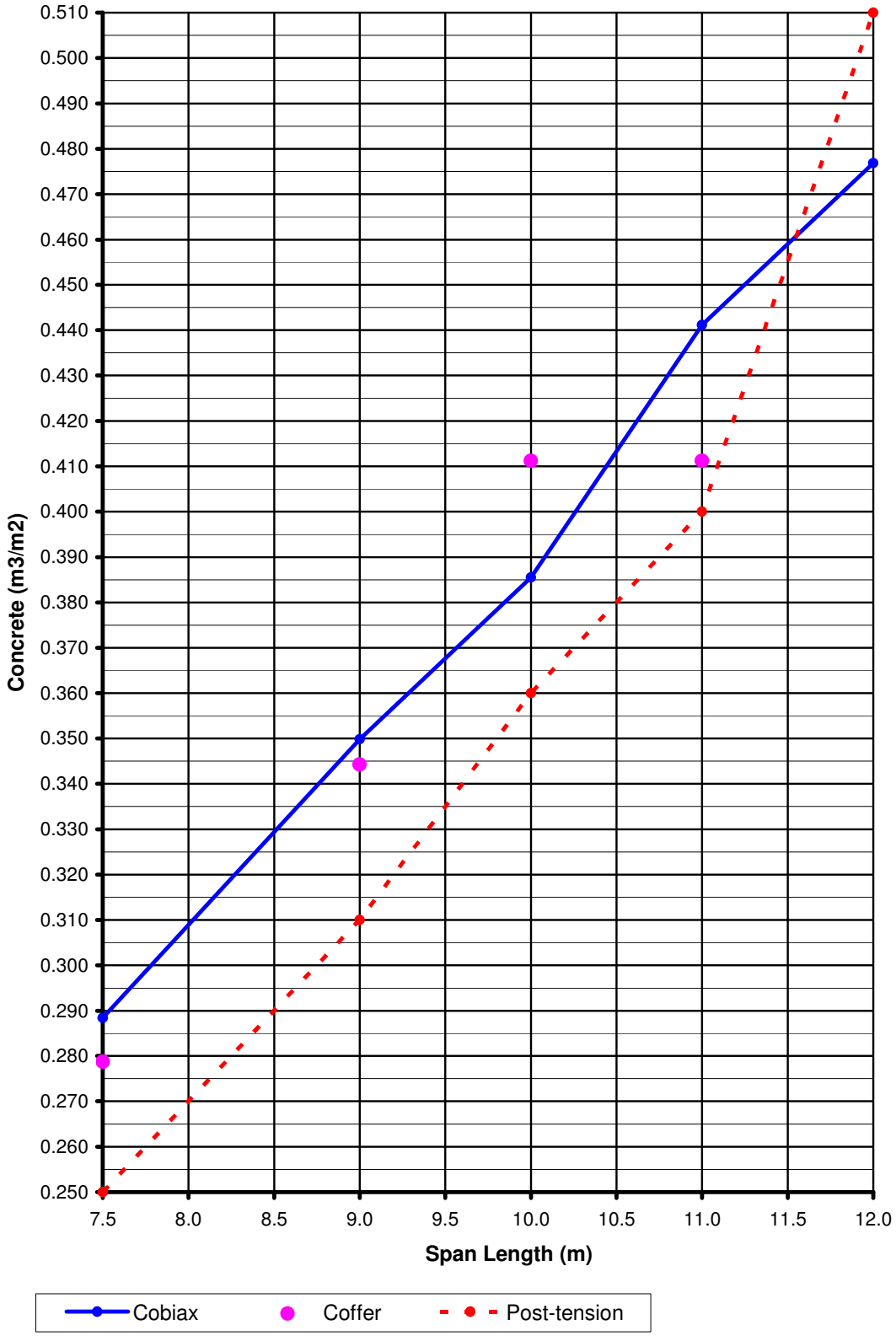

Figure 4.12: Concrete Content of Slab Systems [SDL=5.0kPa & LL=5.0kPa]

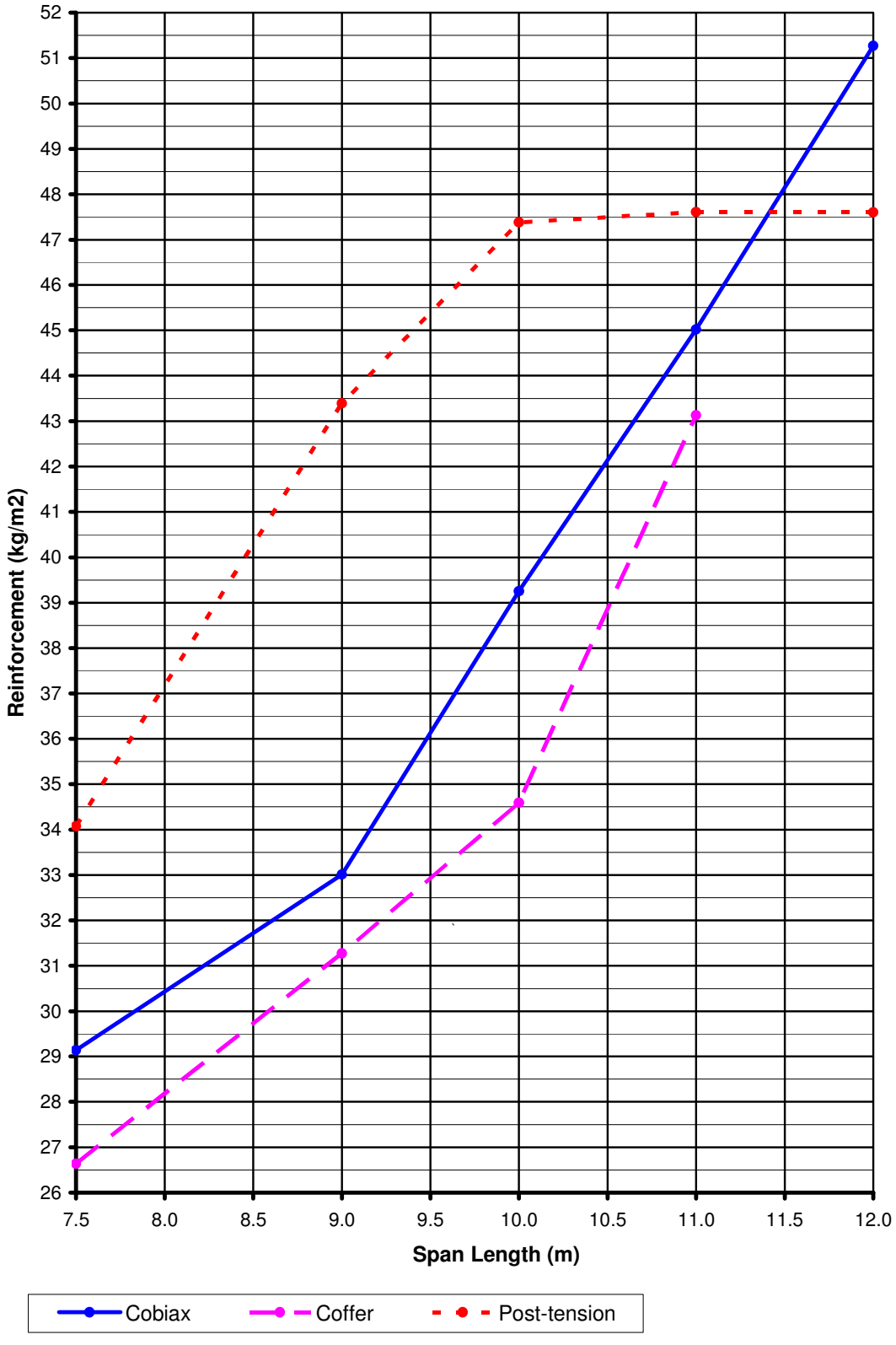

Figure 4.13: Reinforcement Content of Slab Systems [SDL=5.0kPa & LL=5.0kPa]

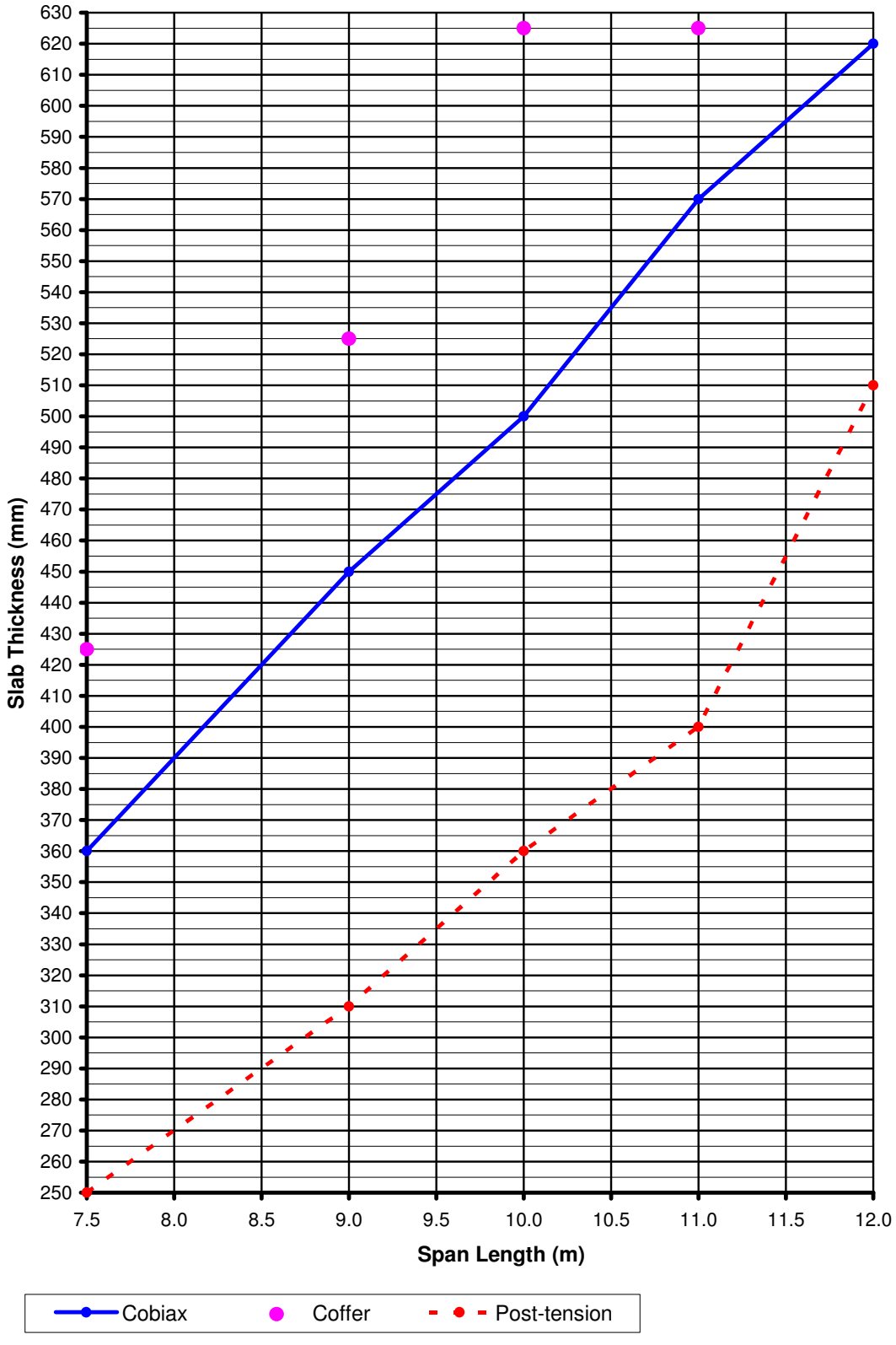

Figure 4.14: Slab Thickness of Slab Systems [SDL=5.0kPa & LL=5.0kPa]

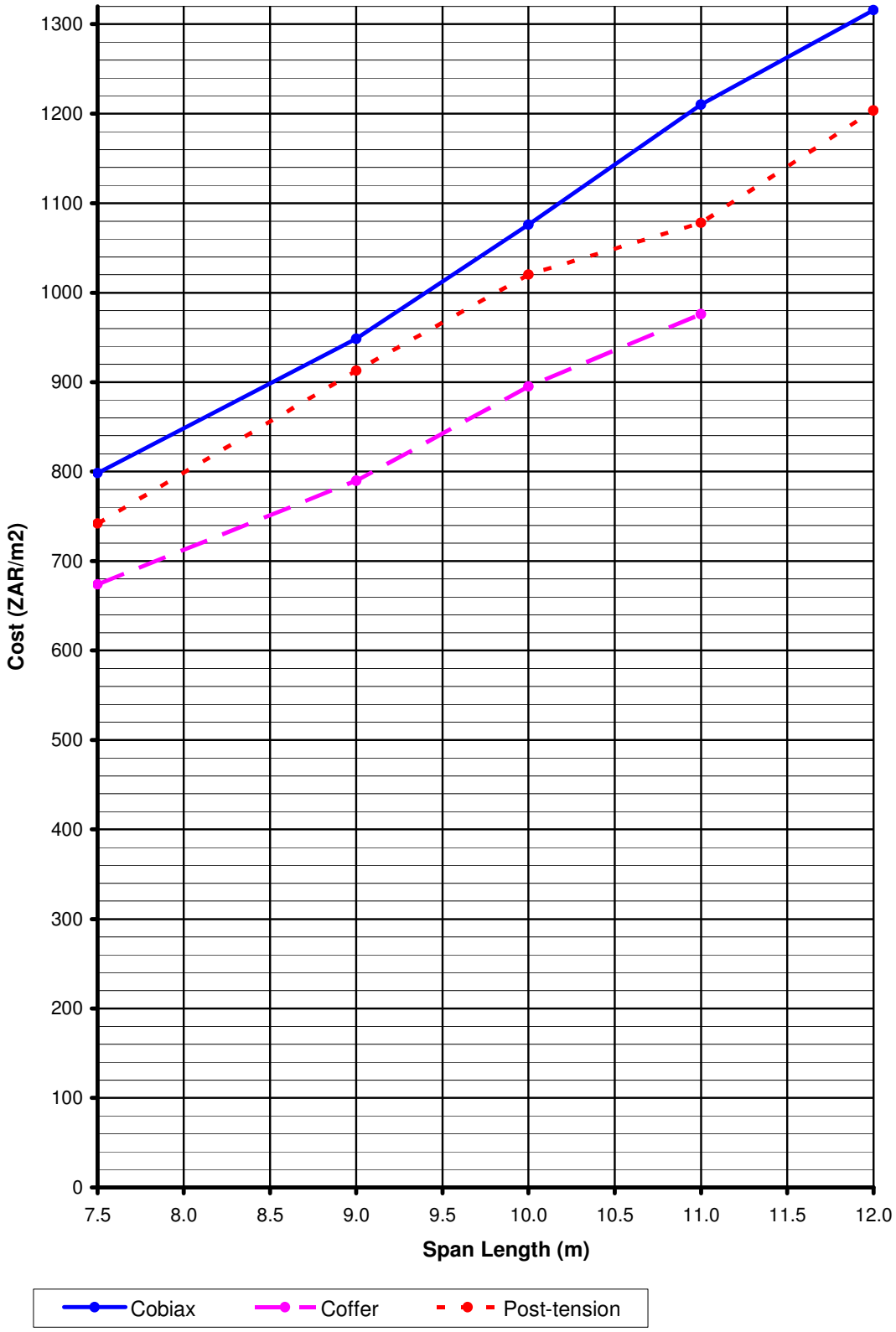

Figure 4.15: Cost of Slab Systems [SDL=5.0kPa & LL=5.0kPa]

5. CONCLUSIONS AND RECOMMENDATIONS

The cost effectiveness of flat-slabs with internal hollow spherical void formers was investigated in this report. The only system of this kind that is available in South Africa is the European Cobiax system. The report did not only investigate the cost relationship of Cobiax to that of other large span slab systems in the country, but also how the SANS 10100-01:2000 concrete design code applies to the system.

Experimental test at the University of Pretoria showed the Cobiax system to operate at higher shear resistance levels than obtained in German research. This was mainly due to the fact that German researchers conservatively ignored the additional shear capacity of the Cobiax steel cages. The shear reduction factor of 0.55 can be taken as 0.85 according to the laboratory tests done in South Africa, yet further research is required to establish whether this a higher factor will result in cost benefits. The probability that a higher factor is likely to be applicable should rather serve to ease the mind of the design engineer after applying the 0.55 factor to v_c.

In order to establish a more exact factor due to the contribution of the Cobiax cages, further test should be performed on Cobiax slabs, comparing solid samples, with solid samples plus cages, with samples containing both the hollow spheres and their cages. The design code formula for normal shear reinforcement will not be applicable for the vertical bars of the cages, since these cages are not fully anchored. Therefore testing samples as described above will display much more trustworthy results. Such testing is already in progress in Germany.

The conditions at the cold joint due to the two pour system with Cobiax slabs will have sufficient horizontal shear capacity according to the results in this report, but will not fulfill the minimum horizontal shear reinforcement requirements, unless the cages are made up of the following reinforcement diameters:

- 6 mm diameter bars for 180 mm and 225 mm diameter Cobiax sphere cages
- 8 mm diameter bars for 270 mm and 315 mm diameter Cobiax sphere cages
- 10 mm diameter bars for 360 mm and 405 mm diameter Cobiax sphere cages
- 12 mm diameter bars for 450 mm diameter Cobiax sphere cages

The cost comparison that was performed included Cobiax, coffer and unbonded post-tensioned flat-slabs, where all systems were considered to have no drop or column heads. Span lengths ranged from 7.5 m to 12 m spans, and light to heavy loading for normal commercial buildings only was

applied. Strand7 finite element analysis software was used to perform the analysis on 45 different models for the various slab types and conditions.

This was done to establish the cost effectiveness of the Cobiax flat-slab system in South Africa. The costs were based on concrete, reinforcement, formwork, post-tension (for post-tensioned slabs alone), and Cobiax (for Cobiax slabs alone) content. These costs were mainly based on direct slab material costs, and the quantity surveyor should investigate other economical implications when choosing a specific slab system as well.

The Cobiax system, based on the direct cost of the slab, turned out to be more expensive than the other two systems for all conditions. This can partly be remedied by introducing Halfen shear links in South Africa, since punching shear dominates Cobiax slab thicknesses, that increases costs. One would rather have thinner slabs dominated by deflection requirements. Halfen shear stirrups will allow the designer to use thinner Cobiax slabs for the same conditions, being much more effective in shear resistance than the normal South African shear clips, and easier to install. This will not only reduce the concrete content of Cobiax, but also the weight on columns and foundations, as well as the overall building height. Cost savings will be a result. The designer can also rather use the Eurocode 2 design code for his slab design, since the requirements for shear resistance are less strenuous than that of SANS 10100.

Cobiax nevertheless shows a cost benefit for light loading such as car parking levels. Due to less concrete content than other slab systems investigated, indirect cost savings can be considerable in terms of column and foundation types and sizes, especially for high, multilevel parking buildings.

Cobiax will also be a very efficient system when dealing with long span slab systems with complex column gridlines and openings in the slabs, or scattered columns. Here coffers and post-tensioning might be difficult to apply.

Due to the thinner slab thicknesses of Cobiax and post-tensioned slabs, lower overall building heights are possible. Especially with high multi-storey buildings, there can be considerable savings on vertical construction material (such as brickwork), services and finishes, by reducing the building's total height.

Cobiax slabs can be safely designed with the SANS 10100-01:2000 design code in combination with suggestions made in this report. Although the direct material cost of Cobiax slabs is higher than coffer and post-tensioned slabs, the Cobiax system can be utilised especially with the construction of high multi-level buildings, with large cost benefits as a result.

4.8. CONCLUSION

After modelling various equal span three-span by three-span slab models in Strand7 with eight-noded rectangular finite element plate elements, a cost comparison between Cobiax (representing SVFS in South Africa), coffer, and unbonded post-tensioned slabs could be executed in accordance with SANS 10100 (2000) and TMH7 Part 3 (1989). The cost comparison included direct material costs only, taking the effect of various span lengths between 7.5 m and 12 m and uniformly distributed load applications into account.

The SVFS (Cobiax) system resulted in the most expensive large span slab system, with coffer slabs being the cheapest for almost every span length and load application scenario, this mainly being the result of the high Cobiax component costs (Cobiax cages and spheres).

6. REFERENCES

ACI 318-08 2005. *Building Code Requirements for Structural Concrete and Commentary.* Committee 318, USA.

Allen, A.H. 1988. *Reinforced Concrete Design to BS8110: Simply Explained*, E. & F.N. Spon, London, 239 pp.

BS 8110-1 1997. *Structural use of concrete. Code of practice for design and construction*. Committee B/525/2, London.

CBD-MS&CRO 2006. *Cobiax Technology Handbook*, Cobiax Technologies AG Zug, Switzerland.

Concrete Society Technical Report No. 43. *Post-tensioned concrete floors: Design handbook*, The Concrete Society, UK.

Cope, R.J. and Clark, L.A. 1984. *Concrete Slabs Analysis and Design*, Elsevier Applied Science Publishers, London, 502 pp.

DIN 1045-1 2000. *Tragwerke aus Beton, Stahlbeton und Spannbeton, Teil 1 Bemessung und Konstruktion*. Germany.

Dr John Robberts 2007. *Private communication*.

EN2 1992. Eurocode 2 - *Design of concrete structures*. CEN, UK.

Fung, Y. and Tong, P. 2001. *Classical and Computational Solid Mechanics.* World Scientific, USA.

Goodchild, C.H. 1997. *Economic Concrete Frame Elements*, British Cement Association, Berkshire.

Gupta, A.K. 1986. "*Combined Membrane and Flexural Reinforcement in Plates and Shells*," *Journal of Structural Engineering*, ASCE, V. 112, No. 3, pp. 550-557.

Jan Kotze 2007. *Private communication*.

Kani, G.N.J. 1966. *Basic Facts Concerning Shear Failure, Journal ACI, Vol. 63, June, pp. 675-692*.

Kong, F.K. and Evans, R.H. 1987. *Reinforced and Prestressed Concrete, 3rd ed*, Chapman & Hall, London, 508 pp.

Leonhardt, F. 1965. *"Reducing Shear Reinforcement in Concrete Beams and Slabs," Magazine of Concrete Research, Vol. 17, No. 53, Dec., pp. 187-198. (This is a brief summary of the original work done by Leonhardt Walther in Stuttgart from 1961 to 1963).*

Marshall, V & Robberts, J. M. 2000. *Prestressed Concrete Design and Practice*, Concrete Society of Southern Africa.

Mosley, W.H., Hulse, R., and Bungey, J.H. 1996. *Reinforced Concrete Design to Eurocode 2*, MacMillan Press, London, 426 pp.

Park, R. and Gamble, W. L. 2000. *Reinforced Concrete Slabs,* 2nd ed, John Wiley & Sons, Canada.

Park, R. and Paulay, T. 1975. *Reinforced Concrete Structures*, John Wiley & Sons, New York, 769 pp.

Pfeffer, K. 2002. *Untersuchung zum Beige- und Durchstanz- tragverhalten von zweiachsigen Hohlkörperdecken,* Germany.

PROKON, 2006. *Prokon Structural Analysis and Design Software.* Prokon Software Consultants Ltd, Pretoria.

Reddy, J.N. 1999. *Theory and Analysis of Elastic Plates.* Taylor & Francis, USA.

Report 110 1985. Construction Industry Research and Information Association. *Design of reinforced concrete flat slabs to BS 8110*, London.

Report No.2. 1989. *The South African Institution of Civil Engineers - Design of Prestressed Concrete Flat Slabs.* The Joint Structural Division of The South African Institution of Civil Engineers and the Institution of Structural Engineers, Johannesburg.

Rowe, R.E., Sommerville, G., Beeby, A.W., Menzies, J.B., Forrest, J.C.M., Harrison, T.A., Moore, J.F.A., Newman, K., Taylor, H.P.J., Threfall, A.J. and Whittle, R. 1987. *Handbook to British Standard BS 8110: 1985: Structural Use of Concrete*, Palladian Publications Ltd., London, 206 pp.

SABS 0160 1989. South African Bureau of Standards 1994. *Code of Practice for the General Procedures and Loadings to be adopted in the Design of Buildings (as amended 1990, 1991 and 1993)*, SABS, Pretoria.

SABS 0144 1995. South African Bureau of Standards. *Detailing of steel reinforcement for concrete, SANS 10144,* SABS, Pretoria, 143 pp.

SANS 10100-1 2000. South African National Standards 200. *Code of Practice for The Structural Use of Concrete Part 1*, SABS, Pretoria.

SANS 10160 1989. South African National Standards 200. *Basis of structural design and actions for buildings and indaustrial structures*, SABS, Pretoria.

Schellenbach-Held, M., Pfeffer, K. 1999. *Transverse force capability of the BubbleDeck*, Technical University Darmstadt's Institute for Solid Construction (in German), Germany.

Shear Study Group 1969. *The Shear Strength of Reinforced Concrete Beams*, Institution of Structural Engineers, London, 170 pp.

Strand7, 2006. *Strand7 Finite Element Analysis Software*. Strand7 Pty Ltd, Australia.

Technical Report No.43 (1994). The Concrete Society. *Post-Tensioned Concrete Floors – Design Handbook*, London.

TMH7 Part 3 1989. Committee of State Road Authorities. *Code of Practice for the Design of Highway Bridges and Culverts in South Africa,* Department of Transport, Pretoria.

Vecchio, F.J. & Collins, M.P. 1986. *The Modified Compression-Field Theory for Reinforced-Concrete Elements Subject to Shear.* Journal of the American Concrete Institute, Vol. 83, No. 2, pp. 219-231.

Wood, R.H. 1968. *The Reinforcement of Slabs in Accordance with a Pre-Determined Field of Moment*, Concrete, V. 2, No. 2, pp. 69-76. (A discussion by Armer).

APPENDIX A

Reinforcement Provided

Cobiax - Reinforcement Content (mm^2/m)

CS - Column strip; MS - Middle strip

Load	Span (m)	Slab Area (m^2)	h (mm)	Shear steel (kg/m^2)	Minimum (mm^2)
7.5m light load	7.5	506	280	0.2	364
7.5m medium load	7.5	506	280	0.4	364
7.5m heavy load	7.5	506	360	0.8	468
9m light load	9	729	300	0.2	390
9m medium load	9	729	340	0.5	442
9m heavy load	9	729	450	0.7	585
10m light load	10	900	340	0.4	442
10m medium load	10	900	400	0.5	520
10m heavy load	10	900	500	0.8	650
11m light load	11	1089	400	0.4	520
11m medium load	11	1089	460	0.5	598
11m heavy load	11	1089	570	0.9	741
12m light load	12	1296	460	0.4	598
12m medium load	12	1296	520	0.7	676
12m heavy load	12	1296	620	1.0	806

Load	Bottom Steel - Edge Span		Bottom Steel - Internal Span		Top Steel - Supports		Total
	CS	MS	CS	MS	CS	MS	kg/m^2
7.5m light load	628	524	452	377	1608	377	16.8
7.5m medium load	905	524	452	377	2513	377	22.0
7.5m heavy load	1047	804	524	452	3272	628	29.1
9m light load	1005	670	565	377	2454	524	23.8
9m medium load	1340	754	524	524	3272	524	29.8
9m heavy load	1340	1005	670	565	3272	785	33.0
10m light load	1047	754	524	524	3272	670	28.4
10m medium load	1340	905	670	628	3272	628	31.6
10m heavy load	1608	1137	804	670	3927	1005	39.3
11m light load	1257	905	628	628	3217	628	30.6
11m medium load	1257	1047	804	670	3927	670	35.1
11m heavy load	1636	1340	754	754	5362	754	45.0
12m light load	1257	1257	628	628	3927	628	35.3
12m medium load	1636	1257	754	804	4909	804	42.8
12m heavy load	1963	1340	905	754	6434	754	51.3

Coffer - Reinforcement Content (mm²/m)

CS - Column strip; MS - Middle strip

Load	**Span (m)**	**Slab Area (m²)**	**h (mm)**	**Shear steel (kg/m²)**	Web Width (mm)	Minimum (mm²)		
						Solid Zone	Voided Zone	Provided
7.5m light load	7.5	506	425	0.0	193	553	148	168
7.5m medium load	7.5	506	425	0.2	193	553	148	168
7.5m heavy load	7.5	506	425	0.4	193	553	148	168
9m light load	9	729	425	0.1	193	553	148	168
9m medium load	9	729	425	0.3	193	553	148	168
9m heavy load	9	729	525	0.5	213	683	201	262
10m light load	10	900	425	0.2	193	553	148	168
10m medium load	10	900	525	0.2	213	683	201	262
10m heavy load	10	900	625	0.6	233	813	262	314
11m light load	11	1089	525	0.2	213	683	201	262
11m medium load	11	1089	625	0.3	233	813	262	262
11m heavy load	11	1089	625	0.5	233	813	262	262
12m light load	12	1296	625	0.2	233	813	262	262
12m medium load	12	1296	625	0.4	233	813	262	314

Load	**Bottom Steel - Edge Span**		**Bottom Steel - Internal Span**		**Top Steel - Supports**		**Total**
	CS	MS	CS	MS	CS	MS	kg/m²
7.5m light load	447	349	174	174	1340	262	13.3
7.5m medium load	502	447	174	174	1636	524	16.5
7.5m heavy load	893	698	174	174	3272	524	26.6
9m light load	698	502	174	174	2094	524	19.5
9m medium load	893	698	174	174	2681	670	24.6
9m heavy load	1091	893	349	349	3272	670	31.3
10m light load	893	698	174	174	2681	670	24.5
10m medium load	893	698	349	349	3272	670	28.6
10m heavy load	1091	893	349	349	3927	754	34.6
11m light load	893	698	349	349	3272	670	28.5
11m medium load	1091	893	349	349	3272	754	31.2
11m heavy load	1397	1091	349	349	5362	1047	43.1
12m light load	1091	893	349	349	3272	754	31.1
12m medium load	1397	1091	349	349	3927	754	37.1

Post-tension - Reinforcement Content (m

CS - Column strip; MS - Middle strip

Load	Span (m)	Slab Area (m²)	h (mm)	Shear steel (kg/m²)	Minimum (mm²)
7.5m light load	7.5	506	220	0.0	286
7.5m medium load	7.5	506	230	0.0	299
7.5m heavy load	7.5	506	250	0.1	325
9m light load	9	729	270	0.0	351
9m medium load	9	729	280	0.1	364
9m heavy load	9	729	310	0.3	403
10m light load	10	900	310	0.1	403
10m medium load	10	900	325	0.1	423
10m heavy load	10	900	360	0.3	468
11m light load	11	1089	350	0.1	455
11m medium load	11	1089	370	0.1	481
11m heavy load	11	1089	400	0.5	520
12m light load	12	1296	380	0.1	494
12m medium load	12	1296	410	0.3	533
12m heavy load	12	1296	510	0.6	663

Load	Bottom Steel - Edge Span		Bottom Steel - Internal Span		Top Steel - Supports		Total
	CS	MS	CS	MS	CS	MS	kg/m²
7.5m light load	628	452	314	314	1608	452	15.9
7.5m medium load	785	565	393	393	2454	393	20.9
7.5m heavy load	1608	754	628	377	3927	670	34.1
9m light load	785	565	393	393	2454	565	21.3
9m medium load	1047	754	524	524	3272	670	28.2
9m heavy load	1636	1047	754	524	5362	1047	43.4
10m light load	1047	670	524	524	2681	524	24.9
10m medium load	1340	754	524	524	3272	670	29.8
10m heavy load	2094	1340	670	524	5362	1047	47.4
11m light load	1047	754	1047	754	3272	670	30.2
11m medium load	1608	905	628	628	3927	804	35.7
11m heavy load	2094	1340	754	524	5362	1047	47.6
12m light load	1257	905	628	628	3927	804	33.6
12m medium load	1571	1005	565	565	4021	1005	36.8
12m heavy load	2094	1340	754	524	5362	1047	47.6

APPENDIX B

Cobiax – Reinforcement Required – Strand7

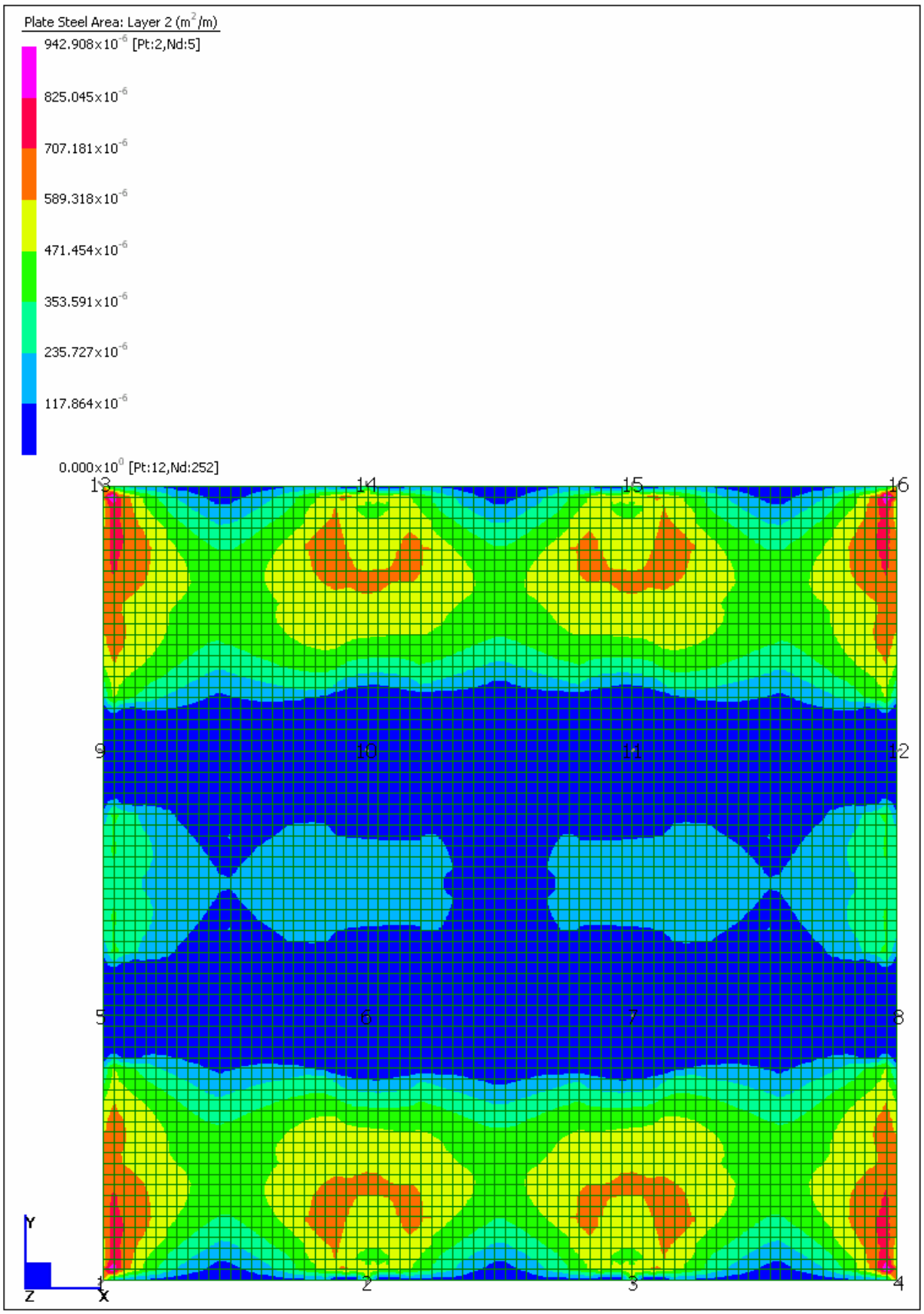
Plate Steel Area: Layer 2 (m²/m)
942.908x10⁻⁶ [Pt:2,Nd:5]
825.045x10⁻⁶
707.181x10⁻⁶
589.318x10⁻⁶
471.454x10⁻⁶
353.591x10⁻⁶
235.727x10⁻⁶
117.864x10⁻⁶
0.000x10⁰ [Pt:12,Nd:252]
13
14
15
16
9
10
11
12
5
6
7
8
1
2
3
4
Y
Z
X
Strand7 Release 2.3.8 [Licenced to:COBIAX]

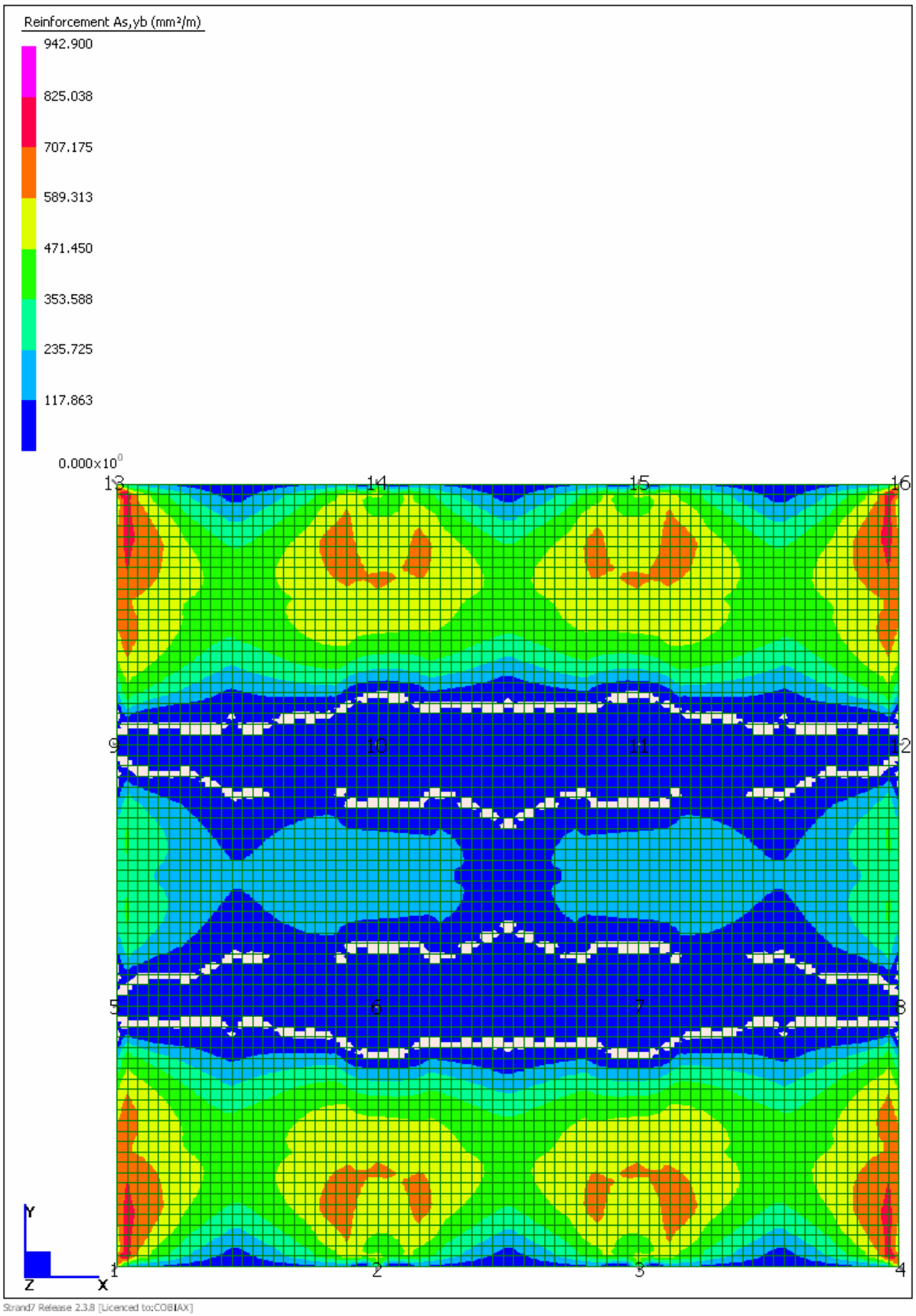
Reinforcement As,yb (mm²/m)
942.900
825.038
707.175
589.313
471.450
353.588
235.725
117.863
0.000x10^0
13
14
15
16
9
10
11
12
5
6
7
8
1
2
3
4
Y
Z
X
Strand7 Release 2.3.8 [Licenced to:COBIAX]

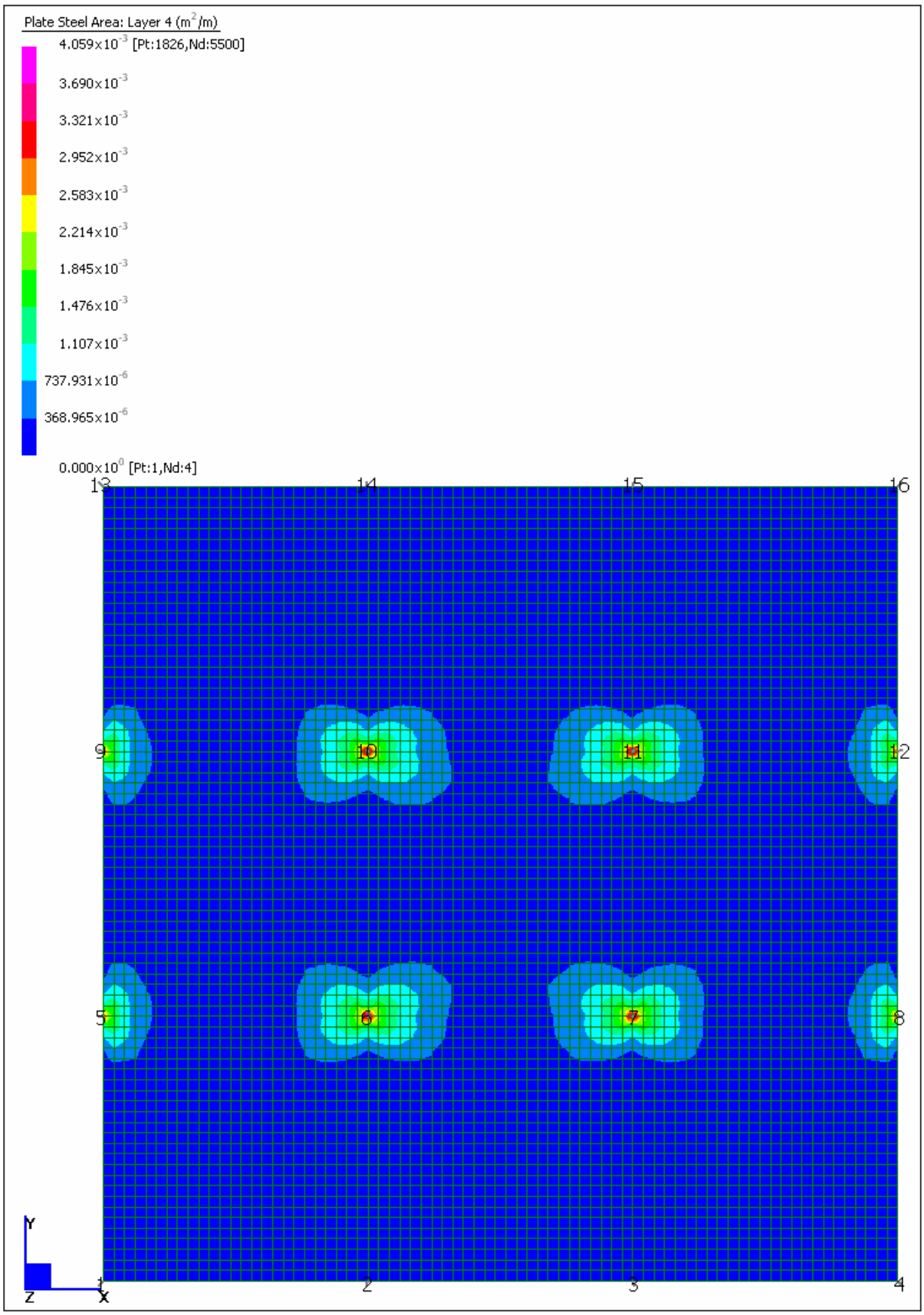
Plate Steel Area: Layer 4 (m²/m)
4.059x10⁻³ [Pt:1826,Nd:5500]
3.690x10⁻³
3.321x10⁻³
2.952x10⁻³
2.583x10⁻³
2.214x10⁻³
1.845x10⁻³
1.476x10⁻³
1.107x10⁻³
737.931x10⁻⁶
368.965x10⁻⁶
0.000x10⁰ [Pt:1,Nd:4]
13
14
15
16
9
10
11
12
5
6
7
8
1
2
3
4
Y
Z
X

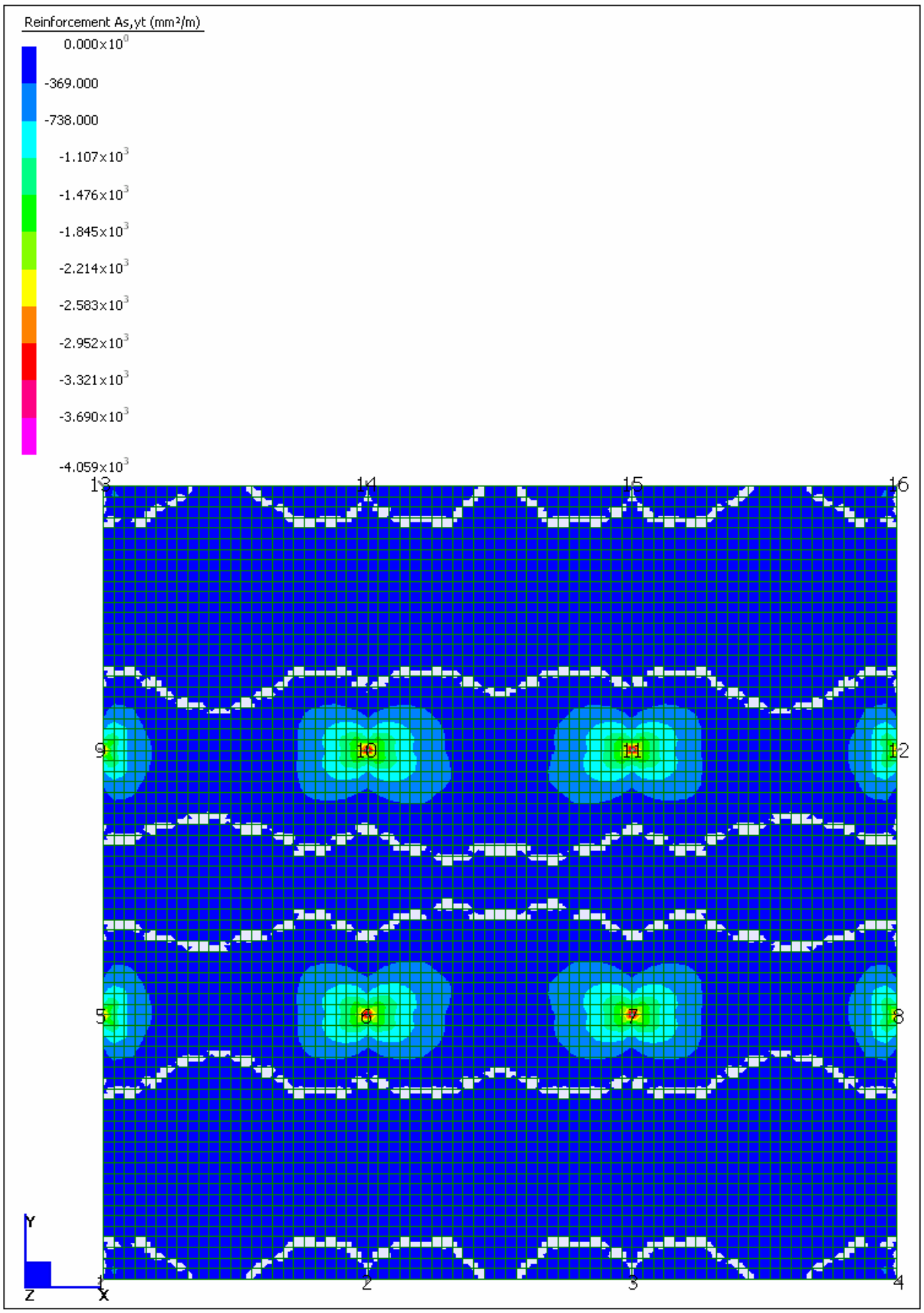
Reinforcement As,yt (mm²/m)
0.000x10^0
-369.000
-738.000
-1.107x10^3
-1.476x10^3
-1.845x10^3
-2.214x10^3
-2.583x10^3
-2.952x10^3
-3.321x10^3
-3.690x10^3
-4.059x10^3
13
14
15
16
9
10
11
12
5
6
7
8
1
2
3
4
Y
Z
X
Strand7 Release 2.3.8 [Licenced to:COBIAX]

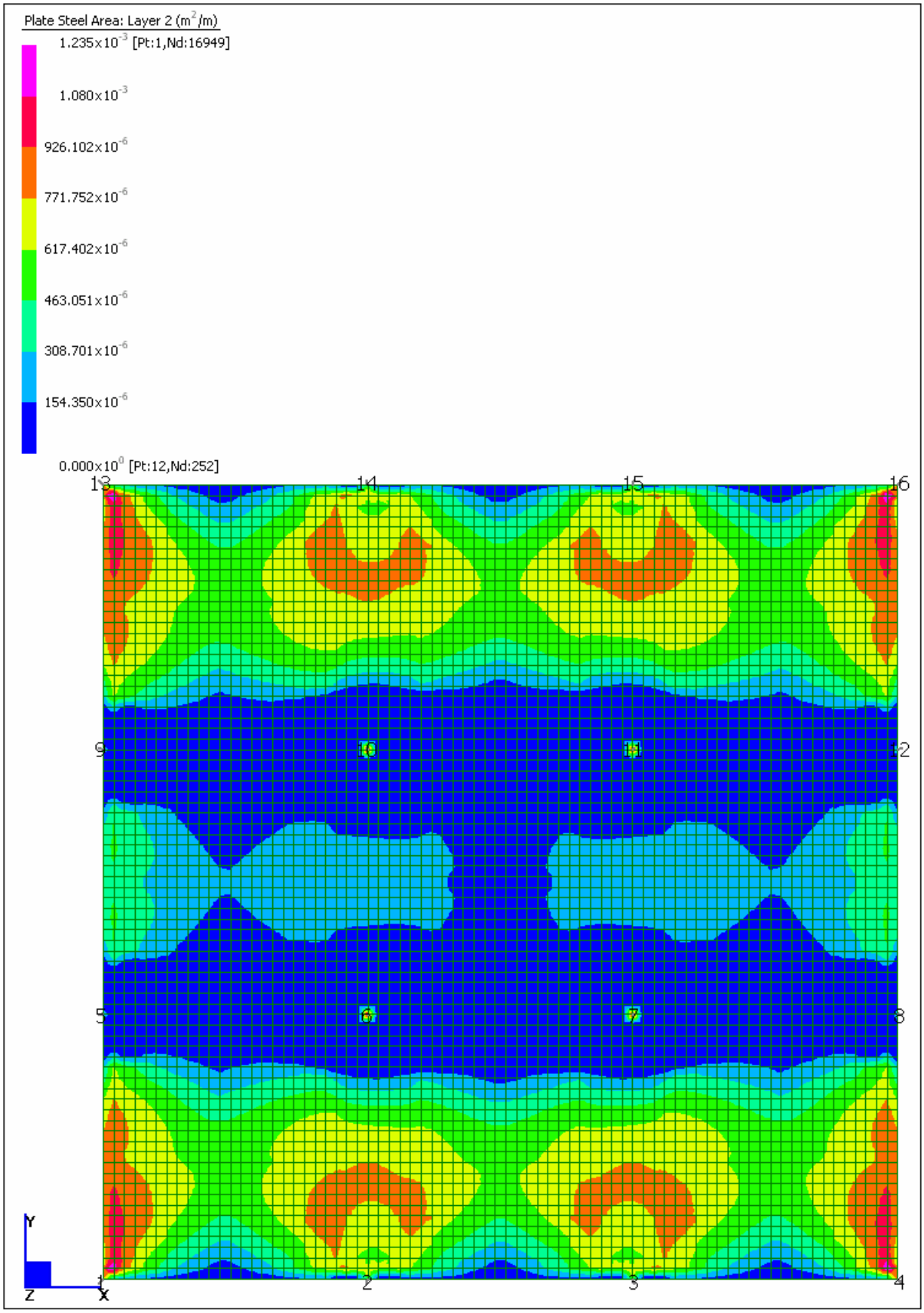
Plate Steel Area: Layer 2 (m²/m)
1.235x10⁻³ [Pt:1,Nd:16949]
1.080x10⁻³
926.102x10⁻⁶
771.752x10⁻⁶
617.402x10⁻⁶
463.051x10⁻⁶
308.701x10⁻⁶
154.350x10⁻⁶
0.000x10⁰ [Pt:12,Nd:252]
13
14
15
16
9
10
11
12
5
6
7
8
1
2
3
4
Y
Z
X
Strand7 Release 2.3.8 [Licenced to:COBIAX]

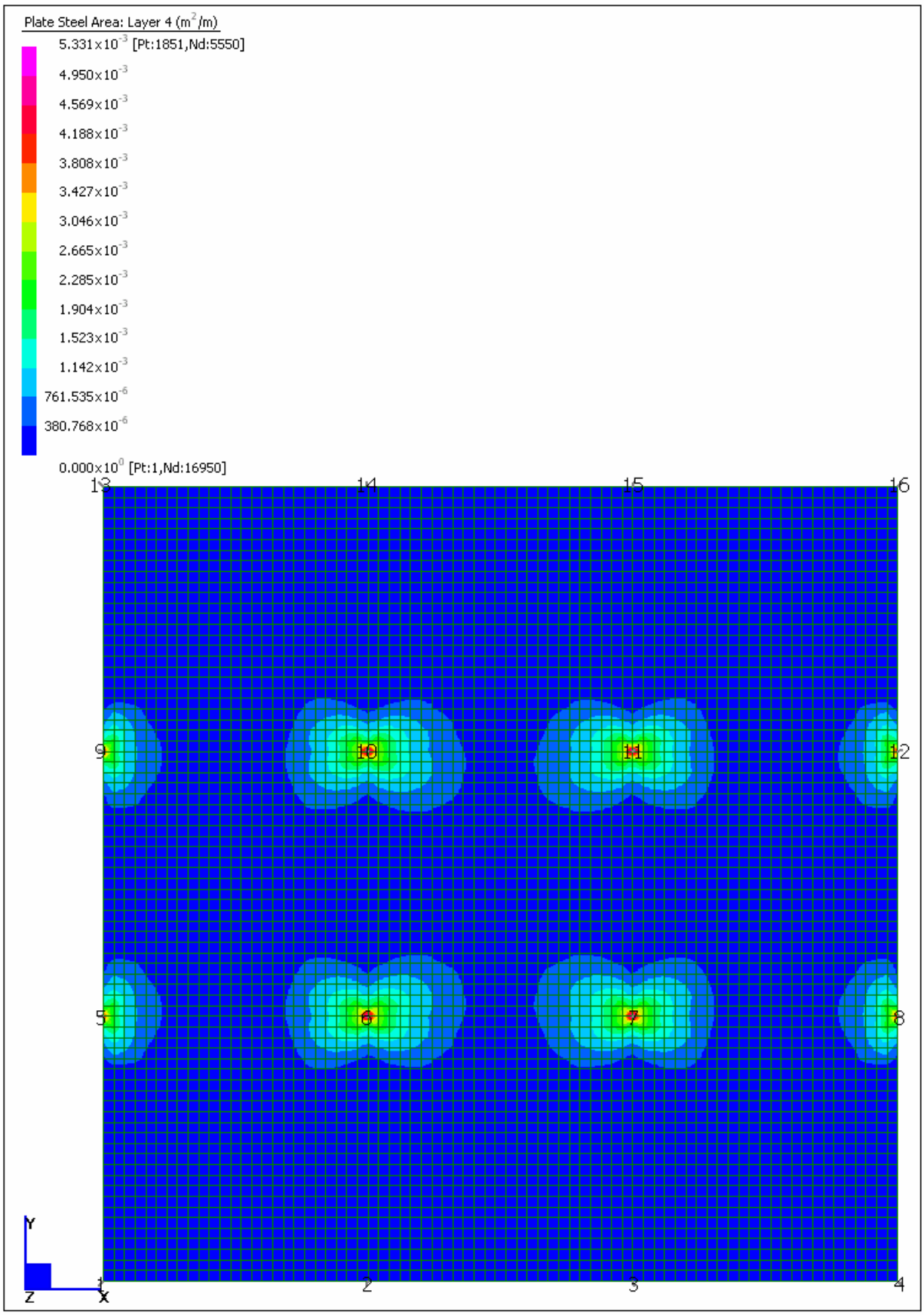

Strand7 Release 2.3.8 [Licenced to:COBIAX]

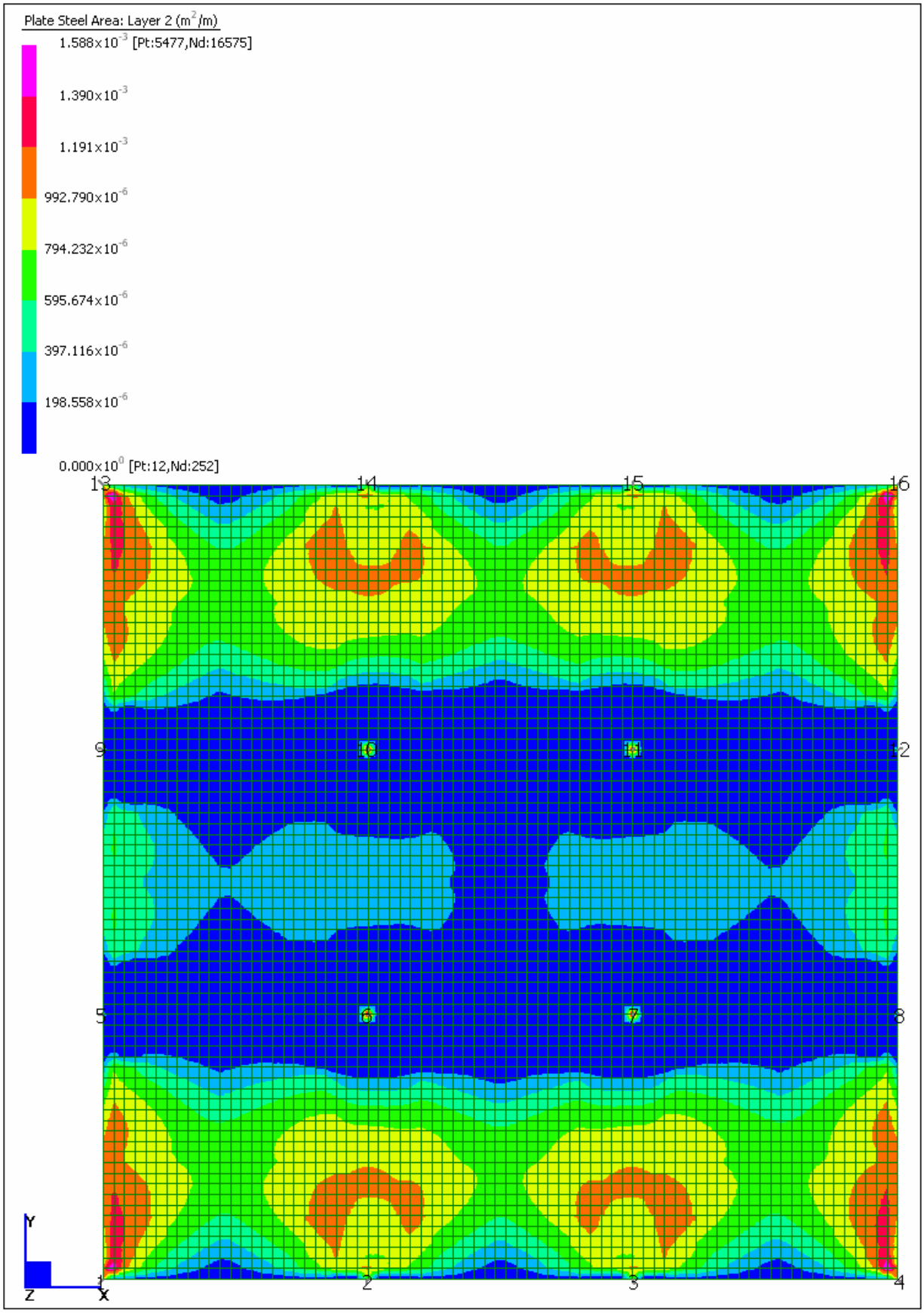
Plate Steel Area: Layer 2 (m²/m)
1.588x10⁻³ [Pt:5477,Nd:16575]
1.390x10⁻³
1.191x10⁻³
992.790x10⁻⁶
794.232x10⁻⁶
595.674x10⁻⁶
397.116x10⁻⁶
198.558x10⁻⁶
0.000x10⁰ [Pt:12,Nd:252]
13
14
15
16
9
10
11
12
5
6
7
8
1
2
3
4
Y
Z
X
Strand7 Release 2.3.8 [Licenced to:COBIAX]

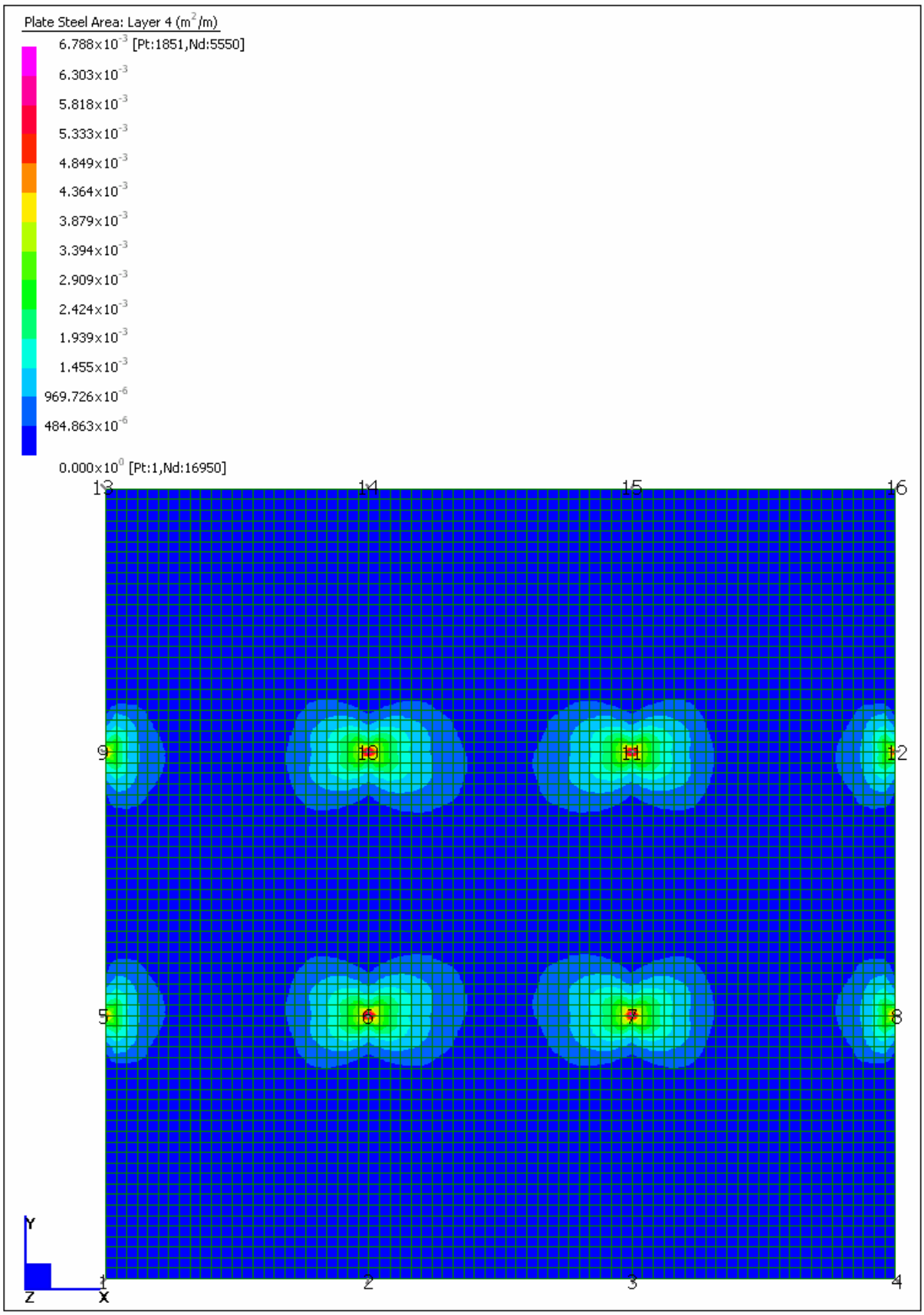

Strand7 Release 2.3.8 [Licenced to:COBIAX]

APPENDIX C

Coffer –Reinforcement Required

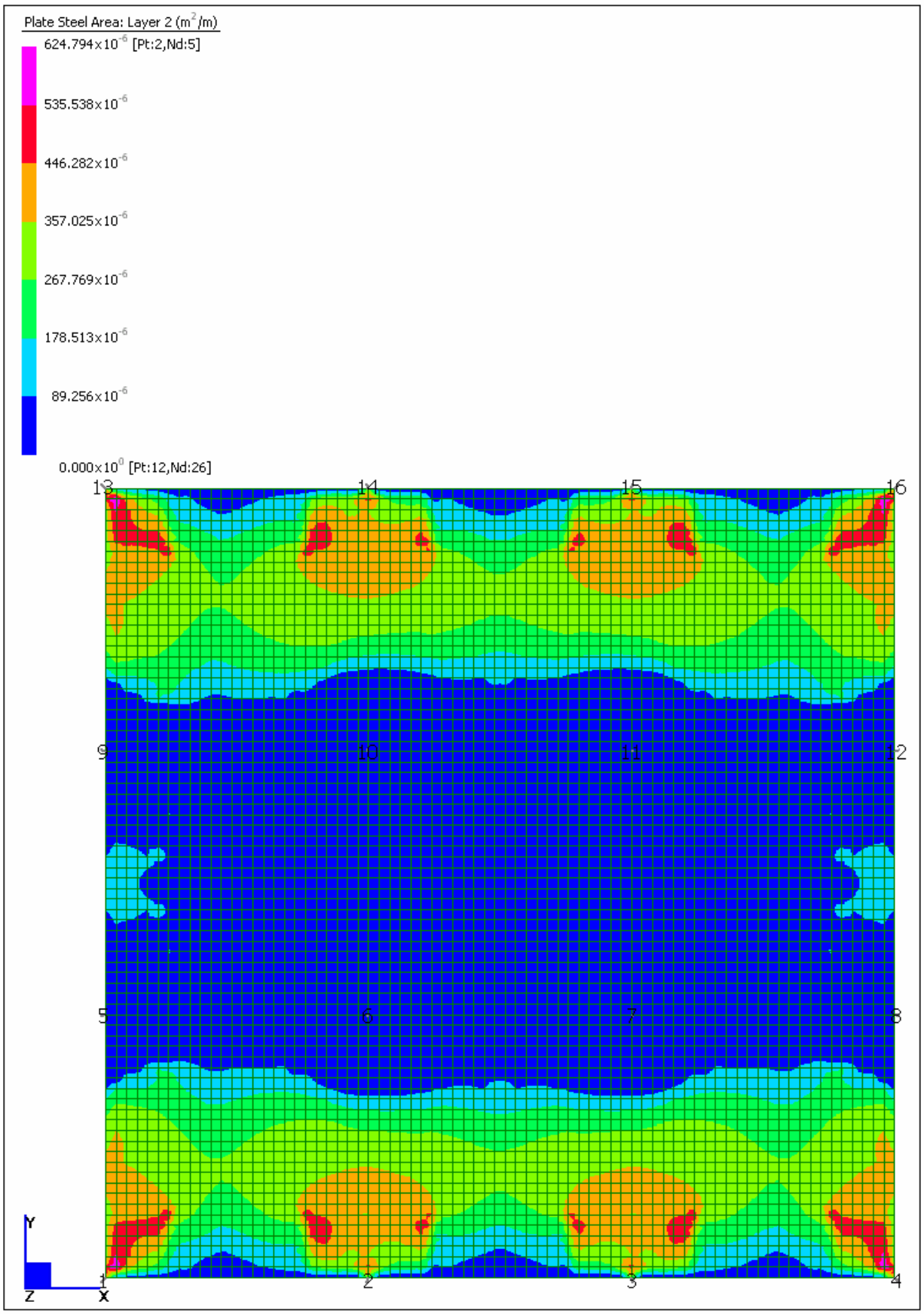
Plate Steel Area: Layer 2 (m²/m)
624.794x10⁻⁶ [Pt:2,Nd:5]
535.538x10⁻⁶
446.282x10⁻⁶
357.025x10⁻⁶
267.769x10⁻⁶
178.513x10⁻⁶
89.256x10⁻⁶
0.000x10⁰ [Pt:12,Nd:26]
13
14
15
16
9
10
11
12
5
6
7
8
1
2
3
4
Y
Z
X
Strand7 Release 2.3.8 [Licenced to:COBIAX]

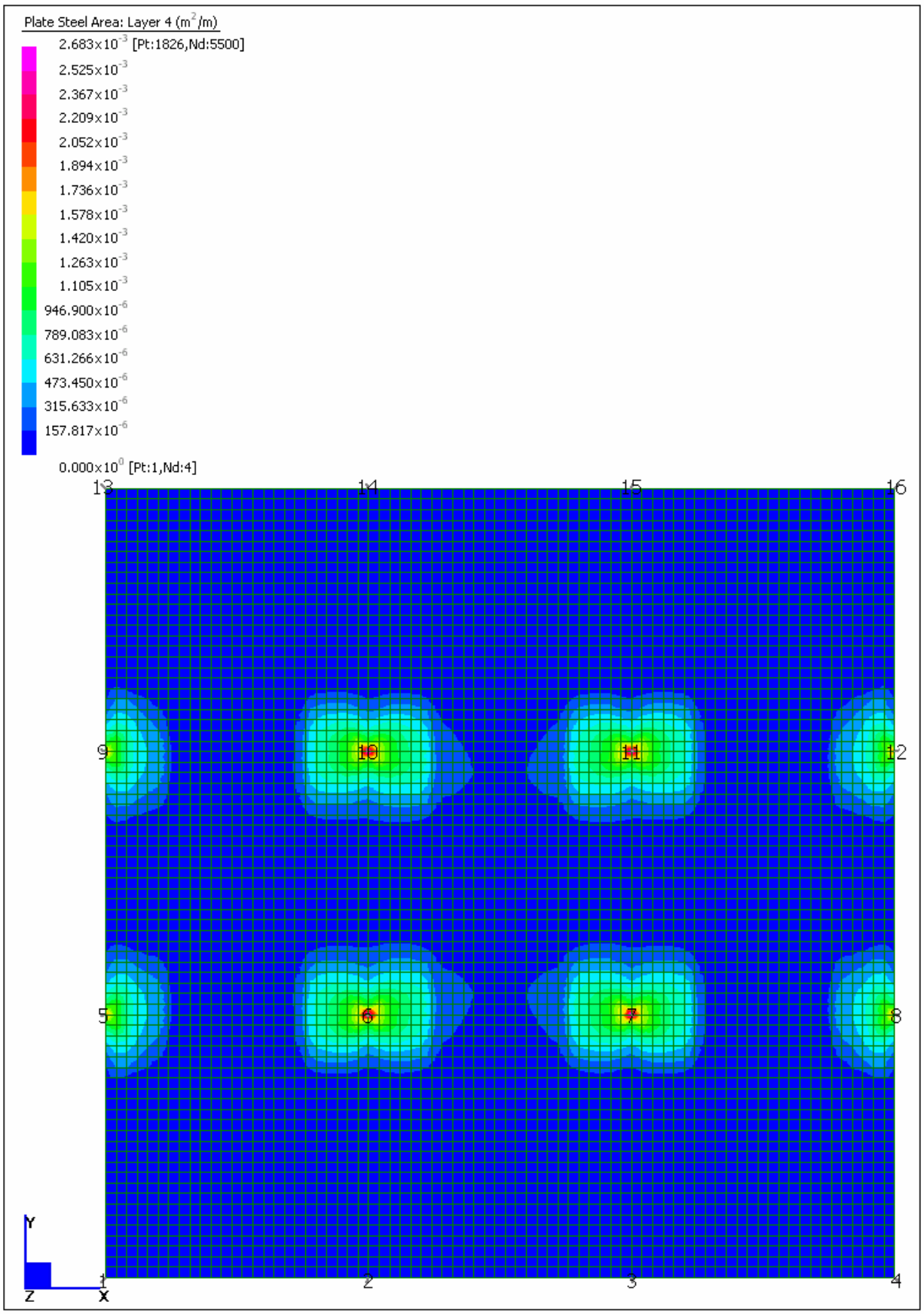
Plate Steel Area: Layer 4 (m²/m)
2.683x10⁻³ [Pt:1826,Nd:5500]
2.525x10⁻³
2.367x10⁻³
2.209x10⁻³
2.052x10⁻³
1.894x10⁻³
1.736x10⁻³
1.578x10⁻³
1.420x10⁻³
1.263x10⁻³
1.105x10⁻³
946.900x10⁻⁶
789.083x10⁻⁶
631.266x10⁻⁶
473.450x10⁻⁶
315.633x10⁻⁶
157.817x10⁻⁶
0.000x10⁰ [Pt:1,Nd:4]
13
14
15
16
9
10
11
12
5
6
7
8
1
2
3
4
Y
Z
X

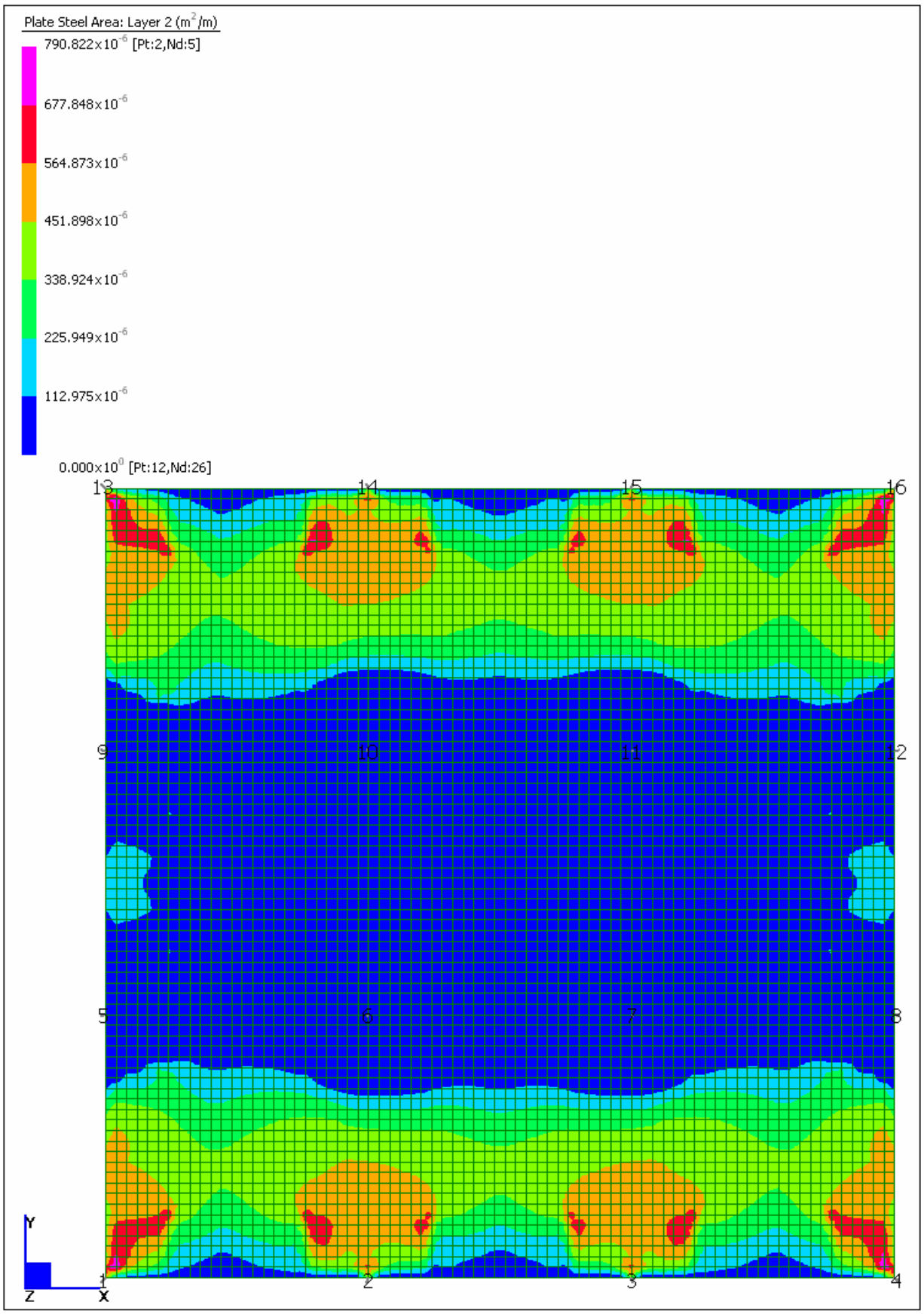
Plate Steel Area: Layer 2 (m²/m)
790.822x10⁻⁶ [Pt:2,Nd:5]
677.848x10⁻⁶
564.873x10⁻⁶
451.898x10⁻⁶
338.924x10⁻⁶
225.949x10⁻⁶
112.975x10⁻⁶
0.000x10⁰ [Pt:12,Nd:26]
13
14
15
16
9
10
11
12
5
6
7
8
1
2
3
4
Y
Z
X
Strand7 Release 2.3.8 [Licenced to:COBIAX]

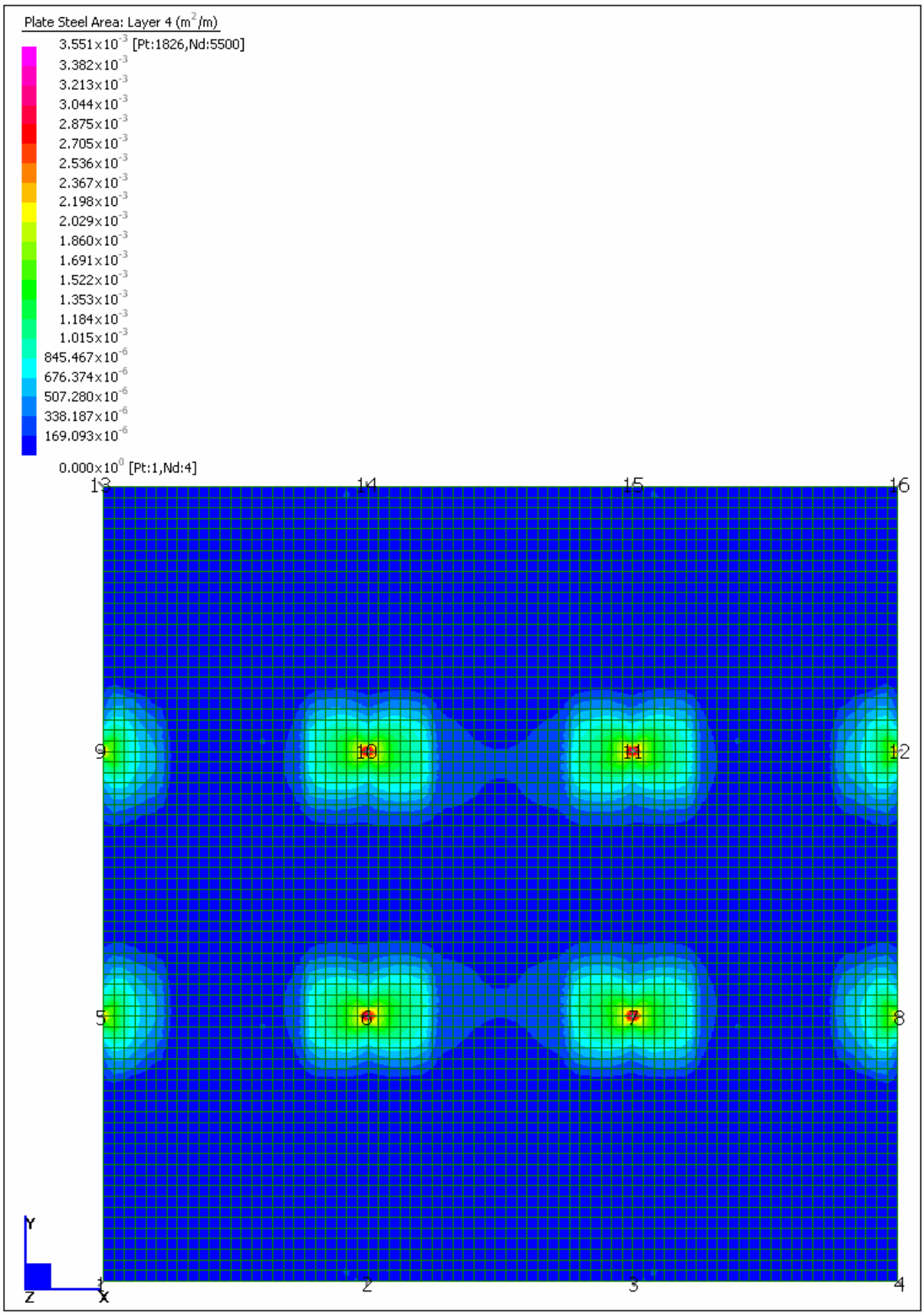

Strand7 Release 2.3.8 [Licenced to:COBIAX]

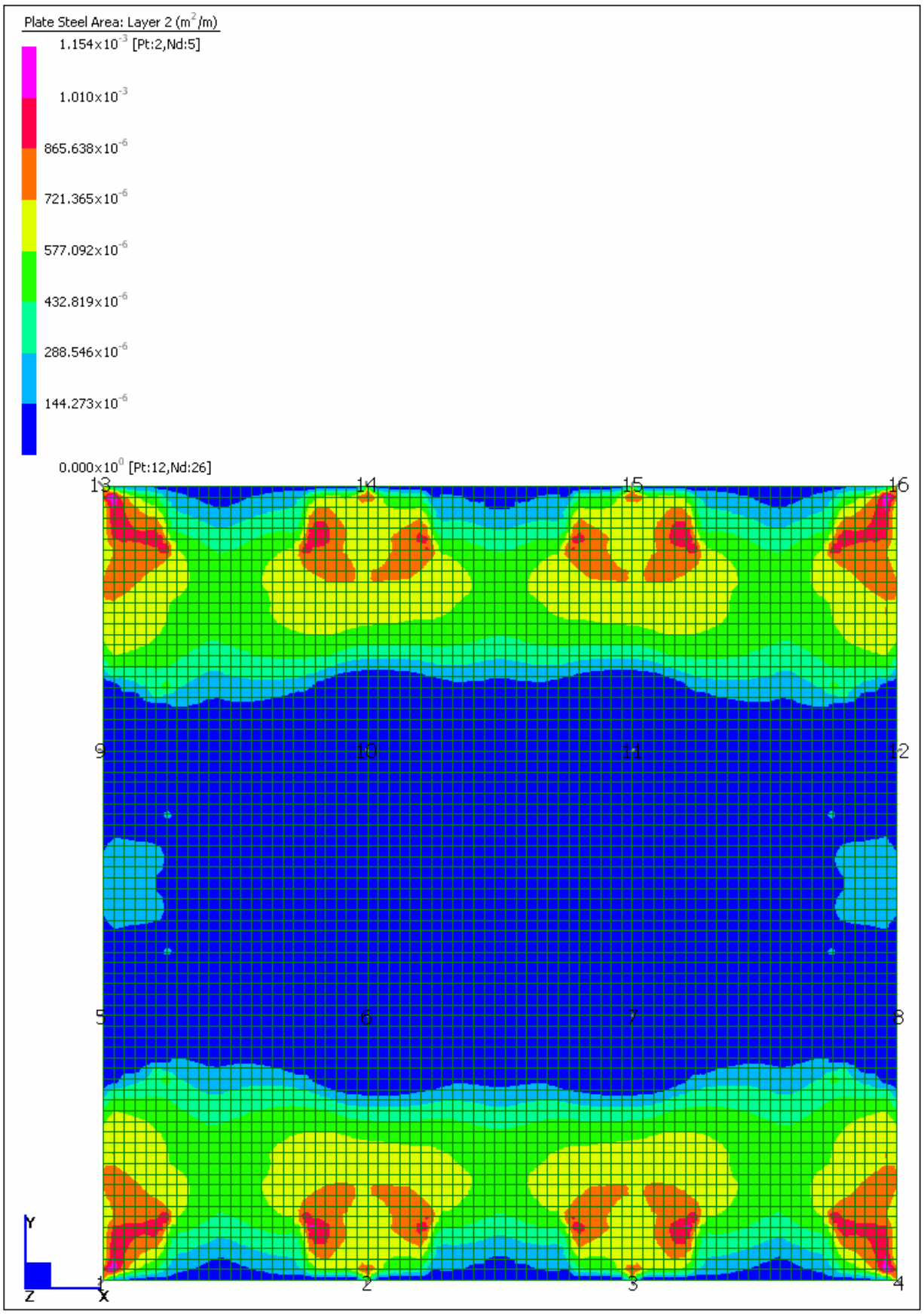
Plate Steel Area: Layer 2 (m²/m)
1.154x10⁻³ [Pt:2,Nd:5]
1.010x10⁻³
865.638x10⁻⁶
721.365x10⁻⁶
577.092x10⁻⁶
432.819x10⁻⁶
288.546x10⁻⁶
144.273x10⁻⁶
0.000x10⁰ [Pt:12,Nd:26]
13
14
15
16
9
10
11
12
5
6
7
8
1
2
3
4
Y
Z
X

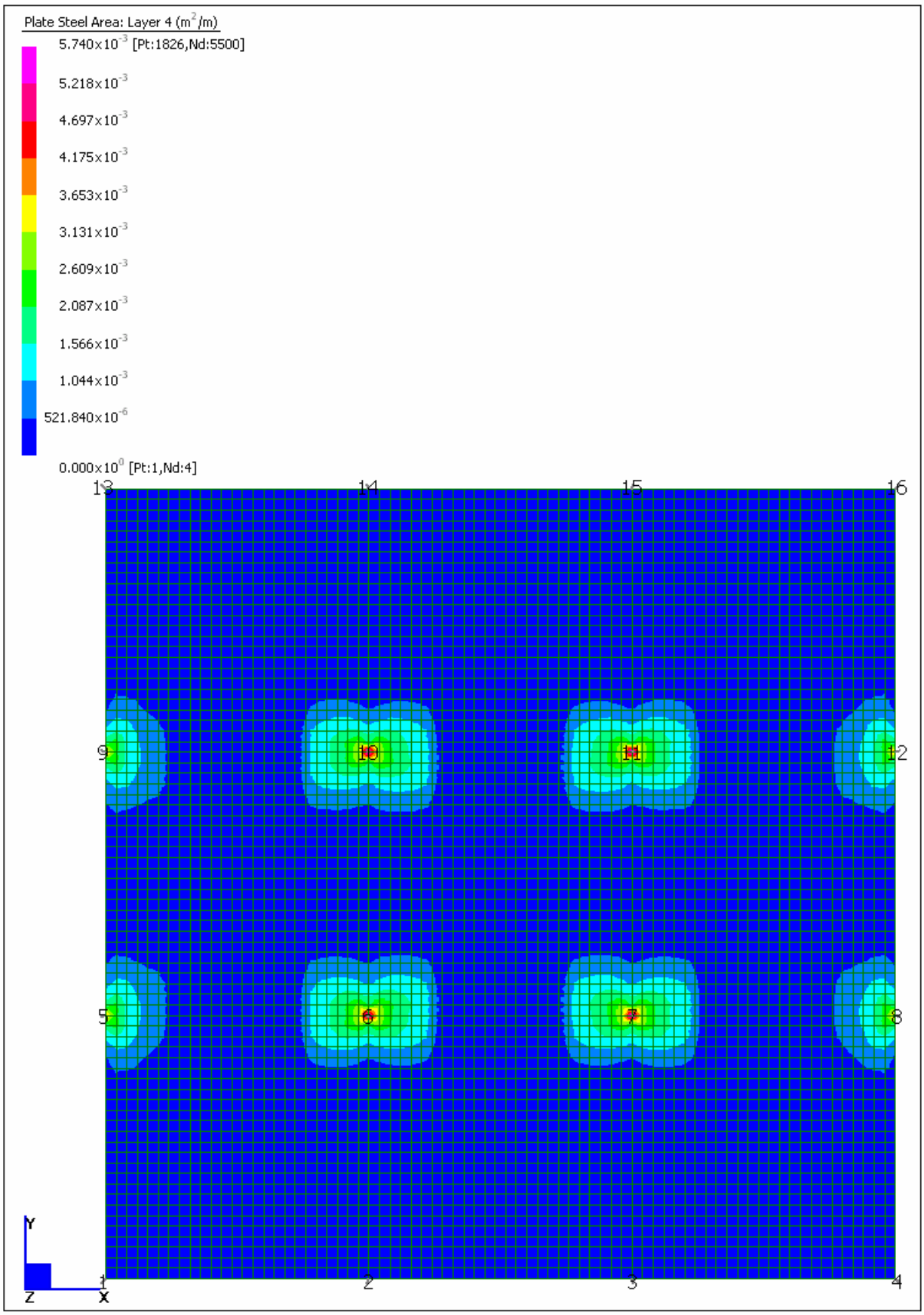
Plate Steel Area: Layer 4 (m²/m)
5.740x10⁻³ [Pt:1826,Nd:5500]
5.218x10⁻³
4.697x10⁻³
4.175x10⁻³
3.653x10⁻³
3.131x10⁻³
2.609x10⁻³
2.087x10⁻³
1.566x10⁻³
1.044x10⁻³
521.840x10⁻⁶
0.000x10⁰ [Pt:1,Nd:4]
13
14
15
16
9
10
11
12
5
6
7
8
1
2
3
4
Y
Z
X
Strand7 Release 2.3.8 [Licenced to:COBIAX]

APPENDIX D

Post-tension – Normal Reinforcement Required

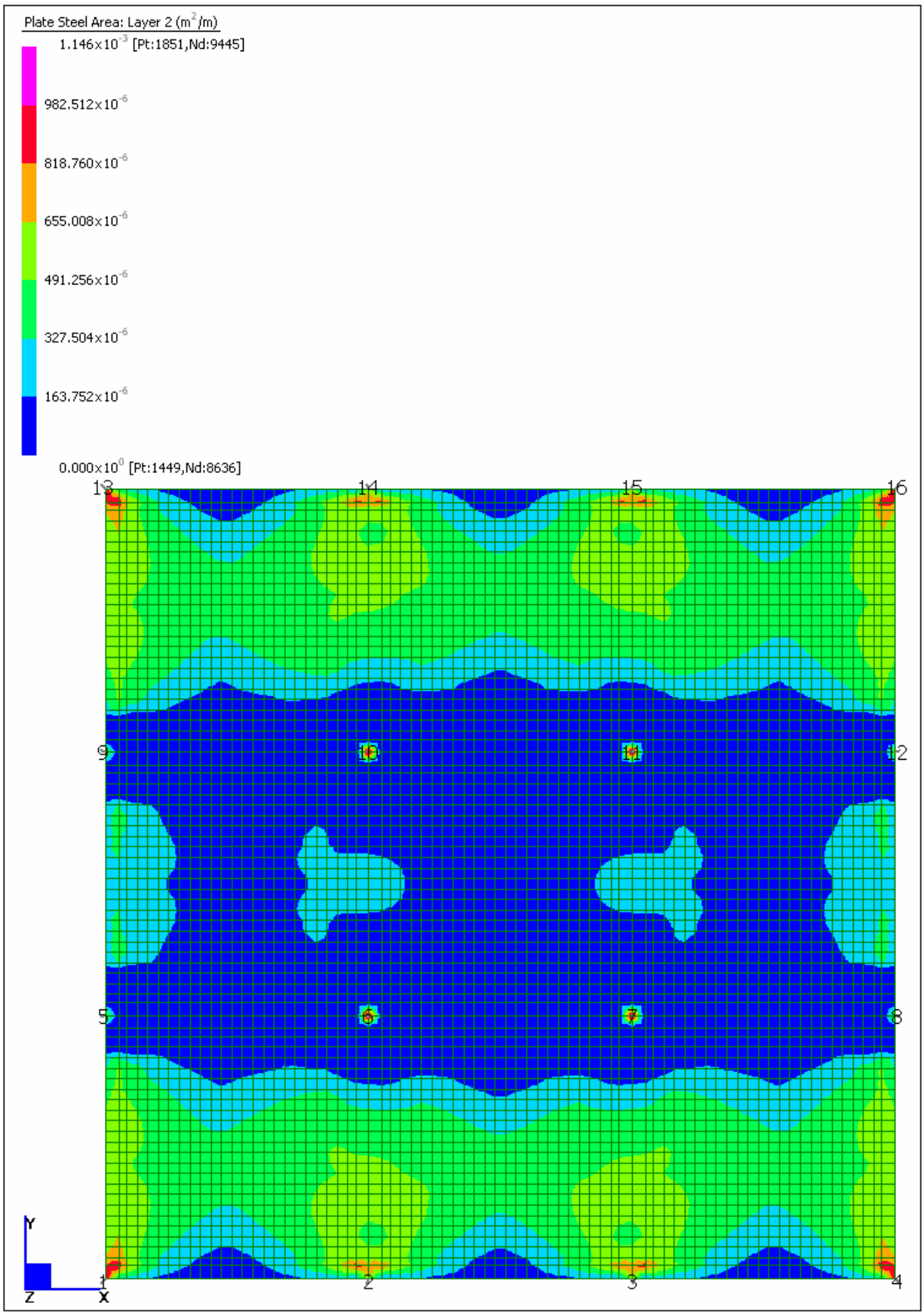
Plate Steel Area: Layer 2 (m²/m)
1.146x10⁻³ [Pt:1851,Nd:9445]
982.512x10⁻⁶
818.760x10⁻⁶
655.008x10⁻⁶
491.256x10⁻⁶
327.504x10⁻⁶
163.752x10⁻⁶
0.000x10⁰ [Pt:1449,Nd:8636]
13
14
15
16
9
10
11
12
5
6
7
8
1
2
3
4
Y
Z
X

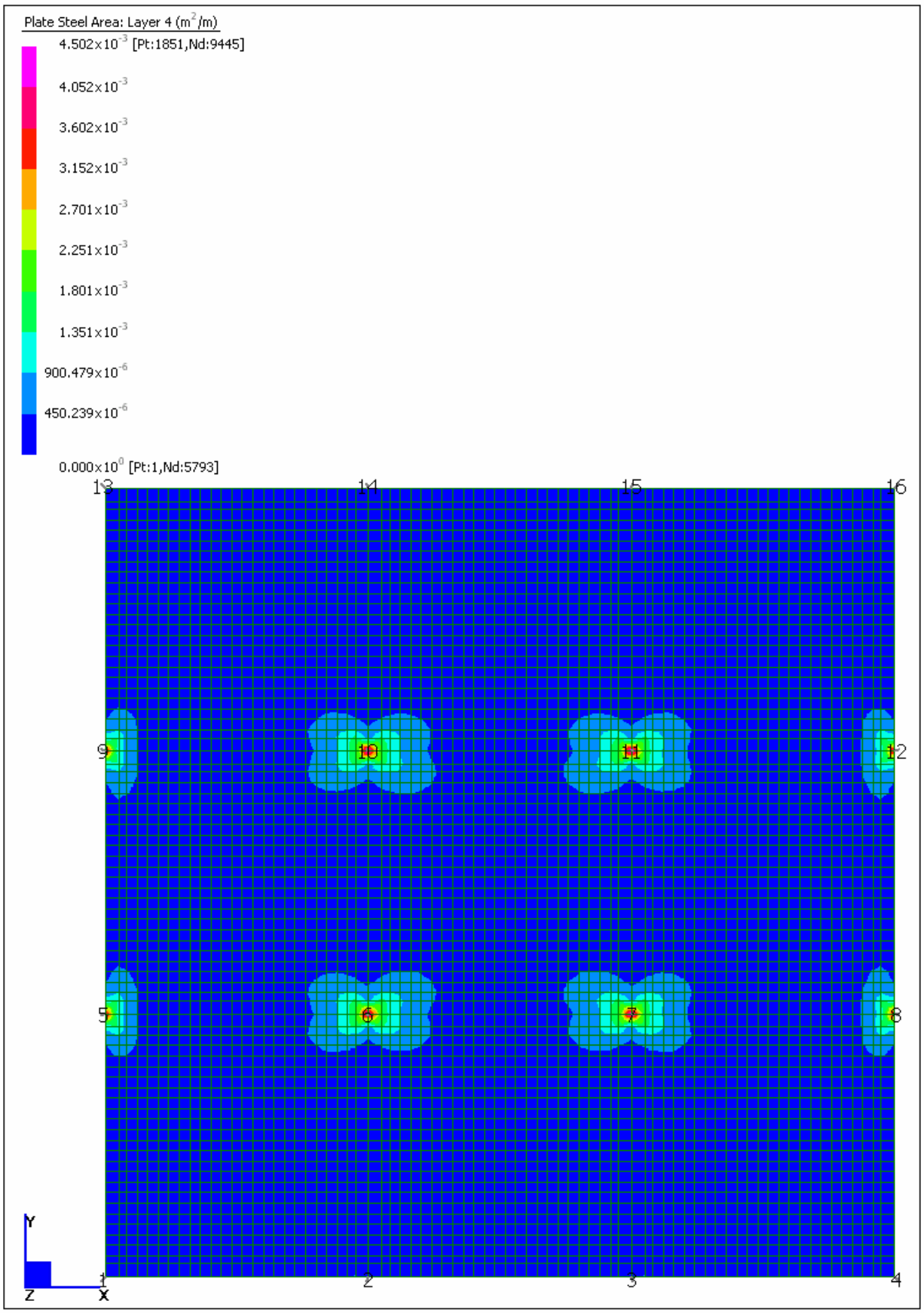
Plate Steel Area: Layer 4 (m²/m)
4.502x10⁻³ [Pt:1851,Nd:9445]
4.052x10⁻³
3.602x10⁻³
3.152x10⁻³
2.701x10⁻³
2.251x10⁻³
1.801x10⁻³
1.351x10⁻³
900.479x10⁻⁶
450.239x10⁻⁶
0.000x10⁰ [Pt:1,Nd:5793]
13
14
15
16
9
10
11
12
5
6
7
8
1
2
3
4
Y
Z
X
Strand7 Release 2.3.8 [Licenced to:COBIAX]

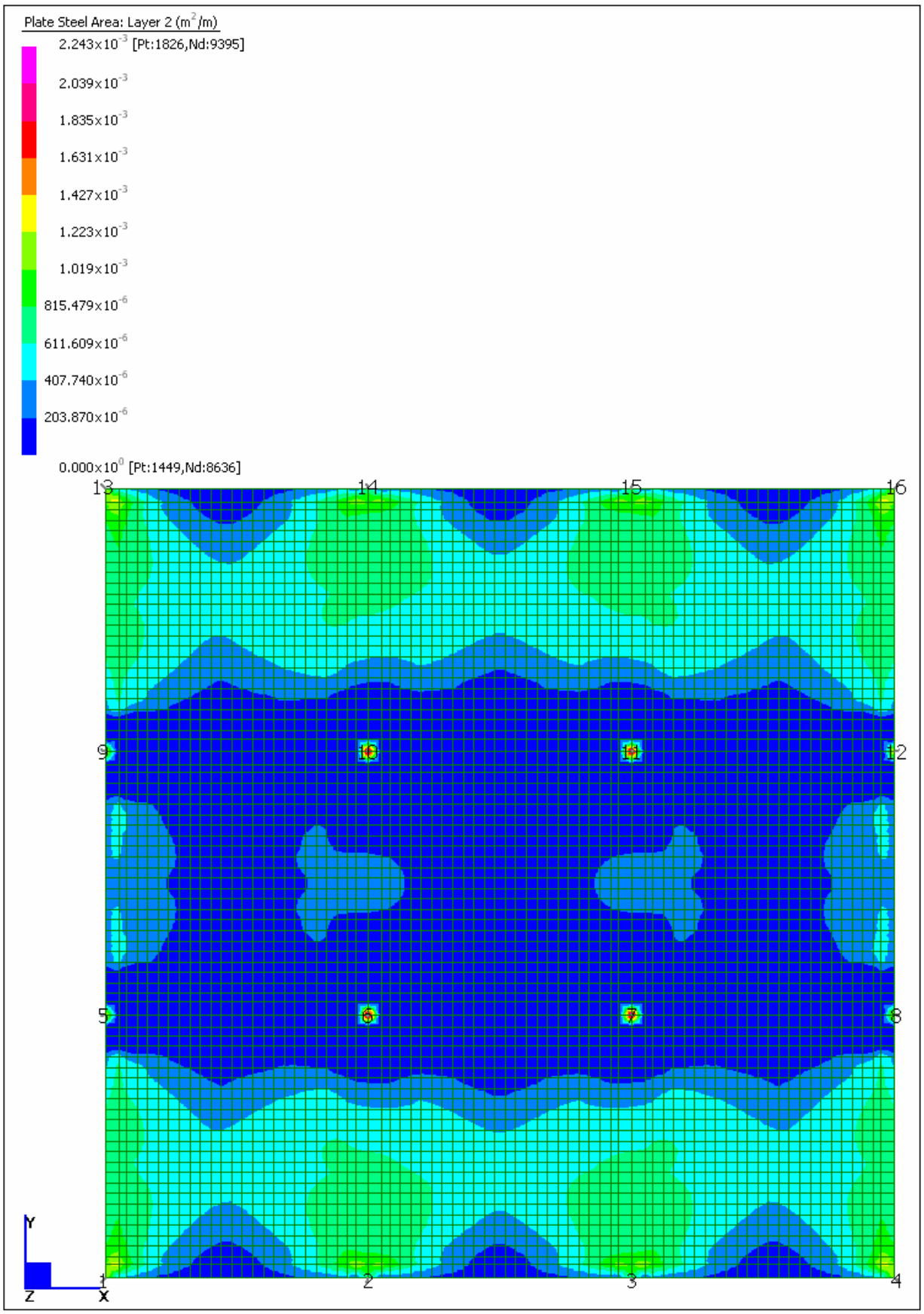
Plate Steel Area: Layer 2 (m²/m)
2.243x10⁻³ [Pt:1826,Nd:9395]
2.039x10⁻³
1.835x10⁻³
1.631x10⁻³
1.427x10⁻³
1.223x10⁻³
1.019x10⁻³
815.479x10⁻⁶
611.609x10⁻⁶
407.740x10⁻⁶
203.870x10⁻⁶
0.000x10⁰ [Pt:1449,Nd:8636]
13
14
15
16
9
10
11
12
5
6
7
8
1
2
3
4
Y
Z
X

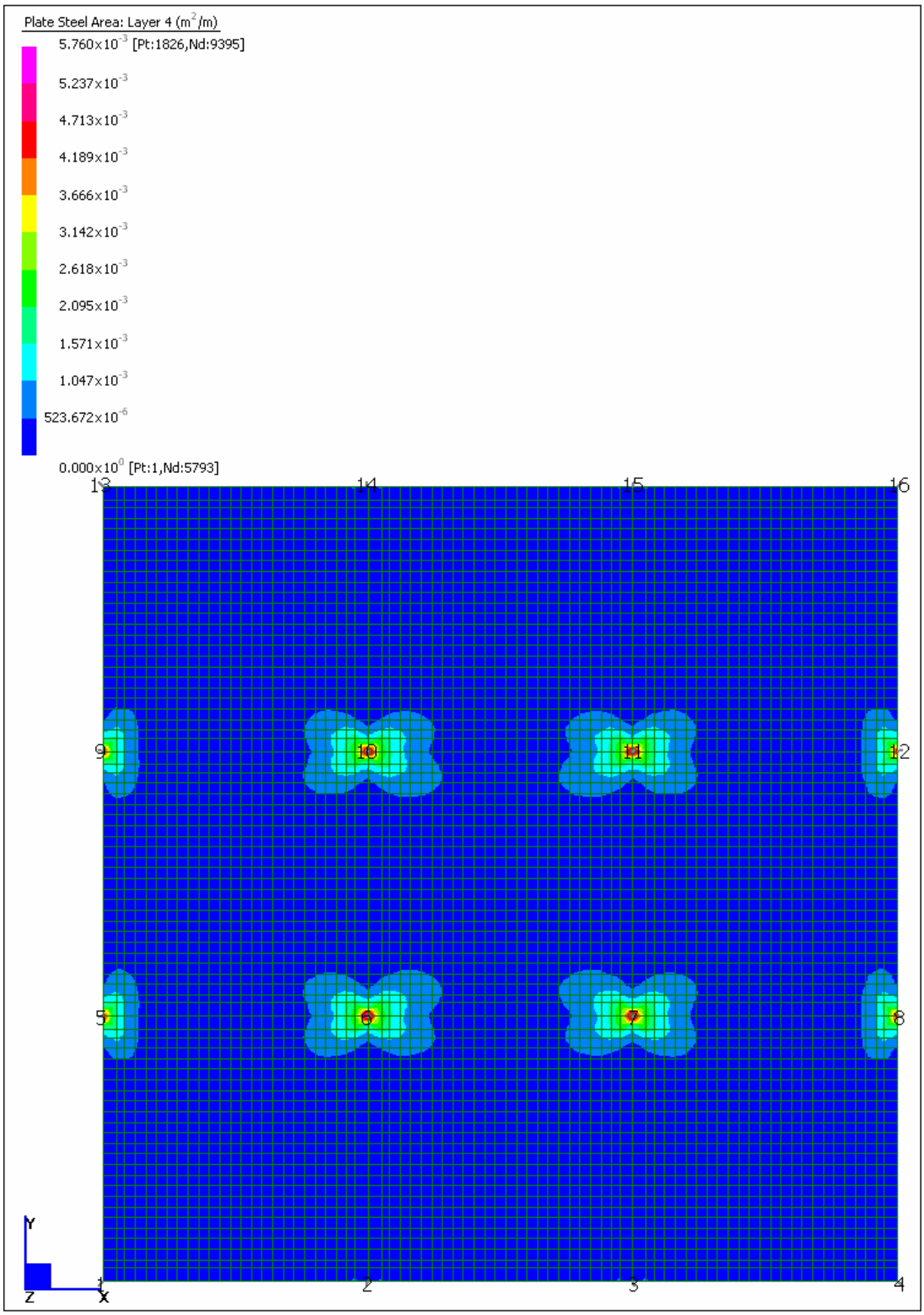

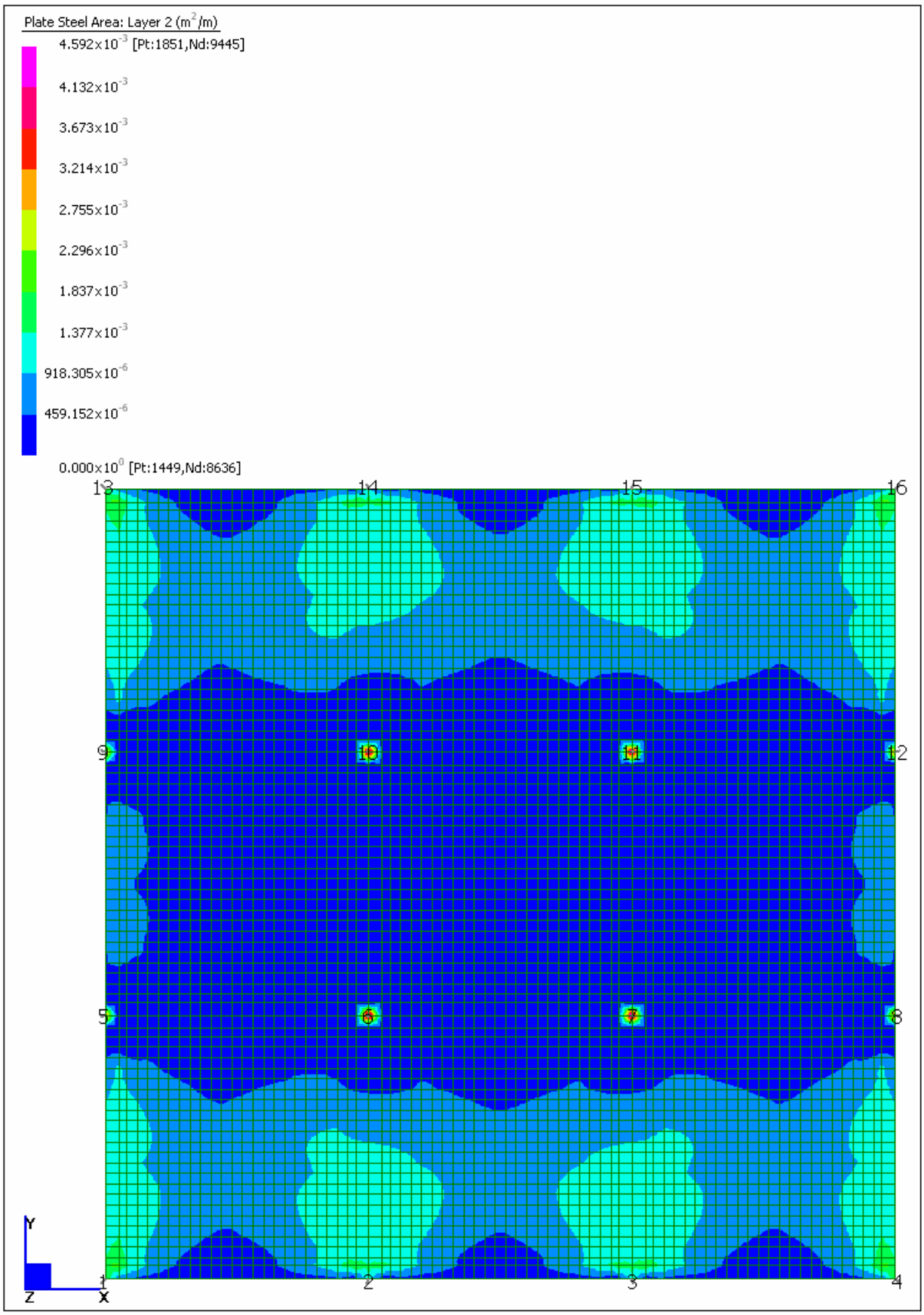
Plate Steel Area: Layer 2 (m²/m)
4.592x10⁻³ [Pt:1851,Nd:9445]
4.132x10⁻³
3.673x10⁻³
3.214x10⁻³
2.755x10⁻³
2.296x10⁻³
1.837x10⁻³
1.377x10⁻³
918.305x10⁻⁶
459.152x10⁻⁶
0.000x10⁰ [Pt:1449,Nd:8636]
13
14
15
16
9
10
11
12
5
6
7
8
1
2
3
4
Y
Z
X

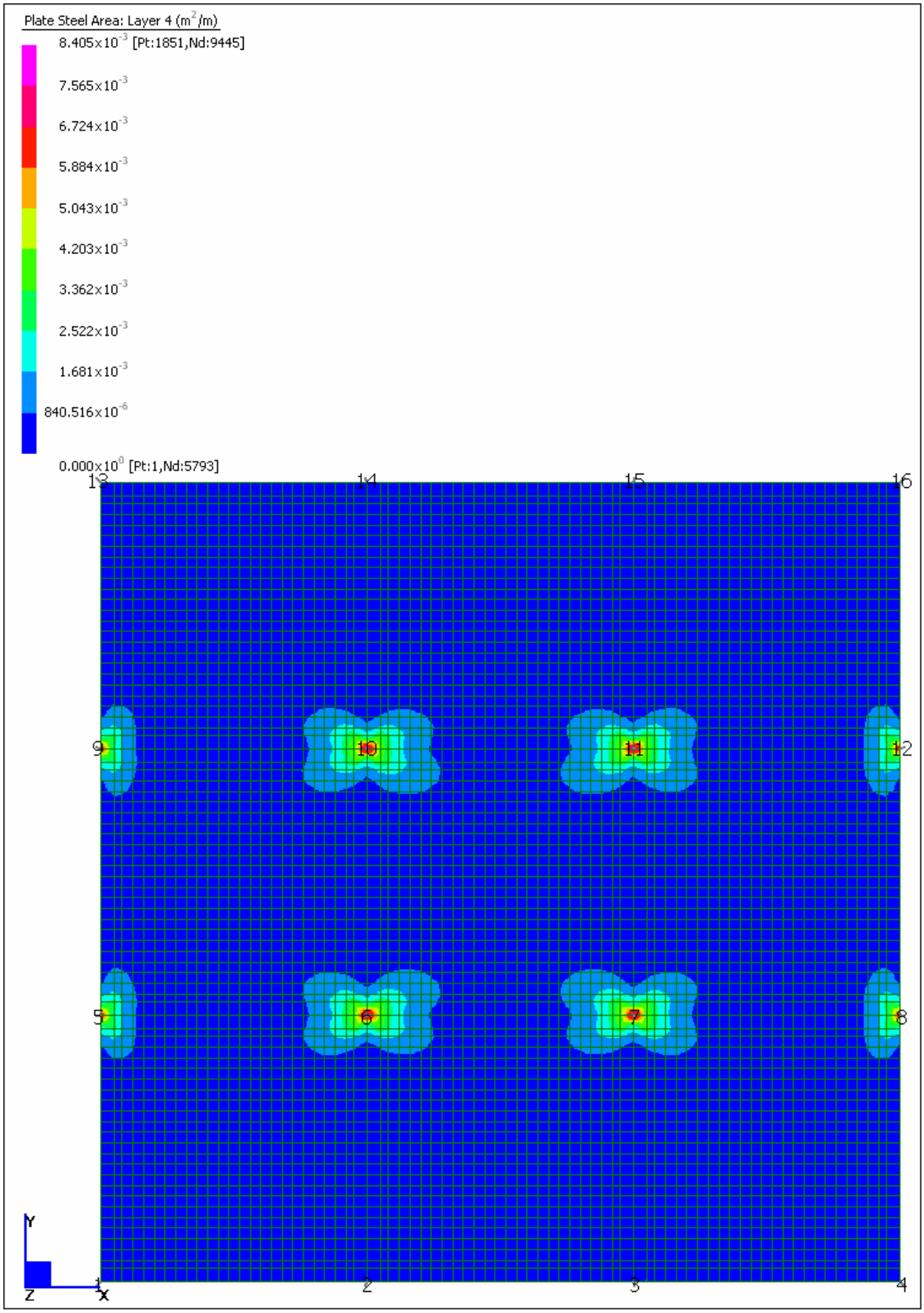
Plate Steel Area: Layer 4 (m²/m)
8.405x10⁻³ [Pt:1851,Nd:9445]
7.565x10⁻³
6.724x10⁻³
5.884x10⁻³
5.043x10⁻³
4.203x10⁻³
3.362x10⁻³
2.522x10⁻³
1.681x10⁻³
840.516x10⁻⁶
0.000x10⁰ [Pt:1,Nd:5793]
13
14
15
16
9
10
11
12
5
6
7
8
1
2
3
4
Y
Z
X

APPENDIX E

Formwork Cost Analysis

UNIVERSITEIT VAN PRETORIA
UNIVERSITY OF PRETORIA
YUNIBESITHI YA PRETORIA

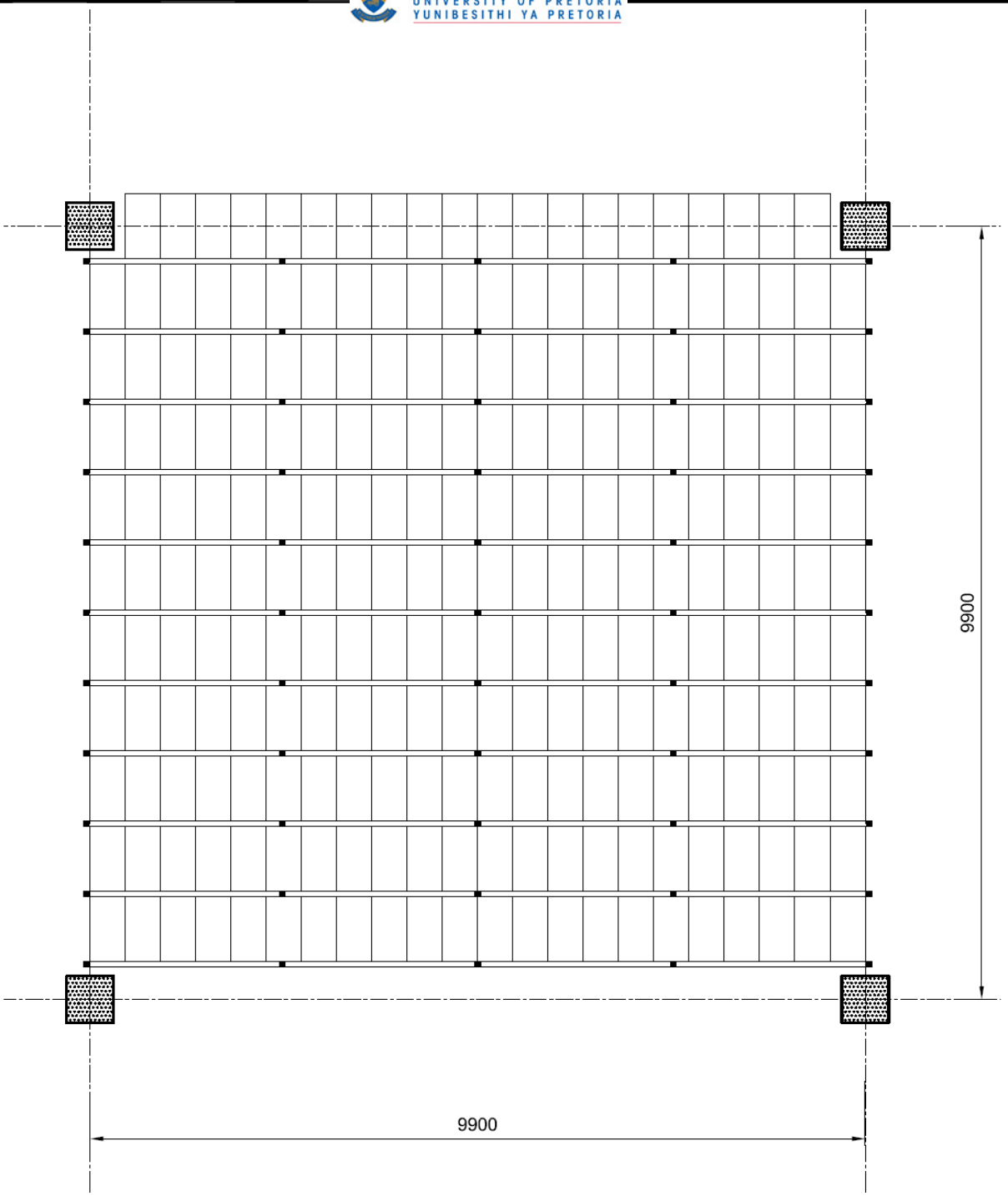

No.	Amendment	By	Auth.	Date
A	FIRST ISSUE	????????????		Year-Month-Day

WIEHAHN
4 Setter Road Midrand Industrial Park
Gauteng 1685
Tel : +27(11) 729 2300
Fax: +27(11) 729 2560
www.perlwiehahn.co.za design@wiehahn.co.za
Authorised PERI distributor

Project Description:

COBIAX SLAB LAYOUT

Contactor:

Scale:	Drawn:	Design review:	Date:
Drawing No:			Revision:

UNIVERSITEIT VAN PRETORIA
UNIVERSITY OF PRETORIA
YUNIBESITHI YA PRETORIA

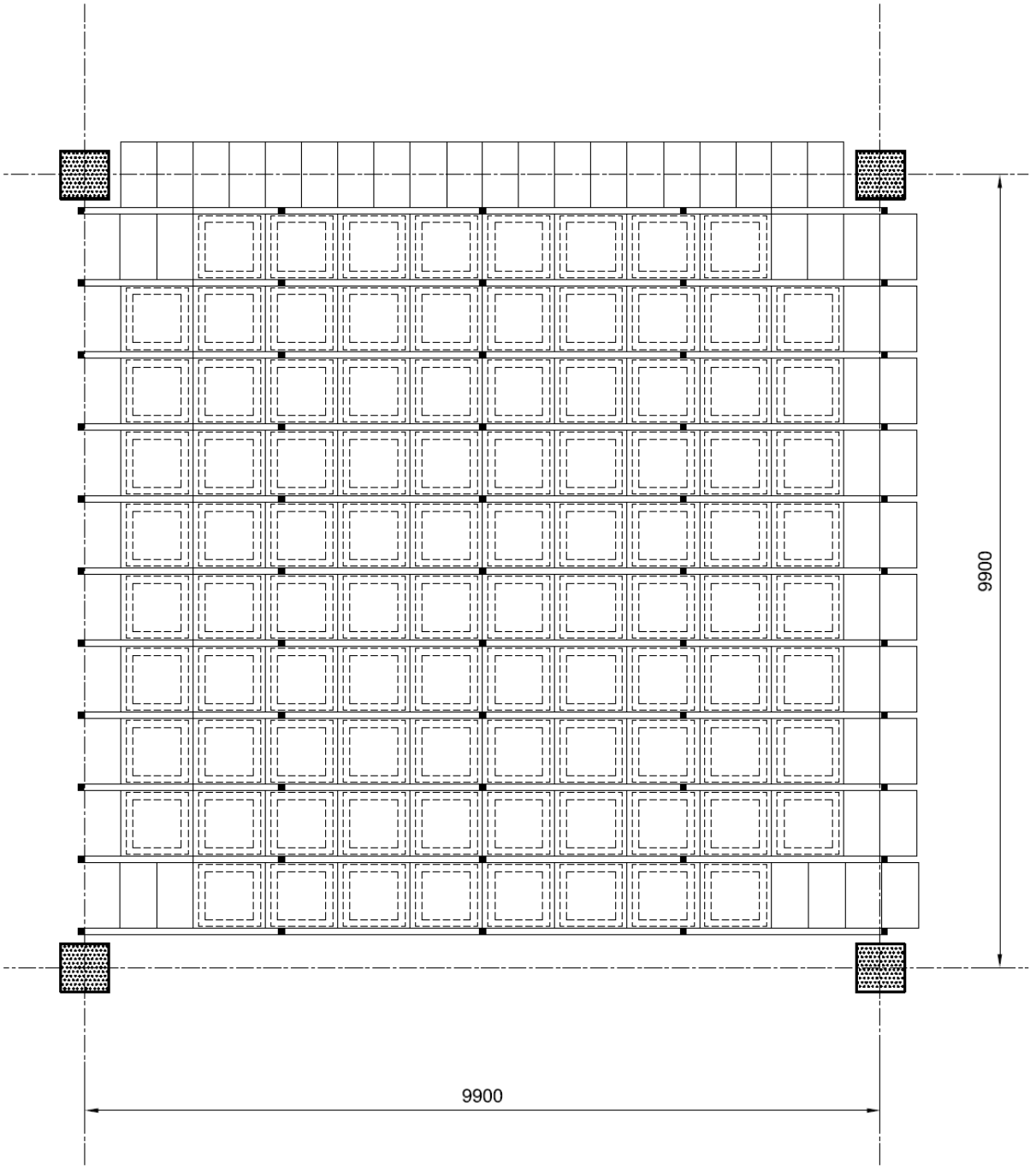

No.	Amendment	By	Auth.	Date

WIEHAHN
4 Setter Road Midrand Industrial Park
Gauteng 1685
Tel : +27(11) 729 2300
Fax: +27(11) 729 2560
www.perlwiehahn.co.za design@wiehahn.co.za
Authorised PERI distributor

Project Description:

COFFERED SLAB LAYOUT

Contactor:

Scale:	Drawn:	Design review:	Date:
Drawing No:			Revision:

ITEM	OP CODE	D E S C R I P T I O N	UNIT	BILLED QUANTITY	NETT RATE	NETT AMOUNT
A	FW002	315 COBIAX SLAB 9900x9900 GRID	m²	98	14.16	1 387.68
B	FW002L	LABOUR ONLY TO ITEM C ABOVE	m²	98	36.00	3 528.00
C	FW001S	SUPPORT WORK TO A ABOVE (NO RE-PROPPING INCLUDED)	m²	98	13.85	1 357.30
		Page 2 total				6 272.98

ITEM	OP CODE	D E S C R I P T I O N	UNIT	BILLED QUANTITY	NETT RATE	NETT AMOUNT
A	FW001	900x900x425 COFFERED SLAB 9900x9900 GRID	m²	98	46.69	4 575.62
B	FW001L	LABOUR ONLY TO ITEM A ABOVE	m²	98	48.00	4 704.00
C	FW001L2	ADDITIONAL LABOUR FOR COFFER PLACEMENT	m²	98	4.90	480.20
D	FW001S	SUPPORT WORK TO A ABOVE (NO RE-PROPPING INCLUDED)	m²	98	13.85	1 357.30
		Page 1 total				11 117.12

APPENDIX F

Typical Solid Zones for Cobiax and Coffer Slabs – Strand7

Shear Contours for Slab Solid Zones

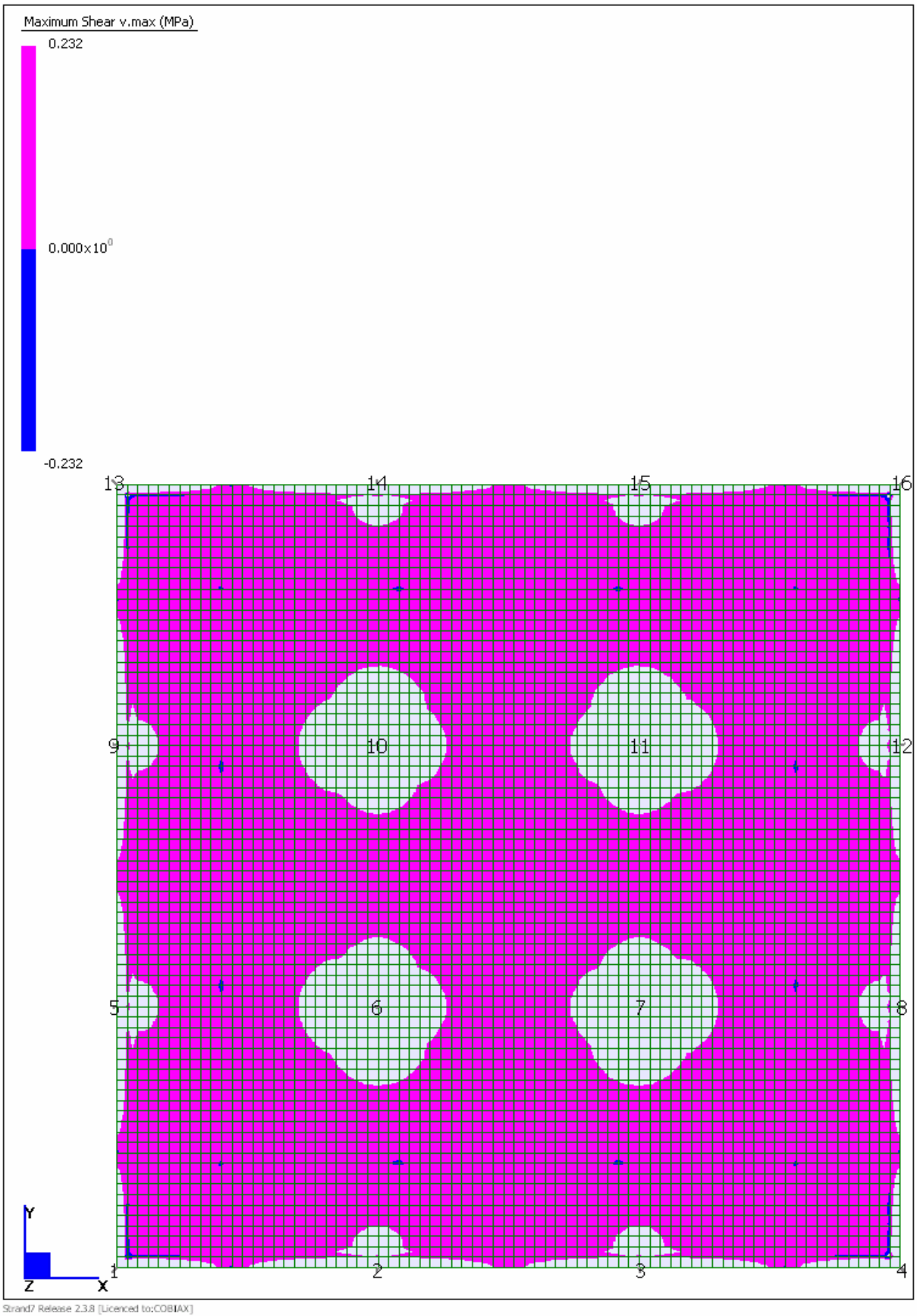

Shear Contours In[illegible]d Zones – 10m Light

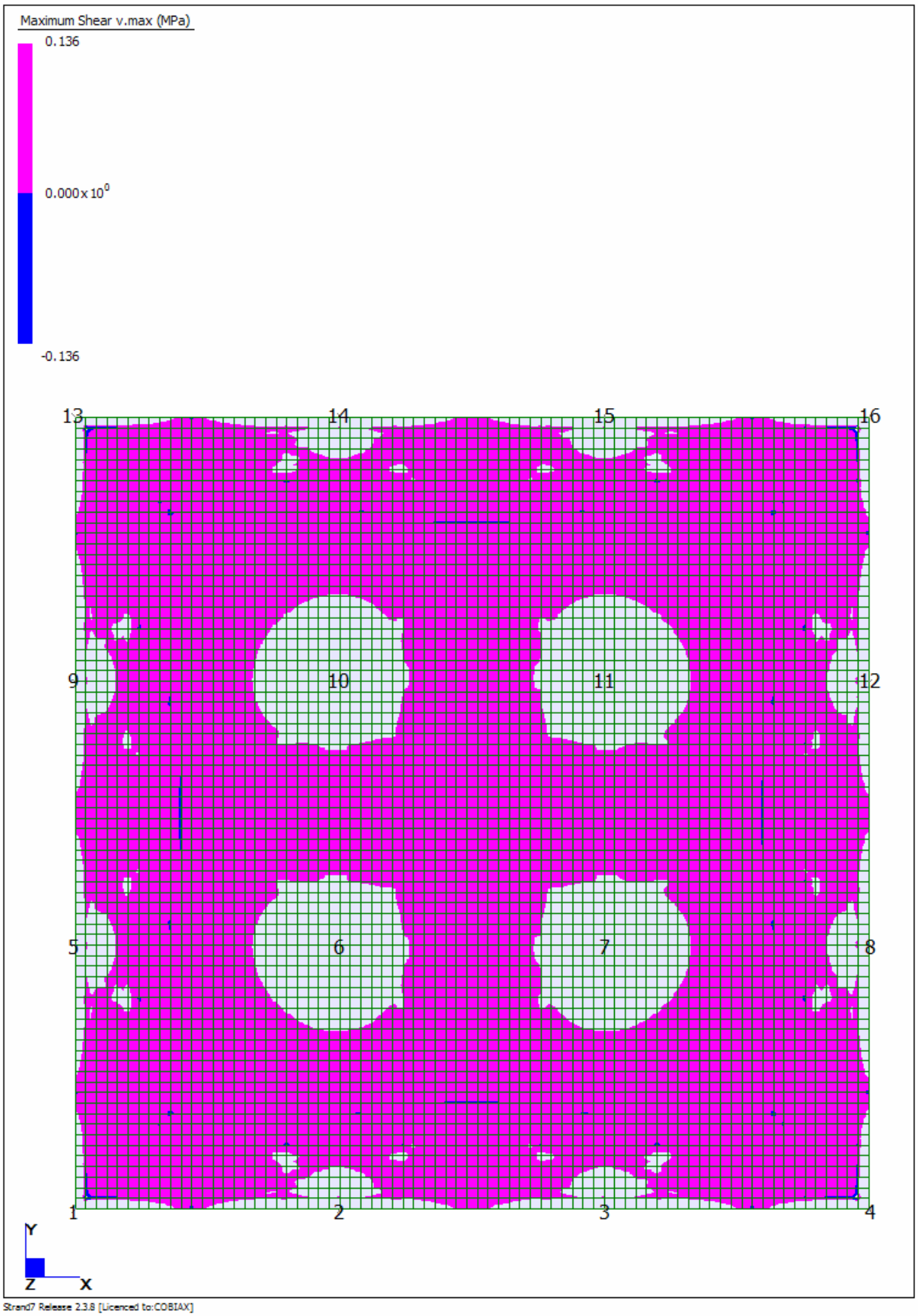

APPENDIX G

Cobiax – Punching Shear Reinforcement

PROKON
Software Consultants (Pty) Ltd
Internet: http://www.prokon.com
E-Mail : mail@prokon.com

Job Number		Sheet
Job Title	Cobiax 7.5m Light	
Client		
Calcs by	Checked by	Date

C23

Punching Shear Design :

Input Data

Column width A	(mm)	450
Column breadth B	(mm)	450
Effective slab depth deff	(mm)	243
Nearest edge X-direction	(mm)	7500
Nearest edge Y-direction	(mm)	7500
fcu	(MPa)	30
fy flexural reinforcement	(MPa)	450
fyv shear reinforcement	(MPa)	450
X-reinforcement crossing perimeter 1		Y10@150
Perimeter 2	(mm^2)	Y10@150
Perimeter 3	(mm^2)	Y10@150
Perimeter 4	(mm^2)	Y10@150
Y-reinforcement crossing perimeter 1		Y10@150
Perimeter 2	(mm^2)	Y10@150
Perimeter 3	(mm^2)	Y10@150
Perimeter 4	(mm^2)	Y10@150
Shear head present	(Y/[N])	
Max. link/tie size	(mm)	16

Load Cases

Load Case	Description	ULS Shear Vt (kN)	ULS X-moment (kNm)	ULS Y-moment (kNm)
1	1	706		

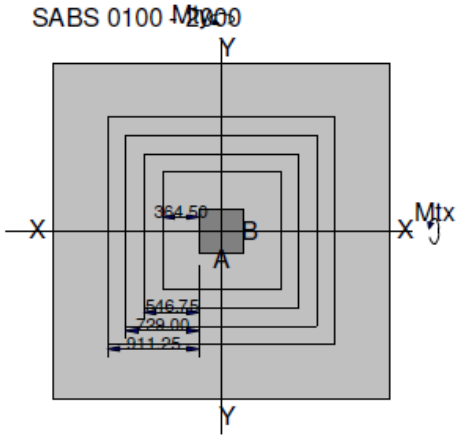

Output for Load Case 1:1

Critical load case: 1:1	Load Case 1:1			
Perimeter	1	2	3	4
Distance from Column face (mm)	365	547	729	911
Critical length (mm)	4716	6174	7632	9090
Allowable shear stress vc (MPa)	0.39	0.39	0.39	0.39
Shear force capacity Vc (kN)	443	580	717	854
Effective shear force Veff (kN)	812	812	812	812
Total reqd. reinforcement Asv (mm^2)	1600	1533	1895	0
Suggested reinforcement configurations	32Y8	31Y8	25Y10	
	1608 mm^2	1558 mm^2	1963 mm^2	
	21Y10	20Y10	17Y12	
	1649 mm^2	1571 mm^2	1923 mm^2	
	15Y12	14Y12	10Y16	
	1696 mm^2	1583 mm^2	2011 mm^2	
	8Y16	8Y16	7Y20	
	1608 mm^2	1608 mm^2	2199 mm^2	

Shear reinforment should be placed in a band 1.5-d wide inside each critcical perimeter. Maximum spacing 0.75-d.

PROKON
Software Consultants (Pty) Ltd
Internet: http://www.prokon.com
E-Mail : mail@prokon.com

Job Number		Sheet
Job Title	Cobiax 7.5m Medium	
Client		
Calcs by	Checked by	Date

C23

Punching Shear Design :

Input Data

Column width A	(mm)	450
Column breadth B	(mm)	450
Effective slab depth deff	(mm)	243
Nearest edge X-direction	(mm)	7500
Nearest edge Y-direction	(mm)	7500
fcu	(MPa)	30
fy flexural reinforcement	(MPa)	450
fyv shear reinforcement	(MPa)	450
X-reinforcement crossing perimeter		Y12@125
Perimeter 2	(mm^2)	Y12@125
Perimeter 3	(mm^2)	Y12@125
Perimeter 4	(mm^2)	Y12@125
Y-reinforcement crossing perimeter		Y12@125
Perimeter 2	(mm^2)	Y12@125
Perimeter 3	(mm^2)	Y12@125
Perimeter 4	(mm^2)	Y12@125
Shear head present	(Y/[N])	
Max. link/tie size	(mm)	16

Load Cases

Load Case	Description	ULS Shear Vt (kN)	ULS X-moment (kNm)	ULS Y-moment (kNm)
1	1	923		

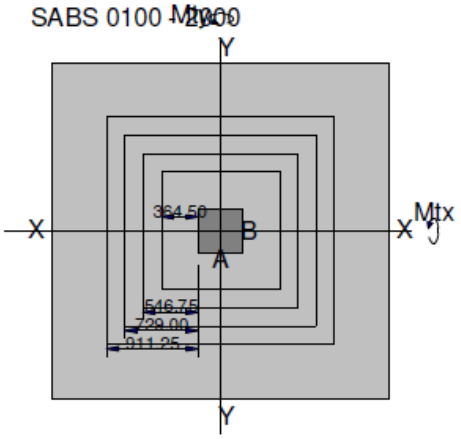

PROKON
Software Consultants (Pty) Ltd
Internet: http://www.prokon.com
E-Mail : mail@prokon.com

Job Number		Sheet
Job Title	Cobiax 7.5m Medium	
Client		
Calcs by	Checked by	Date

Output for Load Case 1:1

Critical load case: 1:1	Load Case 1:1			
Perimeter	1	2	3	4
Distance from Column face (mm)	365	547	729	911
Critical length (mm)	4716	6174	7632	9090
Allowable shear stress vc (MPa)	0.46	0.46	0.46	0.46
Shear force capacity Vc (kN)	532	696	860	1025
Effective shear force Veff (kN)	1061	1061	1061	1061
Total reqd. reinforcement Asv (mm^2)	2700	1533	1895	2257
Suggested reinforcement configurations	35Y10	31Y8	25Y10	29Y10
	2749 mm^2	1558 mm^2	1963 mm^2	2278 mm^2
	24Y12	20Y10	17Y12	20Y12
	2714 mm^2	1571 mm^2	1923 mm^2	2262 mm^2
	14Y16	14Y12	10Y16	12Y16
	2815 mm^2	1583 mm^2	2011 mm^2	2413 mm^2
	9Y20	8Y16	7Y20	8Y20
	2827 mm^2	1608 mm^2	2199 mm^2	2513 mm^2

Shear reinforment should be placed in a band 1.5-d wide inside each critcical perimeter. Maximum spacing 0.75-d.

PROKON
Software Consultants (Pty) Ltd
Internet: http://www.prokon.com
E-Mail : mail@prokon.com

Job Number		Sheet
Job Title	Cobiax 7.5m Heavy	
Client		
Calcs by	Checked by	Date

C23

Punching Shear Design :

Input Data

Column width A	(mm)	450
Column breadth B	(mm)	450
Effective slab depth deff	(mm)	319
Nearest edge X-direction	(mm)	7500
Nearest edge Y-direction	(mm)	7500
fcu	(MPa)	30
fy flexural reinforcement	(MPa)	450
fyv shear reinforcement	(MPa)	450
X-reinforcement crossing perimeter 1		Y16@125
Perimeter 2	(mm^2)	Y16@125
Perimeter 3	(mm^2)	Y16@125
Perimeter 4	(mm^2)	Y16@125
Y-reinforcement crossing perimeter 1		Y16@125
Perimeter 2	(mm^2)	Y16@125
Perimeter 3	(mm^2)	Y16@125
Perimeter 4	(mm^2)	Y16@125
Shear head present	(Y/[N])	
Max. link/tie size	(mm)	16

Load Cases

Load Case	Description	ULS Shear Vt (kN)	ULS X-moment (kNm)	ULS Y-moment (kNm)
1	1	1532		

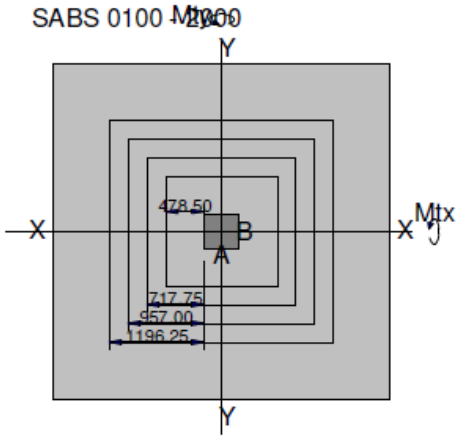

Output for Load Case 1:1

Critical load case: 1:1	Load Case 1:1			
Perimeter	1	2	3	4
Distance from Column face (mm)	479	718	957	1196
Critical length (mm)	5628	7542	9456	11370
Allowable shear stress vc (MPa)	0.48	0.48	0.48	0.48
Shear force capacity Vc (kN)	861	1154	1446	1739
Effective shear force Veff (kN)	1762	1762	1762	1762
Total reqd. reinforcement Asv (mm^2)	4756	2458	3082	3706
Suggested reinforcement configurations	43Y12	32Y10	40Y10	33Y12
	4863 mm^2	2513 mm^2	3142 mm^2	3732 mm^2
	24Y16	22Y12	28Y12	19Y16
	4825 mm^2	2488 mm^2	3167 mm^2	3820 mm^2
	16Y20	13Y16	16Y16	12Y20
	5027 mm^2	2614 mm^2	3217 mm^2	3770 mm^2
	10Y25	8Y20	10Y20	8Y25
	4909 mm^2	2513 mm^2	3142 mm^2	3927 mm^2
Warning: Shear stress v exceeds 2*vc ! justification of the design required				
Shear reinforment should be placed in a band 1.5-d wide inside each critcical perimeter. Maximum spacing 0.75-d.				

APPENDIX H

Shear Contours for 620 mm Thick Cobiax Slab – Strand7

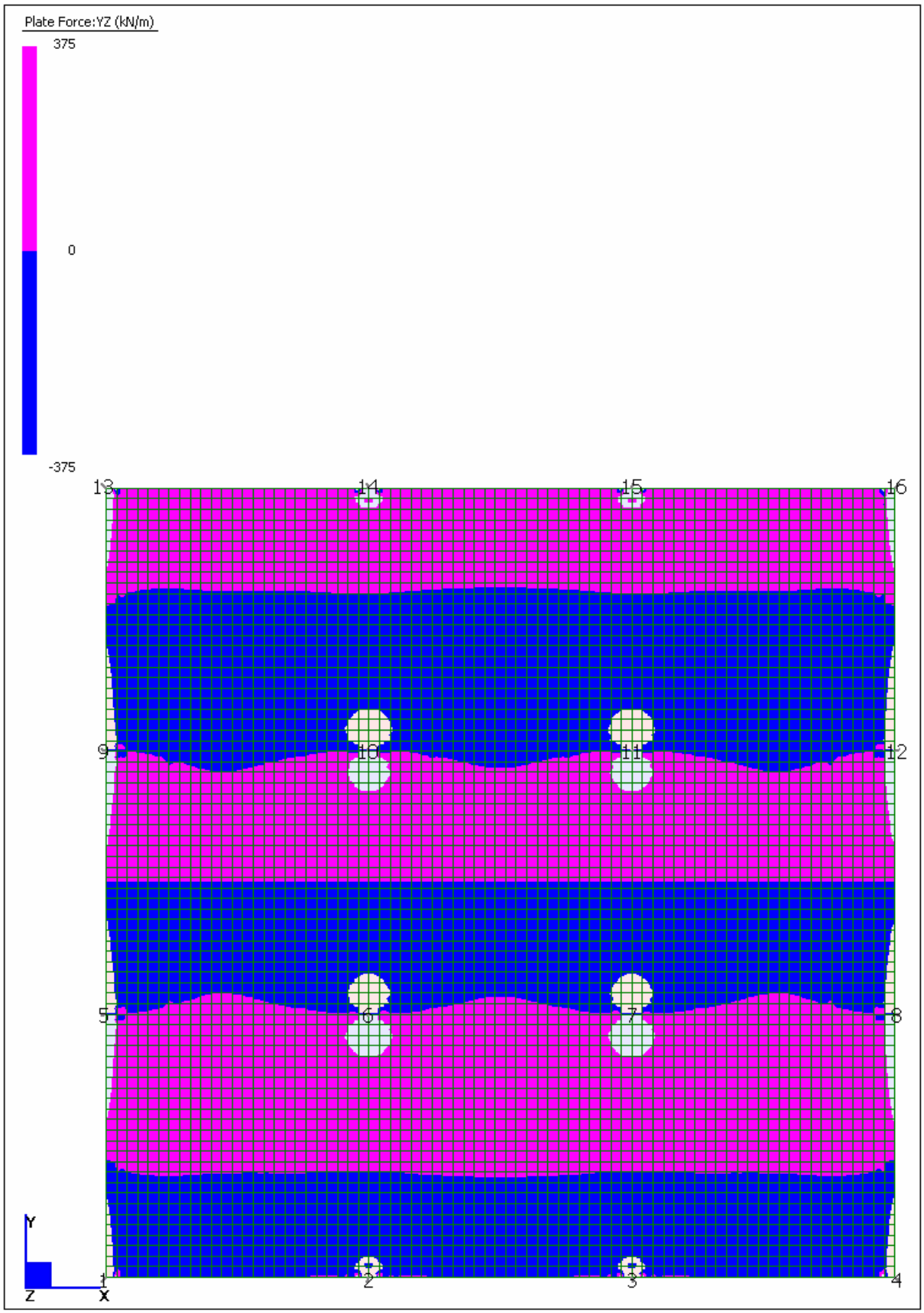
Plate Force:YZ (kN/m)
375
0
-375
13
14
15
16
9
10
11
12
5
6
7
8
1
2
3
4
Y
Z
X
Strand7 Release 2.3.8 [Licenced to:COBIAX]

APPENDIX I

Coffer – Punching Shear Reinforcement

PROKON
Software Consultants (Pty) Ltd
Internet: http://www.prokon.com
E-Mail : mail@prokon.com

Job Number		Sheet
Job Title	Coffer - 7.5m Light	
Client		
Calcs by	Checked by	Date

C23

Punching Shear Design :

Input Data

Column width A	(mm)	450
Column breadth B	(mm)	450
Effective slab depth deff	(mm)	384
Nearest edge X-direction	(mm)	7500
Nearest edge Y-direction	(mm)	7500
fcu	(MPa)	30
fy flexural reinforcement	(MPa)	450
fyv shear reinforcement	(MPa)	450
X-reinforcement crossing perimeter		Y16@150
Perimeter 2	(mm^2)	Y16@150
Perimeter 3	(mm^2)	Y16@150
Perimeter 4	(mm^2)	Y16@150
Y-reinforcement crossing perimeter		Y16@150
Perimeter 2	(mm^2)	Y16@150
Perimeter 3	(mm^2)	Y16@150
Perimeter 4	(mm^2)	Y16@150
Shear head present	(Y/[N])	
Max. link/tie size	(mm)	16

Load Cases

Load Case	Description	ULS Shear Vt (kN)	ULS X-moment (kNm)	ULS Y-moment (kNm)
1	1	706		

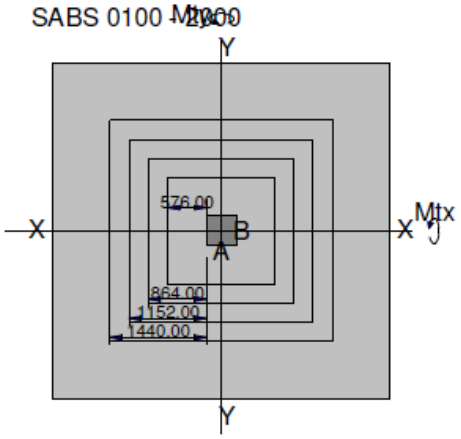

Output for Load Case 1:1

Critical load case: 1:1	Load Case 1:1			
Perimeter	1	2	3	4
Distance from Column face (mm)	576	864	1152	1440
Critical length (mm)	6408	8712	11016	13320
Allowable shear stress vc (MPa)	0.40	0.40	0.40	0.40
Shear force capacity Vc (kN)	996	1355	1713	2071
Effective shear force Veff (kN)	812	812	812	812
Total reqd. reinforcement Asv (mm^2)	0	0	0	0
Suggested reinforcement configurations				
Shear reinforment should be placed in a band 1.5-d wide inside each critcical perimeter. Maximum spacing 0.75-d.				

PROKON
Software Consultants (Pty) Ltd
Internet: http://www.prokon.com
E-Mail : mail@prokon.com

Job Number		Sheet
Job Title	Coffer - 7.5m Medium	
Client		
Calcs by	Checked by	Date

C23

Punching Shear Design :

Input Data

Column width A	(mm)	450
Column breadth B	(mm)	450
Effective slab depth deff	(mm)	375
Nearest edge X-direction	(mm)	7500
Nearest edge Y-direction	(mm)	7500
fcu	(MPa)	30
fy flexural reinforcement	(MPa)	450
fyv shear reinforcement	(MPa)	450
X-reinforcement crossing perimeter 1		Y25@300
Perimeter 2	(mm^2)	Y25@300
Perimeter 3	(mm^2)	Y25@300
Perimeter 4	(mm^2)	Y25@300
Y-reinforcement crossing perimeter 1		Y25@300
Perimeter 2	(mm^2)	Y25@300
Perimeter 3	(mm^2)	Y25@300
Perimeter 4	(mm^2)	Y25@300
Shear head present	(Y/[N])	
Max. link/tie size	(mm)	16

Load Cases

Load Case	Description	ULS Shear Vt (kN)	ULS X-moment (kNm)	ULS Y-moment (kNm)
1	1	1057		

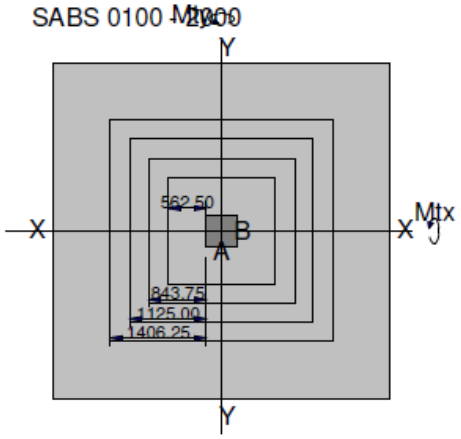

Output for Load Case 1:1

Critical load case: 1:1	Load Case 1:1			
Perimeter	1	2	3	4
Distance from Column face (mm)	563	844	1125	1406
Critical length (mm)	6300	8550	10800	13050
Allowable shear stress vc (MPa)	0.44	0.44	0.44	0.44
Shear force capacity Vc (kN)	1037	1407	1777	2147
Effective shear force Veff (kN)	1216	1216	1216	1216
Total reqd. reinforcement Asv (mm^2)	2414	0	0	0
Suggested reinforcement configurations	31Y10			
	2435 mm^2			
	22Y12			
	2488 mm^2			
	13Y16			
	2614 mm^2			
	8Y20			
	2513 mm^2			
Shear reinforment should be placed in a band 1.5-d wide inside each critcical perimeter. Maximum spacing 0.75-d.				

PROKON
Software Consultants (Pty) Ltd
Internet: http://www.prokon.com
E-Mail : mail@prokon.com

Job Number		Sheet
Job Title	Coffer - 7.5m Heavy	
Client		
Calcs by	Checked by	Date

Punching Shear Design :

Input Data

Column width A	(mm)	450
Column breadth B	(mm)	450
Effective slab depth deff	(mm)	375
Nearest edge X-direction	(mm)	7500
Nearest edge Y-direction	(mm)	7500
fcu	(MPa)	30
fy flexural reinforcement	(MPa)	450
fyv shear reinforcement	(MPa)	450
X-reinforcement crossing perimeter 1		Y25@150
Perimeter 2	(mm^2)	Y25@150
Perimeter 3	(mm^2)	Y25@150
Perimeter 4	(mm^2)	Y25@150
Y-reinforcement crossing perimeter 1		Y25@150
Perimeter 2	(mm^2)	Y25@150
Perimeter 3	(mm^2)	Y25@150
Perimeter 4	(mm^2)	Y25@150
Shear head present	(Y/[N])	
Max. link/tie size	(mm)	16

Load Cases

Load Case	Description	ULS Shear Vt (kN)	ULS X-moment (kNm)	ULS Y-moment (kNm)
1	1	1550		

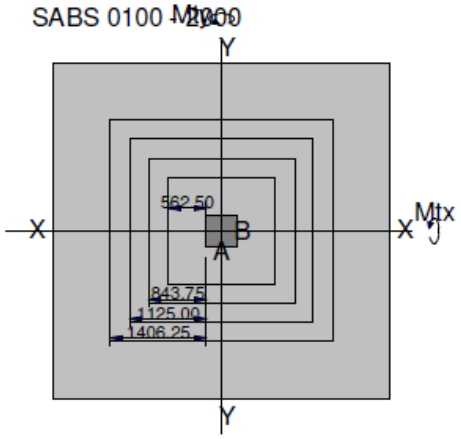

PROKON
Software Consultants (Pty) Ltd
Internet: http://www.prokon.com
E-Mail : mail@prokon.com

Job Number		Sheet
Job Title	Coffer - 7.5m Heavy	
Client		
Calcs by	Checked by	Date

Output for Load Case 1:1

Critical load case: 1:1	Load Case 1:1			
Perimeter	1	2	3	4
Distance from Column face (mm)	563	844	1125	1406
Critical length (mm)	6300	8550	10800	13050
Allowable shear stress vc (MPa)	0.55	0.55	0.55	0.55
Shear force capacity Vc (kN)	1306	1773	2239	2706
Effective shear force Veff (kN)	1783	1783	1783	1783
Total reqd. reinforcement Asv (mm^2)	2414	3276	0	0
Suggested reinforcement configurations	31Y10	29Y12		
	2435 mm^2	3280 mm^2		
	22Y12	17Y16		
	2488 mm^2	3418 mm^2		
	13Y16	11Y20		
	2614 mm^2	3456 mm^2		
	8Y20	7Y25		
	2513 mm^2	3436 mm^2		

Shear reinforment should be placed in a band 1.5-d wide inside each critcical perimeter. Maximum spacing 0.75-d.

APPENDIX J

Post-tension Slab – Punching Shear Reinforcement

PROKON
Software Consultants (Pty) Ltd
Internet: http://www.prokon.com
E-Mail : mail@prokon.com

Job Number		Sheet
Job Title	PT 7.5m Light	
Client		
Calcs by	Checked by	Date

Punching shear data: column 3

Design data

A	(mm)	450
B	(mm)	450
C	(mm)	0
D	(mm)	0
DeffX	(mm)	185
DeffY	(mm)	185
X	(mm)	7500
Y	(mm)	7500
Corner	(Y,N)	N
Vt	(kN)	635.4
Mtx	(kNm)	53.5
Mty	(kNm)	53.5
Pcx	(kN)	4254.4
Pcy	(kN)	709.0
UDL	(kN/m²)	10.4
slope-X		0.0521
slope-Y		0.0521
Cable type no.		1
N cables	X	Y
Perim 1	10	1
Perim 2	12	2
Perim 3	12	2
Perim 4	12	3
Ast (mm²)	X	Y
Perim 1	524.0	524.0
Perim 2	524.0	524.0
Perim 3	524.0	524.0
Perim 4	524.0	524.0

Perimeter output

Perimeter	Ucrit (mm)	vc (MPa)	Vcap (kN)	Veff (kN)	Asv (mm²)
1	4020.00	0.79	586.55	460.04	0.00
2	5130.00	0.81	765.66	452.44	0.00
3	6240.00	0.77	884.13	443.01	0.00
4	7350.00	0.75	1024.90	431.74	0.00

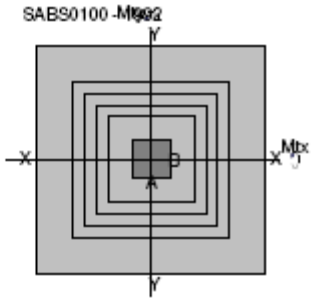

PROKON
Software Consultants (Pty) Ltd
Internet: http://www.prokon.com
E-Mail : mail@prokon.com

Job Number		Sheet
Job Title	PT 7.5m Medium	
Client		
Calcs by	Checked by	Date

Punching shear data: column 3

Design data

A	(mm)	450
B	(mm)	450
C	(mm)	0
D	(mm)	0
DeffX	(mm)	195
DeffY	(mm)	195
X	(mm)	7500
Y	(mm)	7500
Corner	(Y,N)	N
Vt	(kN)	850.0
Mtx	(kNm)	69.7
Mty	(kNm)	69.7
Pcx	(kN)	4555.0
Pcy	(kN)	1051.0
UDL	(kN/m²)	13.9
slope-X		0.0544
slope-Y		0.0544
Cable type no.		1
N cables	X	Y
Perim 1	10	2
Perim 2	13	3
Perim 3	16	3
Perim 4	16	4
Ast (mm²)	X	Y
Perim 1	524.0	524.0
Perim 2	524.0	524.0
Perim 3	524.0	524.0
Perim 4	524.0	524.0

Perimeter output

Perimeter	Ucrit (mm)	vc (MPa)	Vcap (kN)	Veff (kN)	Asv (mm²)
1	4140.00	0.81	656.43	655.41	0.00
2	5310.00	0.82	847.34	644.36	0.00
3	6480.00	0.80	1007.51	630.58	0.00
4	7650.00	0.78	1170.89	614.07	0.00

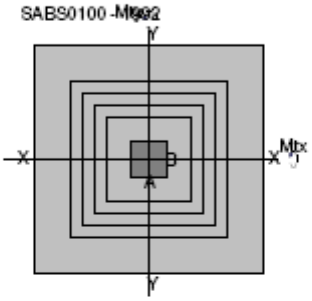

APPENDIX K

Post-tension Slabs – Cable Design

MATHCAD V12.0

Prestressed Flat Slab - Light loading - 7.5m spans

{3 Span X 3 Span Slab Configuration}

Adapted from an example by Marshall & Robberts

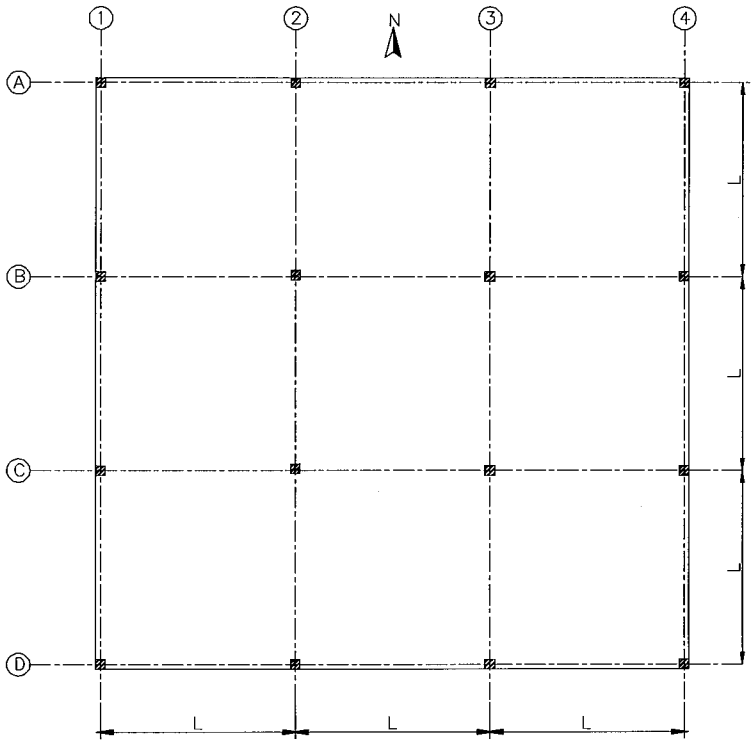

Figure 1: Layout

Design Codes:

SANS 10100-1: 2000
SABS 0160: 1989

Unit Declarations:

$GPa := Pa \cdot 10^{9}$ $MPa := Pa \cdot 10^{6}$ $kPa := Pa \cdot 10^{3}$ $kN := N \cdot 10^{3}$

Material Properties:

Concrete Parameters:

28-day compressive strength $f_{cu} := 30MPa$

Compressive strength at transfer $f_{ci} := 18MPa$

$K_o := 20 \cdot GPa$

Modulus of elasticity at 28 days $E_c := K_o + 0.2GPa \cdot \frac{f_{cu}}{MPa}$ $E_c = 26 \cdot GPa$

Modulus of elasticity at transfer $E_{ct} := E_c \cdot \left(0.4 + 0.6 \cdot \frac{f_{ci}}{f_{cu}}\right)$ $E_{ct} = 19.76 \cdot GPa$

Unit weight of concrete $\gamma_c := 25 \frac{kN}{m^3}$

Non-prestressed reinforcement:

Main $fy := 450MPa$

Shear $fyv := 450MPa$

Modulus of elasticity $Es := 200GPa$

Diameter bottom rebar $\phi_b := 10mm$

Diameter top rebar $\phi_t := 10mm$

Prestressed Reinforcement

Unbonded prestress

(15.7mm diameter 7-wire unbonded low relaxation super grade strand)

Characteristic breaking load per strand	$P_{tnd} := 265kN$
Steel area per strand	$A_{ps} := 150mm^2$
Modulus of elasticity	$E_p := 195GPa$

Loads:

Service Loads

Assume	$h := 220mm$	
Slab Self-weight	$w_{sw} := h \cdot \gamma_c$	$w_{sw} = 5.5 \cdot kPa$
Additional Dead Load	$w_{ADL} := 0.5kPa$	
Total dead load	$w_D := w_{sw} + w_{ADL}$	$w_D = 6.0 \cdot kPa$
Imposed Live Load	$w_L := 2kPa$	

Ultimate Loads

Ultimte UDL	$w_{ult} := 1.2 \cdot w_D + 1.6 \cdot w_L$	$w_{ult} = 10.4 \cdot kPa$
Percentage Dead Load to be Balanced		$Bal_D := 70\%$
Load Balanced	$w_{bal} := w_D \cdot Bal_D$	$w_{bal} = 4.2 \cdot kPa$

Dimensional Parameters:

Slab span $L := 7500mm$ {Assuming equal spans}

Calculation of slab depth

Factors $K_1 := 0.9$ (0.9 for End-Span and 1.0 for Internal Span)

$K_2 := 1.0$ (0.95 for temperature or shrinkage cracking and 1.0 for cracking not likely)

$$K_3 := \left(\frac{E_c}{26 \cdot GPa}\right)^{\frac{1}{3}} \qquad K_3 = 1$$

$K_4 := 1.0$ (1.0 no drops & 1.15 drops present)

Slab Depth

$$h := \frac{L}{\left[14 + \frac{53}{\left(\frac{3.5 \cdot w_D + w_L - 3.32 \cdot Bal_D \cdot w_D}{kPa}\right)^{\frac{1}{3}}}\right] \cdot K_1 \cdot K_2 \cdot K_3 \cdot K_4}$$

$h = 211.36 \cdot mm$

Keep $h := 220mm$

Allowable slab depth $h := \max(h, 200mm)$ $h = 220 \cdot mm$

Cover to reinforcement

Top $C_{top} := 25mm$

Bottom $C_{bot} := 25mm$

Tendon Profile:

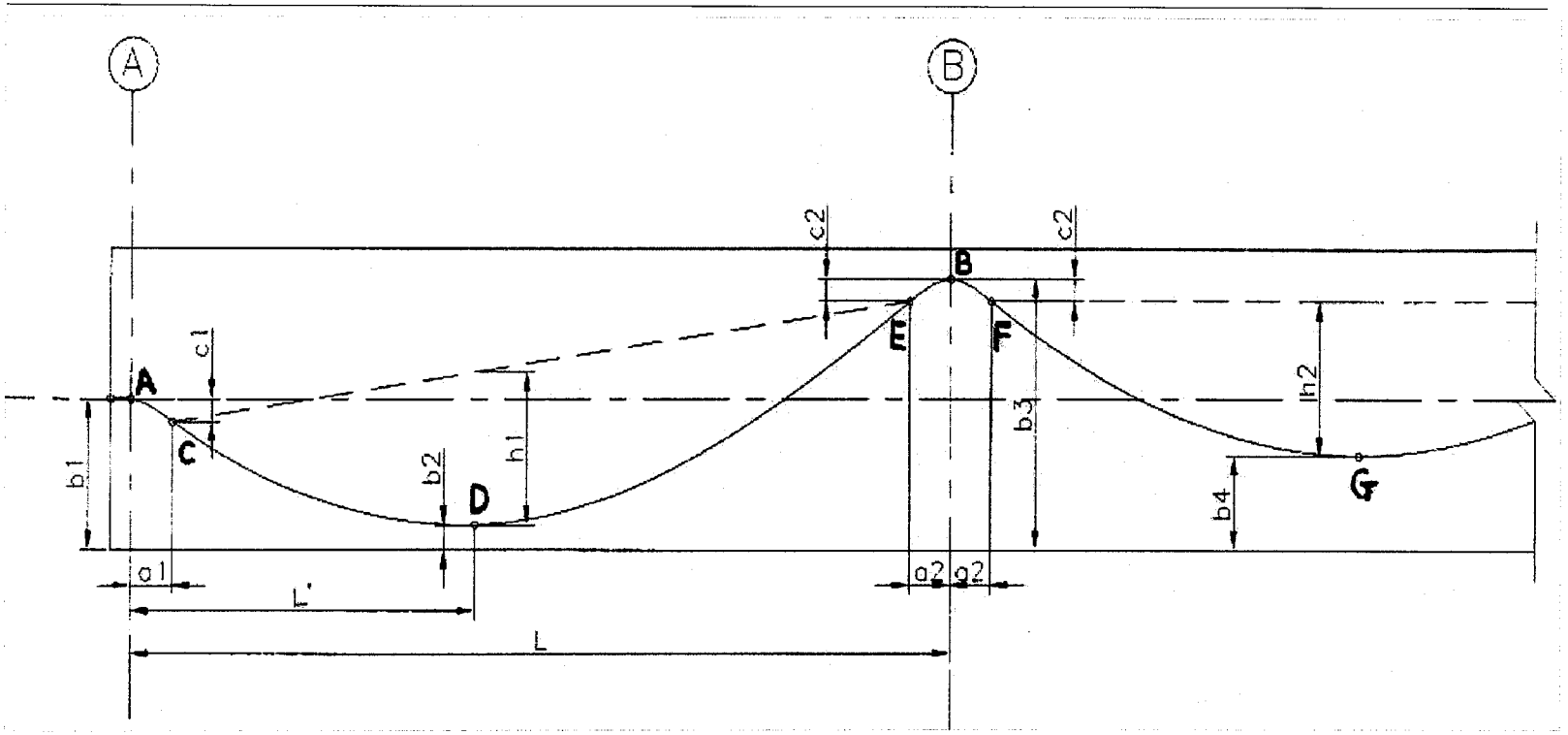

Figure 2: Tendon Profile Parameters

Maximum drape in North-south direction. Distance from centre of supports to the inflection points of the profile taken equal to 0.05 times the span.

$a_1 := 0.05 \cdot L$ $\quad a_1 = 375 \cdot mm$

$a_2 := 0.05L$ $\quad a_2 = 375 \cdot mm$

$b_1 := \frac{h}{2}$ $\quad b_1 = 110 \cdot mm$

$S_p := 9mm$ (Strand position in sheath)

$b_2 := C_{bot} + \phi_b + 9mm$ $b_2 = 44 \cdot mm$

Distance top to centre tendon direction 1 $t_1 := C_{top} + \phi_t + 9mm$ $t_1 = 44 \cdot mm$

$b_3 := h - t_1$ $b_3 = 176 \cdot mm$

$l := b_3 - b_1$ $l = 66 \cdot mm$

$m_1 := (2 \cdot L - a_2) \cdot (b_1 - b_2) - a_1 \cdot (b_3 - b_2)$ $m_1 = 9.158 \times 10^5 \cdot mm^2$

$n := -(b_1 - b_2) \cdot (L - a_2) \cdot L$ $n = -3.527 \times 10^9 \cdot mm^3$

$$L' := \frac{-m_1 + \sqrt{m_1^2 - 4 \cdot l \cdot n}}{2l}$$ $L' = 3140.5 \cdot mm$

$$c_1 := \frac{[(b_1 - b_2) \cdot a_1]}{L'}$$ $c_1 = 7.881 \cdot mm$

$$c_2 := \frac{[(b_3 - b_2) \cdot a_2]}{(L - L')}$$ $c_2 = 11.355 \cdot mm$

Drape $$h_1 := \frac{(b_1 - b_2) \cdot (L - a_1 - a_2)^2}{4 \cdot L' \cdot (L' - a_1)}$$ $h_1 = 86.559 \cdot mm$

Prestressing Force

$w_b=(8Ph)/(L-a_1-a_2)^2$

Per column Strip :

Load to be balanced $w_b := L \cdot w_{bal}$ $w_b = 31.5 \cdot \frac{kN}{m}$

Required Prestressing Force

$$P := \frac{w_b \cdot (L - a_1 - a_2)^2}{8 \cdot h_1} \qquad P = 2.073 \times 10^3 \cdot kN$$

Required internal span drape to maintain load balancing

$$h_2 := \frac{\left[w_b \cdot (L - a_2 - a_2)^2\right]}{8 \cdot P} \qquad h_2 = 86.559 \cdot mm$$

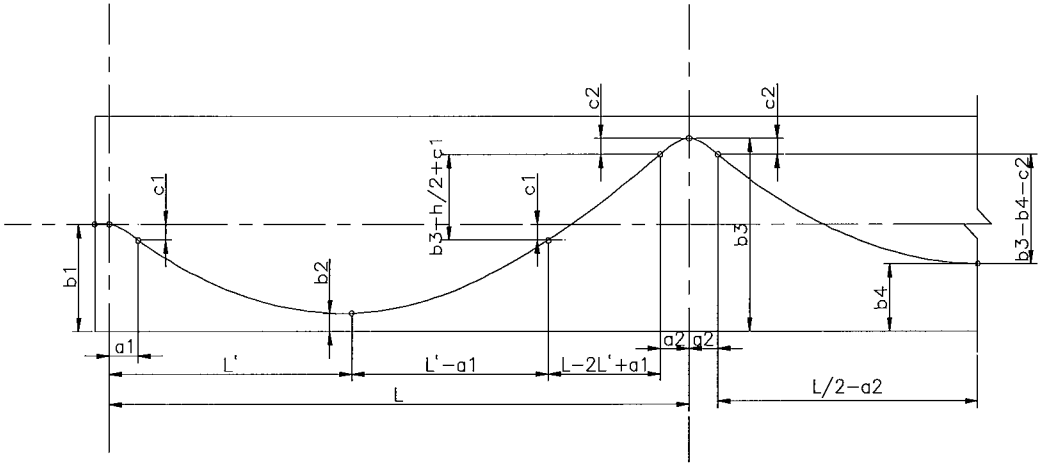

Figure 3: Parameter Calculations

PRESTRESSING LOSSES

Percentage Stressed $P_{Stressed} := 80\%$

SHORT-TERM LOSSES

Coefficient of Friction $\mu := 0.06$

Wobble coefficient $K_w := 0.00025 \cdot m^{-1}$

Anchorage seating $\delta := 5mm$

Cumulative Change in angle:

$$\theta_{AC} := \operatorname{atan}\left(\frac{2c_1}{a_1}\right) \qquad \theta_{AC} = 0.04201 \cdot rad$$

$$\theta_{CD} := \operatorname{atan}\left[\frac{2(b_1 - c_1 - b_2)}{L' - a_1}\right] \qquad \theta_{CD} = 0.04201 \cdot rad$$

$$\theta_{DE} := \operatorname{atan}\left[\frac{2(b_3 - c_2 - b_2)}{L - L' - a_2}\right] \qquad \theta_{DE} = 0.06048 \cdot rad$$

$$\theta_{EB} := \operatorname{atan}\left(\frac{2c_2}{a_2}\right) \qquad \theta_{EB} = 0.06048 \cdot rad$$

$$\theta_{BF} := \operatorname{atan}\left(\frac{2c_2}{a_2}\right) \qquad \theta_{BF} = 0.06048 \cdot rad$$

$$\theta_{FG} := \operatorname{atan}\left[\frac{2(b_3 - c_2 - b_4)}{\frac{L}{2} - a_2}\right] \qquad \theta_{FG} = 0.05125 \cdot rad$$

Angle changes over entire span lengths displayed in Figure 1

$\alpha_{AB} := \theta_{AC} + \theta_{CD} + \theta_{DE} + \theta_{EB}$ $\alpha_{AB} = 0.2050 \cdot rad$

$\alpha_{BC} := 2\theta_{FG} + 2\theta_{BF}$ $\alpha_{BC} = 0.2235 \cdot rad$

$\alpha_{AC} := \alpha_{AB} + \alpha_{BC}$ $\alpha_{AC} = 0.4284 \cdot rad$

$\alpha_{AD} := 2 \cdot \alpha_{AB} + \alpha_{BC}$ $\alpha_{AD} = 0.6334 \cdot rad$

Half of the tendons are tensioned from one end while the remainder is tensioned from the opposite end.

Percentage stressed $P_{Stressed} = 80 \cdot \%$

Jacking force per tendon $P_{tndJ} := P_{Stressed} \cdot -P_{tnd}$ $P_{tndJ} = -212 \cdot kN$

$Loss_{tot} := 0.185$ (Assumed total losses)

$$n_{tnd} := \text{round}\left[\frac{P}{\left(1 - Loss_{tot}\right) \cdot \left(-P_{tndJ}\right)}\right] \qquad n_{tnd} = 12$$

Tendon forces after friction losses

$$P_{AA} := \frac{n_{tnd}}{2} \cdot P_{tndJ} \qquad P_{AA} = -1.272 \times 10^{3} \cdot kN$$

$$P_{BA} := P_{AA} \cdot e^{-\left(\mu \cdot \alpha_{AB} + K_w \cdot L\right)} \qquad P_{BA} = -1.254 \times 10^{3} \cdot kN$$

$$P_{CA} := P_{AA} \cdot e^{-\left(\mu \cdot \alpha_{AC} + K_w \cdot 2 \cdot L\right)} \qquad P_{CA} = -1.235 \times 10^{3} \cdot kN$$

$$P_{DA} := P_{AA} \cdot e^{-\left(\mu \cdot \alpha_{AD} + K_w \cdot 3 \cdot L\right)} \qquad P_{DA} = -1.218 \times 10^{3} \cdot kN$$

The change in tendon force is approximated by using the jacking force (at A) and tendon force (at D):

$$p := \frac{P_{AA} - P_{DA}}{3L} \qquad p = -2.414 \cdot \frac{kN}{m}$$

$$\Delta P_L := \left[\frac{\delta \cdot \frac{n_{tnd}}{2} \cdot A_{ps} \cdot E_p}{3L} - (-p \cdot 3L) \right] \qquad \Delta P_L = -15.305 \cdot kN$$

Since $\Delta P_L < 0$ the tendon force at D will remain the same

$$P_{DA} = -1.218 \times 10^3 \cdot kN$$

For a second attempt, the change in tendon force is approximated by using the jacking force (at A) and tendon force (at C)

$$p := \frac{P_{AA} - P_{CA}}{2L} \qquad p = -2.462 \cdot \frac{kN}{m}$$

Due to anchorage seating:

$$\Delta P_L := \left[\frac{\delta \cdot \frac{n_{tnd}}{2} \cdot A_{ps} \cdot E_p}{2L} - (-p \cdot 2L) \right] \qquad \Delta P_L = 21.577 \cdot kN$$

Tendon forces after anchorage seating

Since $\Delta P_L > 0$ the tendon force at C will become:

$P_{CA} := P_{CA} + \Delta P_L$ $\quad P_{CA} = -1.214 \times 10^3 \cdot kN$

$P_{AA} := P_{CA} \cdot e^{-\left(\mu \cdot \alpha_{AC} + K_w \cdot 2L\right)}$ $\quad P_{AA} = -1.178 \times 10^3 \cdot kN$

$P_{BA} := P_{AA} \cdot e^{\left(\mu \cdot \alpha_{AB} + K_w \cdot L\right)}$ $\quad P_{BA} = -1.195 \times 10^3 \cdot kN$

From symmetry, taking the jacking force at D:

$P_{AD} := P_{DA}$

$P_{BD} := P_{CA}$

$P_{CD} := P_{BA}$

$P_{DD} := P_{AA}$

The total prestressing force is the summation of the tendon forces tensioned from A and D:

$P_A := P_{AA} + P_{AD}$ $\quad P_A = -2.396 \times 10^3 \cdot kN$

$P_B := P_{BA} + P_{BD}$ $\quad P_B = -2.409 \times 10^3 \cdot kN$

$P_C := P_{CA} + P_{CD}$ $\quad P_C = -2.409 \times 10^3 \cdot kN$

$P_D := P_{DA} + P_{DD}$ $\quad P_D = -2.396 \times 10^3 \cdot kN$

Elastic shortening of concrete:

Average cable force	$P_{avg} := \frac{(P_A + P_B + P_C + P_D)}{4}$	$P_{avg} = -2.402 \times 10^3 \cdot kN$
Area of concrete section	$A := h \cdot L$	$A = 1.650 \times 10^6 \cdot mm^2$
Average stress produced by prestress at the centroid of the section	$f_{c.cgsPJ'} := \frac{P_{avg}}{A}$	$f_{c.cgsPJ'} = -1.456 \cdot MPa$
Change in steel stress	$\Delta f_{pES} := \frac{1}{2} \cdot f_{c.cgsPJ'} \cdot \frac{E_p}{E_{ct}}$	$\Delta f_{pES} = -7.184 \cdot MPa$
Loss in prestress	$\Delta P_{ES} := -n_{tnd} \cdot A_{ps} \cdot \Delta f_{pES}$	$\Delta P_{ES} = 12.931 \cdot kN$

Prestressing force at transfer

$P_{tA} := P_A + \Delta P_{ES}$	$P_{tA} = -2.383 \times 10^3 \cdot kN$
$P_{tB} := P_B + \Delta P_{ES}$	$P_{tB} = -2.396 \times 10^3 \cdot kN$
$P_{tC} := P_C + \Delta P_{ES}$	$P_{tC} = -2.396 \times 10^3 \cdot kN$
$P_{tD} := P_D + \Delta P_{ES}$	$P_{tD} = -2.383 \times 10^3 \cdot kN$

LONG-TERM LOSSES

30 year Shrinkage Strain

Assuming 50% Humidity

Approximation from SABS chart

$$\varepsilon_{su} := \begin{cases} \left[\frac{(h - 150mm)}{300mm - 150mm}\cdot(350 - 400) + 400\right]\cdot -10^{-6} & \text{if } 150mm \le h \le 300mm \\ \left[\frac{(h - 300mm)}{600mm - 300mm}\cdot(290 - 350) + 350\right]\cdot -10^{-6} & \text{if } 300mm < h \le 600mm \\ 350\cdot -10^{-6} & \text{otherwise} \end{cases}$$

$$\varepsilon_{su} = -377 \times 10^{-6}$$

{50% Humidity -
150 Slab : 400
300 Slab : 350
600 Slab : 290}

30 year Creep Coefficient

Approximation from SABS chart

$$\phi_u := \begin{cases} \left[\frac{(h - 150mm)}{300mm - 150mm}\cdot(3.1 - 4) + 4\right] & \text{if } 150mm \le h \le 300mm \\ \left[\frac{(h - 300mm)}{600mm - 300mm}\cdot(2.8 - 3.1) + 3.1\right] & \text{if } 300mm < h \le 600mm \\ 3 & \text{otherwise} \end{cases}$$

$$\phi_u = 3.6$$

{50% Humidity, 3 days -
150 Slab : 4
300 Slab : 3.1
600 Slab : 2.8}

Relaxation Losses

Average prestressing force immediatley after transfer

$$P_{tavg} := \frac{\left(P_{tA} + P_{tB} + P_{tC} + P_{tD}\right)}{4} \qquad P_{tavg} = -2389\cdot kN$$

P_{tavg} expressed as a percentage of characteristic breaking load of the tendons

$$Per_P := \frac{P_{tavg}\cdot 100}{n_{tnd}\cdot -P_{tnd}} \qquad Per_P = 75.13\,\%$$

Percentage relaxation loss

$$PR_{Loss} := \left| \begin{array}{l} \varepsilon \leftarrow 500 \cdot 10^{-6} \\ \left[\frac{1}{2} \cdot \left[3 + \left(\frac{8.5 - 3}{80 - 50} \right) \cdot \left(Per_P - 50 \right) \right] \right] \text{ if } \varepsilon \geq 500 \cdot 10^{-6} \\ \frac{1}{2} \cdot \left[3 + \left(\frac{10 - 3}{80 - 50} \right) \cdot \left(Per_P - 50 \right) \right] \text{ otherwise} \end{array} \right.$$

$$PR_{Loss} = 3.804$$

Loss of prestress due to relaxation of the steel $\Delta P_r := -PR_{Loss} \cdot \% \cdot P_{tavg}$ $\Delta P_r = 90.896 \cdot kN$

Shrinkage Losses

$\varepsilon_{su} = -377 \times 10^{-6}$

Loss of steel stress due to shrinkage of concrete $\Delta f_{ps} := \varepsilon_{su} \cdot E_p$ $\Delta f_{ps} = -73.45 \cdot MPa$

Loss in force due to shrinkage $\Delta P_s := -\Delta f_{ps} \cdot n_{tnd} \cdot A_{ps}$ $\Delta P_s = 132.21 \cdot kN$

Creep Losses

Stress in concrete at the level of the centroid of the prestressing steel $f_c := \frac{P_{tavg}}{A}$ $f_c = -1.448 \cdot MPa$

Creep Strain $\varepsilon_c := \phi_u \cdot \frac{f_c}{E_{ct}}$ $\varepsilon_c = -262.36 \times 10^{-6}$

Loss of steel sress due to creep of the concrete $\Delta f_{pC} := \varepsilon_c \cdot E_p$ $\Delta f_{pC} = -51.16 \cdot MPa$

Loss of force due to creep $\Delta P_c := -\left(\Delta f_{pC} \cdot n_{tnd} \cdot A_{ps}\right)$ $\Delta P_c = 92.087 \cdot kN$

Creep plus shrinkage strain $Strain := \left|\varepsilon_{su} + \varepsilon_c\right|$ $Strain = 639.02 \times 10^{-6}$ which is greater than 500E-6 as assumed

Final Prestressing Force

Total long-time loss of prestressing force $\Delta P_{time} := \Delta P_r + \Delta P_s + \Delta P_c$ $\Delta P_{time} = 315.193 \cdot kN$

Final prestressing force after all losses

$P_A := P_{tA} + \Delta P_{time}$ $P_A = -2.068 \times 10^3 \cdot kN$

$P_B := P_{tB} + \Delta P_{time}$ $P_B = -2.08 \times 10^3 \cdot kN$

$P_C := P_{tC} + \Delta P_{time}$ $P_C = -2.08 \times 10^3 \cdot kN$

$P_D := P_{tD} + \Delta P_{time}$ $P_D = -2.068 \times 10^3 \cdot kN$

Total loss $\Delta P_{total} := n_{tnd} \cdot P_{tndJ} - \dfrac{P_A + P_B + P_C + P_D}{4}$

$\Delta P_{total} = -469.841 \cdot kN$

Actual Losses (Percentage of Jacking Force) $PLosses_{Act} := \dfrac{\Delta P_{total}}{n_{tnd} \cdot P_{tndJ}}$ $PLosses_{Act} = 18.5 \cdot \%$ which is the same as assumed

Equivalent Loads *{Equivalent loads imposed by the prestressing tendons on the concrete}*

At transfer

External Support	External Span	Internal support	Internal Span
$w_{bACt} := \left\lvert \frac{2P_{tavg} \cdot c_1}{a_1^{\,2}} \right\rvert$	$w_{bCEt} := \left\lvert \frac{8P_{tavg} \cdot h_1}{(L - a_1 - a_2)^2} \right\rvert$	$w_{bEFt} := \left\lvert \frac{2P_{tavg} \cdot c_2}{a_2^{\,2}} \right\rvert$	$w_{bFGt} := \left\lvert \frac{8P_{tavg} \cdot h_2}{(L - a_1 - a_2)^2} \right\rvert$
$w_{bACt} = 267.807 \cdot kN \cdot m^{-1}$	$w_{bCEt} = 36.314 \cdot kN \cdot m^{-1}$	$w_{bEFt} = 385.849 \cdot kN \cdot m^{-1}$	$w_{bFGt} = 36.314 \cdot kN \cdot m^{-1}$

Spacing of banded tendons over columns: $S_{tndB} := 100mm$

Width containing banded tendons: $Band := n_{tnd} \cdot S_{tndB}$ $\quad Band = 1200 \cdot mm$

After Transfer

$$P_{avg} := \frac{P_A + P_B + P_C + P_D}{4} \qquad P_{avg} = -2074 \cdot kN$$

	External Support	**External Span**	**Internal support**	**Internal Span**
	$w_{bAC} := \left\lvert \frac{2P_{avg} \cdot c_1}{a_1^{\,2}} \right\rvert$	$w_{bCE} := \left\lvert \frac{8P_{avg} \cdot h_1}{(L - a_1 - a_2)^2} \right\rvert$	$w_{bEF} := \left\lvert \frac{2P_{avg} \cdot c_2}{a_2^{\,2}} \right\rvert$	$w_{bFG} := \left\lvert \frac{8P_{avg} \cdot h_2}{(L - a_1 - a_2)^2} \right\rvert$
	$w_{bAC} = 232.479 \cdot kN \cdot m^{-1}$	$w_{bCE} = 31.524 \cdot kN \cdot m^{-1}$	$w_{bEF} = 334.95 \cdot kN \cdot m^{-1}$	$w_{bFG} = 31.524 \cdot kN \cdot m^{-1}$
	$a_1 = 375 \cdot mm$		$a_2 = 375 \cdot mm$	
UDL banded	$W_{1B} := \frac{w_{bAC}}{Band}$ $\quad W_{1B} = 194 \cdot kPa$	$W_{2B} := \frac{w_{bCE}}{Band}$ $\quad W_{2B} = 26.3 \cdot kPa$	$W_{3B} := \frac{w_{bEF}}{Band}$ $\quad W_{3B} = 279 \cdot kPa$	$W_{4B} := \frac{w_{bFG}}{Band}$ $\quad W_{4B} = 26.3 \cdot kPa$
UDL uniform	$W_{1U} := \frac{w_{bAC}}{L}$ $\quad W_{1U} = 31 \cdot kPa$	$W_{2U} := \frac{w_{bCE}}{L}$ $\quad W_{2U} = 4.2 \cdot kPa$	$W_{3U} := \frac{w_{bEF}}{L}$ $\quad W_{3U} = 44.7 \cdot kPa$	$W_{4U} := \frac{w_{bFG}}{L}$ $\quad W_{4U} = 4.2 \cdot kPa$

Shear reinforcement for punching:

Assume 450mm x 450mm columns:

Column width: $b_c := 450mm$

Average depth of tension steel: $d := h - \phi_t - C_{top}$ $d = 185 \cdot mm$

Spacing of banded tendons over columns: $S_{tndB} := 100mm$

Width containing banded tendons: $Band := n_{tnd} \cdot S_{tndB}$ $Band = 1200 \cdot mm$

Spacing of uniformly distributed tendons over columns: $S_{tndU} := \frac{L}{n_{tnd} - 1}$ $S_{tndU} = 681.818 \cdot mm$

Side lengths of critical perimeters:		No of banded tendons passing through:		No of uniformly distributed tendons passing through:	
$s_1 := 2 \cdot \left(\frac{b_c}{2} + 1.5 \cdot d \right)$	$s_1 = 1005 \cdot mm$	$n_{1B} := round\left(\frac{if(Band < s_1, Band, s_1)}{S_{tndB}} \right)$	$n_{1B} = 10$	$n_{1U} := round\left(\frac{s_1}{S_{tndU}} \right)$	$n_{1U} = 1$
$s_2 := 2 \cdot \left(\frac{b_c}{2} + 1.5 \cdot d + .75 \cdot d \right)$	$s_2 = 1282 \cdot mm$	$n_{2B} := round\left(\frac{if(Band < s_2, Band, s_2)}{S_{tndB}} \right)$	$n_{2B} = 12$	$n_{2U} := round\left(\frac{s_2}{S_{tndU}} \right)$	$n_{2U} = 2$
$s_3 := 2 \cdot \left(\frac{b_c}{2} + 1.5 \cdot d + 2 \cdot 0.75 \cdot d \right)$	$s_3 = 1560 \cdot mm$	$n_{3B} := round\left(\frac{if(Band < s_3, Band, s_3)}{S_{tndB}} \right)$	$n_{3B} = 12$	$n_{3U} := round\left(\frac{s_3}{S_{tndU}} \right)$	$n_{3U} = 2$
$s_4 := 2 \cdot \left(\frac{b_c}{2} + 1.5 \cdot d + 3 \cdot 0.75 \cdot d \right)$	$s_4 = 1837 \cdot mm$	$n_{4B} := round\left(\frac{if(Band < s_4, Band, s_4)}{S_{tndB}} \right)$	$n_{4B} = 12$	$n_{4U} := round\left(\frac{s_4}{S_{tndU}} \right)$	$n_{4U} = 3$

Cost Parameters:

Nominal Mass of prestressing tendons $\gamma_{ps} := \text{if}\left(P_{tnd} = 186\text{kN}, 0.785\frac{\text{kg}}{\text{m}}, 1.18\frac{\text{kg}}{\text{m}}\right)$ $\gamma_{ps} = 1.18\frac{\text{kg}}{\text{m}}$

Cost of Tendons per kg $\text{UwCostTnds} := 33.00\text{kg}^{-1}$

Cost of Dead Anchor $\text{UCostDAnch} := 58.00$

Cost of Stressing Anchor $\text{UCostSAnch} := 65.00$

Tendon Length:

Perimeter of Parabola Lp= 2x $\sqrt{B_p^2 + \frac{4}{3}H_p^2}$

$L_{p1} := \sqrt{a_1^2 + \frac{4}{3}c_1^2}$ $L_{p1} = 375\cdot\text{mm}$

$L1 := L - 2L' + a_1$ $L1 = 1594\cdot\text{mm}$

$L2 := b_3 - \frac{h}{2} + c_1$ $L2 = 74\cdot\text{mm}$

$L_{p2} := 2\cdot\sqrt{\left(L' - a_1\right)^2 + \frac{4}{3}\left(\frac{h}{2} - b_2 - c_1\right)^2} + \sqrt{L1^2 + L2^2}$ $L_{p2} = 7128\cdot\text{mm}$

{Part of Parabola approximated as a straight line}

$L_{p3} := 2\cdot\sqrt{a_2^2 + \frac{4}{3}c_2^2}$ $L_{p3} = 750\cdot\text{mm}$

$L_{p4} := 2\cdot\sqrt{\left(\frac{L}{2} - a_2\right)^2 + \frac{4}{3}\cdot\left(b_3 - b_4 - c_2\right)^2}$ $L_{p4} = 6753\cdot\text{mm}$

Length of Prestressing tendon: $L_{t1} := 2 \cdot L_{p1} + 2 \cdot L_{p2} + 2L_{p3} + L_{p4}$ $L_{t1} = 23.261 \cdot m$

Weight of tendon: $W_{ten} := \gamma_{ps} \cdot L_{t1}$ $W_{ten} = 27.448\,kg$

Weight of tendons over total slab area: $W_{tenT} := W_{ten} \cdot 2 \cdot n_{tnd}$ $W_{tenT} = 659\,kg$

Total cost of prestressing:

$Cost_{PT} := 2 \cdot n_{tnd}\left(W_{ten} \cdot UwCostTnds + UCostDAnch + UCostSAnch\right)$ $Cost_{PT} = 24690.59$

COST / m2

$$COST_{PT} := \frac{Cost_{PT}}{(3 \cdot L)^2} \qquad COST_{PT} = 48.77 \cdot m^{-2}$$

Cost of Reinforcement per kg $UCostR := 9.50 kg^{-1}$

Cost of Concrete per m^3 $UCostC := 1100.00 m^{-3}$

PROKON
Software Consultants (Pty) Ltd
Internet: http://www.prokon.com
E-Mail : mail@prokon.com

Job Number		Sheet
Job Title	PT 7.5m Heavy	
Client		
Calcs by	Checked by	Date

Punching shear data: column 3

Design data

A	(mm)	450
B	(mm)	450
C	(mm)	0
D	(mm)	0
DeffX	(mm)	215
DeffY	(mm)	215
X	(mm)	7500
Y	(mm)	7500
Corner	(Y,N)	N
Vt	(kN)	1316.3
Mtx	(kNm)	87.1
Mty	(kNm)	87.1
Pcx	(kN)	4870.0
Pcy	(kN)	1391.0
UDL	(kN/m²)	21.5
slope-X		0.0592
slope-Y		0.0592
Cable type no.		1
N cables	X	Y
Perim 1	11	3
Perim 2	14	4
Perim 3	17	4
Perim 4	20	5
Ast (mm²)	X	Y
Perim 1	1340.0	1340.0
Perim 2	1340.0	1340.0
Perim 3	1340.0	1340.0
Perim 4	1340.0	1340.0

Perimeter output

Perimeter	Ucrit (mm)	vc (MPa)	Vcap (kN)	Veff (kN)	Asv (mm²)
1	4380.00	0.84	794.87	1113.45	962.15
2	5670.00	0.83	1016.62	1093.41	1245.52
3	6960.00	0.81	1212.87	1068.24	0.00
4	8250.00	0.81	1429.38	1037.92	0.00